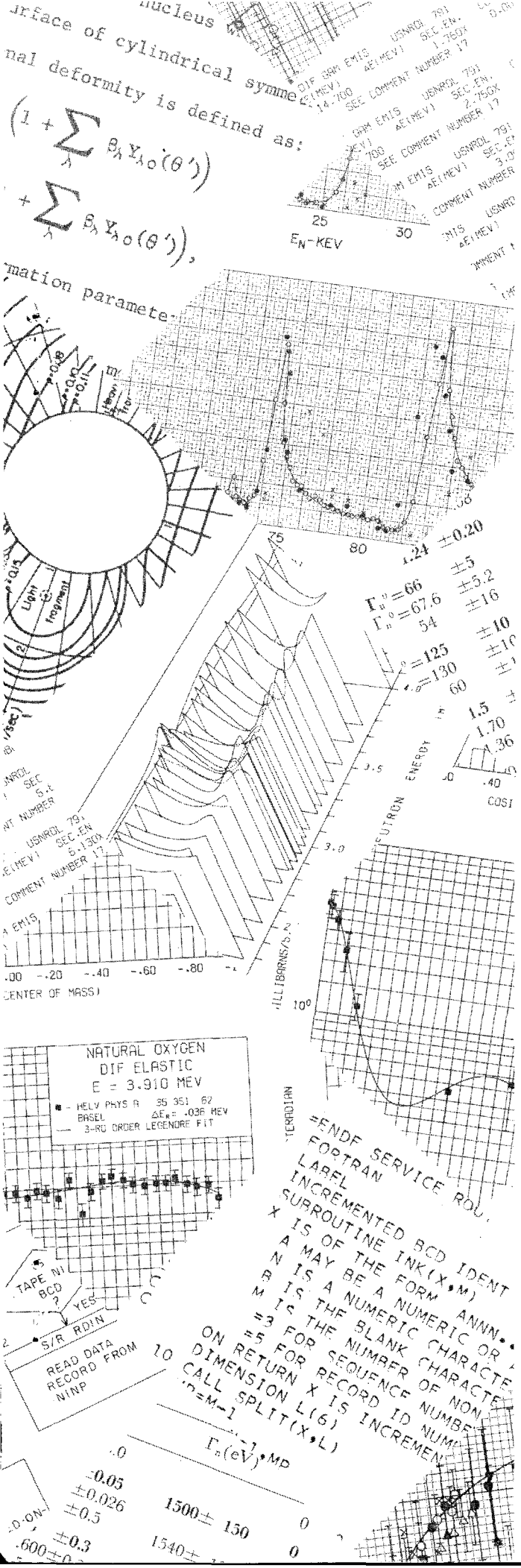

BNL-NCS-20406
ERDA/NDC-2
NEANDC(US)-195/U
INDC(USA)-72/U
Informal Report
Limited Distribution

REPORTS TO THE ERDA NUCLEAR DATA COMMITTEE

Edited by
NATIONAL NEUTRON CROSS SECTION CENTER
for the
U.S. Energy Research and Development Administration
Nuclear Data Committee

May 1975

BROOKHAVEN NATIONAL LABORATORY
ASSOCIATED UNIVERSITIES, INC.
UPTON, NEW YORK 11973

National Neutron Cross Section Center

BNL-NCS-20406
ERDA/NDC-2

REPORTS TO
THE ERDA NUCLEAR DATA COMMITTEE

May 1975

Edited by
NATIONAL NEUTRON CROSS SECTION CENTER
for the
U.S. Energy Research and Development Administration
Nuclear Data Committee

NATIONAL NEUTRON CROSS SECTION CENTER

BROOKHAVEN NATIONAL LABORATORY

ASSOCIATED UNIVERSITIES, INC.

UNDER CONTRACT NO. E(30-1)-16 WITH THE

UNITED STATES ENERGY RESEARCH AND DEVELOPMENT ADMINISTRATION

PREFACE

The reports in this document were submitted to the United States Nuclear Data Committee (USNDC) in May 1975. The reporting laboratories are those having a substantial effort in measuring neutron and nuclear cross sections of relevance to the U.S. applied nuclear energy program. The material contained in these reports is to be regarded as comprised of informal statements of recent developments and preliminary data. Persons wishing to make use of these data should contact the individual experimenter for further details. The data which appear in this document should be quoted only by permission of the contributor and should be referenced as private communication, and not by this document number. Appropriate subjects are listed as follows:

1. Microscopic neutron cross sections relevant to the nuclear energy program, including shielding. Inverse reactions where pertinent are included.

2. Charged particle cross sections, where they are relevant to 1) above, and where relevant to developing and testing nuclear models.

3. Gamma-ray production, radioactive decay, and theoretical developments in nuclear structure which are applicable to nuclear energy programs.

4. Proton and alpha-particle cross sections, at energies of up to 1 GeV, which are of interest to the space program.

These reports cannot be regarded as a complete summary of the nuclear research efforts in the U.S. A number of laboratories, whose research is less programmatically oriented do not submit reports; neither do the submitted reports reflect all the work related to nuclear data in progress at the submitting laboratory.

This compilation has been produced almost completely from master copies prepared by the individual contributors listed in the Table of Contents.

TABLE OF CONTENTS

The CINDA-type index which follows was prepared by Ms. Gail Thompson, National Neutron Cross Section Center, Brookhaven National Laboratory, Upton, New York.

ELEMENT S	A	QUANTITY	TYPE	ENERGY MIN	ENERGY MAX	DOCUMENTATION REF	VOL	PAGE	DATE	LAB	COMMENTS
H	001	ABSORPTION	EXPT-PROG	NDG		ERDA-NDC-2	7	575		ANC	SMITH,EXPT,AT,NBS,TBC.
T	003	TOTAL XSECT	EXPT-PROG	+4	+7	ERDA-NDC-2	74	575		LRL	PHILLIPS+TBC,NDG.
T	003	TOTAL XSECT	EXPT-PROG	50+4	50+7	ERDA-NDC-2	86	575		LAS	SEAGRAVE+WITH,LRL,NDG,TBC.
HE	003	POLARIZATION	EXPT-PROG	NDG		ERDA-NDC-2	175	575		OKE	LISOWSKI+NDG,SCT.OF,POL,NTS.
HE	003	SCATTERING	EXPT-PROG	NDG		ERDA-NDC-2	175	575		OKE	LISOWSKI+NDG,SCT.OF,POL,NTS.
HE	004	DIFF ELASTIC	EXPT-PROG	80+6	16+7	ERDA-NDC-2	174	575		OKE	MACK+RECOIL ANG.DIST.
HE	004	POLARIZATION	EXPT-PROG	NDG		ERDA-NDC-2	175	575		OKE	LISOWSKI+NDG,SCT.OF,POL,NTS.
HE	004	POLARIZATION	EXPT-PROG	20+6	60+6	ERDA-NDC-2	221	575		YAL	FIRK+POL,OF,NTS,IN SCT,BY 4-HE,NDG,
HE	004	SCATTERING	EXPT-PROG	NDG		ERDA-NDC-2	175	575		OKE	LISOWSKI+NDG,SCT.OF,POL,NTS.
HE	004	SCATTERING	EXPT-PROG	20+6	60+6	ERDA-NDC-2	221	575		YAL	FIRK+POL,OF,NTS,IN SCT, BY 4-HE,NDG,
LI		INELST GAMMA	EXPT-PROG	70+5	20+7	ERDA-NDC-2	126	575		ORL	CHAPMAN+NDG,
LI	006	TOTAL XSECT	THEO-PROG	NDG		ERDA-NDC-2	85	575		LAS	HALE,CALC,FROM NT RESULTS SIG=11.1B,
LI	006	TOTAL XSECT	EXPT-PROG	24+3	50+5	ERDA-NDC-2	128	575		ORL	HARVEY+TABLE,ORELA,
LI	006	DIFF ELASTIC	EXPT-PROG	90+6	15+7	ERDA-NDC-2	172	575		OKE	GLASGOW+NDG,TBC.
LI	006	DIFF INELAST	EXPT-PROG	90+6	15+7	ERDA-NDC-2	172	575		OKE	GLASGOW+NDG,TBC.
LI	006	N, TRITON	EXPT-PROG	NDG		ERDA-NDC-2	85	575		LAS	HALE,PCS VALUE=3.4 B.
LI	006	N, TRITON	EXPT-PROG	96+5		ERDA-NDC-2	105	575		MHO	STEPHANY+SIG=356 MB+- 12.PERCENT.
LI	006	N, TRITON	EXPT-PROG	25+4		ERDA-NDC-2	115	575		NBS	SCHRODER+ANG,ANISOT,NDG.
BE	009	DIFF ELASTIC	EXPT-PROG	60+6		ERDA-NDC-2	89	575		LAS	AUCHAMPAUGH+TABLE.
BE	009	DIFF ELASTIC	EXPT-PROG	10+7		ERDA-NDC-2	89	575		LAS	AUCHAMPAUGH+TABLE.
BE	009	DIFF ELASTIC	EXPT-PROG	14+7		ERDA-NDC-2	89	575		LAS	AUCHAMPAUGH+TABLE.
BE	009	DIFF ELASTIC	EXPT-PROG	90+6	15+7	ERDA-NDC-2	172	575		OKE	GLASGOW+NDG,TBC.
BE	009	DIFF ELASTIC	EXPT-PROG	76+6		ERDA-NDC-2	212	575		BRL	BUCHER+EN=7,55MEV,SMALL ANG.EL.SCT,
BE	009	DIFF ELASTIC	EXPT-PROG	11+7		ERDA-NDC-2	212	575		BRL	BUCHER+SMALL ANG. EL.SCT,NDG.
BE	009	DIFF ELASTIC	EXPT-PROG	14+7		ERDA-NDC-2	212	575		BRL	BUCHER+SMALL ANG. EL.SCT,NDG.
BE	009	POLARIZATION	EXPT-PROG	NDG		ERDA-NDC-2	221	575		YAL	FIRK+POL,OF,NTS,IN SCT,BY 9-BE,TBL,
BE	009	DIFF INELAST	EXPT-PROG	90+6	15+7	ERDA-NDC-2	172	575		OKE	GLASGOW+NDG,TBC.
BE	009	SCATTERING	EXPT-PROG	NDG		ERDA-NDC-2	221	575		YAL	FIRK+POL,OF,NTS,IN SCT,BY 9-BE,TBL,
BE	009	NONELASTIC	EXPT-PROG	60+6		ERDA-NDC-2	89	575		LAS	AUCHAMPAUGH+TABLE.
BE	009	NONELASTIC	EXPT-PROG	10+7		ERDA-NDC-2	89	575		LAS	AUCHAMPAUGH+TABLE.
BE	009	NONELASTIC	EXPT-PROG	14+7		ERDA-NDC-2	89	575		LAS	AUCHAMPAUGH+TABLE.
BE	009	N, TRITON	EXPT-PROG	13+7	15+7	ERDA-NDC-2	77	575		LRL	DIETRICH+GRPH.
B	010	N,ALPHA REAC	EXPT-PROG	30+5	10+6	ERDA-NDC-2	108	575		NBS	SCHRACK+TOF,NDG,TBC,
C	012	TOTAL XSECT	EXPT-PROG	10+5	50+6	ERDA-NDC-2	18	575		ANL	HOLT+R-MATR,ANAL.
C	012	DIFF ELASTIC	EXPT-PROG	18+6	40+6	ERDA-NDC-2	18	575		ANL	HOLT+GRPH.

ELEMENT S	A	QUANTITY	TYPE	ENERGY MIN	ENERGY MAX	DOCUMENTATION REF	VOL	PAGE	DATE	LAB	COMMENTS
C	012	DIFF ELASTIC	EXPT-PROG	90+6	15+7	ERDA-NDC-2	172	575		OKE	GLASGOW+NDG,NAT,CARB,
C	012	DIFF ELASTIC	EXPT-PROG	76+6		ERDA-NDC-2	212	575		BRL	BUCHER+ENE7,55MEV,SMALL ANG.EL.SCT,
C	012	DIFF ELASTIC	EXPT-PROG	11+7		ERDA-NDC-2	212	575		BRL	BUCHER+SMALL ANG. EL.SCT,NDG,
C	012	DIFF ELASTIC	EXPT-PROG	14+7		ERDA-NDC-2	212	575		BRL	BUCHER+SMALL ANG. EL.SCT,NDG,
C	012	DIFF INELAST	EXPT-PROG	90+6	15+7	ERDA-NDC-2	172	575		OKE	GLASGOW+NDG,NAT,CARB,
C	012	INELST GAMMA	EXPT-PROG	70+5	20+7	ERDA-NDC-2	126	575		ORL	CHAPMAN+NDG,
N	014	DIFF ELASTIC	EXPT-PROG	77+6	14+7	ERDA-NDC-2	213	575		BRL	HOLLANDSWORTH+ SES,7.65-14.0MEV,NDG,
N	014	INELST GAMMA	EXPT-PROG	70+5	20+7	ERDA-NDC-2	126	575		ORL	CHAPMAN+NDG,
O	016	DIFF ELASTIC	EXPT-PROG	10+7	14+7	ERDA-NDC-2	213	575		BRL	HOLLANDSWORTH+ 4ES,10.25-14.1 MEV,
O	016	INELST GAMMA	EXPT-PROG	70+5	20+7	ERDA-NDC-2	126	575		ORL	CHAPMAN+NDG,
O	018	GAMMA,N	EXPT-PROG	NDG		ERDA-NDC-2	75	575		LRL	BERMAN+NDG,
F	019	TOTAL XSECT	EXPT-PROG		20+5	ERDA-NDC-2	55	575		COL	HACKEN+RES,PARAMS,STF,AVG,LVL,SPACE,
F	019	TOTAL XSECT	EXPT-PROG	50+0	20+7	ERDA-NDC-2	125	575		ORL	JOHNSON+NDG,
F	019	INELST GAMMA	EXPT-PROG	10+5	20+7	ERDA-NDC-2	125	575		ORL	DICKENS+NDG,
F	019	INELST GAMMA	EXPT-PROG	70+5	20+7	ERDA-NDC-2	126	575		ORL	CHAPMAN+NDG,
F	019	RESON PARAMS	EXPT-PROG	NDG		ERDA-NDC-2	55	575		COL	HACKEN+
F	019	STRNGTH FUNC	EXPT-PROG	NDG		ERDA-NDC-2	55	575		COL	HACKEN+
NA	023	TOTAL XSECT	EXPT-PROG	30+5	31+6	ERDA-NDC-2	164	575		RPI	BROWN+NA CS AT MINIMA,TBL,GRPH,
NA	023	N, GAMMA	EXPT-PROG	THR		ERDA-NDC-2	26	575		ANL	WILSON+GRPH,COMP G SPC,TO 2.8KEV SPC
NA	023	N, GAMMA	EXPT-PROG	28+3		ERDA-NDC-2	26	575		ANL	WILSON+GRPH,COMP G SPC,TO THR. SPC,
NA	023	INELST GAMMA	EXPT-PROG		20+6	ERDA-NDC-2	16	575		ANL	SMITH,
MG		TOTAL XSECT	EXPT-PROG		50+5	ERDA-NDC-2	55	575		COL	HACKEN+RES,PARAMS,STF,AVG,LVL,SPACE,
MG		DIFF ELASTIC	EXPT-PROG	11+7		ERDA-NDC-2	156	575		OHO	FERRER+NDG,TOF,
MG		SPECT N,GAMM	EXPT-PROG	14+7		ERDA-NDC-2	90	575		LAS	DRAKE+TABLE
MG		INELST GAMMA	EXPT-PROG	70+5	20+7	ERDA-NDC-2	126	575		ORL	CHAPMAN+NDG,
MG		RESON PARAMS	EXPT-PROG	NDG		ERDA-NDC-2	55	575		COL	HACKEN+
MG		STRNGTH FUNC	EXPT-PROG	NDG		ERDA-NDC-2	55	575		COL	HACKEN+
AL	027	DIFF ELASTIC	EXPT-PROG	11+7		ERDA-NDC-2	156	575		OHO	FERRER+NDG,TOF,
AL	027	DIFF ELASTIC	EXPT-PROG	26+7		ERDA-NDC-2	156	575		OHO	CARLSON+NDG,
AL	027	DIFF ELASTIC	EXPT-PROG	76+6		ERDA-NDC-2	212	575		BRL	BUCHER+ENE7,55MEV,SMALL ANG.EL.SCT,
AL	027	DIFF ELASTIC	EXPT-PROG	11+7		ERDA-NDC-2	212	575		BRL	BUCHER+SMALL ANG. EL.SCT,NDG,
AL	027	DIFF ELASTIC	EXPT-PROG	14+7		ERDA-NDC-2	212	575		BRL	BUCHER+SMALL ANG. EL.SCT,NDG,
AL	027	SPECT N,GAMM	EXPT-PROG	14+7		ERDA-NDC-2	90	575		LAS	DRAKE+TABLE
AL	027	INELST GAMMA	EXPT-PROG	70+5	20+7	ERDA-NDC-2	126	575		ORL	CHAPMAN+NDG,
AL	027	N, PROTON	EXPT-PROG	TR	10+7	ERDA-NDC-2	16	575		ANL	MEADOWS+NDG,

ELEMENTS	A	QUANTITY	TYPE	ENERGY MIN	ENERGY MAX	DOCUMENTATION REF	VOL	PAGE	DATE	LAB	COMMENTS
AL	027	N,ALPHA REAC	EXPT-PROG	21+7	26+7	ERDA-NDC-2	92	575		LAS	BAYHURST+NDG,
SI		TOTAL XSECT	EXPT-PROG	50+0	70+5	ERDA-NDC-2	125	575		ORL	JOHNSON+NDG,
SI		INELST GAMMA	EXPT-PROG	70+5	20+7	ERDA-NDC-2	126	575		ORL	CHAPMAN+NDG,
SI	028	TOTAL XSECT	EXPT-PROG	NDG		ERDA-NDC-2	173	575		OKE	CLEMENT+NDG,
SI	028	SCATTERING	THEO-PROG		40+6	ERDA-NDC-2	177	575		OKE	DIVADEENAM+SHELL MDL,CALC,DOORWAY ST
SI	028	RESON PARAMS	THEO-PROG	NDG		ERDA-NDC-2	178	575		OKE	MARIPUU+CALC,RES,WIDS,WITH SHELL MDL
S		DIFF ELASTIC	EXPT-PROG	11+7		ERDA-NDC-2	156	575		OHO	FERRER+NDG,TOF,
S		DIFF ELASTIC	EXPT-PROG	11+7		ERDA-NDC-2	156	575		OHO	BAINUM+NDG,
S		DIFF ELASTIC	EXPT-PROG	26+7		ERDA-NDC-2	156	575		OHO	BAINUM+NDG,
S	032	TOTAL XSECT	EXPT-PROG	NDG		ERDA-NDC-2	173	575		OKE	CLEMENT+NDG,
S	032	DIFF ELASTIC	EXPT-PROG	11+7		ERDA-NDC-2	157	575		OHO	FERRER+NDG,
S	032	RESON PARAMS	THEO-PROG	NDG		ERDA-NDC-2	178	575		OKE	MARIPUU+CALC,RES,WIDS,WITH SHELL MDL
S	033	TOTAL XSECT	EXPT-PROG	NDG		ERDA-NDC-2	173	575		OKE	CLEMENT+NDG,
S	033	N, GAMMA	EXPT-PROG	25+3	85+5	ERDA-NDC-2	130	575		ORL	HALPERIN+ORELA,TOF,NDG,
S	033	RES INT CAPT	EXPT-PROG	50-1	55+5	ERDA-NDC-2	130	575		ORL	HALPERIN+RIG=33,4+-5,0MB,FRM,DIF,DAT
S	033	RESON PARAMS	EXPT-PROG		55+5	ERDA-NDC-2	130	575		ORL	HALPERIN+39 RESONANCES,NDG,
S	033	LVL DENSITY	EXPT-PROG	13+4	24+5	ERDA-NDC-2	130	575		ORL	HALPERIN+D=9,1+-0,9 KEV,
S	034	TOTAL XSECT	EXPT-PROG	NDG		ERDA-NDC-2	173	575		OKE	CLEMENT+NDG,
CL		TOTAL XSECT	EXPT-PROG		40+5	ERDA-NDC-2	55	575		COL	HACKEN+RES,PARAMS,STF,AVG,LVL,SPACE,
CL	035	RESON PARAMS	EXPT-PROG	NDG		ERDA-NDC-2	55	575		COL	HACKEN+
CL	035	STRNGTH FUNC	EXPT-PROG	NDG		ERDA-NDC-2	55	575		COL	HACKEN+
CL	037	RESON PARAMS	EXPT-PROG	NDG		ERDA-NDC-2	55	575		COL	HACKEN+
CL	037	STRNGTH FUNC	EXPT-PROG	NDG		ERDA-NDC-2	55	575		COL	HACKEN+
AR		TOTAL XSECT	EXPT-PROG		58+5	ERDA-NDC-2	55	575		COL	HACKEN+RES,PARAMS,STF,AVG,LVL,SPACE,
AR	040	TOTAL XSECT	EXPT-PROG	NDG		ERDA-NDC-2	173	575		OKE	CLEMENT+NDG,
AR	040	RESON PARAMS	EXPT-PROG	NDG		ERDA-NDC-2	55	575		COL	HACKEN+
AR	040	STRNGTH FUNC	EXPT-PROG	NDG		ERDA-NDC-2	55	575		COL	HACKEN+
AR	040	LVL DENSITY	EXPT-PROG	NDG		ERDA-NDC-2	55	575		COL	HACKEN+ D0=87+13-11EV,D1=24+5-4EV,
CA		TOTAL XSECT	EXPT-PROG		55+5	ERDA-NDC-2	55	575		COL	HACKEN+RES,PARAMS,STF,AVG,LVL,SPACE,
CA		DIFF ELASTIC	EXPT-PROG	11+7		ERDA-NDC-2	156	575		OHO	FERRER+NDG,TOF,
CA		SCATTERING	THEO-PROG	NDG		ERDA-NDC-2	177	575		OKE	DIVADEENAM,SHELL MDL +VIBR,DOORWAY
CA		INELST GAMMA	EXPT-PROG	70+5	20+7	ERDA-NDC-2	126	575		ORL	CHAPMAN+NDG,
CA	040	DIFF ELASTIC	EXPT-PROG	11+7		ERDA-NDC-2	157	575		OHO	FERRER+NDG,
CA	040	N, GAMMA	EXPT-PROG	NDG		ERDA-NDC-2	132	575		ORL	MUSGROVE+RES,PARAMS,NDG,
CA	040	RESON PARAMS	EXPT-PROG	NDG		ERDA-NDC-2	55	575		COL	HACKEN+

ELEMENT S	A	QUANTITY	TYPE	ENERGY MIN	ENERGY MAX	DOCUMENTATION REF	VOL	PAGE	DATE	LAB	COMMENTS
CA	040	RESON PARAMS	EXPT-PROG		36+5	ERDA-NDC-2	132	575	ORL	MUSGROVE+AVG S,P,D NG/WID,AVG,EL/WID	
CA	040	STRNGTH FUNC	EXPT-PROG	NDG		ERDA-NDC-2	55	575	COL	HACKEN+	
CA	040	STRNGTH FUNC	EXPT-PROG		36+5	ERDA-NDC-2	132	575	ORL	MUSGROVE+S0,S1,S2 GIVEN.	
CA	040	LVL DENSITY	EXPT-PROG		36+5	ERDA-NDC-2	132	575	ORL	MUSGROVE+D=37+-3 KEV.	
SC	045	N2N REACTION	EXPT-PROG	15+7	24+7	ERDA-NDC-2	92	575	LAS	VEESER,LIQ,SCIN,TANK,DOSIM,APPL.	
SC	045	N2N REACTION	EXPT-PROG	75+6	28+7	ERDA-NDC-2	92	575	LAS	BAYHURST+NDG.	
SC	045	N3N REACTION	EXPT-PROG	15+7	24+7	ERDA-NDC-2	92	575	LAS	VEESER,LIQ,SCIN,TANK,DOSIM,APPL.	
TI	046	N, PROTON	EXPT-PROG	TR	10+7	ERDA-NDC-2	16	575	ANL	MEADOWS+NDG.	
TI	047	N, PROTON	EXPT-PROG	TR	10+7	ERDA-NDC-2	16	575	ANL	MEADOWS+NDG.	
TI	048	N, PROTON	EXPT-PROG	TR	10+7	ERDA-NDC-2	16	575	ANL	MEADOWS+NDG.	
V	051	DIFF ELASTIC	EXPT-PROG		11+7	ERDA-NDC-2	156	575	OHO	FERRER+NDG,TOF.	
V	051	INELST GAMMA	EXPT-PROG		20+6	ERDA-NDC-2	16	575	ANL	SMITH.	
CR		SPECT N,GAMM	EXPT-PROG	14+7		ERDA-NDC-2	90	575	LAS	DRAKE+TABLE	
MN	055	DIFF ELASTIC	EXPT-PROG		11+7	ERDA-NDC-2	156	575	OHO	FERRER+NDG,TOF.	
MN	055	ABSORPTION	EXPT-PROG	NDG		ERDA-NDC-2	7	575	ANC	SMITH,EXPT,AT,NBS,TBC.	
FE		DIFF ELASTIC	EXPT-PROG		11+7	ERDA-NDC-2	156	575	OHO	FERRER+NDG,TOF.	
FE		DIFF ELASTIC	EXPT-PROG		26+7	ERDA-NDC-2	156	575	OHO	CARLSON+NDG.	
FE		DIFF ELASTIC	EXPT-PROG		76+6	ERDA-NDC-2	212	575	BRL	BUCHER+EN=7,55MEV,SMALL ANG.EL.SCT.	
FE		DIFF ELASTIC	EXPT-PROG		11+7	ERDA-NDC-2	212	575	BRL	BUCHER+SMALL ANG. EL.SCT,NDG.	
FE		DIFF ELASTIC	EXPT-PROG		14+7	ERDA-NDC-2	212	575	BRL	BUCHER+SMALL ANG. EL.SCT,NDG.	
FE		SPECT N,GAMM	EXPT-PROG		14+7	ERDA-NDC-2	90	575	LAS	DRAKE+TABLE	
FE		INELST GAMMA	EXPT-PROG		20+6	ERDA-NDC-2	16	575	ANL	SMITH.	
FE		INELST GAMMA	EXPT-PROG	70+5	20+7	ERDA-NDC-2	126	575	ORL	CHAPMAN+NDG.	
FE	054	TOTAL XSECT	EXPT-PROG		60+5	ERDA-NDC-2	129	575	ORL	PANDEY+NDG,R-MAT.ANALYS.	
FE	054	N, PROTON	EXPT-PROG	TR	10+7	ERDA-NDC-2	16	575	ANL	MEADOWS+NDG.	
FE	054	LVL DENSITY	EXPT-PROG		60+5	ERDA-NDC-2	129	575	ORL	PANDEY+FOR 1/2+ STATES D=25 KEV.	
FE	056	TOTAL XSECT	EXPT-PROG	20+4	10+6	ERDA-NDC-2	129	575	ORL	PANDEY+NDG,R-MAT.ANALYS.	
FE	056	N, PROTON	EXPT-PROG	TR	10+7	ERDA-NDC-2	16	575	ANL	MEADOWS+NDG.	
FE	056	LVL DENSITY	EXPT-PROG		50+5	ERDA-NDC-2	129	575	ORL	PANDEY+FOR 1/2+ STATES D=27 KEV.	
FE	057	LVL DENSITY	EXPT-PROG		50+4	ERDA-NDC-2	129	575	ORL	PANDEY+FOR 0- AND 1- STATES D= 5 KEV	
FE	058	LVL DENSITY	EXPT-PROG	NDG		ERDA-NDC-2	129	575	ORL	PANDEY+NDG.	
CO	059	DIFF ELASTIC	EXPT-PROG		11+7	ERDA-NDC-2	156	575	OHO	FERRER+NDG,TOF.	
CO	059	N, GAMMA	EXPT-PROG	35+5	75+5	ERDA-NDC-2	15	575	ANL	POENITZ,NDG.	
CO	059	N2N REACTION	EXPT-PROG	15+7	24+7	ERDA-NDC-2	92	575	LAS	VEESER,LIQ,SCIN,TANK,DOSIM,APPL.	
CO	059	N3N REACTION	EXPT-PROG	15+7	24+7	ERDA-NDC-2	92	575	LAS	VEESER,LIQ,SCIN,TANK,DOSIM,APPL.	

ELEMENT S	A	QUANTITY	TYPE	ENERGY MIN	ENERGY MAX	DOCUMENTATION REF	VOL	PAGE	DATE	LAB	COMMENTS
CO	059	N, PROTON	EXPT-PROG	TR	10+7	ERDA-NDC-2	16	575		ANL	MEADOWS+NDG,
CO	059	N,ALPHA REAC	EXPT-PROG		10+7	ERDA-NDC-2	16	575		ANL	MEADOWS+NDG,
NI		DIFF ELASTIC	EXPT-PROG	11+7		ERDA-NDC-2	156	575		OHO	FERRER+NDG,TOF,
NI		DIFF ELASTIC	EXPT-PROG	76+6		ERDA-NDC-2	212	575		BRL	BUCHER+EN=7,55MEV,SMALL ANG.EL.SCT,
NI		DIFF ELASTIC	EXPT-PROG	11+7		ERDA-NDC-2	212	575		BRL	BUCHER+SMALL ANG. EL,SCT,NDG,
NI		DIFF ELASTIC	EXPT-PROG	14+7		ERDA-NDC-2	212	575		BRL	BUCHER+SMALL ANG. EL,SCT,NDG,
NI		N, GAMMA	EXPT-PROG	35+5	75+5	ERDA-NDC-2	15	575		ANL	POENITZ,NDG,
NI		SPECT N,GAMM	EXPT-PROG	14+7		ERDA-NDC-2	90	575		LAS	DRAKE+TABLE
NI		INELST GAMMA	EXPT-PROG		20+6	ERDA-NDC-2	16	575		ANL	SMITH,
NI		INELST GAMMA	EXPT-PROG	70+5	20+7	ERDA-NDC-2	126	575		ORL	CHAPMAN+NDG,
NI	058	N, PROTON	EXPT-PROG	TR	10+7	ERDA-NDC-2	16	575		ANL	MEADOWS+NDG,
NI	059	ABSORPTION	EXPT-PROG	20-2	30+1	ERDA-NDC-2	127	575		ORL	RAMAN+RES,PARAMS,2200M/S SIG=66+-5 B
NI	059	N, GAMMA	EXPT-PROG	NDG		ERDA-NDC-2	28	575		ANL	WILSON+G-RAY SPC.GRPH,
NI	059	N, GAMMA	EXPT-PROG	THR		ERDA-NDC-2	87	575		LAS	JURNEY,SIG=53+-4 BARNS,GRPH,
NI	059	N, GAMMA	EXPT-PROG	+6	12+7	ERDA-NDC-2	87	575		LAS	JURNEY,GRPH,
NI	059	N, GAMMA	EXPT-PROG	THR		ERDA-NDC-2	127	575		ORL	RAMAN+RES,PARAMS,SIG=51+-8 BARNS,
NI	059	N2N REACTION	EXPT-PROG	75+6	28+7	ERDA-NDC-2	92	575		LAS	BAYHURST+NDG,
NI	059	RESON PARAMS	EXPT-PROG	20+2	91+3	ERDA-NDC-2	127	575		ORL	RAMAN+TOT,AND,ELAS,WIDS GIVEN,
NI	060	TOTAL XSECT	EXPT-PROG	NDG		ERDA-NDC-2	173	575		OKE	CLEMENT+NDG,
NI	063	N, GAMMA	EXPT-PROG	NDG		ERDA-NDC-2	28	575		ANL	WILSON+G-RAY SPC.GRPH,
CU		DIFF ELASTIC	EXPT-PROG	76+6		ERDA-NDC-2	212	575		BRL	BUCHER+EN=7,55MEV,SMALL ANG.EL.SCT,
CU		DIFF ELASTIC	EXPT-PROG	11+7		ERDA-NDC-2	212	575		BRL	BUCHER+SMALL ANG. EL,SCT,NDG,
CU		DIFF ELASTIC	EXPT-PROG	14+7		ERDA-NDC-2	212	575		BRL	BUCHER+SMALL ANG. EL,SCT,NDG,
CU		N, GAMMA	EXPT-PROG	35+5	75+5	ERDA-NDC-2	15	575		ANL	POENITZ,NDG,
CU		SPECT N,GAMM	EXPT-PROG	14+7		ERDA-NDC-2	90	575		LAS	DRAKE+TABLE
CU		INELST GAMMA	EXPT-PROG	70+5	20+7	ERDA-NDC-2	126	575		ORL	CHAPMAN+NDG,
CU	065	N, PROTON	EXPT-PROG		10+7	ERDA-NDC-2	16	575		ANL	MEADOWS+NDG,
ZN		N, GAMMA	EXPT-PROG	35+5	75+5	ERDA-NDC-2	15	575		ANL	POENITZ,NDG,
ZN		INELST GAMMA	EXPT-PROG	70+5	20+7	ERDA-NDC-2	126	575		ORL	CHAPMAN+NDG,
ZN	064	N, PROTON	EXPT-PROG	TR	10+7	ERDA-NDC-2	16	575		ANL	MEADOWS+NDG,
ZN	066	N, PROTON	EXPT-PROG		10+7	ERDA-NDC-2	16	575		ANL	MEADOWS+NDG,
ZN	068	INELST GAMMA	EXPT-PROG	54+6		ERDA-NDC-2	126	575		ORL	DICKENS,LVL,STRUCT,ZN-68,
SR		TOTAL XSECT	EXPT-PROG	NDG		ERDA-NDC-2	173	575		OKE	CLEMENT+NDG,
Y	089	TOTAL XSECT	EXPT-PROG	20+4	25+5	ERDA-NDC-2	74	575		LRL	CAMARDA,TRANSM,MEASMT,NDG,
Y	089	ELASTIC SCAT	EXPT-PROG	27+6		ERDA-NDC-2	60	575		KTY	MC+DANIEL+NDG

ELEMENT S	A	QUANTITY	TYPE	ENERGY MIN	ENERGY MAX	DOCUMENTATION REF	VOL	PAGE	DATE	LAB	COMMENTS
Y	089	TOT INELASTI	EXPT-PROG	27+6		ERDA-NDC-2	60	575	KTY		MC+DANIEL+NDG
Y	089	SCATTERING	THEO-PROG	NDG		ERDA-NDC-2	177	575	DKE		DIVADEENAM,THEOR,CALC,SHELL MDL,
Y	089	N2N REACTION	EXPT-PROG	15+7	24+7	ERDA-NDC-2	92	575	LAS		VEESER,LIQ,SCIN,TANK,DOSIM,APPL,
Y	089	N2N REACTION	EXPT-PROG	75+6	28+7	ERDA-NDC-2	92	575	LAS		BAYHURST+NDG,
Y	089	N3N REACTION	EXPT-PROG	15+7	24+7	ERDA-NDC-2	92	575	LAS		VEESER,LIQ,SCIN,TANK,DOSIM,APPL,
Y	089	N3N REACTION	EXPT-PROG	75+6	28+7	ERDA-NDC-2	92	575	LAS		BAYHURST+NDG,
ZR	090	ELASTIC SCAT	EXPT-PROG	27+6		ERDA-NDC-2	60	575	KTY		MC+DANIEL+NDG
ZR	090	TOT INELASTI	EXPT-PROG	27+6		ERDA-NDC-2	60	575	KTY		MC+DANIEL+NDG
ZR	090	N, GAMMA	EXPT-PROG	30+3	20+5	ERDA-NDC-2	133	575	ORL		BOLDEMAN+VALENCE COMPON,NDG,
ZR	090	N2N REACTION	EXPT-PROG	75+6	28+7	ERDA-NDC-2	92	575	LAS		BAYHURST+NDG,
ZR	090	N3N REACTION	EXPT-PROG	75+6	28+7	ERDA-NDC-2	92	575	LAS		BAYHURST+NDG,
ZR	090	STRNGTH FUNC	EXPT-PROG	NDG		ERDA-NDC-2	133	575	ORL		BOLDEMAN+S,P STF GIVEN
ZR	092	ELASTIC SCAT	EXPT-PROG	27+6		ERDA-NDC-2	60	575	KTY		MC+DANIEL+NDG
ZR	092	TOT INELASTI	EXPT-PROG	27+6		ERDA-NDC-2	60	575	KTY		MC+DANIEL+NDG
ZR	092	INELST GAMMA	EXPT-PROG	22+6	37+6	ERDA-NDC-2	62	575	KTY		GLASGOW+LVL STRUCTURE
ZR	094	INELST GAMMA	EXPT-PROG	22+6	37+6	ERDA-NDC-2	62	575	KTY		GLASGOW+LVL STRUCTURE
NB	093	DIFF ELASTIC	EXPT-PROG	11+7		ERDA-NDC-2	156	575	OHO		FERRER+NDG,TOF,
NB	093	DIFF ELASTIC	EXPT-PROG	26+7		ERDA-NDC-2	156	575	OHO		CARLSON+NDG,
NB	093	DIFF ELASTIC	EXPT-PROG	14+7		ERDA-NDC-2	213	575	BRL		HOLLANDSWORTH+TBC,NDG,SMALL ANG,SCT,
NB	093	N, GAMMA	EXPT-PROG	24+4		ERDA-NDC-2	44	575	BNL		RIMAWI+P-WAVE CAPT,G-RAY SPC,GRPH,
NB	093	N, GAMMA	EXPT-PROG	26+3	70+5	ERDA-NDC-2	131	575	ORL		MACKLIN,TOF,ORELA,NDG,
NB	093	SPECT N,GAMM	EXPT-PROG	14+7		ERDA-NDC-2	90	575	LAS		DRAKE+TABLE
NB	093	INELST GAMMA	EXPT-PROG	70+5	20+7	ERDA-NDC-2	126	575	ORL		CHAPMAN+NDG,
NB	093	N2N REACTION	EXPT-PROG	14+7	15+7	ERDA-NDC-2	71	575	LRL		NETHAWAY,TO NB-92META,STATE,TBC,TBL,
NB	093	N2N REACTION	EXPT-PROG	15+7	24+7	ERDA-NDC-2	92	575	LAS		VEESER,LIQ,SCIN,TANK,DOSIM,APPL,
NB	093	N2N REACTION	EXPT-PROG	TR	20+7	ERDA-NDC-2	101	575	LAS		YOUNG+NDG,
NB	093	N3N REACTION	EXPT-PROG	15+7	24+7	ERDA-NDC-2	92	575	LAS		VEESER,LIQ,SCIN,TANK,DOSIM,APPL,
NB	093	RESON PARAMS	EXPT-PROG		74+3	ERDA-NDC-2	131	575	ORL		MACKLIN,NDG,
NB	093	STRNGTH FUNC	EXPT-PROG		10+5	ERDA-NDC-2	131	575	ORL		MACKLIN,NDG,
MO		SPECT N,GAMM	EXPT-PROG	14+7		ERDA-NDC-2	90	575	LAS		DRAKE+TABLE
MO	092	ELASTIC SCAT	EXPT-PROG	25+6		ERDA-NDC-2	60	575	KTY		MC+DANIEL+NDG
MO	092	DIFF ELASTIC	EXPT-PROG	11+7		ERDA-NDC-2	156	575	OHO		FERRER+NDG,TOF,
MO	092	DIFF ELASTIC	EXPT-PROG	26+7		ERDA-NDC-2	156	575	OHO		CARLSON+NDG,
MO	092	TOT INELASTI	EXPT-PROG	25+6		ERDA-NDC-2	60	575	KTY		MC+DANIEL+NDG
MO	094	ELASTIC SCAT	EXPT-PROG	25+6		ERDA-NDC-2	60	575	KTY		MC+DANIEL+NDG

ELEMENT S	A	QUANTITY	TYPE	ENERGY MIN	ENERGY MAX	DOCUMENTATION REF	VOL	PAGE	DATE	LAB	COMMENTS
MO	094	TOT INELASTI	EXPT-PROG	25+6		ERDA-NDC-2	60	575	KTY		MC+DANIEL+NDG
MO	096	ELASTIC SCAT	EXPT-PROG	25+6		ERDA-NDC-2	60	575	KTY		MC+DANIEL+NDG
MO	096	ELASTIC SCAT	EXPT-PROG	11+7		ERDA-NDC-2	157	575	OHO		CARLSON+NDG,
MO	096	DIFF ELASTIC	EXPT-PROG	11+7		ERDA-NDC-2	156	575	OHO		FERRER+NDG,TOF,
MO	096	DIFF ELASTIC	EXPT-PROG	26+7		ERDA-NDC-2	156	575	OHO		CARLSON+NDG,
MO	096	TOT INELASTI	EXPT-PROG	25+6		ERDA-NDC-2	60	575	KTY		MC+DANIEL+NDG
MO	098	ELASTIC SCAT	EXPT-PROG	27+6		ERDA-NDC-2	60	575	KTY		MC+DANIEL+NDG
MO	098	DIFF ELASTIC	EXPT-PROG	11+7		ERDA-NDC-2	156	575	OHO		FERRER+NDG,TOF,
MO	098	DIFF ELASTIC	EXPT-PROG	26+7		ERDA-NDC-2	156	575	OHO		CARLSON+NDG,
MO	098	TOT INELASTI	EXPT-PROG	27+6		ERDA-NDC-2	60	575	KTY		MC+DANIEL+NDG
MO	100	ELASTIC SCAT	EXPT-PROG	27+6		ERDA-NDC-2	60	575	KTY		MC+DANIEL+NDG
MO	100	DIFF ELASTIC	EXPT-PROG	11+7		ERDA-NDC-2	156	575	OHO		FERRER+NDG,TOF,
MO	100	DIFF ELASTIC	EXPT-PROG	26+7		ERDA-NDC-2	156	575	OHO		CARLSON+NDG,
MO	100	TOT INELASTI	EXPT-PROG	27+6		ERDA-NDC-2	60	575	KTY		MC+DANIEL+NDG
RU	101	N, GAMMA	EXPT-PROG	20+1	15+5	ERDA-NDC-2	162	575	RPI		HOCKENBURY+RPI,LINAC
RU	101	LVL DENSITY	EXPT-PROG	NDG		ERDA-NDC-2	162	575	RPI		HOCKENBURY+D=17.9+-1.9 EV
RU	102	N, GAMMA	EXPT-PROG	20+1	15+5	ERDA-NDC-2	162	575	RPI		HOCKENBURY+RPI,LINAC
RU	102	LVL DENSITY	EXPT-PROG	NDG		ERDA-NDC-2	162	575	RPI		HOCKENBURY+D=109.8+-15.7 EV
RU	104	N, GAMMA	EXPT-PROG	20+1	15+5	ERDA-NDC-2	162	575	RPI		HOCKENBURY+RPI,LINAC
RU	104	LVL DENSITY	EXPT-PROG	NDG		ERDA-NDC-2	162	575	RPI		HOCKENBURY+D=125.1+-19.1 EV
RH	103	N, GAMMA	EXPT-PROG	20+1	90+1	ERDA-NDC-2	162	575	RPI		HOCKENBURY+DERIVED AVG,RES,PAR,NDG,
RH	103	N2N REACTION	EXPT-PROG	15+7	24+7	ERDA-NDC-2	92	575	LAS		VEESER,LIQ,SCIN,TANK,DOSIM,APPL,
RH	103	N3N REACTION	EXPT-PROG	15+7	24+7	ERDA-NDC-2	92	575	LAS		VEESER,LIQ,SCIN,TANK,DOSIM,APPL,
RH	103	RESON PARAMS	EXPT-PROG	NDG		ERDA-NDC-2	162	575	RPI		HOCKENBURY+AVG,NG/WID,NDG,
RH	103	STRNGTH FUNC	EXPT-PROG	NDG		ERDA-NDC-2	162	575	RPI		HOCKENBURY+S,P STF,NDG,
PD	105	N, GAMMA	EXPT-PROG	26+3		ERDA-NDC-2	126	575	ORL		MACKLIN,SIG=12.9BARNS AT 2.665 KEV,
PD	105	N, GAMMA	EXPT-PROG	20+1	90+1	ERDA-NDC-2	162	575	RPI		HOCKENBURY+DERIVED AVG,RES,PAR,NDG,
PD	105	RESON PARAMS	EXPT-PROG	NDG		ERDA-NDC-2	162	575	RPI		HOCKENBURY+AVG,NG/WID,NDG,
PD	105	STRNGTH FUNC	EXPT-PROG	NDG		ERDA-NDC-2	162	575	RPI		HOCKENBURY+S,P STF,NDG,
AG		INELST GAMMA	EXPT-PROG	70+3	20+7	ERDA-NDC-2	126	575	ORL		CHAPMAN+NDG,
AG	107	N2N REACTION	EXPT-PROG	75+6	28+7	ERDA-NDC-2	92	575	LAS		BAYHURST+NDG,
AG	107	N3N REACTION	EXPT-PROG	75+6	28+7	ERDA-NDC-2	92	575	LAS		BAYHURST+NDG,
CD	110	TOTAL XSECT	EXPT-PROG	NDG		ERDA-NDC-2	55	575	BOL		HACKEN+RES,PARAMS,STF,AVG,LVL,SPACE,
CD	110	N, GAMMA	EXPT-PROG	NDG		ERDA-NDC-2	55	575	BOL		HACKEN+ NG/WID CALC,
CD	110	RESON PARAMS	EXPT-PROG	NDG		ERDA-NDC-2	55	575	BOL		HACKEN+TABLE

ELEMENT S A	QUANTITY	TYPE	ENERGY MIN	ENERGY MAX	DOCUMENTATION REF	VOL	PAGE	DATE	LAB	COMMENTS
CD 110	STRNGTH FUNC	EXPT-PROG	NDG		ERDA-NDC-2	55	575	COL		HACKEN+TABLE
CD 110	LVL DENSITY	EXPT-PROG	NDG		ERDA-NDC-2	55	575	COL		HACKEN+ D=174EV+-18EV
CD 111	TOTAL XSECT	EXPT-PROG	NDG		ERDA-NDC-2	55	575	COL		HACKEN+RES,PARAMS,STF,AVG,LVL,SPACE,
CD 111	TOT INELASTI	EXPT-PROG		10+7	ERDA-NDC-2	16	575	ANL		MEADOWS+NDG,TO CD-111 METAST,STATE
CD 111	N, GAMMA	EXPT-PROG	NDG		ERDA-NDC-2	55	575	COL		HACKEN+ NG/WID CALC,
CD 111	RESON PARAMS	EXPT-PROG	NDG		ERDA-NDC-2	55	575	COL		HACKEN+TABLE
CD 111	STRNGTH FUNC	EXPT-PROG	NDG		ERDA-NDC-2	55	575	COL		HACKEN+TABLE
CD 111	LVL DENSITY	EXPT-PROG	NDG		ERDA-NDC-2	55	575	COL		HACKEN+ D=24,0EV+-1,5EV
CD 112	TOTAL XSECT	EXPT-PROG	NDG		ERDA-NDC-2	55	575	COL		HACKEN+RES,PARAMS,STF,AVG,LVL,SPACE,
CD 112	N, GAMMA	EXPT-PROG	NDG		ERDA-NDC-2	55	575	COL		HACKEN+ NG/WID CALC,
CD 112	RESON PARAMS	EXPT-PROG	NDG		ERDA-NDC-2	55	575	COL		HACKEN+TABLE
CD 112	STRNGTH FUNC	EXPT-PROG	NDG		ERDA-NDC-2	55	575	COL		HACKEN+TABLE
CD 112	LVL DENSITY	EXPT-PROG	NDG		ERDA-NDC-2	55	575	COL		HACKEN+ D=137EV+-8EV
CD 113	TOTAL XSECT	EXPT-PROG	NDG		ERDA-NDC-2	55	575	COL		HACKEN+RES,PARAMS,STF,AVG,LVL,SPACE,
CD 113	N, GAMMA	EXPT-PROG	NDG		ERDA-NDC-2	55	575	COL		HACKEN+ NG/WID CALC,
CD 113	RESON PARAMS	EXPT-PROG	NDG		ERDA-NDC-2	55	575	COL		HACKEN+TABLE
CD 113	STRNGTH FUNC	EXPT-PROG	NDG		ERDA-NDC-2	55	575	COL		HACKEN+TABLE
CD 113	LVL DENSITY	EXPT-PROG	NDG		ERDA-NDC-2	55	575	COL		HACKEN+ D=22,1EV+-3,8EV
CD 114	TOTAL XSECT	EXPT-PROG	NDG		ERDA-NDC-2	55	575	COL		HACKEN+RES,PARAMS,STF,AVG,LVL,SPACE,
CD 114	N, GAMMA	EXPT-PROG	NDG		ERDA-NDC-2	55	575	COL		HACKEN+ NG/WID CALC,
CD 114	RESON PARAMS	EXPT-PROG	NDG		ERDA-NDC-2	55	575	COL		HACKEN+TABLE
CD 114	STRNGTH FUNC	EXPT-PROG	NDG		ERDA-NDC-2	55	575	COL		HACKEN+TABLE
CD 114	LVL DENSITY	EXPT-PROG	NDG		ERDA-NDC-2	55	575	COL		HACKEN+ D=183EV+-29EV
CD 116	TOTAL XSECT	EXPT-PROG	NDG		ERDA-NDC-2	55	575	COL		HACKEN+RES,PARAMS,STF,AVG,LVL,SPACE,
CD 116	N, GAMMA	EXPT-PROG	NDG		ERDA-NDC-2	55	575	COL		HACKEN+ NG/WID CALC,
CD 116	RESON PARAMS	EXPT-PROG	NDG		ERDA-NDC-2	55	575	COL		HACKEN+TABLE
CD 116	STRNGTH FUNC	EXPT-PROG	NDG		ERDA-NDC-2	55	575	COL		HACKEN+TABLE
CD 116	LVL DENSITY	EXPT-PROG	NDG		ERDA-NDC-2	55	575	COL		HACKEN+ D=264EV+-38EV
IN	DIFF ELASTIC	EXPT-PROG	11+7		ERDA-NDC-2	156	575	OHO		FERRER+NDG,TOF,
IN 113	TOTAL XSECT	EXPT-PROG	NDG		ERDA-NDC-2	55	575	COL		HACKEN+RES,PARAMS,STF,AVG,LVL,SPACE,
IN 113	TOT INELASTI	EXPT-PROG		10+7	ERDA-NDC-2	16	575	ANL		MEADOWS+NDG,TO IN-113 METAST,STATE
IN 113	N, GAMMA	EXPT-PROG	NDG		ERDA-NDC-2	55	575	COL		HACKEN+ NG/WID CALC,
IN 115	TOTAL XSECT	EXPT-PROG	NDG		ERDA-NDC-2	55	575	COL		HACKEN+RES,PARAMS,STF,AVG,LVL,SPACE,
IN 115	TOT INELASTI	EXPT-PROG		10+7	ERDA-NDC-2	16	575	ANL		MEADOWS+NDG,TO IN-115 METAST,STATE
IN 115	N, GAMMA	EXPT-PROG	24+4		ERDA-NDC-2	40	575	BNL		RIMAWI+ACT,TECH,SIG=469+-28MILLI-B

ELEMENT S	A	QUANTITY	TYPE	ENERGY MIN	ENERGY MAX	DOCUMENTATION REF	VOL	PAGE	DATE	LAB	COMMENTS
IN	115	N, GAMMA	EXPT-PROG	NDG		ERDA-NDC-2	55	575		COL	HACKEN+ NG/WID CALC.
IN	115	N, GAMMA	EXPT-PROG	96+5		ERDA-NDC-2	106	575		MHG	ROBERTSON,NDG,TBC.
IN	115	N, GAMMA	EXPT-PROG	26+5		ERDA-NDC-2	106	575		MHG	ROBERTSON,NDG,TBC.
IN	115	RESON PARAMS	EXPT-PROG	NDG		ERDA-NDC-2	55	575		COL	HACKEN+
IN	115	STRNGTH FUNC	EXPT-PROG	NDG		ERDA-NDC-2	55	575		COL	HACKEN+
IN	115	LVL DENSITY	EXPT-PROG	NDG		ERDA-NDC-2	55	575		COL	HACKEN+ D=9,4EV+-0,2EV
SN		DIFF ELASTIC	EXPT-PROG	76+6		ERDA-NDC-2	212	575		BRL	BUCHER+EN=7,55MEV,SMALL ANG.EL.SCT.
SN		DIFF ELASTIC	EXPT-PROG	11+7		ERDA-NDC-2	212	575		BRL	BUCHER+SMALL ANG. EL.SCT.NDG.
SN		DIFF ELASTIC	EXPT-PROG	14+7		ERDA-NDC-2	212	575		BRL	BUCHER+SMALL ANG. EL.SCT.NDG.
SN		INELST GAMMA	EXPT-PROG	70+5	20+7	ERDA-NDC-2	126	575		ORL	CHAPMAN+NDG.
SN	113	N, GAMMA	EXPT-PROG	NDG		ERDA-NDC-2	136	575		ORL	SLAUGHTER+NEUT.SEPAR.ENS.GIVEN.
SN	117	N, GAMMA	EXPT-PROG	NDG		ERDA-NDC-2	136	575		ORL	SLAUGHTER+NEUT.SEPAR.ENS.GIVEN.
SN	118	N, GAMMA	EXPT-PROG	NDG		ERDA-NDC-2	136	575		ORL	SLAUGHTER+NEUT.SEPAR.ENS.GIVEN.
SN	119	N, GAMMA	EXPT-PROG	NDG		ERDA-NDC-2	136	575		ORL	SLAUGHTER+NEUT.SEPAR.ENS.GIVEN.
SN	120	DIFF ELASTIC	EXPT-PROG	11+7		ERDA-NDC-2	156	575		OHO	FERRER+NDG.TOF.
SN	120	DIFF ELASTIC	EXPT-PROG	26+7		ERDA-NDC-2	156	575		OHO	CARLSON+NDG.
SN	120	N, GAMMA	EXPT-PROG	NDG		ERDA-NDC-2	134	575		ORL	CARLTON+LVL.STRUCT.NDG.
SN	121	N, GAMMA	EXPT-PROG	NDG		ERDA-NDC-2	136	575		ORL	SLAUGHTER+NEUT.SEPAR.ENS.GIVEN.
SN	123	N, GAMMA	EXPT-PROG	NDG		ERDA-NDC-2	136	575		ORL	SLAUGHTER+NEUT.SEPAR.ENS.GIVEN.
SN	125	N, GAMMA	EXPT-PROG	NDG		ERDA-NDC-2	136	575		ORL	SLAUGHTER+NEUT.SEPAR.ENS.GIVEN.
I	127	N, GAMMA	EXPT-PROG	24+4		ERDA-NDC-2	40	575		BNL	RIMAWI+ACT.TECH.SIG=772+-47MILLI-B
BA	138	N, GAMMA	EXPT-PROG		10+5	ERDA-NDC-2	132	575		ORL	MUSGROVE+NDG.
BA	138	RESON PARAMS	EXPT-PROG		10+5	ERDA-NDC-2	132	575		ORL	MUSGROVE+AVG.S AND P NG/WID GIVEN.
BA	138	STRNGTH FUNC	EXPT-PROG		10+5	ERDA-NDC-2	132	575		ORL	MUSGROVE+S0=(0,9+-0,4)E-04&1=0,5E-04
BA	138	LVL DENSITY	EXPT-PROG		10+5	ERDA-NDC-2	132	575		ORL	MUSGROVE+D=7,5+-1,5 KEV
ND	145	N, GAMMA	EXPT-PROG	20+1	15+5	ERDA-NDC-2	162	575		RPI	HOCKENBURY+RPI.LINAC
ND	145	LVL DENSITY	EXPT-PROG	NDG		ERDA-NDC-2	162	575		RPI	HOCKENBURY+D=14,4+-2,0 EV
SM	149	N, GAMMA	EXPT-PROG	20+1	15+5	ERDA-NDC-2	162	575		RPI	HOCKENBURY+RPI.LINAC
SM	149	LVL DENSITY	EXPT-PROG	NDG		ERDA-NDC-2	162	575		RPI	HOCKENBURY+D=2,7+-0,3 EV
SM	152	N, GAMMA	EXPT-PROG	25-2		ERDA-NDC-2	31	575		BNL	CHRIEN+TABLE
EU	151	N, GAMMA	EXPT-PROG	20+1	90+1	ERDA-NDC-2	162	575		RPI	HOCKENBURY+DERIVED AVG.RES.PAR.NDG.
EU	151	N3N REACTION	EXPT-PROG	75+6	28+7	ERDA-NDC-2	92	575		LAS	BAYHURST+NDG.
EU	151	N4N REACTION	EXPT-PROG	75+6	28+7	ERDA-NDC-2	92	575		LAS	BAYHURST+NDG.
EU	151	RESON PARAMS	EXPT-PROG	NDG		ERDA-NDC-2	162	575		RPI	HOCKENBURY+AVG.NG/WID.NDG.
EU	151	RESON PARAMS	EXPT-PROG	NDG		ERDA-NDC-2	162	575		RPI	HOCKENBURY+AVG.NG/WID.NDG.

ELEMENT S	A	QUANTITY	TYPE	ENERGY MIN	ENERGY MAX	DOCUMENTATION REF	VOL	PAGE	DATE	LAB	COMMENTS
EU	151	STRNGTH FUNC	EXPT-PROG	NDG		ERDA-NDC-2	162	575		RPI	HOCKENBURY+S,P STF,NDG.
EU	153	N, GAMMA	EXPT-PROG	20+1	90+1	ERDA-NDC-2	162	575		RPI	HOCKENBURY+DERIVED AVG,RES,PAR,NDG.
EU	153	STRNGTH FUNC	EXPT-PROG	NDG		ERDA-NDC-2	162	575		RPI	HOCKENBURY+S,P STF,NDG.
GD	154	TOTAL XSECT	EXPT-PROG	NDG		ERDA-NDC-2	55	575		COL	HACKEN+RES,PARAMS,STF,AVG,LVL,SPACE.
GD	154	N, GAMMA	EXPT-PROG	NDG		ERDA-NDC-2	55	575		COL	HACKEN+ NG/WID CALC.
GD	154	RESON PARAMS	EXPT-PROG	NDG		ERDA-NDC-2	55	575		COL	HACKEN+
GD	154	STRNGTH FUNC	EXPT-PROG	NDG		ERDA-NDC-2	55	575		COL	HACKEN+S0=2,0+-0.3E-04
GD	154	LVL DENSITY	EXPT-PROG	NDG		ERDA-NDC-2	55	575		COL	HACKEN+ D=14.5EV+-1.5EV
GD	155	N, GAMMA	EXPT-PROG	24+4		ERDA-NDC-2	35	575		BNL	GREENWOOD+LVL,STRUCT,GRPH,TBL.
GD	156	N, GAMMA	EXPT-PROG	25-2		ERDA-NDC-2	31	575		BNL	CHRIEN+TABLE
GD	157	N, GAMMA	EXPT-PROG	24+4		ERDA-NDC-2	35	575		BNL	GREENWOOD+LVL,STRUCT,GRPH,TBL.
GD	158	TOTAL XSECT	EXPT-PROG	NDG		ERDA-NDC-2	55	575		COL	HACKEN+RES,PARAMS,STF,AVG,LVL,SPACE.
GD	158	N, GAMMA	EXPT-PROG	25-2		ERDA-NDC-2	31	575		BNL	CHRIEN+NDG,TBC.
GD	158	N, GAMMA	EXPT-PROG	NDG		ERDA-NDC-2	55	575		COL	HACKEN+ NG/WID CALC.
GD	158	RESON PARAMS	EXPT-PROG	NDG		ERDA-NDC-2	55	575		COL	HACKEN+
GD	158	STRNGTH FUNC	EXPT-PROG	NDG		ERDA-NDC-2	55	575		COL	HACKEN+S0=1,5+-0.2E-04
GD	158	LVL DENSITY	EXPT-PROG	NDG		ERDA-NDC-2	55	575		COL	HACKEN+ D=86EV+-4EV
GD	160	TOTAL XSECT	EXPT-PROG	NDG		ERDA-NDC-2	55	575		COL	HACKEN+RES,PARAMS,STF,AVG,LVL,SPACE.
GD	160	N, GAMMA	EXPT-PROG	25-2		ERDA-NDC-2	31	575		BNL	CHRIEN+NDG,TBC.
GD	160	N, GAMMA	EXPT-PROG	NDG		ERDA-NDC-2	55	575		COL	HACKEN+ NG/WID CALC.
GD	160	RESON PARAMS	EXPT-PROG	NDG		ERDA-NDC-2	55	575		COL	HACKEN+
GD	160	STRNGTH FUNC	EXPT-PROG	NDG		ERDA-NDC-2	55	575		COL	HACKEN+
GD	160	LVL DENSITY	EXPT-PROG	NDG		ERDA-NDC-2	55	575		COL	HACKEN+ D=202EV+-20EV
DY	160	TOTAL XSECT	EXPT-PROG	NDG		ERDA-NDC-2	55	575		COL	HACKEN+RES,PARAMS,STF,AVG,LVL,SPACE.
DY	160	N, GAMMA	EXPT-PROG	NDG		ERDA-NDC-2	55	575		COL	HACKEN+ NG/WID CALC.
DY	160	RESON PARAMS	EXPT-PROG	NDG		ERDA-NDC-2	55	575		COL	HACKEN+TABLE
DY	160	STRNGTH FUNC	EXPT-PROG	NDG		ERDA-NDC-2	55	575		COL	HACKEN+
DY	160	LVL DENSITY	EXPT-PROG	NDG		ERDA-NDC-2	55	575		COL	HACKEN+ D=27.3EV+-1.7EV
DY	161	TOTAL XSECT	EXPT-PROG	NDG		ERDA-NDC-2	55	575		COL	HACKEN+RES,PARAMS,STF,AVG,LVL,SPACE.
DY	161	N, GAMMA	EXPT-PROG	NDG		ERDA-NDC-2	55	575		COL	HACKEN+ NG/WID CALC.
DY	161	RESON PARAMS	EXPT-PROG	NDG		ERDA-NDC-2	55	575		COL	HACKEN+TABLE
DY	161	STRNGTH FUNC	EXPT-PROG	NDG		ERDA-NDC-2	55	575		COL	HACKEN+
DY	161	LVL DENSITY	EXPT-PROG	NDG		ERDA-NDC-2	55	575		COL	HACKEN+ D=2.67EV+-0.13EV
DY	162	TOTAL XSECT	EXPT-PROG	NDG		ERDA-NDC-2	55	575		COL	HACKEN+RES,PARAMS,STF,AVG,LVL,SPACE.
DY	162	N, GAMMA	EXPT-PROG	25-2		ERDA-NDC-2	31	575		BNL	CHRIEN+TABLE

ELEMENT S	A	QUANTITY	TYPE	ENERGY MIN	ENERGY MAX	DOCUMENTATION REF	VOL	PAGE	DATE	LAB	COMMENTS
DY	162	N, GAMMA	EXPT-PROG	NDG		ERDA-NDC-2	55	575	COL		HACKEN+ NG/WID CALC.
DY	162	RESON PARAMS	EXPT-PROG	NDG		ERDA-NDC-2	55	575	COL		HACKEN+TABLE
DY	162	STRNGTH FUNC	EXPT-PROG	NDG		ERDA-NDC-2	55	575	COL		HACKEN+
DY	162	LVL DENSITY	EXPT-PROG	NDG		ERDA-NDC-2	55	575	COL		HACKEN+ D=64.6EV+-1.9EV
DY	163	TOTAL XSECT	EXPT-PROG	NDG		ERDA-NDC-2	55	575	COL		HACKEN+RES.PARAMS.STF.AVG.LVL.SPACE.
DY	163	N, GAMMA	EXPT-PROG	NDG		ERDA-NDC-2	55	575	COL		HACKEN+ NG/WID CALC.
DY	163	RESON PARAMS	EXPT-PROG	NDG		ERDA-NDC-2	55	575	COL		HACKEN+TABLE
DY	163	STRNGTH FUNC	EXPT-PROG	NDG		ERDA-NDC-2	55	575	COL		HACKEN+
DY	163	LVL DENSITY	EXPT-PROG	NDG		ERDA-NDC-2	55	575	COL		HACKEN+ D=6.85EV+-0.54EV
DY	164	TOTAL XSECT	EXPT-PROG	NDG		ERDA-NDC-2	55	575	COL		HACKEN+RES.PARAMS.STF.AVG.LVL.SPACE.
DY	164	N, GAMMA	EXPT-PROG	25-2		ERDA-NDC-2	31	575	BNL		CHRIEN+TABLE
DY	164	N, GAMMA	EXPT-PROG	NDG		ERDA-NDC-2	55	575	COL		HACKEN+ NG/WID CALC.
DY	164	RESON PARAMS	EXPT-PROG	NDG		ERDA-NDC-2	55	575	COL		HACKEN+TABLE
DY	164	STRNGTH FUNC	EXPT-PROG	NDG		ERDA-NDC-2	55	575	COL		HACKEN+
DY	164	LVL DENSITY	EXPT-PROG	NDG		ERDA-NDC-2	55	575	COL		HACKEN+ D=147EV+-9EV
HO	165	DIFF ELASTIC	EXPT-PROG	11+7		ERDA-NDC-2	156	575	OHO		FERRER+NDG,TOF.
HO	165	N, GAMMA	EXPT-PROG	30+5	30+6	ERDA-NDC-2	13	575	ANL		POENITZ,NORM,TO,AU.
ER	164	N, GAMMA	EXPT-PROG	25-2		ERDA-NDC-2	31	575	BNL		CHRIEN+NDG,TBC.
ER	166	N, GAMMA	EXPT-PROG	25-2		ERDA-NDC-2	31	575	BNL		CHRIEN+NDG,TBC.
ER	168	N, GAMMA	EXPT-PROG	25-2		ERDA-NDC-2	31	575	BNL		CHRIEN+NDG,TBC.
ER	170	N, GAMMA	EXPT-PROG	25-2		ERDA-NDC-2	31	575	BNL		CHRIEN+NDG,TBC.
TM	169	N2N REACTION	EXPT-PROG	15+7	24+7	ERDA-NDC-2	92	575	LAS		VEESER,LIQ,SCIN,TANK,DOSIM,APPL.
TM	169	N2N REACTION	EXPT-PROG	75+6	28+7	ERDA-NDC-2	92	575	LAS		BAYHURST+NDG.
TM	169	N2N REACTION	EXPT-PROG	TR	20+7	ERDA-NDC-2	101	575	LAS		YOUNG+NDG.
TM	169	N3N REACTION	EXPT-PROG	15+7	24+7	ERDA-NDC-2	92	575	LAS		VEESER,LIQ,SCIN,TANK,DOSIM,APPL.
TM	169	N3N REACTION	EXPT-PROG	75+6	28+7	ERDA-NDC-2	92	575	LAS		BAYHURST+NDG.
TM	169	N4N REACTION	EXPT-PROG	75+6	28+7	ERDA-NDC-2	92	575	LAS		BAYHURST+NDG.
YB	170	N, GAMMA	EXPT-PROG	25-2		ERDA-NDC-2	31	575	BNL		CHRIEN+TABLE
LU	175	TOTAL XSECT	EXPT-PROG	NDG		ERDA-NDC-2	58	575	COL		HACKEN+
LU	175	N, GAMMA	EXPT-PROG	NDG		ERDA-NDC-2	58	575	COL		HACKEN+ AVG NG/WID= 77MILLI-EV
LU	175	N2N REACTION	EXPT-PROG	15+7	24+7	ERDA-NDC-2	92	575	LAS		VEESER,LIQ,SCIN,TANK,DOSIM,APPL.
LU	175	N2N REACTION	EXPT-PROG	75+6	28+7	ERDA-NDC-2	92	575	LAS		BAYHURST+NDG.
LU	175	N3N REACTION	EXPT-PROG	15+7	24+7	ERDA-NDC-2	92	575	LAS		VEESER,LIQ,SCIN,TANK,DOSIM,APPL.
LU	175	N3N REACTION	EXPT-PROG	75+6	28+7	ERDA-NDC-2	92	575	LAS		BAYHURST+NDG.
LU	175	N4N REACTION	EXPT-PROG	75+6	28+7	ERDA-NDC-2	92	575	LAS		BAYHURST+NDG.

ELEMENT S	A	QUANTITY	TYPE	ENERGY MIN	ENERGY MAX	DOCUMENTATION REF	VOL	PAGE	DATE	LAB	COMMENTS
LU	175	RESON PARAMS	EXPT-PROG		30+3	ERDA-NDC-2	58	575	COL		HACKEN+
LU	175	STRNGTH FUNC	EXPT-PROG	NDG		ERDA-NDC-2	58	575	COL		HACKEN+S0=1,83+-0,12E-04
LU	175	LVL DENSITY	EXPT-PROG	NDG		ERDA-NDC-2	58	575	COL		HACKEN+
LU	176	N, GAMMA	EXPT-PROG	NDG		ERDA-NDC-2	28	575	ANL		WILSON+G-RAY SPC.
LU	177	N, GAMMA	EXPT-PROG	NDG		ERDA-NDC-2	28	575	ANL		WILSON+G-RAY SPC.
TA	180	RESON PARAMS	EXPT-PROG		10+2	ERDA-NDC-2	128	575	ORL		HARVEY+AVG NG/WID=(51+-1EV)E-03.
TA	180	STRNGTH FUNC	EXPT-PROG		10+2	ERDA-NDC-2	128	575	ORL		HARVEY+S0=(2,4+-0,4)E-04.
TA	180	LVL DENSITY	EXPT-PROG		10+2	ERDA-NDC-2	128	575	ORL		HARVEY+D=1,1 +-0.1 EV.
TA	181	DIFF ELASTIC	EXPT-PROG	11+7		ERDA-NDC-2	156	575	OHO		FERRER+NDG,TOF.
TA	181	N, GAMMA	EXPT-PROG	30+5	30+6	ERDA-NDC-2	13	575	ANL		POENITZ,NORM,TO,AU,GRPH.
TA	181	SPECT N,GAMM	EXPT-PROG	14+7		ERDA-NDC-2	90	575	LAS		DRAKE+TABLE
TA	181	INELST GAMMA	EXPT-PROG	10+5	20+7	ERDA-NDC-2	125	575	ORL		DICKENS+NDG,
TA	181	INELST GAMMA	EXPT-PROG	70+5	20+7	ERDA-NDC-2	126	575	ORL		CHAPMAN+NDG,
TA	181	INELST GAMMA	EXPT-PROG	NDG		ERDA-NDC-2	134	575	ORL		DICKENS+LVL,STRUCT,NDG.
TA	181	N2N REACTION	EXPT-PROG	15+7	24+7	ERDA-NDC-2	92	575	LAS		VEESER,LIQ,SCIN,TANK,DOSIM,APPL.
TA	181	N3N REACTION	EXPT-PROG	15+7	24+7	ERDA-NDC-2	92	575	LAS		VEESER,LIQ,SCIN,TANK,DOSIM,APPL.
TA	181	N, GAMMA	THEO-PROG	NDG		ERDA-NDC-2	72	575	LRL		GARDNER,MOL,CALC,NDG.
W		DIFF ELASTIC	EXPT-PROG	76+6		ERDA-NDC-2	212	575	BRL		BUCHER+EN=7,55MEV,SMALL ANG.EL.SCT.
W		DIFF ELASTIC	EXPT-PROG	11+7		ERDA-NDC-2	212	575	BRL		BUCHER+SMALL ANG. EL.SCT,NDG.
W		DIFF ELASTIC	EXPT-PROG	14+7		ERDA-NDC-2	212	575	BRL		BUCHER+SMALL ANG. EL.SCT,NDG.
W		INELST GAMMA	EXPT-PROG	70+5	20+7	ERDA-NDC-2	126	575	ORL		CHAPMAN+NDG,
W	186	DIFF ELASTIC	EXPT-PROG		30+6	ERDA-NDC-2	18	575	ANL		GUENTHER+GRPH,
W	186	DIFF INELAST	EXPT-PROG		30+6	ERDA-NDC-2	18	575	ANL		GUENTHER+GRPH,
OS	186	N, GAMMA	EXPT-PROG	20+0	30+5	ERDA-NDC-2	74	575	LRL		BROWNE+TBC,NDG.
OS	187	N, GAMMA	EXPT-PROG	20+0	30+5	ERDA-NDC-2	74	575	LRL		BROWNE+TBC,NDG.
OS	188	N, GAMMA	EXPT-PROG	THR		ERDA-NDC-2	46	575	BNL		MACPHAIL+POP,ROTA,BANDS,DEF,NUC,GRPH
OS	188	N, GAMMA	EXPT-PROG	NDG		ERDA-NDC-2	46	575	BNL		MACPHAIL+POP,ROTA,BANDS,DEF,NUC,GRPH
OS	188	N, GAMMA	EXPT-PROG	THR		ERDA-NDC-2	50	575	BNL		MACPHAIL+G-DECAY OF 0+ AND 2+ STATES
OS	188	N, GAMMA	EXPT-PROG	94+0		ERDA-NDC-2	50	575	BNL		MACPHAIL+G-DECAY OF 0+ AND 2+ STATES
OS	188	N, GAMMA	EXPT-PROG	13+0		ERDA-NDC-2	50	575	BNL		MACPHAIL+G-DECAY OF 0+ AND 2+ STATES
OS	188	N, GAMMA	EXPT-PROG	20+0	30+5	ERDA-NDC-2	74	575	LRL		BROWNE+TBC,NDG.
OS	189	N, GAMMA	EXPT-PROG	20+0	30+5	ERDA-NDC-2	74	575	LRL		BROWNE+TBC,NDG.
OS	190	N, GAMMA	EXPT-PROG	THR		ERDA-NDC-2	46	575	BNL		MACPHAIL+POP,ROTA,BANDS,DEF,NUC,GRPH
OS	190	N, GAMMA	EXPT-PROG	NDG		ERDA-NDC-2	46	575	BNL		MACPHAIL+POP,ROTA,BANDS,DEF,NUC,GRPH
OS	190	N, GAMMA	EXPT-PROG	THR		ERDA-NDC-2	50	575	BNL		MACPHAIL+G-DECAY OF 0+ AND 2+ STATES

ELEMENT S	A	QUANTITY	TYPE	ENERGY MIN	ENERGY MAX	DOCUMENTATION REF	VOL	PAGE	DATE	LAB	COMMENTS
OS	190	N, GAMMA	EXPT-PROG	67+0		ERDA-NDC-2	50	575		BNL	MACPHAIL+G-DECAY OF 0+ AND 2+ STATES
OS	190	N, GAMMA	EXPT-PROG	89+0		ERDA-NDC-2	50	575		BNL	MACPHAIL+G-DECAY OF 0+ AND 2+ STATES
OS	190	N, GAMMA	EXPT-PROG	10+1		ERDA-NDC-2	50	575		BNL	MACPHAIL+G-DECAY OF 0+ AND 2+ STATES
OS	190	N, GAMMA	EXPT-PROG	20+0	30+5	ERDA-NDC-2	74	575		LRL	BROWNE+TBC,NDG,
OS	192	N, GAMMA	EXPT-PROG	20+0	30+5	ERDA-NDC-2	74	575		LRL	BROWNE+TBC,NDG,
IR	191	N2N REACTION	EXPT-PROG	75+6	28+7	ERDA-NDC-2	92	575		LAS	BAYHURST+NDG,
IR	191	N3N REACTION	EXPT-PROG	75+6	28+7	ERDA-NDC-2	92	575		LAS	BAYHURST+NDG,
IR	191	N4N REACTION	EXPT-PROG	75+6	28+7	ERDA-NDC-2	92	575		LAS	BAYHURST+NDG,
IR	193	TOT INELASTI	EXPT-PROG	75+6	28+7	ERDA-NDC-2	92	575		LAS	BAYHURST+NDG,
IR	193	N2N REACTION	EXPT-PROG	75+6	28+7	ERDA-NDC-2	92	575		LAS	BAYHURST+NDG,
PT		SPECT N,GAMM	EXPT-PROG	14+7		ERDA-NDC-2	90	575		LAS	DRAKE+TABLE
AU	197	N, GAMMA	EXPT-PROG	40+5	35+6	ERDA-NDC-2	11	575		ANL	POENITZ,TOF,ABSOL,MEAS+RATIO,TO,U238
AU	197	N, GAMMA	EXPT-PROG	24+4		ERDA-NDC-2	40	575		BNL	RIMAWI+ADT,TECH,SIG=630+-17MILLI-B
AU	197	N, GAMMA	THEO-PROG	NDG		ERDA-NDC-2	72	575		LRL	GARDNER,MDL,CALC,GRPH,
AU	197	N, GAMMA	EXPT-PROG	30+3	55+5	ERDA-NDC-2	131	575		ORL	MACKLIN+NDG,
AU	197	INELST GAMMA	EXPT-PROG	70+5	20+7	ERDA-NDC-2	126	575		ORL	CHAPMAN+NDG,
AU	197	N2N REACTION	EXPT-PROG	15+7	24+7	ERDA-NDC-2	92	575		LAS	VEESER,LIQ,SCIN,TANK,DOSIM,APPL,
AU	197	N2N REACTION	EXPT-PROG	75+6	28+7	ERDA-NDC-2	92	575		LAS	BAYHURST+NDG,
AU	197	N3N REACTION	EXPT-PROG	15+7	24+7	ERDA-NDC-2	92	575		LAS	VEESER,LIQ,SCIN,TANK,DOSIM,APPL,
AU	197	N3N REACTION	EXPT-PROG	75+6	28+7	ERDA-NDC-2	92	575		LAS	BAYHURST+NDG,
AU	197	N4N REACTION	EXPT-PROG	75+6	28+7	ERDA-NDC-2	92	575		LAS	BAYHURST+NDG,
AU	197	STRNGTH FUNC	EXPT-PROG		15+5	ERDA-NDC-2	131	575		ORL	MACKLIN+NDG,
TL	203	N2N REACTION	EXPT-PROG	75+6	28+7	ERDA-NDC-2	92	575		LAS	BAYHURST+NDG,
TL	203	N3N REACTION	EXPT-PROG	75+6	28+7	ERDA-NDC-2	92	575		LAS	BAYHURST+NDG,
TL	203	N4N REACTION	EXPT-PROG	75+6	28+7	ERDA-NDC-2	92	575		LAS	BAYHURST+NDG,
TL	205	N4N REACTION	EXPT-PROG	75+6	28+7	ERDA-NDC-2	92	575		LAS	BAYHURST+NDG,
PB		TOTAL XSECT	EXPT-PROG	NDG		ERDA-NDC-2	173	575		OKE	CLEMENT+NDG,
PB		DIFF ELASTIC	EXPT-PROG	11+7		ERDA-NDC-2	156	575		OHO	FERRER+NDG,TOF,
PB		DIFF ELASTIC	EXPT-PROG	26+7		ERDA-NDC-2	156	575		OHO	CARLSON+NDG,
PB		DIFF ELASTIC	EXPT-PROG	70+6	14+7	ERDA-NDC-2	212	575		ORL	BUCHER+ANG=3 TO 15 DEG,NDG,
PB		SCATTERING	THEO-PROG	NDG		ERDA-NDC-2	177	575		OKE	DIVADEENAM,SHELL MDL +VIBR,DOORWAY
PB		N, GAMMA	EXPT-PROG	57+6		ERDA-NDC-2	160	575		OHO	BRIEN+G-RAY SPC,NDG,
PB		INELST GAMMA	EXPT-PROG	70+5	20+7	ERDA-NDC-2	126	575		ORL	CHAPMAN+NDG,
PB		INELST GAMMA	EXPT-PROG	60+5	20+7	ERDA-NDC-2	133	575		ORL	CHAPMAN+NDG,
PB	206	DIFF ELASTIC	EXPT-PROG	11+7		ERDA-NDC-2	156	575		OHO	FERRER+NDG,TOF,

ELEMENT S	A	QUANTITY	TYPE	ENERGY MIN	ENERGY MAX	DOCUMENTATION REF	VOL	PAGE	DATE	LAB	COMMENTS
PB	206	SPECT N,GAMM	EXPT-PROG	57+6		ERDA-NDC-2	160	575	OHO	BRIENT+NAICRYS,SPECT,NDG,	
PB	207	SPECT N,GAMM	EXPT-PROG	57+6		ERDA-NDC-2	160	575	OHO	BRIENT+NAICRYS,SPECT,NDG,	
PB	208	SPECT N,GAMM	EXPT-PROG	57+6		ERDA-NDC-2	160	575	OHO	BRIENT+NAICRYS,SPECT,NDG,	
PB	208	INELST GAMMA	EXPT-PROG	NDG		ERDA-NDC-2	134	575	ORL	DICKENS,E(GAM)=5 TO 8 MEV, GRPH,	
BI	209	DIFF ELASTIC	EXPT-PROG		30+6	ERDA-NDC-2	18	575	ANL	GUENTHER+NDG,	
BI	209	DIFF ELASTIC	EXPT-PROG	11+7		ERDA-NDC-2	156	575	OHO	FERRER+NDG,TOF,	
BI	209	DIFF ELASTIC	EXPT-PROG	76+6		ERDA-NDC-2	212	575	BRL	BUCHER+ENR7,55MEV,SMALL ANG.EL.SCT,	
BI	209	DIFF ELASTIC	EXPT-PROG	11+7		ERDA-NDC-2	212	575	BRL	BUCHER+SMALL ANG. EL.SCT,NDG.	
BI	209	DIFF ELASTIC	EXPT-PROG	14+7		ERDA-NDC-2	212	575	BRL	BUCHER+SMALL ANG. EL.SCT,NDG.	
BI	209	DIFF INELAST	EXPT-PROG		30+6	ERDA-NDC-2	18	575	ANL	GUENTHER+NDG,	
BI	209	N2N REACTION	EXPT-PROG	15+7	24+7	ERDA-NDC-2	92	575	LAS	VEESER,LIQ,SCIN,TANK,DOSIM,APPL,	
BI	209	N3N REACTION	EXPT-PROG	15+7	24+7	ERDA-NDC-2	92	575	LAS	VEESER,LIQ,SCIN,TANK,DOSIM,APPL,	
TH	232	N, GAMMA	EXPT-PROG	+1		ERDA-NDC-2	137	575	ORL	HALPERIN+22EV DOUBLET,	
TH	232	RESON PARAMS	EXPT-PROG	22+1		ERDA-NDC-2	137	575	ORL	HALPERIN+EL/WID+G=3,72+-0,11 MILLIEV	
TH	232	GAMMA,N	EXPT-PROG	NDG		ERDA-NDC-2	74	575	LRL	ALVAREZ+TBC,NDG,	
TH	232	PHOTO-FISSN	EXPT-PROG	NDG		ERDA-NDC-2	74	575	LRL	ALVAREZ+TBC,NDG,	
U		DIFF ELASTIC	EXPT-PROG	70+6	14+7	ERDA-NDC-2	212	575	BRL	BUCHER+ANG=3 TO 15 DEG,NDG,	
U	233	FISSION	EXPT-PROG	10+3	30+7	ERDA-NDC-2	70	575	LRL	CARLSON+REL,TO U-235 FISS,	
U	233	ETA	EXPT-PROG	NDG		ERDA-NDC-2	7	575	ANC	SMITH,REANAL,DATA,ETA=2,295+-0,009	
U	234	FISSION	EXPT-PROG	10+3	30+7	ERDA-NDC-2	70	575	LRL	CARLSON+REL,TO U-235 FISS,	
U	235	SPECT N,GAMM	EXPT-PROG	14+7		ERDA-NDC-2	90	575	LAS	DRAKE+TABLE	
U	235	FISSION	EXPT-PROG	53+6	10+7	ERDA-NDC-2	16	575	ANL	MEADOWS,RATIO U238/U235 FISS.CS,GRPH	
U	235	FISSION	EXPT-PROG	NDG		ERDA-NDC-2	59	575	GOL	FELVINCI+TOF,LOW EN,QUANT,NUMS,	
U	235	FISSION	EXPT-PROG	80+3	20+7	ERDA-NDC-2	70	575	LRL	CZIRR+REL,TO N-P SCAT,NDG,	
U	235	FISSION	EXPT-PROG	THR	10+6	ERDA-NDC-2	70	575	LRL	CZIRR+REL TO LI-6(N,ALPHA),NDG,	
U	235	FISSION	EXPT-PROG	NDG		ERDA-NDC-2	89	575	LAS	KEYWORTH+POL,NTS,AND TARG,RES,SPNS,	
U	235	FISSION	EXPT-PROG	26+5		ERDA-NDC-2	104	575	MHG	ROBERTSON+PRELIM,SIG=1,32BARNS,	
U	235	FISSION	EXPT-PROG	80+3	50+6	ERDA-NDC-2	108	575	NBS	CARLSON,TBC,	
U	235	ETA	EXPT-PROG	NDG		ERDA-NDC-2	7	575	ANC	SMITH,REANAL,DATA,ETA=2,081+-0,009	
U	235	NUBAR,(NU)	EXPT-PROG		20+7	ERDA-NDC-2	71	575	LRL	HOWE+PRELIM,GRPH,TBC,	
U	235	SPECT FISS N	EVAL-PROG	NDG		ERDA-NDC-2	119	575	NBS	GRUNDL+COMP,AND,EVAL,	
U	235	RESON PARAMS	EXPT-PROG		15+5	ERDA-NDC-2	89	575	LAS	KEYWORTH+SPINS ASSIGN,TO RESONANCES,	
U	235	GAMMA,N	EXPT-PROG	NDG		ERDA-NDC-2	74	575	LRL	ALVAREZ+TBC,NDG,	
U	235	PHOTO-FISSN	EXPT-PROG	NDG		ERDA-NDC-2	74	575	LRL	ALVAREZ+TBC,NDG,	
U	236	FISSION	EXPT-PROG	10+3	30+7	ERDA-NDC-2	70	575	LRL	CARLSON+REL,TO U-235 FISS,	

ELEMENTS	A	QUANTITY	TYPE	ENERGY MIN	ENERGY MAX	DOCUMENTATION REF	VOL	PAGE	DATE	LAB	COMMENTS
U	236	GAMMA,N	EXPT-PROG	NDG		ERDA-NDC-2	74	575		LRL	ALVAREZ+TBC,NDG,
U	236	PHOTO-FISSN	EXPT-PROG	NDG		ERDA-NDC-2	74	575		LRL	ALVAREZ+TBC,NDG,
U	238	TOTAL XSECT	EXPT-PROG		10+3	ERDA-NDC-2	136	575		ORL	OLSEN+TRANS,ORELA,NDG,
U	238	DIFF ELASTIC	EXPT-PROG		30+6	ERDA-NDC-2	18	575		ANL	GUENTHER+GRPH,
U	238	DIFF INELAST	EXPT-PROG		30+6	ERDA-NDC-2	18	575		ANL	GUENTHER+GRPH,
U	238	N, GAMMA	EXPT-PROG	24+4		ERDA-NDC-2	40	575		BNL	RIMAWI+ACT,TECH,SIG=475+-36MILLI-B
U	238	N, GAMMA	THEO-PROG	NDG		ERDA-NDC-2	143	575		ORL	PEREZ+STAT,TESTS ON EXPT,DATA,
U	238	NEUT EMISSN	EXPT-PROG	14+7		ERDA-NDC-2	76	575		LRL	WONG,PLSD,SPHER,MEASMT,TBL,GRPH,
U	238	FISSION	EXPT-PROG	53+6	10+7	ERDA-NDC-2	16	575		ANL	MEADOWS,RATIO U238/U235 FISS,CS,GRPH
U	238	FISSION	EXPT-PROG	10+3	30+7	ERDA-NDC-2	70	575		LRL	CARLSON+REL,TO U-235 AND U-233 FISS,
U	238	FISSION	THEO-PROG	NDG		ERDA-NDC-2	144	575		ORL	JAMES+STAT,TESTS ON EXPT,DATA,
U	238	FISSION	EXPT-PROG	10+0	35+4	ERDA-NDC-2	163	575		RPI	BLOCK+GRPH,
U	238	RESON PARAMS	EXPT-PROG	NDG		ERDA-NDC-2	59	575		COL	MELKONIAN+CORRELATION OF EL/WID,
U	238	RESON PARAMS	EXPT-PROG	67+0	37+1	ERDA-NDC-2	163	575		RPI	BLOCK+NF/WIDS MEASD,
U	238	GAMMA,N	EXPT-PROG	NDG		ERDA-NDC-2	74	575		LRL	ALVAREZ+TBC,NDG,
U	238	PHOTO-FISSN	EXPT-PROG	NDG		ERDA-NDC-2	74	575		LRL	ALVAREZ+TBC,NDG,
U	239	TOTAL XSECT	EXPT-PROG	10+1	25+6	ERDA-NDC-2	72	575		LRL	GARDNER,ABST,NDG,
U	239	ELASTIC SCAT	EXPT-PROG	10+1	25+6	ERDA-NDC-2	72	575		LRL	GARDNER,ABST,NDG,
U	239	TOT INELASTI	EXPT-PROG	10+1	25+6	ERDA-NDC-2	72	575		LRL	GARDNER,ABST,NDG,
U	239	N, GAMMA	EXPT-PROG	10+1	25+6	ERDA-NDC-2	72	575		LRL	GARDNER,ABST,NDG,
U	239	FISSION	EXPT-PROG	10+1	25+6	ERDA-NDC-2	72	575		LRL	GARDNER,ABST,NDG,
NP	237	N, GAMMA	EXPT-PROG	NDG		ERDA-NDC-2	139	575		ORL	WESTON+TBC,NDG,
PU	239	N, GAMMA	EXPT-PROG	10+2	20+5	ERDA-NDC-2	139	575		ORL	GWIN+NORM,TO 2200M/S,
PU	239	SPECT N,GAMM	EXPT-PROG	14+7		ERDA-NDC-2	90	575		LAS	DRAKE+TABLE
PU	239	FISSION	EXPT-PROG	NDG		ERDA-NDC-2	104	575		MHO	ROBERTSON+NDG,TBC,
PU	239	FISSION	EXPT-PROG	10+2	20+5	ERDA-NDC-2	139	575		ORL	GWIN+NORM,TO 2200M/S,
PU	239	ETA	EXPT-PROG	NDG		ERDA-NDC-2	7	575		ANC	SMITH,REANAL,DATA,ETA=2.110+-0.008
PU	240	N, GAMMA	EXPT-PROG	THR	30+5	ERDA-NDC-2	139	575		ORL	WESTON+NDG,REL TO 10B(N,A)+6LI(N,A)
PU	240	FISSION	EXPT-PROG	THR	30+5	ERDA-NDC-2	139	575		ORL	WESTON+NDG,REL TO 10B(N,A)+6LI(N,A)
PU	241	N, GAMMA	EXPT-PROG	THR	30+5	ERDA-NDC-2	139	575		ORL	WESTON+NDG,REL TO 10B(N,A)+6LI(N,A)
PU	241	FISSION	EXPT-PROG	THR	30+5	ERDA-NDC-2	139	575		ORL	WESTON+NDG,REL TO 10B(N,A)+6LI(N,A)
PU	241	ETA	EXPT-PROG	NDG		ERDA-NDC-2	7	575		ANC	SMITH,REANAL,DATA,ETA=2.169+-0.010
PU	241	P NEUT DELAY	EXPT-PROG	15+5	50+6	ERDA-NDC-2	18	575		ANL	MEADOWS,AVG,YIELD=0.0142+-0.0011NT/F
PU	242	N, GAMMA	EXPT-PROG	NDG		ERDA-NDC-2	139	575		ORL	WESTON+TBC,NDG,
PU	242	N, GAMMA	EXPT-PROG	50+3	70+4	ERDA-NDC-2	162	575		RPI	HOCKENBURY+

ELEMENT S	A	QUANTITY	TYPE	ENERGY MIN	ENERGY MAX	DOCUMENTATION REF	VOL	PAGE	DATE	LAB	COMMENTS
AM	241	N, GAMMA	EXPT-PROG	THR	30+5	ERDA-NDC-2	139	575		ORL	WESTON+NDG,REL TO 10B(N,A)+6LI(N,A)
AM	241	FISSION	EXPT-PROG	THR	30+5	ERDA-NDC-2	139	575		ORL	WESTON+NDG,REL TO 10B(N,A)+6LI(N,A)
CF	252	NUBAR,(NU)	EXPT-PROG	NDG		ERDA-NDC-2	105	575		MHG	BOZORGMANESH, NDG,TBC.
CF	252	SPECT FISS N	EVAL-PROG	SPON		ERDA-NDC-2	119	575		NBS	GRUNDL+COMP,AND,EVAL.

IDAHO NATIONAL ENGINEERING LABORATORY, AEROJET NUCLEAR COMPANY
IDAHO FALLS, IDAHO

A. EVALUATED DECAY-SCHEME DATA FOR THE ILRR PROGRAM (Helmer, Greenwood)

For many years, the nuclear physics community has had available two general files of decay scheme data. These are the data sheets from the Nuclear Data Group at ORNL and the Table of Isotopes from LBL. These files have attempted to include essentially all quantities related to nuclear structure and radioactive decay. These files represent both a compilation (i.e., a list of all data or, at least, all references) and an evaluation (i.e., a judgment as to the best information).

In the last few years, a great use has developed for a number of specialized files of decay scheme data. These specialized files are usually needed for one of the following two reasons. First, due to the large amount of experimental data to be treated, it has not been possible to keep the evaluation work of the two general files up to date. Second, some special files can justify more evaluation effort in obtaining specific quantities (e.g., absolute γ intensities) than can be warranted for these quantities in assembling the general files.

As reported earlier, we have prepared a specialized evaluation of decay scheme data for the Interlaboratory LMFBR Reaction Rate (ILRR) program. This program was organized in 1971 for the purpose of making a series of precise measurements of rates of neutron induced reactions for a set of well-defined and reproducible neutron spectra. For most of these reactions, the rates are determined by measurements of the γ-ray spectra from the decay of radioactive reaction products.

With respect to the accuracy of the γ-ray counting, the goals of the ILRR program are:

> to provide absolute nonfission reaction rates which are accurate to ±5% (at the 68% confidence level); and
>
> to provide absolute fission-product production rates accurate to ±2½%.

These reaction rates R depend on two parameters of the decay scheme: the half-life $T_{\frac{1}{2}}$ and the absolute γ-ray intensity (or branching ratio) B. For the calculation of the reaction rates for the ILRR program, a careful determination of the associated uncertainties is needed. Differentiation of the expression for R and rearrangement gives the following contributions to the fractional error, $\sigma(R)/R$,

$$\frac{\sigma(R)}{R} = -\frac{\sigma(B)}{B}$$

$$\frac{\sigma(R)}{R} = -\frac{\sigma(T_{\frac{1}{2}})}{T_{\frac{1}{2}}}\left(1 + \lambda\tau - \frac{\lambda T e^{-\lambda T}}{1-e^{-\lambda T}} - \frac{\lambda t e^{-\lambda t}}{1-e^{-\lambda t}}\right)$$

from the decay scheme parameters. Here T = count time, t = irradiation time, and τ = decay time.

For careful γ counting, the contribution to $\sigma(R)$ from the counting is taken to be between 1% and 2% by the various laboratories involved in the ILRR measurements. This means that to meet a goal of $\sigma(R)/R < 2\frac{1}{2}\%$ the decay scheme contributions must total (when added in quadrature) $\leq 2\%$ for the fission products. Because of these rather stringent goals, an evaluation effort was needed within the ILRR program to provide the current best values of these parameters. In this case, published evaluations were not completely satisfactory because they either were out of date by several years or did not place a sufficient emphasis on obtaining precise values of these particular quantities.

One of the purposes of any specialized data evaluation is to identify those experimental data which are not accurate enough for the program. To facilitate the comparison of the quality of the evaluated data with the ILRR goals, the contributions to $\sigma(R)/R$ from the γ-ray intensity and half-life errors are given in Table A-1. The latter contribution is given for typical irradiation and count times (namely, 2.2 and 8.3 hours, respectively) and two decay times (0 and the lesser of $2T_{\frac{1}{2}}$ and 60 days). These data indicate that the ±5% goal for the nonfission reactions can be met, but that more stringent goals would be impossible for several isotopes (e.g., ^{64}Cu, ^{115m}In). With the present parameters, the fission reaction goal of $\pm 2\frac{1}{2}\%$ cannot be met for ^{103}Ru, ^{132}Te and ^{144}Ce-Pr due to the large uncertainty in the absolute γ-ray intensities. In no case is the uncertainty in the half-life a limiting factor with respect to these goals.

TABLE A-1

UNCERTAINTY IN REACTION RATE R

Contributions to $\sigma(R)/R$ from the errors in decay scheme parameters for an irradiation of 30,000 sec and count duration of 8,000 sec. τ is the decay time.

Isotope	Half-Life	Fractional Uncertainty in R (%) from γ-Intensity	from Half-Life $\tau=0$	$\tau=2T_{1/2}$	$\tau = 60$ d
		nonfission reactions			
^{24}Na	15 h	0.002	0.10	0.08	
^{27}Mg	9.5 m	0.7; 0.004[a]	0.21	0.50	
^{46}Sc	84 d	0.006	0.12		0.06
^{47}Sc	3.4 d	3.6	1.1	0.51	
^{48}Sc	44 h	0.002	0.21	0.11	
^{54}Mn	313 d	0.02	0.10		0.08
^{58}Co	71 d	0.05	0.21		0.09
^{59}Fe	45 d	2.7; 0.1[a]	0.22		0.01
^{60}Co	5.3 y	0.002	0.09		0.09
^{64}Cu	13 h	4.3	0.04	0.04	
^{115m}In	4.5 h	4.3	0.15	0.47	
^{116m}In	54 m	1.8; 0.01[a]	0.23	0.74	
^{198}Au	2.7 d	0.10	0.07	0.03	
^{239}Np	2.4 d	1.4	0.16	0.08	
		fission reactions			
^{95}Zr	64 d	0.9	0.77		0.27
^{103}Ru	39 d	3.4	0.25		0.01
^{132}Te	78 h	6.8	0.61	0.28	
^{137}Cs	30 y	0.35	0.50		0.50
^{140}Ba-La	13 d	0.17	0.08	0.03	
^{144}Ce-Pr	284 d	5.2	0.14		0.12

[a] The second value applies if the sum of the intensities of two γ rays is used.

B. INTEGRAL CROSS SECTION MEASUREMENTS (Harker, Anderl, Rogers)

A continuing effort in our laboratory in support of the LMFBR development program has been the measurement of the integral capture cross sections, reactivity worths, and precise reaction rates for fission product isotopes, structural and control element materials, materials for neutron dosimetry, and transuranic nuclides in the intermediate and fast neutron field of the Coupled Fast Reactivity Measurement Facility (CFRMF). Since the last USNDC report, our efforts have concentrated in the measurement of precise reaction rates for dosimetry materials in the CFRMF, testing of the dosimetry data file for ENDF/B-IV, the characterization of the central neutron energy spectrum for the CFRMF, and the development of the capabilities for preparation of highly enriched fission product samples and the preparation of transuranic samples for integral cross section measurements.

A summary of some of the results of precise reaction rate measurements* for dosimetry related materials and their use in data testing of the ENDF/B-IV dosimetry file is presented in Table B-1. For these reactions the fission rate of ^{235}U is used as a standard and all reactions are normalized to that value. Calculations were performed using the broad group (0.25 lethargy) version of the CFRMF spectrum and the ENDF/B-IV dosimetry file. The results of these tests indicate the following average discrepancies between calculation and experiment: for all reactions, -4.3%; for the resonance (broad energy responce) reaction alone, 0.46%, and for the threshold (high energy response) reaction alone, 9.0%. Similar tests are being performed for the $\Sigma\Sigma$ facility (Mol, Belgium), the BIG-10 facility (LASL), the fission spectrum and a 1/E spectrum. The analysis of these tests is expected to indicate deficiencies in the cross section and spectral data and point the direction to improved representation of both.

Measurements of the central neutron flux in the CFRMF have been made by Li-6 neutron spectrometry. The analysis of these measurements is underway and is expected to more precisely define the neutron spectrum from 1 keV to 10 MeV. These results along with the results of earlier proton-recoil measurements will be correlated with multifoil dosimetry measurements and reactor code calculations using ENDF/B-IV cross section data to arrive at an evaluated neutron spectrum for the CFRMF. Such a spectrum is necessary for reliable interpretation of the integral measurements, for data testing of ENDF/B, and for establishing the CFRMF as a benchmark neutron spectrum.

At the present time experiments for measuring the integral capture cross sections for ^{152}Sm, ^{152}Gd and ^{137}Cs and the integral capture and fission cross sections for ^{242}Pu are underway.

---

*Performed as part of the Interlaboratory LMFBR Reaction Rate Program.

A re-evaluation was made of the capture cross section measurements in the CFRMF for ^{151}Eu, ^{153}Eu and ^{181}Ta for which preliminary results were presented in an earlier USNDC report[1]. The capture cross section for ^{151}Eu has been determined to be 2.59 ± 0.15 b/atom with isomer ratios of 8.1×10^{-4}, 0.41, and 0.59 for production of $^{152m_2}Eu$ (96 m), $^{152m_1}Eu$ (9.3 h) and ^{152g}Eu (13.2 y) respectively. The capture cross section for ^{153}Eu is 1.51 ± 0.12 b/atom. For ^{181}Ta a capture cross section of 0.54 ± 0.04 b/atom was determined with isomer ratios of 1.0×10^{-3} and 0.999 for production of ^{182m}Ta (15.9 m) and ^{182g}Ta (115 d), respectively. These results along with the measurement in the CFRMF of the $^{10}B(n,\alpha)$ cross section[2] were used to estimate relative reactivity worths for Eu_2O_3, B_4C and Ta in different fast neutron fields[3].

We have developed the capability in the isotope separator laboratory for producing milligram quantities of highly enriched rare earth samples for cross section measurements in EBR II and CFRMF. At the present time samples of ^{147}Sm, ^{149}Sm, ^{143}Nd, ^{145}Nd and ^{154}Gd are being prepared. Highly enriched samples are required to permit the use of mass spectrometry in the cross section determinations.

Experiments are planned for measuring the integral capture cross sections for ^{152}Eu, ^{154}Eu, ^{144}Ce, ^{111}Cd, ^{151}Sm, ^{134}Cs, ^{90}Sr and ^{135}Cs in the CFRMF. The isotope separator is required for several of these measurements. Of the transuranic nuclides, cross section measurements for ^{243}Am, ^{244}Cm, ^{241}Pu and ^{241}Am are planned.

---

1. Y. D. Harker, "Integral Cross Section Measurements", USNDC-9 (28-29 November, 1973) p. 6.
2. Harry Farrar, IV, et al., Nuclear Technology 25, 305 (February 1975).
3. R. A. Anderl, et al., "Integral Capture Cross Section Measurements in the CFRMF for LMFBR Control Materials", Conference on Nuclear Cross Sections and Technology, Washington, D.C., March 3-7, 1975.

TABLE B-1

Comparison of Measured and Calculated
Reaction Rates for Dosimetry Related Materials

Reaction	Measured* Reaction Rate	Calculated* Reaction Rate	C/E
$^{27}Al(n,p)$	.000562	.000562	1.0
$^{27}Al(n,\alpha)$	.000104	.000107	1.029
$^{59}Co(n,\gamma)$	.0589	.0538	.913
$^{235}U(n,f)$	1.0 (Ref.)	1.0 (Ref.)	--
$^{238}U(n,f)$	.0489	.0438	.896
$^{238}U(n,\gamma)$	.114	.145	1.27
$^{237}Np(n,f)$	.357	.345	.966
$^{239}Pu(n,f)$	1.17	1.12	.957
$^{6}Li(n,\alpha)$	.543	.622	1.15
$^{10}B(n,\alpha)$	1.17	1.07	.915
$^{197}Au(n,\gamma)$	.273	.260	.952
$^{115}In(n,n')$	.0320	.0275	.869
$^{63}Cu(n,\gamma)$	.0292	.0298	1.02
$^{45}Sc(n,\gamma)$	.0151	.0127	.841
$^{115}In(n,\gamma)$	.181	.190	1.05
$^{54}Fe(n,p)$	.0112	.0104	.929
$^{59}Fe(n,\gamma)$	.00394	.00386	.980
$^{59}Ni(n,p)$	.0154	.0138	.896
$^{46}Ti(n,p)$	.00168	.00136	.810
$^{48}Ti(n,p)$	.00268	.00298	1.11
$^{48}Ti(n,p')$	.0000443	.0000267	.603

* Normalized to the fission rate of ^{235}U.

C. DISCREPANCIES BETWEEN η AND $\bar{\nu}$ (Smith)

Manganese bath systematic effects involved in the MTR η measurements were reevaluated. The reappraisal took into consideration information gained from suggestions by De Volpi[1], the Monte Carlo calculation of the η experiment by Mitchell and Emert[2], and recent cross section evaluations. Minor modifications were indicated for values of several of the corrections to the experiment. Using the revised set of corrections, least squares analyses were made of (1) the original (1964) MTR η data[3], (2) the second set of data collected in 1967, when η for ^{241}Pu was also measured[4], and (3) both sets together. The 1967 data had not previously been analyzed by the full least-squares treatment. The results of the reanalysis are shown in Table C-1. The changes in the corrections essentially balanced each other out. The differences between the Table C-1 values and the results of the original analysis[3] are not statistically significant. This study was reported at the Conference on Nuclear Cross Sections and Technology at Washington in March, 1975.[5]

A joint experiment with the National Bureau of Standards will measure the ratio of the absorption cross sections of hydrogen and manganese. The measurement will be made by determining, as a function of manganese concentration, the activity induced in a manganese bath by a thermal beam. In addition to the σ_H/σ_{Mn} ratio to be derived, the purpose of this experiment is to look for systematic effects that could be responsible for the 1.4% difference in this ratio observed by De Volpi and Axton. In preparation for this experiment, studies have been made of methods for determining manganese concentration. These studies suggest that the σ_H/σ_{Mn} discrepancy might be due largely to errors in determining manganese concentration. Accordingly, three methods for determining manganese concentration will be used in the experiment at NBS. These will be (1) a gravimetric determination by weighing the dried salts from an evaporated volume of the solution, (2) a volumetric determination by a complexiметric titration with ethylenediamine tetraacetic acid (EDTA), and (3) a densimetric determination by comparing the measured density of the solution with a set of pre-determined calibration curves. All three methods are subject to errors due to impurities present. Present indications are that the largest uncertainties are associated with the densimetric method. To be valid, the calibration curves must be prepared for the same solution

---

1. A. De Volpi, ANL-7830 (1971).
2. J. A. Mitchell and C. J. Emert, Proc. 3rd Conf. Neutron Cross Sections and Technology CONF-710301 (Vol. 2) p. 605, (1971).
3. J. R. Smith et al., IDO-17083 (1966).
4. J. R. Smith and S. D. Reeder, in "Neutron Cross Sections and Technology", NBS Spec. Publ. 299 1, 590 (1968).
5. J. R. Smith, Conf. on Nucl. Cross Sections and Tech., paper DB-9, Washington, D.C., March 3-7, 1975.

matrix as will be used in the measurements. In particular, the same amount of sulfuric acid should be present and the same temperature should be used. Sulfuric acid is commonly used to stabilize the solution. Differences of 0.5% have been observed in concentration due to differences in the amount of sulfuric acid present. To provide a controlled acidity for the solutions, we are planning to use a constant molar concentration of hydroxyl amine sulfate in the place of sulfuric acid.

TABLE C-1

REANALYZED η VALUES

Nucleus	η (1964 data)	η (1967 data)	η (all data)
U-233	2.298 ± 0.009	2.291 ± .010	2.295 ± .009
U-235	2.080 ± .010	2.082 ± .009	2.081 ± .009
Pu-239	2.110 ± .008	2.106 ± .009	2.110 ± .008
Pu-241	not measured	2.166 ± .010	2.165 ± .010

A. CHARGED PARTICLE REACTIONS

1. Reactions Relevant to Controlled Thermonuclear Research

a. Cross Sections for Neutrons from ^{6}Li + d Reactions at Low Energies: (A. J. Elwyn, R. E. Holland, F. J. Lynch, J. E. Monahan, and F. P. Mooring)

As part of a program for determining absolute cross sections for various nuclear particles emitted in charged-particle induced reactions on light nuclei we have measured the differential and total cross sections for the outgoing neutrons in the bombardment of ^{6}Li by 0.2 to 0.9 MeV deuterons accelerated in the ANL Dynamitron. Knowledge of the properties of nuclear reactions of deuterons with ^{6}Li is of importance to the needs of the controlled thermonuclear research program in connection with the evaluation of advanced fusion fuels and the concept of fusion chain reactions. At the same time such measurements can contribute to the understanding of the nuclear structure of light nuclei and the relative importance of the various reaction mechanisms that could produce a neutron in the final state. Differential and total cross sections for the neutrons corresponding to the excitation of the final ^{7}Be nucleus in its ground and 0.431 MeV excited state (in the ^{6}Li(d, n) reaction) and for the continuum neutrons that arise in the breakup of ^{7}Be into ^{3}He and ^{4}He have been determined by the use of stilbene scintillator detectors and standard time-of-flight techniques. Target thickness and detector efficiencies have been obtained with sufficient accuracy to allow absolute cross section measurements to ~16%. Total cross sections are presented in Table A-1. An attempt to interpret the measured neutron spectra associated with three-body breakup in terms of a consistent reaction mechanism is in progress. The observed results are qualitatively different from the spectra expected from direct breakup. An analysis based on sequential decay (i.e. multi-step processes) in terms of various possible final-state interactions appears promising.

b. Cross Sections for Charged Particles from ^{6}Li + d Reactions at Low Energies: (C. N. Davids, A. J. Elwyn, R. E. Holland, L. Meyer-Schützmeister, and F. P. Mooring)

Experiments designed to determine absolute cross sections for charged particles emitted in d + ^{6}Li reactions at low energies have been

TABLE A-1. Total cross sections (in mb) for neutrons emitted in d + ^{6}Li reactions.

E_d(MeV) (± .005)	σ_t(g.s.) (± 16%)	σ_t(431 keV) (± 16%)	$\sigma_t(E_n \geq .5$ MeV) (± 18%)
0.873	56.0	29.9	
0.779	49.9	25.5	61.7
0.578	45.0	19.5	41.2
0.482	41.2	14.6	
0.379	29.0	9.45	
0.375	30.4	10.1	22.1
0.328	24.3	7.78	
0.242	10.0	2.68	
0.238	11.8	3.12	7.64
0.204	7.67	2.16	5.29

initiated. Motivation for such investigations is as presented in the previous contribution. Preliminary relative differential cross sections for the protons in the ^{6}Li(d, p)^{7} Li reaction and the α-particles in the ^{6}Li(d, α) ^{4}He have been obtained at angles between 15 and 165° at a number of deuteron energies between 0.2 and 0.8 MeV by use of silicon surface barrier detectors and a 30" diameter scattering chamber. Thin targets of ^{6}Li F evaporated on carbon backings are being utilized, and effects due to the energy dependence of the change of beam charge state and scattering within the target are being investigated. The study of the low energy charged particles that arise in the breakup of ^{7}Li and ^{7}Be in the d + ^{6}Li reactions will in all likelihood require the use of time-of-flight and perhaps other more specialized techniques.

2. Nuclear Structure Studies

Lifetimes of the 1/2 + [631] → 5/2 + [622] E2 Transitions in some Actinide Nuclei (S. W. Yates, I. Ahmad, A. M. Friedman, F. J. Lynch, and Re. E. Holland)

Lifetimes of the E2 transitions from the 1/2 + [631] state to the 5/2 + [622] state have been measured in several actinide nuclei using pulsed beam and delayed coincidence techniques. The 1/2 + [631] level was excited in ^{239}U and ^{243}Pu by the (d, p) reaction and in ^{241}Pu by the (d, t) reaction and the subsequent γ-ray decay to the 5/2 + [622] level was observed between beam pulses. The corresponding E2 transitions were observed in ^{243}Cm and ^{245}Cm from the radioactive decay of ^{243}Bk and ^{245}Bk, respectively, and the lifetimes were determined from electron-photon delayed coincidence experiments. The half-lives from these measurements are: ^{239}U (0.78 ± 0.04 μs); ^{241}Pu (0.88 ± 0.05 μs); ^{243}Pu (0.33 ± 0.03 μs); ^{243}Cm (1.08 ± 0.03 μs); and ^{245}Cm (0.29 ± 0.02 μs). Comparisons are made between the experimental transition probabilities and theoretical estimates. The differences between the transition rates in these nuclei are understood when pairing interactions are taken into account.

B. FAST NEUTRON PHYSICS

1. Fast Neutron Capture Cross Section Measurements of ^{197}Au and ^{238}U. (W. P. Poenitz)

Absolute measurements of the capture cross section of ^{197}Au were carried out in the 400-3500 keV energy range. Ratios of the

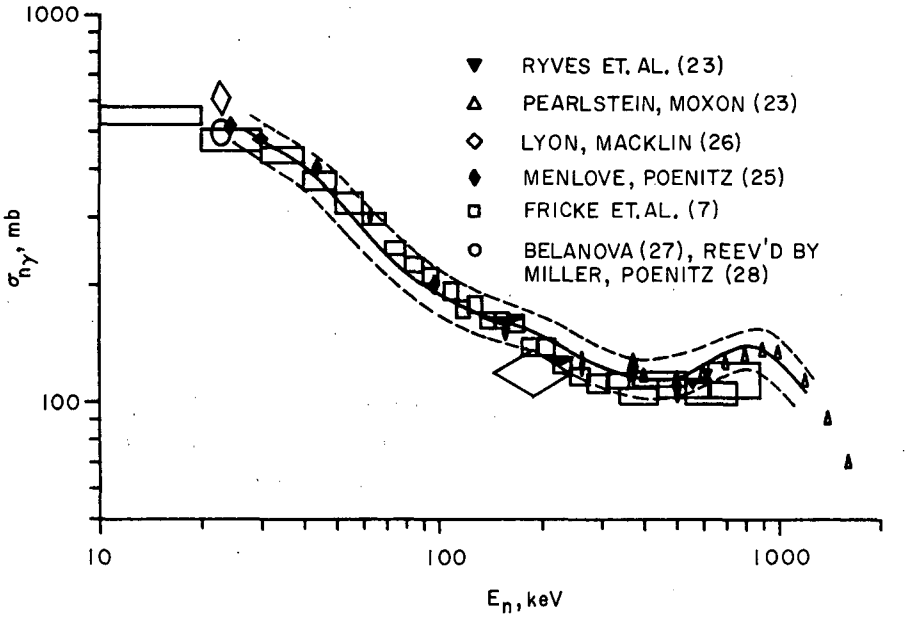

Fig. B-1. Neutron radiative capture cross sections of ^{238}U. The present results and associated uncertainties are indicated by the curves. Previously reported values are also given for comparison.

capture cross sections of ^{238}U to ^{197}Au were measured from 20 to 1200 keV. Values for $\sigma_{n,\gamma}(^{238}U)$ were derived by utilizing evaluated and present data for $\sigma_{n,\gamma}(^{197}Au)$. The time-of-flight technique and a large liquid scintillator were used for the detection of the prompt capture gamma rays, and the Grey Neutron Detector, the Black Neutron Detector, and an ^{6}Li-glass detector were used for the measurement and monitoring of the neutron flux.

The absolute values for the capture cross section of ^{197}Au agree well with evaluated data and measurements reported relative to the ^{235}U fission cross section. The present results for the ^{238}U neutron capture cross section are shown in Fig. B-1 as a solid line. The dashed curves indicate the uncertainty range. A comparison is made between the present measurements and other absolute data.

2. Capture Cross Section Measurements and Model Calculations on ^{165}Ho and ^{181}Ta. (W. P. Poenitz)

Measurements of the fast neutron capture cross sections of ^{165}Ho and ^{181}Ta were carried out in the energy range from 0.3 to 3.0 MeV. Monoenergetic neutrons were used and the time-of-flight technique was utilized for background suppression. The Grey Neutron Detector was used as a neutron flux monitor and the data were normalized with a cross section of 138 mb for gold at 0.5 MeV.

Fast neutron capture and activation cross sections were calculated in terms of the statistical model. The Hauser-Freshbach formalism and a gamma cascade model previously described were used[1]. Of specific interest here are the capture and activation of ^{181}Ta as a test example for the present calculations because the daughter nucleus, ^{182}Ta, has an isomeric state with a high spin value (10^-) and thus a very small activation cross section for this isomeric state. Experimental values for the activation cross section exist up to 1.6 MeV[2].

Fig. B-2 shows the results from the present calculations in comparison with the present experimental results for the capture cross

---

[1] W. P. Poenitz, Z. f. Physik 197, 262 (1966).

[2] S. A. Cox, Phys. Rev. 133, B378 (1964).

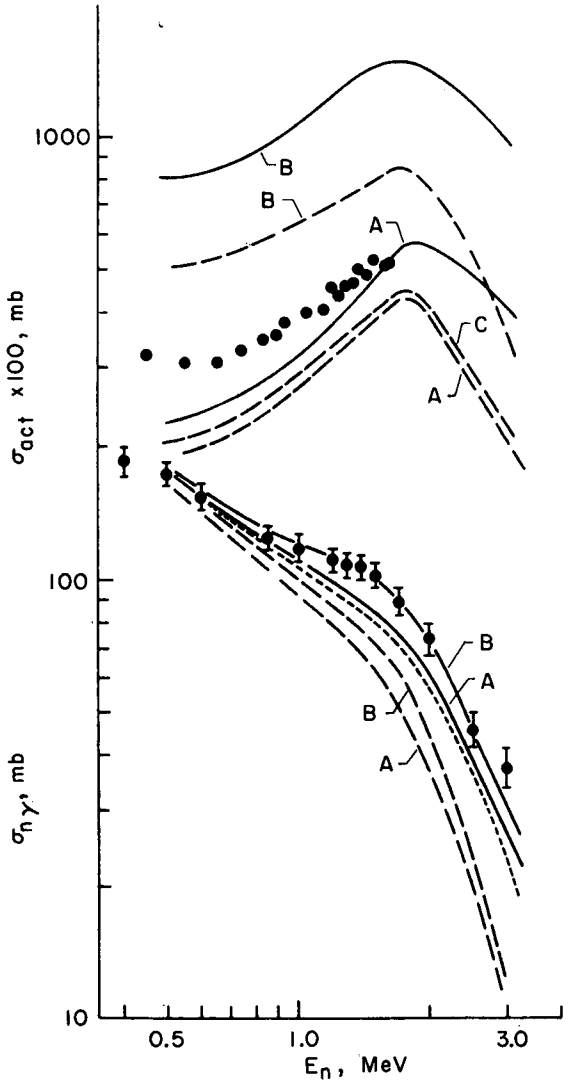

Fig. B-2. Neutron radiative capture cross sections of tantalum. The present experimental values are indicated by data points. The results of calculations are indicated by curves as described in the text.

section and the measurements by Cox[2] for the isomeric state. All curves labeled with A are for parameters in the level density formulas and transition probabilities applicable to a wide range of nuclei. The only normalization used is the value for $<\Gamma_\gamma>/<D>$ which was obtained from experimental values in the eV-energy range. The improvement obtained for the capture cross section by using Axel instead of Weisskopf is similar as recently reported by Gardner[3], however, the difference between the inclusion or exclusion or exclusion of 1 percent Pigmy resonance is much smaller than obtained by Brzosko et al.[4]. The most satisfactory result of the present calculations is the good agreement obtained for the isomeric cross section which is about two orders of magnitude smaller than the capture cross section. Inclusion of quadrupole radiation in the γ-ray cascades changes the isomeric cross section very little, however, increasing the spin cut-off factor in the level density formula to a value desirable for a deformed nucleus improves the agreement for the capture cross section but increases the isomeric cross section excessively.

---

[3]D. G. Gardner, Bull. Am. Phys. Soc., Vol. 19, No. 9, 1017 (1974).

[4]J. S. Brzoski et al., Can. J. Physics 47, 2849 (1969).

3. Neutron Capture Cross Section Measurements on Co, Ni, Cu and Zn in the 350-750 keV Energy Range (W. P. Poenitz)

Measurements of the capture cross sections of Co, Ni, Cu and Zn were carried out in the 350-750 keV energy range using white source neutron time-of-flight techniques. These capture cross sections show some structure which is most pronounced for Co and Ni. The fluctuations exceed 30 percent for Ni above 500 keV. The data for Co and Ni were compared with total cross sections. These values were obtained from an evaluated data file[1] and averaged with the same resolution as the experimental capture cross sections. The structure is ver similar in both the total and the capture cross sections; however, differences in the amplitudes at some energies are apparent.

---

[1]A. B. Smith, ANL-NDM-1 and private communication.

4. The delayed Neutron Yield of ^{241}Pu (J. W. Meadows)

The total delayed neutron yield of ^{241}Pu has been measured as a function of the incident neutron energy. The measure-

ments extend from 0.15 to 5 MeV and show no significant energy dependence. The average yield is 0.0142 ± .0011 delayed neutrons per fission.

5. The ^{238}U: ^{235}U Fission Cross Section Ratio (J. W. Meadows)

The ^{238}U: ^{235}U fission cross section ratios have been measured from 5.33 to 10.32 MeV at intervals of ~0.25 MeV. The estimated errors are 1.5 to 2%. The D(d, n) ^{3}He reaction was used as the source of neutrons and the data were corrected for neutrons from (d, n) reactions with the target structure and also from the D(d, pn) D reaction. The details of the equipment, procedures, data analysis, sample assay and sources of error are similar to the previously reported measurements at lower energies[1]. The results are shown in Fig. B-3.

---

[1] J. W. Meadows, Nucl. Sci. Eng. 49, 310 (1972).

6. Fast-Neutron Activation Cross Section Studies (J. W. Meadows and D. L. Smith)

Data obtained on (n, p) reactions for ^{27}Al, $^{46,47,48}Ti$, $^{54,56}Fe$, ^{58}Ni, ^{59}Co and ^{64}Zn from near threshold to ~10 MeV has been completely processed and reported[1]. These data have also been farwarded to the National Neutron Cross Section Center.

Measurements were recently made on the $^{111}Cd(n, n')^{111m}Cd$ (49m), $^{113}In(n, n')^{113m}In$(.73h), $^{115}In(n, n')^{115m}In$ (4.4h), $^{66}Zn(n, p)^{66}Cu$, $^{59}Co(n, \alpha)^{56}Mn$ and $^{65}Cu(n, p)^{65}Ni$ reactions at energies below ~10 MeV. These data are being processed.

---

[1] D. L. Smith and J. W. Meadows, ANL/NDM-10, Argonne National Laboratory (January 1975).

7. Gamma-Ray Production Cross Section Studies (D. L. Smith)

A program of cross section measurements for (n, n'γ) reactions on sodium, vanadium, iron and nickel at energies below ~2 MeV was described in an earlier report[1]. Data obtained from differential cross section measurements at 55° have been partially processed. Gamma-ray angular distribution measurements for these elements have been completed up to ~2 MeV.

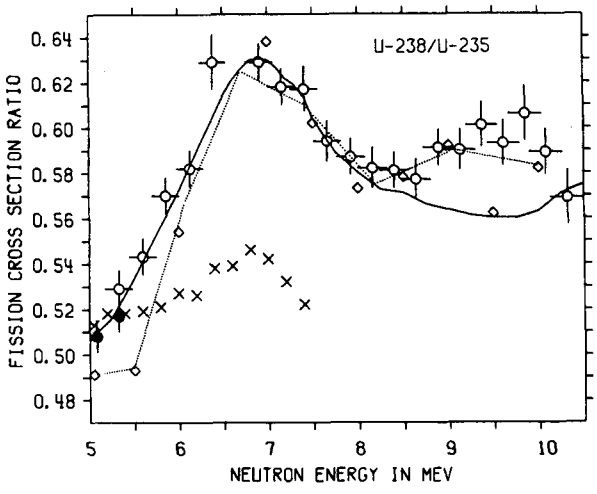

Fig. B-3. The ^{238}U:^{235}U fission cross section ratios. ○ this experiment, ● Meadows (1972), ◇ Hansen et al. (1967), × Fursov et al. (1973). The dashed line connects points from Davey's (1968) evaluation. The solid curve is calculated from ENDF/B-III cross sections.

The problems associated with absorption and multiple scattering of neutrons and gamma rays within the samples used for these measurements have been investigated extensively. Measurements have been made with scattering samples of various sizes to provide data for comparison with calculations. The results of these studies are being utilized in the processing of cross section data.

---

[1] D. L. Smith, USNDC-11, p. 20 (1974).

8. Observation and Analysis of Elastic Neutron Scattering from ^{12}C. (R. J. Holt, A. B. Smith and J. F. Whalen)

Angular distributions of neutrons elastically scattered from ^{12}C were measured with high resolution (20-50 keV) in the energy range 1.8 to 4.0 MeV and at 20 to 90 scattering angles between 20^{o} and 160^{o}. The differential cross sections were determined relative to those of the H(n, n) reaction. In addition, total neutron cross sections were deduced from nearly monoenergetic ($\Delta E \cong 2$ keV) neutron transmissions in the energy range 0.1 to 5.0 MeV. The results were interpreted in terms of a general multi-level R-function analysis in which the R-Matrix parameters were fitted to the angular distributions and the total cross sections and neutron polarizations were predicted. The quality of the R-Matrix analysis of the angular distributions is illustrated in Fig. B-4. A self-consistent set of R-Matrix parameters was found which describe all observations of the $^{12}C(n, n)^{12}C$ reaction below 5 MeV. In particular, the present data were found to be physically consistent with the total cross section measurements of Schwartz et al[1] and the neutron polarization observations of Holt et al.[2]

---

[1] R. B. Schwartz, R. A. Schruck and H. T. Heaton, II, "MeV total Neutron Cross Sections", National Bureau of Standards (1974).

[2] R. J. Holt, F. W. K. Firk, R. North and H. L. Schultz, Nucl. Phys. A213 (1973) 147

9. Fast Neutron Scattering from Heavy Nuclei (P. Guenther and A. Smith)

The on-going program of fast neutron scattering studies from heavy nuclei gave emphasis to elastic and inelastic scattering from ^{209}Bi, ^{186}W and ^{238}U to incident energies of 3.0 MeV. Elastic angular

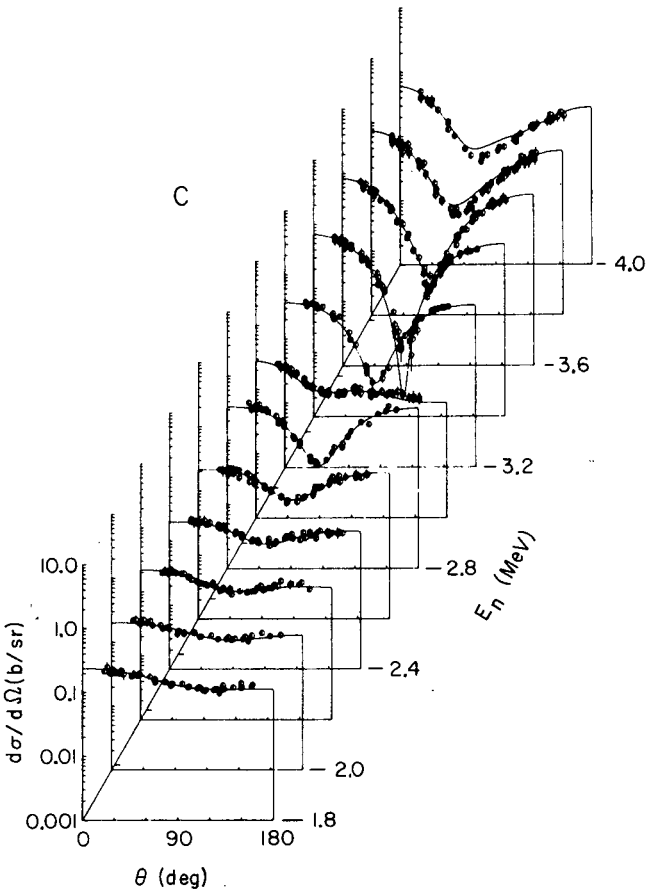

Fig. B-4. A comparison of the measured angular distributions for the $^{12}C(n, n)\ ^{12}C$ reaction with the results of the R-Matrix analysis at selected energies between 1.8 and 4.0 MeV.

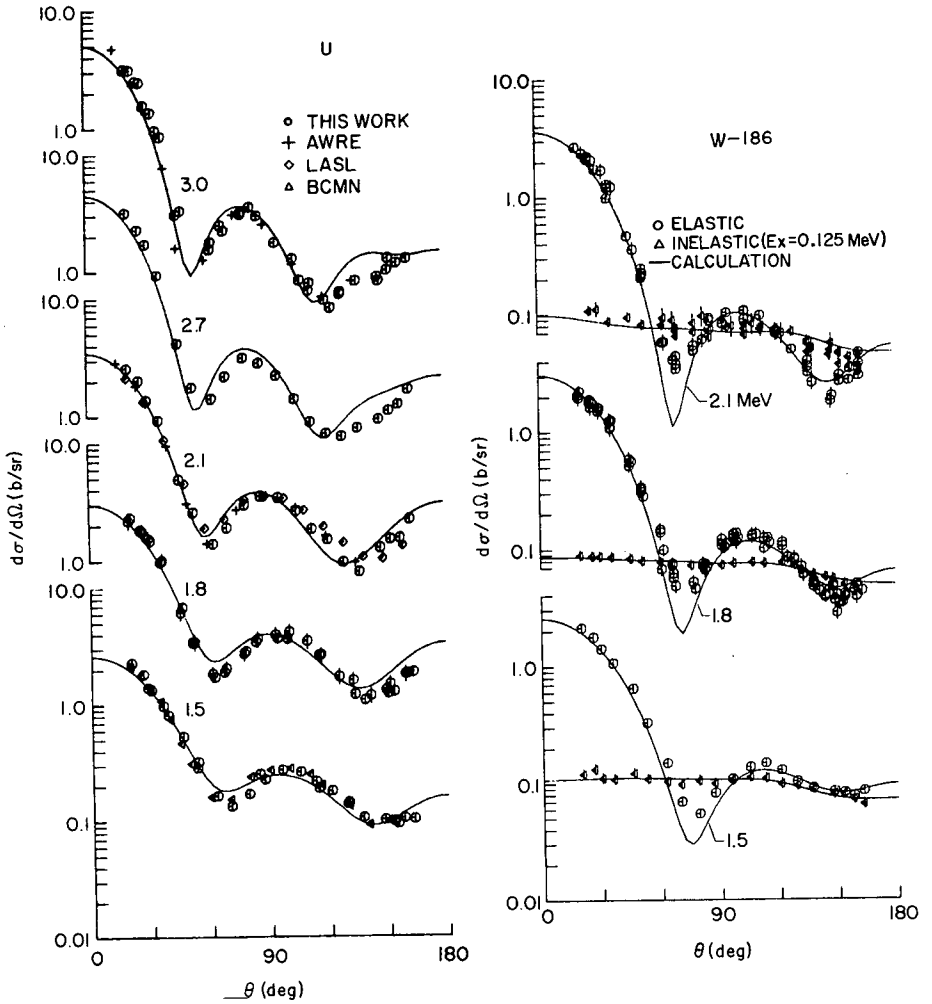

Fig. B-5 Differential elastic and inelastic neutron scattering from ^{186}W and ^{238}U. The present results are indicated by the noted data points. Previously reported values are as follows: AWRE = Batchelor et al., Nucl. Phys. 65, 236, LASL = L. Cranberg LA-2177, and BCMN = Knitter et al. Z. Phys. 244, 358. The curves are the results of calculations using the coupled channel model of LaGrange (EANDC Topical Discussion, Tokyo, 1974).

distributions were determined at up to 50 scattering angles at incident neutron energy intervals of approximately 0.3 MeV. Some illustrative results for ^{186}W and ^{238}U are shown in Fig. B-5. Cross sections for the inelastic excitation of more than 19 states in ^{186}W were determined. Analysis now in progress suggests a number of collective spectroscopic configurations. Particular attention was given to the inelastic neutron excitation of the ground state rotational band of ^{238}U (2 + 45 keV, 4 + 148 keV states). The contribution due to the excitation of the prominant 45 keV state was reasonably resolved to 3.0 MeV. The results are illustrated in Fig. B-6. It is clear that direct reaction mechanisms play an important part in the excitation of the 2 + 45 keV state but is very much less significant for the higher energy levels. Measurements of the cross sections for the states in ^{238}U at excitation energies of greater than 1.0 MeV are in progress. Thus far cross sections for more than 12 states in ^{238}U have been obtained. Concurrent with the above measurement program is an analysis effort some results of which are indicated in Figs. B-5 and B-6.

10. Why the Hauser-Feshbach Formula Works (P.A. Moldauer)

A theoretical study of the Hauser-Feshbach Formula has resulted in the following conclusions. Flux conservation requires substantial channel-channel correlations of resonance amplitudes. These, together with the effects of level-level correlations and other terms conspire to cancel the large additive corrections to the Hauser-Feshbach formula for the fluctuation cross section. The remaining multiplicative corrections become negligible for nonelastic cross sections when many channels are open. In other cases, approximation formulas provide estimates that are adequate for most purposes. However, the Bohr independence hypothesis is not always satisfied when fewer than about 20 channels are open. The cross section correlation width is shown to differ markedly from the average width. The use of the former for estimating the Hauser- Feshbach denominator is found to be justified. All of these results are verified by means of statistical model calculations of resonance parameters and of cross sections.

C. PHOTONUCLEAR PHYSICS

1. Photodisintegration of the Deuteron Near Threshold (H. E. Jackson, R. J. Holt, and W. M. Wilson).

Although the photodisintegration cross section of the deuteron is known to be discrepant with current theories at high energies, no precision absolute measurements have been made in the region near

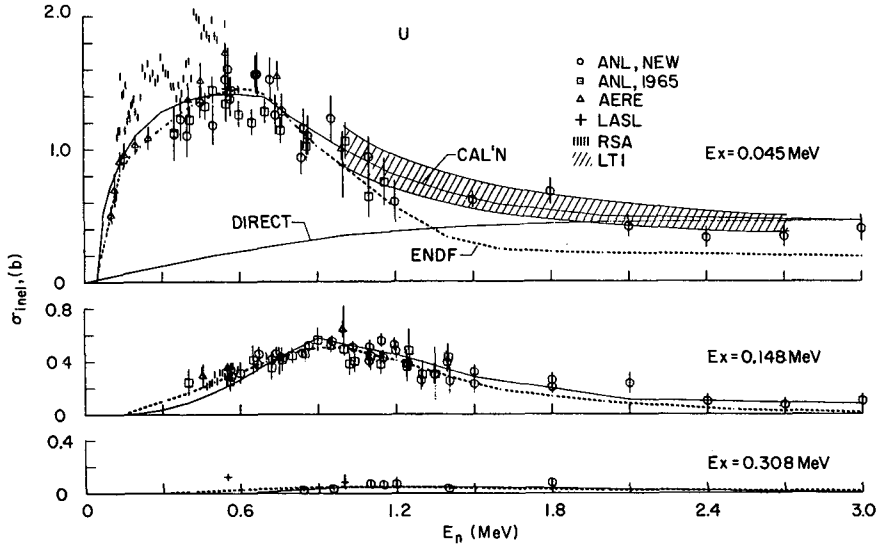

Fig. B-6. Cross sections for the inelastic neutron excitation of the ground-state rotational band of ^{238}U. The present values are indicated by circular data points. Other reported values are as follows: ANL-65 = A. Smith, Nucl. Phys. 47, 633, AERE = Barnard et al., Nucl. Phys. 80, 46, LASL = Cranberg and Levin, Phys. Rev. 109, 2063, RSA = Barnard et al., Helsinki Conf. 1971, and LTI = Marcella et al., Bull. Am. Phys. Soc. 19, 575. Solid curves indicate the results of model calculations and the dashed curve the respective values from ENDF/B-IV.

threshold. The cross section in this region is of particular interest because of its sensitivity to the relative strength of the photomagnetic and photoelectric disintegration amplitudes. The only information available in this region comes from the inverse reaction, i.e., thermal capture in hydrogen. The capture cross section is observed to be enhanced over predicted values by about 10%. Recently this enhancement has been attributed to the effects of meson exchange currents. A study of deuteron photodisintegration in the threshold region $E_\gamma < 3.0$ MeV was begin in 1974. The experiments are performed by irradiating a deuterium target with pulsed bremsstrahlung and measuring the photoneutron energy spectrum by neutron time-of-flight at 90° and 135°. The objective of the measurements in progress is to determine the angular distribution of the photoneutrons. A comparison of the observed distribution with predictions of the simple effective-range theory can be used to put limits on any final state interaction or momentum-dependent component in the nucleon potential. Such effects would cause spin mixing and lead to an interference term in the photoneutron distribution. Such terms are absent in the predictions of the effective-range theory.

2. Nonresonant (γ, n) Reactions in the Mass Region $A \approx 60$
(H. E. Jackson, R. J. Holt, and W. M. Wilson)

The nuclei in the region of Cr and Ni are of particular importance in the channel theory of neutron capture. Strong nonresonant reactions which vary rapidly with changing atomic mass are predicted. The reaction amplitudes for such processes can be established in photoneutron spectra directly from the asymmetry produced by the interference between the reaction amplitude due to an isolated resonance and the underlying nonresonant amplitude. The threshold photoneutron technique is particularly well suited for measuring resonance shapes because of the absence of significant multiple scattering of the emerging neutron. Precision measurements of the line shapes for low energy s-wave resonances in ^{53}Cr and ^{61}Ni have been performed at the ANL threshold-photoneutron facility. The initial analysis of the data indicates that a very strong nonresonant amplitude is present in the $^{53}Cr(\gamma, n)$ reaction, but almost zero within experimental error in the reaction ^{61}Ni (γ, n). This is precisely the trend predicted in the original theoretical intermediate-coupling calculations of channel capture. Efforts are continuing to explore the connection between such nonresonance reactions and correlations between the strengths for neutron and radiative decay of the resonant states.

3. Ground-State Radiation Widths Near Photoneutron Threshold for the A = 140 Mass Region (R. J. Holt and H. E. Jackson)

The E1 and M1 ground-state radiation widths have been measured for levels in ^{138}Ba and ^{140}Ce using the threshold-photo neutron method. The time-of-flight spectra for a target of ^{138}Ba are shown in Fig. C-1. The multipolarities of these states were determined by observing the photoneutron spectra simultaneously at reaction angles of 90° and 135°. The M1 ground-state radiation widths are expected to be enhanced for nuclei with A ≈ 140, since nuclei in this mass region are near a closed neutron shell ($1h_{11/2}$) and the $1h_{9/2}$ neutron orbital is vacant. In addition, the protons in the $1g_{9/2}$ orbital can also be excited to the vacant $1g_{7/2}$ orbital by M1 radiation. Hence, we expect a collective M1 resonance in this mass region. We have discovered and evidence of a giant M1 resonance in the ^{138}Ba nucleus at an excitation energy of 8.6 MeV. In addition, the E1 photon reduced widths were deduced for the ^{140}Ce(γ, n_0) ^{139}Ce and ^{138}Ba(γ, n_0) ^{137}Ba reactions. For this purpose, a new method has been developed for extracting ground-state radiation widths in the presence of nonground-state transitions.

4. Threshold Photoneutron Polarization in the ^{208}Pb$(\gamma, \vec{n}_0)$ ^{207}Pb Reaction: A New Method for Threshold Photoneutron Spectroscopy (R. J. Holt, H. E. Jackson, and W. M. Wilson)

Preliminary measurements of the threshold-photoneutron polarization from the ^{208}Pb$(\gamma, \vec{n}_0)$ reaction have been performed. This work represents the first time that polarization of photoneutrons has been measured as a continuous function of energy near threshold. The need for observing the polarization of the photoneutrons in this reaction arises from the fact that a measurement of the angular distribution of the photoneutrons is not sufficient to determine the multipolarity of the photoexcitation. The ^{208}Pb nucleus is particularly interesting, since the theoretical calculations involving the M1 spin-flip transitions have been performed in detail. These calculations predict that an M1 giant resonance exists in ^{208}Pb at an excitation energy of 7.9 MeV. The polarization of the photoneutrons was detected using a liquid ^{16}O polarimeter. In order to reduce systematic errors in the polarization measurement to negligible amounts, we are presently constructing a neutron spin-precision solenoid which is suitable for use with a continuous spectrum of neutrons. The preliminary polarization measurements indicate that there is considerable M1 strength in ^{208}Pb at excitation energies near 7.9 MeV.

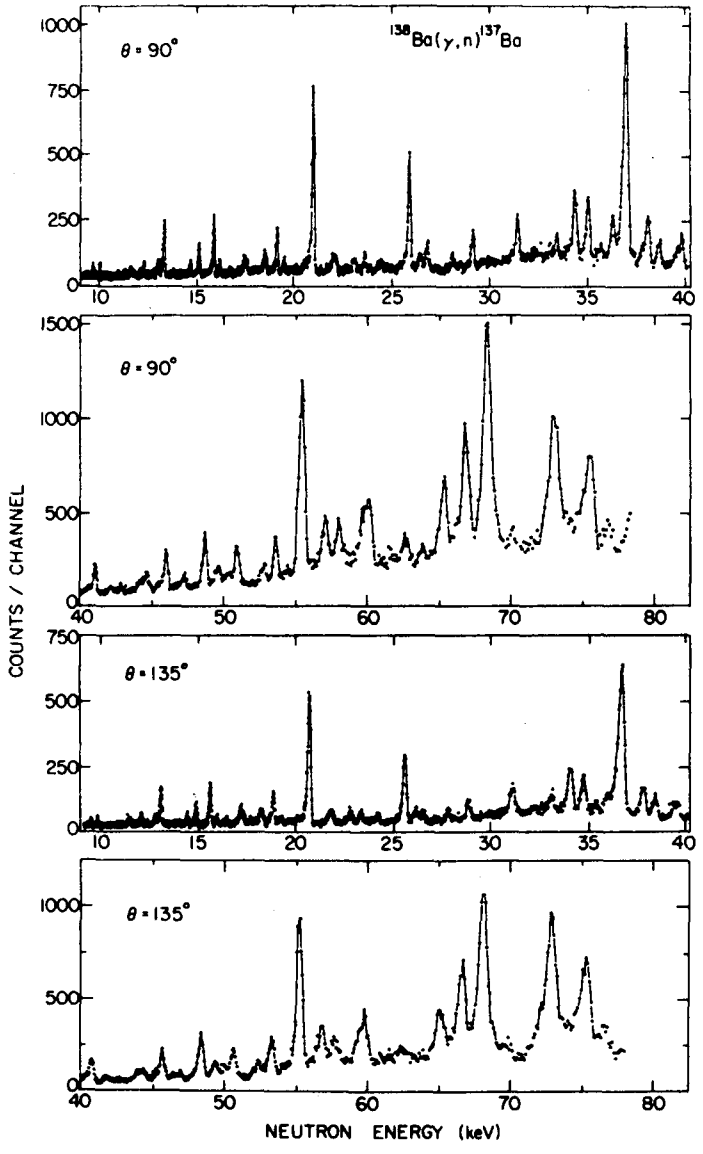

Fig. C-1. Photoneutron time-of-flight spectrum for $^{138}Ba(\gamma,n)^{137}Ba$ at angles of 90° and 135°.

5. Nuclear Raman Scattering of 11.4-MeV Photons (H. E. Jackson, G. E. Thomas, and K. J. Wetzel)

Studies of the elastic and inelastic scattering of 11.4 MeV photons were completed during 1974 at the internal-target facility of the CP-5 reactor, and a paper summarizing the results was completed The beam of 11.4-MeV photons used in these measurements was generated by an internal capture target enriched in ^{59}Ni. This target was obtained by irradiating a 25-g sample of normal Ni for 90 days in the HFIR reactor at ORNL and transferring it to the CP-5 internal target facility. Absolute differential cross sections were measured for photon scattering by nuclei ranging from ^{141}Pr to ^{238}U. Inelastic scattering which leaves the residual nucleus in a state of the ground-state rotational band was measured relative to elastic scattering. The data confirm the trends observed in earlier ANL measurements at 10.83 MeV. The strength of inelastic scattering is systematically weaker than predicted by a simple models of the giant-dipole resonance. The discrepancies are significant in the lanthanide region and may be viewed as evidence for the existence of a small direct nonresonant reaction component in the region of the giant-dipole state.

D. SLOW NEUTRON PHYSICS

1. A Comparison of the γ-ray Spectra from Thermal Neutron Capture and 2.81keV Neutron Capture in ^{23}Na (W. M. Wilson, G. E. Thomas, and H. E. Jackson)

The γ-ray spectra from thermal neutron capture and neutron capture in the 2.8 keV resonance by ^{23}Na have been measured with the high-resolution annihilation pair spectrometer at the internal target facility of CP-5. The thermal measurement involved standard techniques. The 2.8-keV resonance was populated by using the "average resonance" technique: a 1/4 in filter of ^{10}B surrounding the Na sample reduced capture below ~2 keV to a negligible level; capture above 2.8 keV is negligible because of the $1/E$ spectrum of incident neutrons and because the nearest resonance having an appreciable neutron width is at $E_n \approx 53$ keV. The average spectrum is shown in Fig. D-1 where the arrows refer to the strongest Na lines determined in preliminary analysis. For each of these lines a corresponding capture line is observed in the thermal spectrum. Captive predominantly in the 2.8-keV resonance is indicated by a ~2 keV shift in the energies of these (primary) transitions relative to those observed in the thermal capture. A comparison will be made between the relative intensities of each measurement to determine the extent to which the 2.8-keV resonance contributes to the thermal

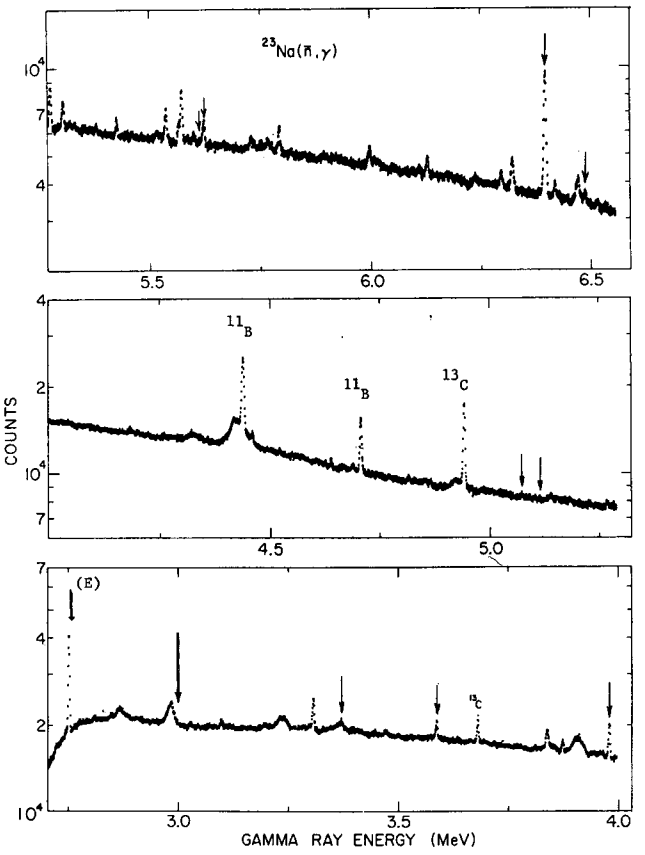

Fig. D-1. Neutron capture gamma-ray spectrum for a sample of ^{23}Na surrounded by a 1/4" - ^{10}B filter. The filter selectively removes slow energy neutrons and thus reduces capture below the 2.8-keV resonance to a negligible level. The arrows refer to primary transitions from the 2.8-keV resonance as determined from a preliminary analysis.

capture cross section.

2. Average Method of Neutron Capture γ-Ray Spectroscopy: ^{176}Lu, ^{177}Lu (W. M. Wilson, G. E. Thomas and H. E. Jackson)

The γ-ray spectra from neutron capture in a broad band of states in ^{175}Lu and ^{176}Lu has been measured at the internal target facility of the research reactor CP-5. A 1/4 in ^{10}B filter surrounding the lutetium sample reduced thermal capture to a negligible level and thus provides an average over many states in the compound nuclei ^{176}Lu and ^{177}La. Preliminary analysis indicates a clear separator between the relative strengths of the E1 transitions and M1 transitions. This information enables one to determine the parities of and place limits on the spins of the final states. Of greater interest is the absolute magnitude of the E1 and M1 strength functions. Additional measurements, which complement the present measurement, must be made to determine the absolute strengths. Several techniques to do this are presently being investigated.

3. Thermal Neutron Capture Gamma Rays from Neutron Capture in ^{59}Ni and ^{63}Ni. (W. M. Wilson, G. E. Thomas, and H. E. Jackson.

The thermal neutron capture γ-ray spectra of ^{60}Ni and ^{64}Ni were measured with the high resolution annihilation pair spectrometer at the internal target facility of the research reactor CP-5. The sample, consisting of the long-lived ^{59}Ni and ^{63}Ni isotopes (as well as the stable isotopes ^{58}Ni, ^{60}Ni, ^{61}Ni, ^{67}Ni and ^{64}Ni) was prepared by irradiating natural nickel in a high neutron flux at the Oak Ridge high flux isotope reactor (HFIR). The data are plotted in fig. D-2 where the arrows indicate primary transitions from the nickel compound nuclei. The improved precision of the present data results in more accurate estimates of neutron binding energies of the nickel isotopes than was previously available; for ^{64}Ni, $B_n = 9656.7 \pm 0.4$ keV; ^{62}Ni, $B_n = 10595.6 \pm 0.7$ keV; ^{61}Ni, $B_n = 7819.4 \pm 0.4$ keV; ^{60}Ni, $B_n = 11387.9 \pm 0.7$ keV; ^{59}Ni, $B_n = 9000.0 \pm 10.4$ keV. The distribution of the γ-ray strength provides a qualitative test of the predicted strong correlations between the γ-ray reduced transition probabilities and the (d, p) single particle strengths of the final states. The correlations have been verified for neutron capture by, and (d,p) stripping on, even mass target nuclei. The γ-ray strength is observed to be peaked at high energies corresponding to the large single particle strengths of the final states. Until now,

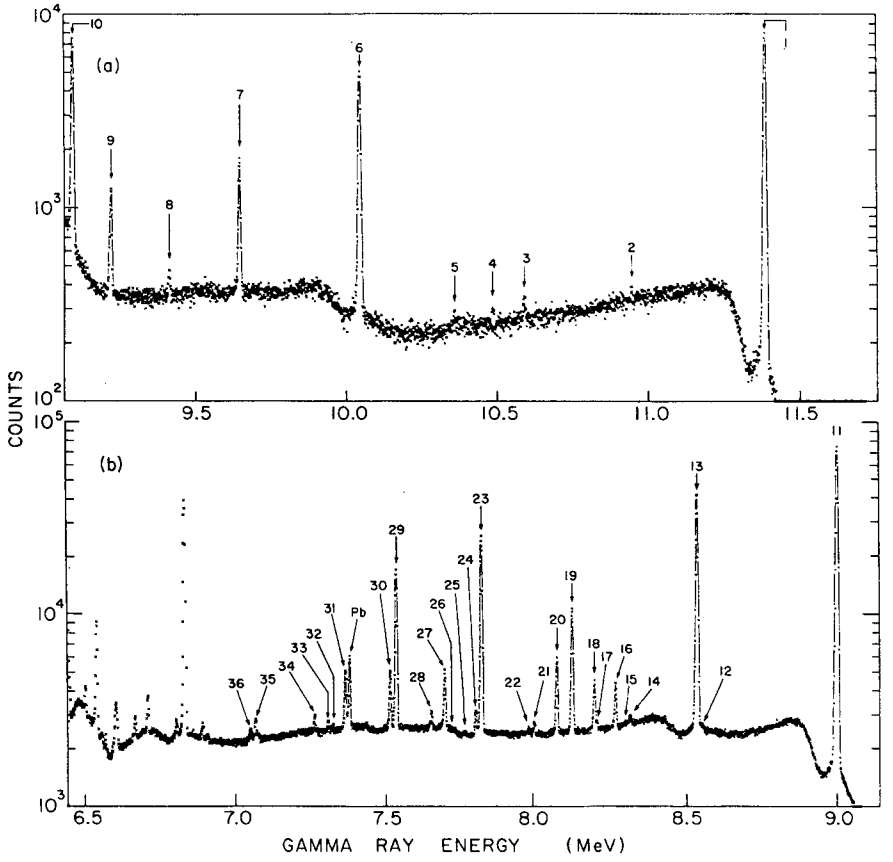

Fig. D-2. Thermal neutron capture γ-ray spectrum above 7.0 MeV for irradiated nickel.

no test was made for odd mass target nuclei. It is expected that the γ-ray strength will not be as strongly peaked at high energy since the single particle strengths for (d,p) stripping on odd mass target nuclei are much smaller than those for even mass target nuclei. The present data support this conjecture: The transitions to the ground and first excited states exhaust only ~20% of the total capture cross section in ^{59}Ni and ~31% in ^{63}Ni compared, for example, to ~62.3% in ^{60}Ni and ~77.3% in ^{62}Ni.

A. NEUTRON-NUCLEAR PHYSICS

1. Fast Chopper

a. Survey of Direct Capture in 4s Giant Resonance
(R. E. Chrien, G. W. Cole and J. B. Garg)

The radiative capture of epithermal neutrons has received extensive theoretical and experimental attention. While the majority of experimental efforts have concerned the properties of capture in discrete resonances, or of average capture, theoretical descriptions of the capture process include a direct, or nonresonant, component which is also significant in any discussion of the reaction mechanism.

The collision matrix $U_{cc'}$ from which the radiative capture cross section is calculated may be decomposed into two components:

$$U = U(ch) + U(int)$$

where U(ch) describes the contribution due to channel interactions, external to the target nucleus, and U(int) arises from the incident nucleon's interactions in the interior of the nucleus. The channel term may be further decomposed,

$$U(ch) = U(ch\ res) + U(hs)$$

where "hs" means "hard sphere." The internal term gives rise to the usual statistical capture process, in which partial radiative widths obey the Porter-Thomas distribution. The channel resonance term, which also gives a cross section having Breit-Wigner resonance shapes, leads to partial radiative widths which are proportional to the resonance reduced neutron widths. Finally, the "hard sphere" term contributes a non-resonant component, proportional to $1/v_{neut}$, to the cross section. While the hard sphere capture is not included in most discussions of statistical behavior of epithermal neutron capture, neither is it non-statistical behavior in the usual sense. Rather it is a consequence of the scattering of the incident neutron by the nuclear potential into a bound final state.

To the extent that U(ch res) is important, the non-resonant, or "direct capture contains a second term

$$U(direct) = U(hs) + U(ch\ res\ dist\ level).$$

The existence of the distant level contribution arises because, in the presence of significant channel capture, partial radiative width amplitudes are no longer random in sign and magnitude. Thus the tails of distant resonances can sum to give a 1/v term in the cross section. This mechanism is the same as that which gives rise to correlations between radiative and neutron widths.

Using the fast-chopper, time-of-flight facility, we have been attempting to identify the direct capture contribution to the collision matrix through its interference with the sharply-varying resonance amplitudes.

The data thus obtained are analyzed according to a multi-level formula for well-separated resonances:

$$\sigma_{n\gamma f}(D) = \pi\lambda\lambda^{o}\sum_{J} g(J)\left| D_{f}^{o}(J) + \sum_{\lambda}(\Gamma_{\lambda n}^{o})^{\frac{1}{2}}(\Gamma_{\gamma\lambda f}^{\frac{1}{2}})/(E-E_{\lambda}+i\Gamma_{\lambda}/2)\right|^{2}$$

where D_{f}^{o} is the energy independent amplitude for direct capture to the final state f, E is the neutron energy and J is the resonance spin. A non-linear least squares technique is used to fit the measured values of $\sigma_{n\gamma f}(E)/\sigma_{n\gamma}(E)$ to this function, yielding a value of the amplitude D_{f}^{o} and its sign with respect to the resonance amplitudes.

In evaluating the results, several points are of importance: 1) the hard sphere and channel components of direct capture cannot be experimentally distinguished; 2) the direct capture cross section depends on the single particle nature of the final states, so that final states of low spectroscopic factors should show little direct capture; 3) as a consequence of 2), we can expect the direct capture process to give spectroscopic information similar to the (d,p) reaction.

For the five targets for which analysis has been completed to date, Table A-1-1 lists the derived values for the direct cross section, evaluated at En = 0.0253 eV. The table also indicates the Nilsson orbital assignments for the final states examined in these nuclides. Where lower and upper limits are given, the ambiguity is due to uncertainty about the relative phases among the local levels included in the multilevel fit. This same ambiguity is responsible for the tabulation of the ^{152}Sm results as upper limits; e.g. in the case of the 36 keV level, one resonance phase set gives $\sigma_{D}\sim 0$, while another set gives $\sigma_{D}\sim 70$mb with an equivalent quality of fit.

For the dysprosium isotopes, the states which exhibit

Table A-1-1

Target	Final State (keV)	σ_D(mb)*	J^π	Assignment from (d,p)
^{162}Dy	351	86	$1/2^-$	$1/2^-[521]$
	389	139	$3/2^-$	$1/2^-[521]$
	421	253	$3/2^-$	$3/2^-[521]$
	820	<6	$3/2^-$	a
	1051	<5	$3/2^-$	a
	1057	300	$(1/2^-,3/2^-)$	b
^{164}Dy	108	139	$1/2^-$	$1/2^-[521]$
	158	>100 <500	$3/2^-$	$1/2^-[521]$
	539	<9	$(3/2^+)$	c
	572	<12	$1/2^- + 3/2^-$	d
	606	<12	$(3/2^-)$	γ-vibration
^{152}Sm	36	<70	$3/2^-$	$3/2^-[521]$
	127	>34 <250	$3/2^-$	$3/2^-[532]$
	406	<30	$3/2^-$	$1/2^-[530]$
	630	<55	$3/2^-$	$\{[521],0^+\}+\{[532],0^+\}$
	696	<30	$1/2^-$	e
	750	<36	$3/2^-$	e
^{156}Gd	0	<14.7	$3/2^-$	$3/2^-[521]$
^{170}Yb	0	<15	$1/2^-$	$1/2^-[521]$

* The uncertainty in σ_D is $\sim \pm 20\%$.

a) Not seen in (d,p) reaction.

b) d,p studies place a $1/2^+$ level at 1058 keV. However, the strength of the primary (n,γ) transition implies a negative parity. Each reference lists only one level populated by (d,p) at about this energy.

c) One level, at 535 keV is seen in (d,p). Other work suggests a possible doublet and assign the 535 keV state to a γ-vibration.

d) This level is a doublet, assigned to a γ-vibration.

e) These levels are seen in (d,p), but no assignment is made. The 696 keV level is very strongly populated in (d,p).

significant direct capture are those which are known from the (d,p) experiments to be of good single particle character, while those which show weak direct capture are in general weakly populated by stripping.

In the possible case of a target exhibiting significant partial width correlations, we expect two coherently contributing amplitudes for non-resonant capture. On the other hand, for a nucleus in which ρ is small, the direct capture should be accounted for by the hard sphere term. In this case, the direct capture term provides a spectroscopic probe of the final state. A more sophisticated calculation of the hard sphere capture, taking into account the detailed nature of the final states and the shape of the potential in these deformed nuclei, would allow further information to be extracted from these results.

Recently-run targets in this series include Gd-158, Gd-160, Er-164, Er-166, Er-168 and Er-170. Data analysis is in progress for these nuclides and will be presented in the near future.

A. 2. Tailored Beam Facility

a. Energy Levels of Gd-155 and Gd-157 Populated by the (n,γ) reaction at 24.3 keV

(R. C. Greenwood, C. W. Reich, Aerojet Nuclear Corp.; R. E. Chrien, K. Rimawi, BNL)

The properties of a 24-keV neutron beam, obtained from HFBR through an Fe+Al+S filter, which make it a useful tool in nuclear spectroscopy have been studied. As an application of these techniques, the prompt γ-rays from 24-keV neutron capture in Gd-154 and Gd-156 have been measured.

The initial measurements have been concerned with the low-energy level structure of Gd-155 and Gd-157. While previous decay-scheme and charged-particle-induced reaction studies have provided valuable insight into the structure of these nuclei, there are still serious gaps in our knowledge. Neutron-capture γ-ray studies can provide much additional information about these nuclei but, because of the very large thermal-neutron capture cross sections of the neighboring isotopes Gd-155 and Gd-157 and the fact that most (n,γ) reaction studies are carried out using thermal neutrons, little such data exist. The only such information currently available is that for the Gd-156 (n,γ) reaction. For (n,γ) studies using keV neutrons, however, the Gd-155 and Gd-157 cross sections do not seriously interfere, and the Gd-154(n,γ) and Gd-156(n,γ) reactions can meaningfully be studied using samples with presently obtainable enrichment.

The Fe+Al+S filter arrangement used provides a clean 24-keV neutron beam with an energy width of $\sim$ 2 keV. In consequence, the resultant Gd-154(n,γ) and Gd-156(n,γ) spectra represent an average over $\sim$ 130 and $\sim$ 42 resonances, respectively. Hence, if s-wave capture predominates we expect $I^{\pi} = 1^-/2$ and $3^-/2$ final states to be more strongly populated by primary transitions than those with $I^{\pi} = 1^+/2$ and $3^+/2$, since E1 primary transition strengths are typically a factor of 5-10 greater than M1 strengths in this region. Because I^{π} values for many of the low-lying states in Gd-155 are firmly established it is instructive to examine the spectrum from the Gd-154(n,γ) reaction (Fig. A-2-1) to see to what extent this is found to be true. In this spectrum we note that the final states with $I^{\pi} = 1^+/2, 3^+/2$ and $5^+/2$ are populated with intensities similar to those having $I^{\pi} = 1^-/2$ and $3^-/2$ (see Fig. A-2-2). From this we conclude that the s- and p-wave neutron capture rates at $\sim$ 24 keV are comparable. Even though the s-wave strength function is at a maximum and the p-wave strength function is at a minimum at this mass region, the observation is not unexpected, since a simple estimate of the relative p- and s-wave capture cross sections in this specific case, ignoring the fluctuation

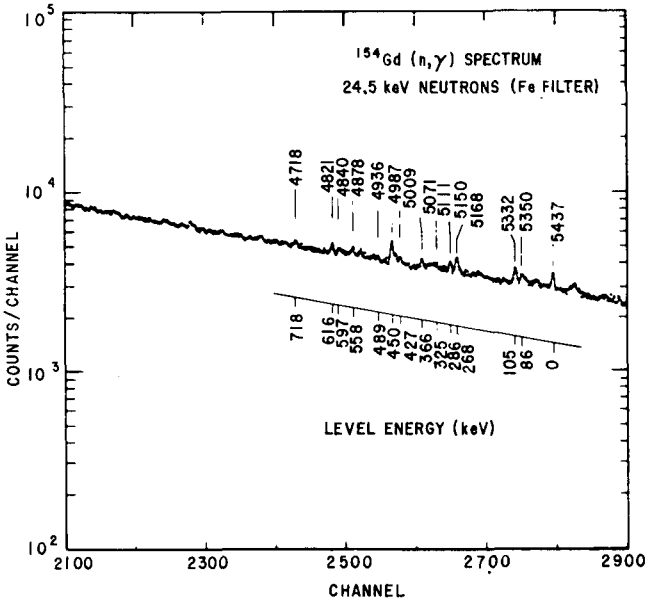

Fig. A-2-1. High-energy portion of the spectrum of γ rays from 24-keV neutron capture in Gd-154.

corrections, gives

$$\frac{\sigma_1}{\sigma_0} \sim \frac{3S_1}{S_1} \frac{\langle \Gamma^0 \rangle}{\langle \Gamma^1 \rangle} (kR)^2 \sim 0.5 \text{ for Gd-154,}$$

$$\text{using } S_0 = 2.0\text{x}10^{-4} \text{ and } S_1 \sim 1\text{x}10^{-4}.$$

This feature of the 24-keV neutron-induced reaction complicates the analysis, in that it makes unambiguous parity assignments for the final states difficult to achieve on the basis of the primary γ-ray intensities alone. This amplification of the primary transition strength to the positive-parity states (relative to the case of only s-wave capture), however, allows with reasonable certainty the observation of all states in Gd-155 with $I^\pi = 1^+/2$ and $3^+/2$, as well as those with $I^\pi = 5^+/2$.

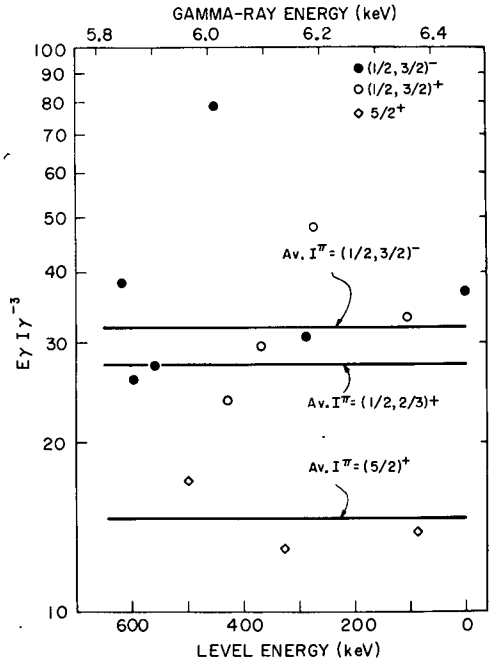

Fig. A-2-2. Plot of reduced transition intensities ($I_\gamma E_\gamma^{-3}$) for the primary γ-rays from the capture of 24-keV neutrons in Gd-156.

In order to distinguish between final states with positive and negative parity, additional experiments are necessary using lower energy neutrons, such as the 2-keV neutrons obtained through a Sc filter or the ~ 1 keV neutrons obtained through the ^{6}Li filter installed in HFBR. The Gd-156(n,γ) spectra shown in Fig. A-2-3 provide a comparison of the spectral structure observed with 24- and 1-keV neutron capture. Using the above estimate for the relative p- and s-wave capture cross sections, we calculate that σ_1/σ_0 are ~ 1.0 and

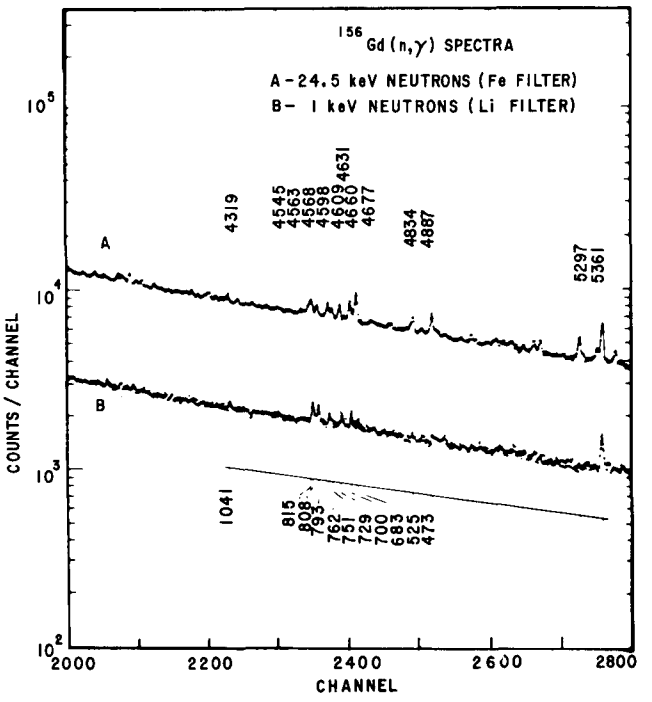

Fig. A-2-3. Comparison of the high-energy γ-ray spectra from capture of 24- and ~ 1-keV neutrons in Gd-156.

~ 0.02 for 24- and 1-keV neutron capture, respectively (using values of $S_0 = 1.8 \times 10^{-4}$ and $S_1 \sim 1 \times 10^{-4}$). Hence, primary transitions to those final states with $I^{\pi} = 1^-/2$ and $3^-/2$ will predominate in the 1-keV neutron capture spectrum, and a comparison of the two spectra should provide unique parity assignments for the final states populated. This spectral change is especially dramatic in the suppression of the primary transitions to the $5^+/2$ states in the 1-keV neutron capture spectrum.

Table A-2-1

Comparison of energies and I^{π} assignments in Gd-157 determined from the Gd-156(n,γ) reaction using the Fe+Al+S and ^{6}Li filtered neutron beams, with energies of 24 and ~ 1 keV respectively, obtained from HFBR.

Levels populated in 24.5 keV neutron capture[a] (keV)	Levels populated in ~1 keV neutron capture[a] (keV)	Proposed I^{π} Assignment	Previous assignments: level energy (I^{π})
0 (38.5)	0 (38.9)	$(1/2,3/2^-)$	0 $(3/2^-)$
63.8 (21.8)	(<6.8)	$(1/2\text{-}5/2^+)$	64.0 $(5/2^+)$
474.0 (30.0)	473.5 (14.5)	$(1/2,3/2^-)$	474.6 $(3/2^+)$
525.6 (18.6)	(<6.5)	$(1/2\text{-}5/2^+)$	527 $(5/2^+)$
683.5 (55.1)	683.3 (14.3)	$(1/2,3/2^-)$	685 $(1/2^+)$
700.8 (32.7)	701.4 (24.0)	$(1/2,3/2^-)$	700 $(3/2^-)$
700.8 (32.7)	701.4 (24.0)	$(1/2,2/2^-)$	702 $(1/2^-)$
729.5 (26.2)	729.1 (23.5)	$(1/2,3/2^-)$	
751.1 (15.1)	(<10.0)	$(1/2\text{-}5/2^+)$	746 $(3/2^-)$
762.6 (24.8)	763.0 (20.7)	$(1/2,3/2^-)$	
792.4 (19.5)	793.9 (36.6)	$(1/2,3/2^-)$	
807.7 (20.5)	809.4 (46.2)	(1/2,3/2)	811 $(3/2^-)$
815.6 (16.3)	(<10.0)	$(1/2\text{-}5/2^+)$	

[a] The values of the reduced intensity (relative $I_{\gamma}E_{\gamma}^{-3}$) are given in parenthesis after the level energies.

A. 2. Tailored Beam Facility

b. Activation Cross Sections at 24.3 keV
(K. Rimawi and R. E. Chrien)

We have measured a number of cross sections by the activation technique by making use of the relatively clean, intense neutron beam available through the iron window at the HFBR tailored-beam facility.

The availability of a strong neutron beam ($\sim 10^7$ n/sec) allows allows the use of thin targets to obtain adequate counting statistics. This reduces multiple scattering effects considerably. The neutron beam was derived from the High Flux Beam Reactor at Brookhaven through a filter composed of 9 inches of iron, 14 inches of aluminum and 2 inches of sulfur. A sheet of cadmium, 0.8 mm thick, was placed at the exit opening of the neutron collimator, which has a square cross section area of 1" x 1".

The cross sections studied were those of In-115, I-127, Au-197 and U-238. Two main points dictated the selection of the nuclei to be used. U-238 was studied because of the importance of this cross section in reactor calculations. The other three were studied since they are widely used as standards in capture measurements.

The sample was viewed by a 12 cm^3 germanium detector whose axis was 90^o with the neutron beam. The detector viewed the sample through a two inch ^6LiH neutron shield. Gamma spectra were accumulated both during the irradiation of the sample and the subsequent decay after the beam was turned off.

The detector efficiency was determined, for the same geometry, using a series of sources with γ-cascades overlapping the region of interest. The portion of the efficiency curve pertinent to these measurements is shown in Fig. A-2-4.

One of the largest sources of uncertainty in activation measurements is the value for the standard cross section used in the experiment. For a standard the $^{10}B(n,\alpha\gamma)^7Li$ reaction was selected since this cross section is well established. A total cross section of 5.9175 barns and a partial $(n,\alpha\gamma)$ cross section of 3.4875 barns as derived from INDEF B-III tabulations, were used.[1]

Boron samples were made of boron powder between two glass plates. The glass was checked for boron content and was determined to be boron-free. The sample was chemically and isotopically analyzed for boron and ^{10}B content. It was found to be 93.14% boron of which 92.818% was boron-10. This sample was used for measuring the gold activation cross section.

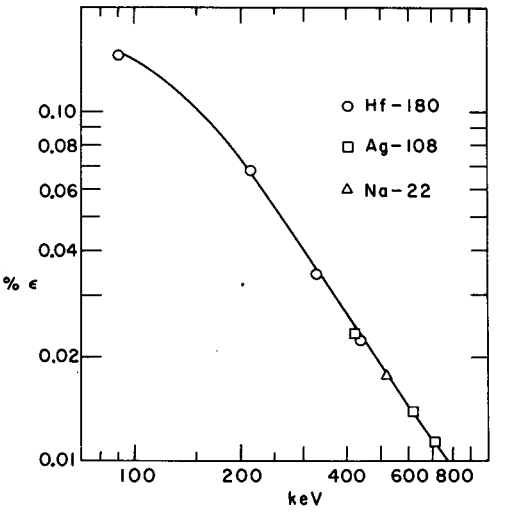

Fig. A-2-4. The efficiency curve for the GeLi detector.

Once a value for the gold cross section was established it was used in turn in conjunction with the other three samples as a standard. This was done to avoid the tendency toward settling exhibited by the powder samples, as well as the problem of water absorption and the effects of sample holder walls.

The branching ratios for the different gamma rays emitted in the decay process were taken from the Table of Isotopes compilation.

Typical counting statistics in the experiment ranged from 0.5% for gold to 2.4% for uranium. Errors in sample thickness and non-uniformities were less than 2.0%. Relative detector efficiency error estimates ranged from negligible (for ^{115}In) to 7% for U-238, while errors in half-lives and branching ratios were in the range of 1.0 to 3.0%. Absorption corrections for neutrons and γ-rays were typically less than 5%, except for U-238 where absorption corrections of up to 12% for the low energy γ-rays had to be applied.

$^{197}Au(n,\gamma)^{198}Au$

The sample consisted of a gold sheet 1.48×10^{-3}

atoms/barn thick combined with a boron sample which was 3.24×10^{-3} atoms/barn thick. We measured the intensitity of the 412 keV line, following Au-198 beta decay against the 478 keV gamma ray emitted in the $^{10}B(n,\alpha\gamma)^{7}Li$ process. The sample was irradiated for a period of 61 hours while the gamma ray spectrum was being recorded. Spectra were also recorded during the decay of ^{198}Au for a period of 129 hours.

Using the above-mentioned values for the boron cross section and correcting for the neutron and gamma ray attenuation in the sample, one obtains a cross section of 630±17 mb, exclusive of error in the ^{10}B standard.

$\underline{^{238}U(n,\gamma)^{239}U}$

The decay of U-239 through Np-239 leads to several excited states in Pu-239, and we used the resulting γ-ray transitions of 228 keV and 278 keV to measure the cross section. These lines were measured relative to the 478 keV B-10$(n,\alpha\gamma)$ line and the 412 keV gold activation γ-ray.

Two separate measurements were carried out. The first measured the uranium cross section relative to that of boron-10. The second used gold as a standard. The uranium samples in both experiments were 4.7×10^{-4} atoms/barn thick. The boron sample was the same used in conjunction in the gold measurement. The sample was irradiated for 65.5 hours. The decay spectrum was accumulated for 46.5 hours.

In the second measurement the sample was made small enough to be entirely covered by the neutron beam. The gold sample was 6.13×10^{-4} atoms/barn thick. The samples were irradiated for a period of 55 hours. The decay run was 84 hours. The two measurements agreed within statistical errors. The cross section averaged over the two measurements was found to be 475 ± 36 mb.

$\underline{^{115}In(n,\gamma)^{116m}In(54.0\ min + 2.2\ sec)}$

The cross section for populating the 60 keV isomeric state in In-116 was determined by counting the 417 keV gamma ray relative to the 412 keV gold line. Three separate measurements were taken with different sample sizes and thicknesses. Gold was used as a standard in all three measurements. The thickest gold sample was 1.45×10^{-3} atoms/barn thick, while the In samples were less than 4.85×10^{-4} atoms/b thick. The runs were typically about 20 hours irradiation time, and a few hours decay time. A cross section of 469 ± 28 mb was obtained from the average of three measurements.

$^{127}I(n,\gamma)^{128}I$

Iodine was obtained in powder form and packaged between glass plates. The 441 keV gamma ray emitted in the decay of ^{128}I was used to measure the activation cross section.

Two measurements were carried out one relating to the cross section of gold, and the second relative to the cross section of In. The I samples were 4.80 x 10^{-3} atoms/barn thick while the gold was 1.54 x 10^{-3} atom/barn and the indium was 5.84 x 10^{-4} atoms/barn thick. The runs consisted of a 22 hour irradiation time for the gold-reference run and two hour irradiations for the In-reference run. Decay times of a few half lives were taken. An average cross section of 722 ± 47 mb was obtained when averaging the two runs.

Discussion of Results:

^{197}Au

The present result of 630 ± 17 mb is in good agreement with the results of Macklin at Oak Ridge. Macklin has measured the Au capture cross section relative to a ^{6}Li flux monitor. When this cross section, measured in 250 eV intervals, is folded into the spectral distribution of the 24 keV Fe-filtered beam, a value of 622 mb is obtained. The agreement between the two methods is excellent.

^{238}U

The interpolated value for $\gamma^{238}U(n,\gamma)$ at 24.3 keV in the ENDF/B IV evaluation is 487 mb. The present value of 475 ± 36 mb is in good agreement with this evaluation.

^{127}I

Activation results with a Sb-Be source from Robertson yield a value of 832 ± 26 mb, while the corrected sphere transmission results of Schmitt and Cook yield 768 ± 90 mb. The same data as interpreted by Bogard and Semler yield 800 ± 80 mb. The present result of 772 ± 47 mb is significantly lower than the Sb-Be measurement, but in agreement with the transmission measurements.

^{115}In (54 min + 2.2 sec)

This activity can be accurately measured by the present technique since the daughter ^{116}Sn contains a γ-ray at 417 keV, close to 412 keV Au standard. The present value of 469 ± 28 mb is lower than the value of 580 ± 40 reported by Chaubey and Seghal, who used an Sb-Be

source. Their value is, however, based on $\sigma_{act}(I)$ = 820 mb at 24 keV. Renormalized to the value measured here, the Chaubey and Seghal result would be 511 ± 35 mb, in reasonable agreement with our measurement.

c. Characteristics of p-Wave Capture γ-Ray
(K. Rimawi and R. E. Chrien)

For s-wave capture in heavy nuclides, the behavior of the partial cross sections for radiative transitions to discrete final states is seen to follow reasonably well the predictions of a statistical decay model; namely that the partial widths $\Gamma_{\gamma\lambda f}$ follow an approximately Porter-Thomas distribution and that correlations between partial widths are small and negligible.

The situation for p-wave capture near the 3p giant neutron resonance is markedly different. In this region the low-lying states have a predominantly ℓ=0 and ℓ=2 character; the strengths of γ-rays feeding these states are correlated with the single particle reduced widths of these states as measured by the (d,p) reaction.

We have previously reported these effects for capture in the even isotopes of Mo. In the present experiment we report similar results obtained for Nb-93. Figure A-2-5 illustrates the spectrum

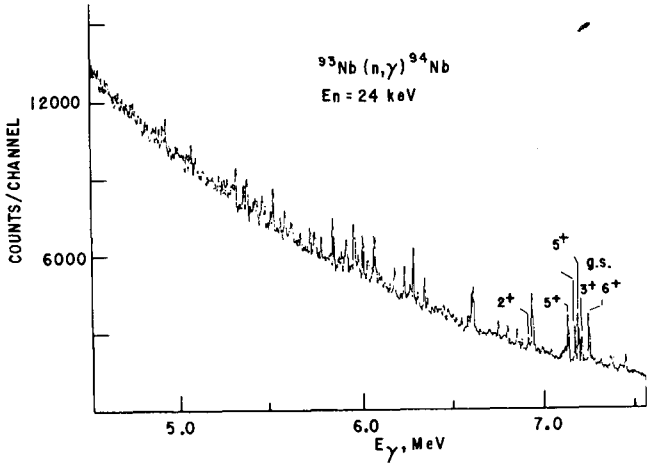

Fig. A-2-5. A portion of the capture spectrum for 24.3 keV neutrons on ^{93}Nb.

obtained for p-wave capture of 24.3 keV neutrons incident on niobium. Consistent with the high level density of ^{94}Nb, we see a complex spectrum. Nevertheless we can observe, qualitatively that all six states of the ground state configuration $\pi(g_{9/2})\nu(d_{5/2})^3$, are populated strongly, including the 2^+ state at 334 keV, and the 7^+ state at 79 keV.

A striking pattern for these radiative transitions is noted when we compare the average (n,γ) strengths to the (d,p) reduced widths in this nuclide. Figure A-2-6 illustrates the intensity patterns obtained for (n,γ) and (d,p) on niobium.

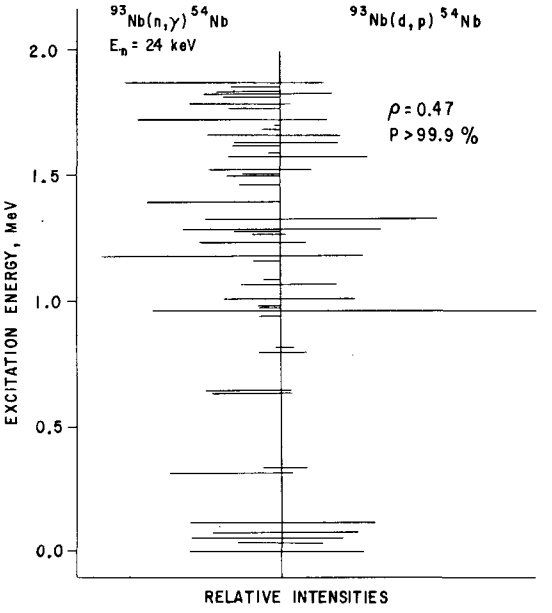

Fig. A-2-6. Partial cross sections for ^{93}Nb(n,γ) compared to (d,p) stripping widths.

We know from our previous resonance γ-ray measurements on Nb-93 that no correlation exists between resonance neutron widths and γ-ray intensities; hence a valence transition model cannot account for the observed correlation with the final state (d,p) spectroscopic factors. It seems plausible, therefore, that several overlapping doorway states exist for Nb-capture, in order to account for the final state correlation.

A.3. Neutron Monochromator

a. Systematics of the Population of Rotational Bands in Deformed Nuclei in the (n,γ) Reaction
(M. R. Macphail, R. F. Casten, and W. R. Kane)

Studies of the population of low-lying levels in the (n,γ) reaction have proved to be an important tool in determining both the statistical properties of nuclei and the specific properties of individual states. For example, Wetzel and Thomas[1] developed a method for determining the spin of a neutron resonance from a knowledge of the relative population of low-lying levels of different spins by γ-ray cascades. Coceva, et al.[2,3] have recently utilized a related technique for assigning the spins of low-lying levels of the product nucleus on the basis of the ratio of the strengths of their population by neutron capture in resonances with different spins.

In thermal neutron capture studies of ^{200}Hg and ^{202}Hg, Breitig et al.[4,5] found that the populations of levels with a given spin decrease smoothly with increasing excitation energy and fall on a curve which is separate and distinct from those for other spins, thus providing an aid for spin determinations.

These results are not unexpected, and in fact, can be reproduced well by statistical model calculations.

This work has now been extended to include deformed nuclei. In this case level populations are found to depend not only upon spin and excitation energy but upon the structure of individual levels as well.

---

1 K. J. Wetzel and G. E. Thomas, Phys. Rev. C1, 1501 (1970).

2 C. Coceva, F. Corvi, P. Giacobbe, and M. Stefanon, Conf. on Nuclear Structure Study with Neutrons (Central Research Institute for Physics, Budapest, 1972), p. 12.

3 C. Coceva, P. Giacobbe, F. Corvi, and M. Stefanon, Nucl. Phys. A218, 61 (1974).

4 D. Breitig, R. F. Casten and G. W. Cole, Phys. Rev. C9, 366, 2088 (1974).

5 D. Breitig, R. F. Casten, W. R. Kane, G. W. Cole and J. Cizewski, Phys. Rev. (in press).

A.3.a. (cont.)

Our new experimental results provide detailed information on the population of low-lying states in ^{188,190}Os in the (n,γ) reaction. The experiments were carried out at the neutron monochromator facility at the Brookhaven High Flux Beam Reactor. Both high and low energy gamma rays from the ^{187}Os(n,γ)Os^{188} and ^{189}Os(n,γ)^{190}Os reactions were studied at thermal and resonant neutron energies. We shall concentrate on ^{190}Os here since its level scheme has been more completely developed.

The principal results are as follows:

In both thermal neutron capture and in individual resonances the population strengths, as expected, generally decrease with excitation energy and may be roughly grouped according to final state spin. However, the deviations from smooth dependencies are significantly greater than observed, for example, in the Hg isotopes. Instead, smooth curves can be drawn through the populations of the levels belonging to a given rotational band. The curves for different bands are closely parallel. The regularity of this effect is striking.

In Fig. A-3-1a the relative population intensities of levels in ^{190}Os in thermal capture are presented, with lines connecting data points for levels of the same spin. Strictly speaking, the data for the 0^+ states should be considered as lower limits, since their decays by E0 transitions have not been observed experimentally, but this contribution is not expected to be significant. As for the Hg isotopes, a general decrease in population with increasing spin and excitation energy takes place, although with significant deviations from a regular behavior. Such irregularities suggest significant differences in the structure of the states concerned and thus in the characteristic channels of deexcitation by which they are populated.

The full significance of the effect of the nuclear structure of individual levels on the population systematics becomes apparent in Fig. A-3-1b, where the same data as in Fig. A-3-1a are presented, but with the curves connecting data points for states in the same rotational band, rather than states with the same spin. A striking systematic behavior is seen, with the points for each band lying on smooth curves which are essentially parallel.

Identical behavior occurs in the data for the three resonances shown in Fig. A-3-2. The curves for the two J = 1 resonances are indistinguishable and the curves for the J = 2 resonance are less steep, as expected for the higher initial spin.

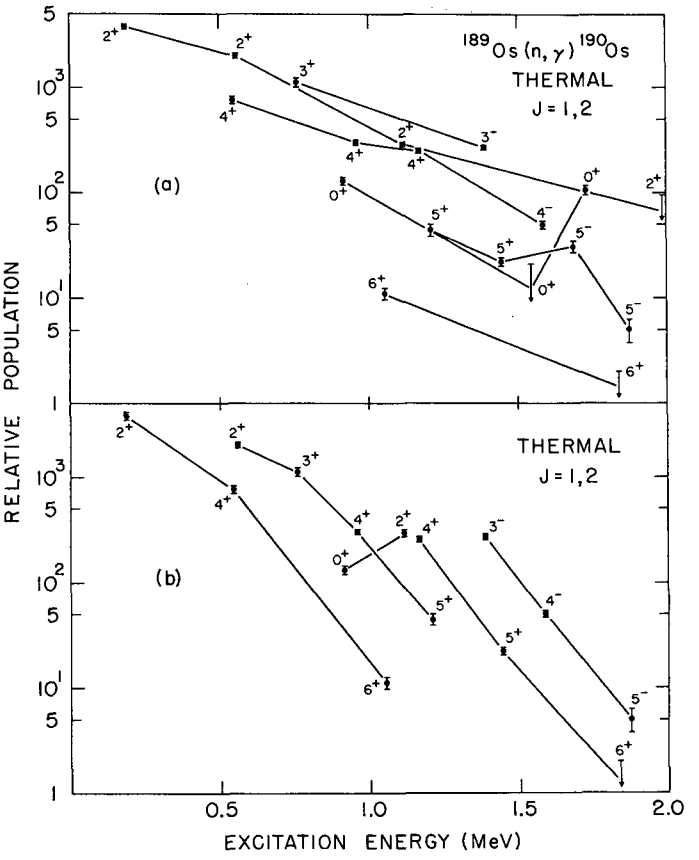

Fig. A-3-1. Relative population of the states in the ^{189}Os(n,γ)^{190}Os reaction at thermal neutron energies. Spin and parity assignments are indicated for each data point. a) The lines are drawn to connect data points for levels with the same spin. b) The same data as for part a) for states assigned to rotational bands. Each line connects the states belonging to a given rotational band.

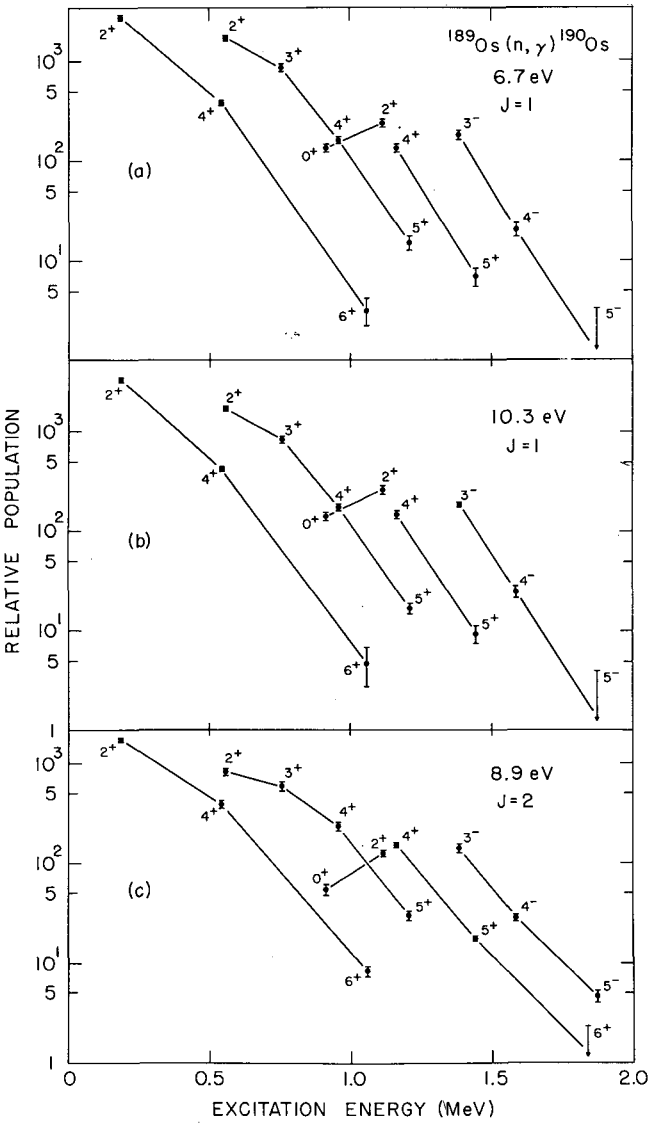

Fig. A-3-2. Relative population of states in the ^{189}Os(n,γ)^{190}Os reaction for three neutron resonances. The resonant energies and capture state spins are indicated. The ordinate scale is arbitrary for each resonance. Each line connects the states belonging to a given rotational band.

A.3.a. (cont.)

The highly systematic behavior of the population of the members of a given rotational band, together with population differences for states with different intrinsic character, can provide a powerful method for assigning states to rotational bands and for studying band structure. For example, for ^{184}W, one can distinguish by this means between two alternative assignments for a pair of states into rotational bands: These assignments are important for interpreting the fragmentation of Nilsson orbitals at high energies. The technique outlined here can also be used to anticipate the strength of transitions from a given level, and thus to test proposed deexcitation branches, or to extend rotational bands to higher spins. Finally, other interesting aspects of this problem deal with the populations of strongly mixed bands, with odd mass nuclei, in particular for $K = \frac{1}{2}$ bands, and with the systematics of overall band population for analogous bands in series of nuclei.

A.3.b. γ Decay of 0^+ and 2^+ States in $^{188,190}Os$
(M. R. Macphail, R. F. Casten, and W. R. Kane)

The level schemes of ^{188}Os and ^{190}Os have been investigated with the neutron monochromator facility at the BNL High Flux Beam Reactor. These nuclei lie between the regions of strongly deformed and spherical nuclei and are not understood simply in terms of the well established nuclear models.

Primary and secondary γ radiations from the (n,γ) reaction were studied with Ge(Li) detectors at thermal neutron energies and at resonant energies of 9.4 and 12.7 eV (for ^{188}Os) and 6.7, 8.9 and 10.3 eV (for ^{190}Os). These experiments have located low spin states up to $\sim$ 2500 keV and have provided information on their γ deexcitation modes, spins and parities.

In particular, four 0^+ excited states in ^{188}Os and three in ^{190}Os, which were established by recent (p,t) studies, are found to have remarkably similar reduced E2 branching ratios. Each of the 0^+ states decays predominantly to the 2^+ state of the γ-vibrational band rather than to the 2^+ state of the ground state band.

Low energy transitions from the 2^+ states at 1305 keV in ^{188}Os and 1114 keV in ^{190}Os show that the states are connected by large E2 matrix elements to the 0^+ states about 200 keV lower in excitation energy. The decays of these 2^+ and 0^+ states provide new confirmation of the pairing-plus-quadrupole model of Kumar and Baranger and appear to rule out recent two phonon model interpretations for these 2^+ states.

B. NATIONAL NEUTRON CROSS SECTION CENTER

1. Data Libraries

The organization and implementation of the CINDA system at NNCSC has been completed. Entries for the neutron literature produced in the USA and Canada are routinely prepared and transmitted to the CCDN at Saclay. Work has been started to upgrade the CINDA entries from the NNCSC area as to correctness and completeness. At the same time, entries relating to the same experiment are blocked together in the CINDA book.

A CINDA storage and retrieval system has been completed. The CCDN master file or updates to that file can be entered directly into the NNCSC data base. Retrievals for both customer and center use are made on a routine basis on request.

In connection with the production of the new edition of BNL-325, Vol. II, an effort is being made to improve the completeness and the correctness of the CSISRS experimental data library. In the past year, new data from 129 references have been compiled and entered into the experimental data files.

ENDF/B, Version IV has been completed. The library consists of 90 materials in the General Purpose File, 27 materials in the Dosimetry File and 770 materials in the Fission Product File. Planning for ENDF/B, Version V has been started with an estimated completion date of mid 1977.

A data file of "Requests for Nuclear Data" and related status comments have been implemented. Extensive revisions to the request and status file were made in the last half of 1974 upon completion of the USNDC review. The center supplied retrievals to the USNDC sub-committees to aid the status reviews.

Two special purpose libraries were prepared in the past year. These are a charged particle library in ENDF format for CTR purposes and a conversion into CSISRS format of the LLL photoneutron experimental data library.

Statistics for data requested from NNCSC between January 1, 1974 and March 1, 1975 are attached.

B. 2. Data Evaluation and Data Testing

Evaluation of 12 fission product nuclei ^{141}Pr, $^{143,145,146,148,150}Nd$, ^{147}Pm, $^{147,149,151,152}Sn$ and ^{155}Eu have been completed. In addition the neutron cross sections of Au were evaluated to provide general purpose files as well as the capture cross section as a standard.

A series of benchmark calculations for fast reactors and for shielding applications have been completed using the ENDF/B Version IV General Purpose File. Several thermal reactor benchmarks have been analyzed using ENDF/B-IV in an attempt to understand the present discrepancy between experiment and calculation. A seminar on U-238 resonance capture was held in March where these discrepancies were analyzed. Extensive tests have been made on the new ENDF/B Dosimetry File and the results published.

3. Publications

BNL-325, Neutron Cross Sections, Third Edition Volume 2 is now being produced from our experimental data files and will be completed in the summer of 1975. This second volume will contain graphical displays of selected experimental data sets for the integral cross sections for all elements and isotopes where such data exists. Also contained will be a more complete bibliography to the available data.

The Formats and Procedures Manual for ENDF (ENDF-102) is passing through a final editing before printing in April. The book of curves for ENDF (ENDF-200) and the summary documentation (ENDF-201) are now being printed.

4. Reactor Core Safety Analysis
(A. Aronson, A. Buslik, S. Cheng, D. Diamond, M. Levine)

The recently issued ENDF/B-IV library has been adopted as the data base to be used in performing neutronics calculations of interest in assessing nuclear reactor safety. The data were processed into thermal and epithermal libraries for use in multigroup analysis codes. The processing codes ETØG3 and HELP generated the epithermal data (0.625 eV - 10.0 MeV). FLANGE2 and LITHE were used to generate the thermal data (0.253 meV - 0.785 eV).

Table B-1

Request Statistics for

Evaluated Information

Jan. 1, 1974 to Dec. 31, 1974

1.	Requests	
	a) Number of requests	350
2.	Origin of Requests	
	a) Government Agencies	38
	b) Educational Institutions	71
	c) Industry	27
	d) Foreign (includes Four-Center Members)	28
	e) CSEWG Members	186
3.	Mode of Requests(may be more than one mode per request)	
	a) Magnetic Tapes	160
	b) Computer Listings	103
	c) Cards	3
	d) Plots	19
	e) Documentation	85
	f) Telephone	24
	g) Teletype	2

Table B-2

Request Statistics for
Experimental Information

Jan. 1, 1974 to Dec. 31, 1974

1.	Requests	
	a) Number of requests	111
2.	Origin of Requests	
	a) Government Agencies	10
	b) Educational Institutions	29
	c) Industry(includes CSEWG members)	25
	d) Foreign	2
	e) Four-Center Members	12
	f) National Laboratories(includes CSEWG members)	33
3.	Mode of Requests(may be more than one mode per request)	
	a) Magnetic Tapes	42
	b) Computer Listing	53
	c) Cards	0
	d) Plots	17
	e) Documentation	13
	f) Telephone	9
	g) Teletype	1

COLUMBIA UNIVERSITY

A. Neutron Velocity Spectrometer Total and Capture Cross Section Measurements (G. Hacken, H. I. Liou, U.N. Singh, J. Rainwater, J.B. Garg)

The NVS publications since 1 May 1974 are in Physical Review C, vol. 10 (1974) and vol. 11 (1975). Their specific references are:

volume	issue	page	element
10	#2	709	Cd
10	#5	1904	Gd
10	#5	1910	In
10	#6	2138	Cl
10	#6	2143	Ca
10	#6	2147	F
10	#6	2150	Mg
11	#2	457	Ar
11	#2	462	Dy

The cadmium results cover the isotopes whose mass number A is 110, 111, 112, 113, 114, 116. They are derived from our 1970 transmission (200 meter) and capture (40 meter) measurements. They include resonance parameters E_0 and $g\Gamma_n^0$ to 10 keV for the even isotopes, and to 2.3 keV for A = 111 and 113. Also included are 181 unassigned resonances to 10 keV. Radiation widths $\Gamma\gamma$ are given for 15 levels in Cd-111, and for 19 levels in Cd-113. Total angular momenta (J) are given for 11 and 14 levels respectively in Cd-111 and Cd-113. The total number of individual resonances covered is 570. Results of the analysis include $\langle\Gamma\gamma\rangle$, $\langle D_0\rangle$, the $\ell = 0$ and $\ell = 1$ strength functions, and orthogonal ensemble (OE) tests. The following summarize the results of these tests.

Final choices of average capture widths, $\ell = 0$ average nearest neighbor spacings, s-wave strength functions, and p-wave strength functions for the Cd isotopes.

Isotope	$\langle\Gamma\gamma\rangle$ (meV)	$\langle D_0\rangle$ (eV)	$10^4 S_0$	$10^4 S_0$
^{110}Cd	101	174 ±18	0.50±0.10	2.8±0.6
^{111}Cd	102	24.0± 1.5	0.38±0.06	3.5±0.7
^{112}Cd	102	137 ± 8	0.53±0.09	2.5±0.5
^{113}Cd	101	22.1± 3.8	0.43±0.07	
^{114}Cd	110	183 ±29	0.70±0.19	3.2±1.0
^{116}Cd		264 ±38	0.20±0.06	

Summary of the results of statistical QE tests (Δ and ρ) for the final s level selections for ^{110}Cd, ^{112}Cd, and ^{111}Cd.

Isotope	(keV)	N	Δexp	Δtheo	ρexp	ρtheo
^{110}Cd	5.0	29	0.41	0.33±0.11	-0.18	-0.27±0.17
^{112}Cd	7.0	52	0.30	0.39±0.11	-0.32	-0.27±0.13
^{114}Cd	3.4	19	0.22	0.29±0.11	-0.28	-0.27±0.22
^{111}Cd	1.8	74	0.63	0.69±0.22	-0.14	-0.21±0.10

The gadolinium isotopes studied were Gd-154, 158, 160. The measurements were transmission and capture measurements. Resonance parameters E_0 and Γ_n^0 go to 1 keV for Gd-154 and to 10 keV for Gd-158 and 160. The number of radiation widths $\Gamma\gamma$ obtained are 25, 27, and 4 for Gd-154, 158, and 160 respectively. The following are results of data analysis on gadolinium: For Gd-154, $\langle\Gamma\gamma\rangle$ = 88 meV, $\langle D_0\rangle$ = (14.5±1.5) eV, $10^4 S_0$= 2.0±0.3. For Gd-158, $\langle\Gamma\gamma\rangle$ = 105 meV, $\langle D_0\rangle$ = (86±4) eV, $10^4 S_0$ = 1.5±0.2. For Gd-160, $\langle\Gamma\gamma\rangle$ = 111 meV, $\langle D_0\rangle$ = (202±20) eV, $10^4 S_0$ = 1.8±.14, $10^4 S_1$ = 1.7±0.3. These are based on a total of 190 individual resonances.

The indium results come from 200 meter transmission and 40 meter capture and self-indication data. Resonance parameters are given to 2 keV for In-113,115. They include 15 $\Gamma\gamma$'s for In-115 and three for In-113. The total number of individual resonances analyzed is 280. Since a separated In-113 sample was not available, and since natural indium is 96% In-115, nuclear parameters were derived for In-115 only. The results are: $\langle\Gamma\gamma\rangle$ = 85 meV, $\langle D_0\rangle$ = (9.4±0.2) eV, $10^4 S_0$ = 0.26±0.03, $10^4 S_1$ = 2.7+1.0 or -0.7 for In-115.

The results for natural chlorine include total cross section to 400 keV and 35 resonance parameters ($ag\Gamma_n$) to 200 keV. We deduce a bound level at E_0 = -130 eV, with ℓ = 0, J = 2, Γ_n^0 = 0.725 eV, and $\Gamma\gamma$ = 0.378 eV. For Cl-35 we obtain 10^4S_0 = 0.12+0.23 or -0.07, and 10^4S_1 = 0.77+0.53 or -0.29. For Cl-37, 10^4S_0 = 0.59+0.66 or -0.28.

For natural calcium, results include σ_{total} vs. E to 550 keV, and E_0, Γ_n, $ag\Gamma_n$ for 31 levels (including 9 s-levels and 22 $\ell \geq 1$ levels). For Ca-40, 10^4S_0 = 2.97+1.95 or -1.05.

For natural fluorine, we have σ_{total} to 200 keV and three p-levels. Result for F-19 is 10^4S_1 = 11.1+12.4 or -5.2.

For natural magnesium, we have σ_{total} to 500 keV and five levels to that energy. The result is 10^4S_1 = 10.5+11.8 or -4.9.

The results for natural argon include σ_{total} (E) to 580 keV, and resonance parameters for 24 levels in Ar-40. Of these 24 levels, six are assigned ℓ = 0, and 18 ℓ = 1. S-levels were analyzed using both area and R-matrix techniques. The s and p strength functions and average level spacings for Ar-40 were found to be: 10^4S_0 = 0.91±0.77 or -0.37; 10^4S_1 = 0.33±0.14 or -0.09; $\langle D_0 \rangle$ = (87+13 or -11) keV; $\langle D_1 \rangle$ = (24+5 or -4) keV.

Results for the following dysprosium isotopes are given, based on 200 meter transmission and 40 meter capture measurements: A = 160, 161, 162, 163, 164. We obtained resonance parameters for 64 levels in Dy-160 to 2 keV, 251 levels in Dy-161 to 1 keV, 142 levels in Dy-162 to 16 keV, 114 levels in Dy-163 to 1 keV, and 116 levels in Dy-164 to 21 keV. The data were analyzed to yield E_0, $g\Gamma_n^0$, $\Gamma\gamma$, S_0, $\langle D_0 \rangle$, S_1, and orthogonal ensemble (OE) results. The respective $\langle \Gamma\gamma \rangle$ values are: 108, 112, 112, 113, 114. The ℓ = 0 strength functions are: 10^4S_0 = (2.00±0.36), (1.73±0.17), (1.88±0.25), (2.02±0.30), and (1070±0.25). The ℓ = 1 strength functions for Dy-162 and Dy-164 are: (1.1±0.4) and (1.3±0.3) respectively. The values of $\langle D_0 \rangle$ for the above isotopes are: (27.3±1.7), (2.67±0.13), (64.6±1.9), (6.85±0.54), and (147±9). The following summarizes the OE results for dysprosium:

Isotope	E_{max} (eV)	n	Δ	Δ_{DM}	ρ	ρ_{OE}
^{161}Dy	140	53	0.62	0.65±0.22	-0.17	-0.25±0.11
^{163}Dy	220	32	0.34	0.55±0.22	-0.21	-0.25±0.15
^{160}Dy	900	33	0.39	0.35±0.11	-0.25	-0.27±0.16
^{162}Dy	3000	48	0.34	0.39±0.11	-0.29	-0.27±0.13
^{162}Dy	4500	70	0.40	0.42±0.11	-0.28	-0.27±0.11
^{164}Dy	5000	34	0.41	0.35±0.11	-0.33	-0.27±0.16

Attached is the abstract of a paper on ^{175}Lu due to be published in April 1975 (Physical Review C).

NEUTRON RESONANCE SPECTROSCOPY. ^{175}LU

H.I. Liou, J. Rainwater, G. Hacken, U.N. Singh
Columbia University, New York, N.Y. 10027

Results are given of high resolution measurements of the neutron resonance parameters (E_0, $g\Gamma_n^0$) for 446 resonances to 3 keV in ^{175}Lu using the Columbia University Nevis Synchrocyclotron. The measurements used the 202.05 m flight path for transmission measurements and the 39.57 m flight path for transmission, capture, and self-indication measurements. Values of $\Gamma\gamma$ from (59±20) to (100±20) meV were obtained for 40 levels, with $\langle\Gamma\gamma\rangle$ = 77 meV. The s-wave strength function is $10^4 S_0$ = (1.83±0.12) and the deduced mean s level spacing is (3.45±0.15) eV. Using recent unpublished J assignments for levels below 238 eV by Namenson, Stolovy, and Smith, we obtain (0.55±0.20) for the ratio of the J = 4 to J = 3 s strength functions. The results to 200 eV agree with values expected from the Orthogonal Ensemble Theory for level spacing systematics.

B. Studies of the Neutron Interactions with Fissile and Fertile Nuclei. J.P. Felvinci, E. Melkonian, D. Cacuci, W.W. Havens, Jr.

Abstracts of the three papers presented at the Nuclear Cross Sections and Technology Conference in Washington, D.C. held 2-7 March 1975 are given below.

LEVEL DENSITY CALCULATION FOR DEFORMED NUCLEI

J.P. Felvinci, D. Cacuci, and E. Melkonian
Columbia University
New York, New York 10027

Level densities for the rare earth and actinide nuclei have been calculated using a modified version of the Ericson formalism. The assumption was made that K (the projection of J on the symmetry axis of the nucleus) is a good quantum number in the compound nucleus. Individual level densities for the different (K,J) values of the compound nucleus formed by low energy neutron interactions were calculated. The results show good agreement with the interpretation of recent results obtained on U-235 in this laboratory. Using the above calculations it is also possible to infer from the measured level densities the locations of the band heads of different K bands in the compound nucleus. The results also indicate that the K bands responsible for the level densities exclude the ground state rotational band. Levels built on the higher lying β and γ vibrational bands and their composites are sufficient in number to explain the observed level densities.

QUANTUM NUMBERS OF LOW LYING NEUTRON RESONANCES IN U-235

J.P. Felvinci, E. Melkonian and W.W. Havens, Jr.
Columbia University
New York, New York 10027

Experiments were performed at ORELA to measure the low energy fission cross section of U-235. Times of flight of the neutrons causing fission and the fission fragment energy detected by a solid state detector were recorded event-by-event. Analysis of the data showed marked pulse height variation among resonances. Several of the large resonances were shown to be composites and the level density obtained is much higher than previously determined. The results were interpreted by the hypothesis that K is a good quantum number in the compound nucleus. This assumption and the systematic variation of the fission fragment energies among resonances enabled us to assign J and K quantum numbers to many levels. Three families of fission resonances were seen, $J = 4^-$; $K = 2$, $J = 4^-$; $K = 1$, and $J = 3^-$; $K = 1$. Our results have implications as to the accuracy of fission cross section measurements and to the calculation of cross sections in the unresolved energy region.

EVIDENCE FOR STRUCTURE IN THE SEQUENCE OF S-WAVE LEVELS IN ^{238}U

E. Melkonian, J.P. Felvinci, and W.W. Havens, Jr.
Columbia University
New York, New York 10027

The levels in ^{238}U show unusual clusterings of large and small levels as evidenced by runs statistics and sequential correlation of values of Γ_n^0. Also, Γ_n^0 is found to show significant correlation with $\Gamma\gamma$. These effects are interpreted in terms of a model which assumes that excitation states are built upon persistent states of collective vibration and that an entering neutron seeks to form those states involving minimum change of particle motion.

UNIVERSITY OF KENTUCKY

A. NEUTRON SCATTERING

1. The Elastic and Inelastic Scattering of 2.75 MeV Neutrons by Isotopes of Molybdenum, Zirconium, and Yttrium (McDaniel, Sinram,* Chung, Brandenberger, McEllistrem, Glasgow,+ and Robertson++)

This work includes part of an extensive study of neutron elastic and inelastic scattering in the mass region A∿90-100 which has been in progress at this laboratory for several years. The immediate goals of this study are the determination of the level and decay schemes and other nuclear structure properties in this mass region, and accurate measurement of elastic and inelastic differential neutron scattering cross sections at several incident energies. The first of the papers dealing with nuclear structure has been presented[1] and is concerned with the 0^+ levels of Mo isotopes. The first paper describing scattering cross section measurements has also been presented,[2] and reports measurements at 1.5 MeV incident energy for Mo and Zr isotopes. The present work includes the results of three sets of measurements carried out over a period of three years at incident energies between 2.5 and 2.75 MeV. The experiments were performed at different times because of limitations on the availability of the isotopically enriched Zr and Mo samples.

Several questions were to be studied through these measurements. First, the behavior of the elastic scattering cross sections as a function of neutron excess in a series of isotopes, and the complementary question of the relationship of Zr and Mo cross sections for nuclei with the same number of neutrons. The variation over a limited number of nuclides was not expected to be great, particularly since all of these nuclei should be spherical, near semi-magic ^{90}Zr. But with sufficiently precise measurements, the influence of changes in Z and N should be discernible. The second question was a related one, whether a consistent complex potential model would fit all of the measurements well. The measurements included are those for neutron elastic and inelastic scattering from ^{92}Mo, ^{94}Mo, and ^{96}Mo at an incident energy (En) of 2.52 MeV, from ^{98}Mo and ^{100}Mo at En = 2.75 MeV in a second measurement set, and from ^{89}Y, ^{90}Zr, and ^{92}Zr in the third set of measurements, also for En = 2.75 MeV.

The experimental apparatus has been presented in detail elsewhere[2] and will be very briefly presented here. The scattered neutron yields were measured using a dynamically biased time-of-flight (TOF) spectrometer developed at the University of Kentucky[3] to reduce backgrounds in wide dynamic range neutron detection. A beam of protons pulsed at a repetition rate of 2.0 MHz and bunched to a pulse width of <1.0 nsec was produced by the University of Kentucky's Van de Graaff accelerator and Mobley beam deflection system. The beam entered a 3.0 cm long gas cell filled with ^{3}H to 1.0 atm through a 0.00036 cm Mo foil. The proton energy losses in the foil and gas were 180 and 60 keV respectively. The average energy of neutrons produced at 0° was 2.75 MeV with an energy spread of 60 keV full width at half maximum (fwhm). These neutrons were incident on a cylindrical scattering sample mounted with its axis perpendicular to the reaction plane and about 6-8 cm from the center of the neutron source. Scattered neutrons were detected in a heavily shielded and collimated liquid organic scintillator (NE218) mounted between 2 and 4 m from the sample.

Complex potential models and the statistical model were used to obtain fits to the differential elastic scattering cross sections and the total cross sections. Striking similarities were found in the data for ^{90}Zr and ^{92}Mo, and also between the data for ^{92}Zr and ^{94}Mo. The analysis did require a definite i-spin dependence for the real potential,

---

* Now at North Texas University, Denton, Texas

** Now at II. Institut für Experimental Physik, 2000-Hamburg-Bahrenfeld Luruper Chaussee-149, W. Germany

\+ Now at Department of Radiology, Washington University, St. Louis, Mo.

++ Now at Prestonsburg Community College, Prestonsburg, Ky.

1 McEllistrem, Brandenberger, Sinram, Glasgow, and Chung, Phys. Rev. C9, 690 (1974).

2 McDaniel, Brandenberger, Glasgow, and Leighton, Phys. Rev. C10, 1087 (1974).

3 J. D. Brandenberger and T. B. Grandy, Nucl. Instr. and Meth. 93, 495 (1971).

of the form $V=V_0-V_1[N-Z]/A$. The coefficient V_1 was $V\simeq 25$, comparable to that[1] required for global fit analyses of proton scattering and some limited neutron scattering surveys. Details of the measurements, analyses and conclusions are contained in a paper to be submitted for publication.

2. Structure Studies in ^{92}Zr, ^{94}Zr (Glasgow, McDaniel, Weil, Brandenberger and McEllistrem)

The nuclear level structures of ^{92}Zr and ^{94}Zr are of especial interest because of the proximity of these isotopes in the periodic table to ^{90}Zr, which in its ground state has protons filling the $2p_{1/2}$ sub-shell at Z = 40 and a closed neutron $1g_{9/2}$ shell at N = 50. The level structure of ^{92}Zr and ^{94}Zr have previously been studied in transfer reactions, inelastic scattering, β-decay, and thermal neutron capture. The results have been compiled by Wood[1], Kocher and Horen[2], and Kocher[3].

Kocher and Horen's[2] compilation for ^{92}Zr includes a recently up-dated level scheme. The energies in keV, and spin-parities of the levels below 2.0 MeV, adopted by the compilers[2], are: 934.46, 2^+; 1383.0, 0^+; 1495.6, 4^+; and 1847.3, 2^+.

Kocher and Horen[2] note that above 2.4 MeV, the correspondence between the levels observed in various experiments is not good, primarily because of imprecise energy determinations in the reaction studies. Spins have been tentatively adopted[2] for four of the levels above 2.4 MeV. While many ^{92}Zr de-excitation γ-rays recently have been identified, excitation functions have been measured only for the nine γ-rays originating from the levels below 2.4 MeV. None have been measured for the γ-rays from the levels above this energy and no γ-ray angular distribution data exists.

Kocher's[3] recently released compilation for ^{94}Zr indicates a similar situation for this isotope. The energies, in keV, and spin-parities of the levels of ^{94}Zr adopted by Kocher[3], are: 918.24, 2^+; 1299.99, 0^+; 1468.34, 4^+; and 1668.74, 2^+. Only two spins are known[3] for levels above 2.4 MeV.

A puzzle exists in the ^{94}Zr level structure near 2.4 MeV. Tessler and Glickstein[17] note that the $^{94}Zr(n,n'\gamma)^{94}Zr$ reaction excited a 4^+ level not observed in $^{92}Zr(t,p)$

^{94}Zr and ^{96}Zr(p,t)^{94}Zr reactions,[3,4] while these latter two reactions excited a 2^+ level not observed in their (n,n'γ) study. Gamma-ray excitation functions have been measured for the de-excitation γ-rays from the levels below 2.4 MeV but few γ-rays have been identified from the levels above this energy and no γ-ray angular distribution data exist.

An additional interest in ^{92}Zr and ^{94}Zr stems from the use of zirconium as a structural material in nuclear reactors. The need for zirconium neutron inelastic scattering cross sections stimulated the recent (n,n'γ) measurements on ^{90}Zr, ^{91}Zr and ^{94}Zr by Tessler, Glickstein, and Carrol.[4] Neutron time-of-flight studies at Kentucky have recently been made of neutron elastic and inelastic scattering cross sections for ^{90}Zr, ^{92}Zr and ^{94}Zr at 1.5, 2.75, and 3.5 MeV. These neutron time-of-flight experiments provide the most direct measure of the neutron inelastic scattering cross sections, but finite energy resolution prohibits the measurement of cross sections for closely spaced levels. Inelastic scattering cross sections inferred from (n,n'γ) studies provide the best cross section information about the scattering to closely spaced energy levels. This technique can be validated by comparing the inferred values to the cross sections of well-resolved levels measured in time-of-flight experiments.

This work includes the results of ^{92}Zr and ^{94}Zr (n,n'γ) experiments performed to determine the energies, excitation functions, angular distributions, and branching ratios of the de-excitation γ-rays of these isotopes. These experiments consisted of γ-ray excitation function measurements on each isotope using neutrons with energies from 2.22 MeV to 3.70 MeV and angular distribution measurements at incident neutron energies of 3.20 MeV and 3.70 MeV for ^{92}Zr and at 3.10 MeV for ^{94}Zr . Using this information, the ^{92}Zr and ^{94}Zr level structure near and above 2.4 MeV has been investigated and the spins of certain levels uniquely determined or limited to a few choices. Multipole mixing ratios were also determined for many of the γ-rays. These results are compared to previously reported results. Neutron inelastic scattering cross sections inferred from the present measurements are compared to other measurements of these cross sections.

The physical equipment and electronics used in these experiments were similar to those previously used in (n,n'γ) studies in this laboratory.[5] Protons of the desired energy,

produced by a CN Van de Graaff accelerator pulsed at 2 MHz entered a Mobley pulse compression system and were bunched to about a 1 ns pulse width. The protons passed through a 3.61 μm molybdenum foil into 1.0 atm of tritium contained in a stainless steel gas cell 32 mm in length and 10 mm in diameter to produce neutrons by the $T(p,n)^3He$ reaction. The neutron energy spread was about 60 keV. The cylindrical scattering samples were suspended 50 mm from the end of the gas cell. Table I lists the samples isotopic composition and Table II gives their dimensions and masses.

A 34 cm^3 Ge(Li) detector in a lead, Li_2CO_3, and paraffin neutron shield viewed the de-excitation γ-rays. The detector was further shielded from the $T(p,n)^3He$ neutron source by a tungsten shadow bar. The sample to detector distance was 65 cm. The detector energy resolution was 2.5 keV FWHM. Time-of-flight techniques were used to discriminate between the prompt γ-rays following neutron inelastic scattering from the samples and background γ-rays produced when neutrons struck the detector or inelastically scattered from near-by laboratory materials.

This spectroscopic study of the gamma radiations following the inelastic scattering of neutrons with energies from 2.22 MeV to 3.70 MeV from nearly pure isotopic samples of ^{92}Zr and ^{94}Zr shows that the (n,n'γ) reaction and related experimental techniques are an excellent means of styding nuclear structure. The 2.5 keV FWHM spectral resolution obtained with a 35 cm^3 Ge(Li) detector allowed many weak γ-rays to be identified. The accurate measurement of the γ-ray energies to within 1 keV, combined with the measurement of their 90° production cross sections at 50 keV increments in the incident neutron energy, properly placed the γ-rays in the isotope decay schemes, determined the level schemes, and established the level energies to within 1 keV. The agreement of many of the γ-ray energies, 90° production cross sections, level branching ratios, and level energies measured in this study to previously reported values of these quantities justifies confidence in the values of these quantities that are reported for the first time in this work.

The ^{92}Zr excitation function experiment identified 51 γ-rays, several of which were previously unreported, from 26 levels through 3472.0 keV. Two new levels, 2903.8 keV and 3407.9 keV, were discovered in this study. The remainder of the level energies measured agree best with those reported by Fanger *et al.*[12] and this agreement aids in clarifying the

level structure of ^{92}Zr. The ^{92}Zr 3.20-MeV angular distribution study yielded 24 angular distributions of γ-rays from the levels through 3056.5 keV while the 3.70-MeV study yielded 39 angular distributions of γ-rays from the levels through 3370.9 keV. The analysis of these distributions resulted in the following unique or limiting spin assignments (level energies in keV are followed by the acceptable J values): 2398.0, 3, 4; 2485.1, 5; 2742.6, 3, 4; 2818.0, 2, 3; 2863.6, 3-5; 2903.8, 0; 2909.0, 2, 3; 3056.5, 2, 3; 3124.4, 1-3; 3177.2, 2-5; 3190.8, 2-5; 3232.6, 2-5; 3275.9, 1-3; 3288.7, 2-4; 3407.9, (1,2); 3452.2, 2-4; and 3472.0, 2-4. Gamma-ray level branching ratios were measured and the γ-ray multipole mixing ratios were obtained for the indicated spin assignments.

The ^{94}Zr excitation studies identified 28 γ-rays, 15 of which were previously unreported, from 20 levels below 3361.2 keV. A previously reported ambiguity concerning 2^+ and 4^+ levels in the 2320 keV to 2365 keV energy region has been resolved. We have shown that there are two γ-decaying levels in this energy region; a J = 4 level at 2329.0 keV and a 2^+ level at 2365.4 keV. New levels were discovered at 2507.6, 2698.0, and 2825.2 keV, and tentatively, 2859.8 keV. The 3.10-MeV ^{94}Zr angular distribution experiment yielded 18 angular distributions of γ-rays from the ^{94}Zr levels through 2887.0 keV. Unique or limitng spin assignments were made to the following five levels of ^{94}Zr for which the spins were previously unknown: 2507.6, 3; 2698.0, 0; 2825.2, 2, 3; 2859.8, (5); and 2887.7, 0-3. The γ-ray multipole mixing ratios were obtained as well as γ-ray level branching ratios.

---

1 J. L. Wood, Center for Nuclear REsearch, Karlsruhe, Germany, External Report 1/72-1 (1972).

2 D. C. Kocher and D. J. Horen, Nucl. Data B7, 299 (1972).

3 D. C. Kocher, Nucl. Data A10, 264 (1973).

4 G. Tessler, S. S. Glickstein, and E. E. Carroll, Jr., Phys. Rev. C2, 2390 (1970); S. S. Glickstein, G. Tessler, and M. E. Goldsmith, Phys. Rev. C4, 1822 (1971).

3. Comparisons of (n,n') Cross Sections from n and γ-ray Detection (Glasgow, McDaniel, Weil, Brandenberger, McEllistrem)

As noted above, the neutron inelastic scattering cross sections $\sigma_{n'}$ inferred from the results of the (n,n'γ) experiments can be compared to those measured directly in (n,n') experiments. These two types of neutron experiments normally have different objectives and usually are not undertaken at the same incident neutron energies. The excitation functions measured in the (n,n'γ) studies can be used to extrapolate the angle integrated γ-ray production cross sections σ_γ to the proper energy so the inelastic neutron cross sections can be inferred and compared to the directly measured values. If the inferred cross sections are to agree with the directly measured ones, certain criteria must be satisfied. The range of the extrapolation should not be large because the anisotropies of the γ-ray angular distribtuions can change rapidly with energy. All γ-rays cascading to and emitted from a level must be identified and their angle integrated cross sections accurately measured. Failure to include even one strong γ-ray introduces serious error. Based on excitation function data, $4\pi\sigma_\gamma(90°)$ cross sections often can be used to approximate the cross sections of those γ-rays for which angular distributions were not obtained. However, this approximation introduces additional uncertainties into the inferred neutron inelastic scattering cross sections. Consistent and similar sample-size corrections must be made to the data from the (n,n') and (n,n'γ) experiments.

The angle integrated γ-ray production cross sections obtained from the ^{92}Zr 3.20 MeV angular distribution experiment satisfy these criteria and have been extrapolated to 2.75 MeV. Table I compares the inelastic neutron cross sections inferred from these results to those measured directly from an (n,n') experiment at 2.75 MeV, an experiment referred to above. The inferred and directly measured neutron inelastic cross sections for the 934.1- and 1381.9-keV levels agree very well. The cross sections for the remaining three levels agree within their respective uncertainties. The difference between the measured and inferred values for the levels at 1846.4 keV and 2066.1 keV result from insufficient energy resolution to separate the two neutron groups in the (n,n') study. The sum of the inelastic cross sections of these two levels agrees with the sum of those inferred from this study. This is an example of the situation of closely spaced levels mentioned in the introduction, in which

the (n,n'γ) technique gives more precise values of the inelastic cross sections than does a direct (n,n') measurement.

Table I. A comparison of ^{92}Zr inferred and directly measured neutron inelastic scattering cross sections at 2.75 MeV. The energy above each column is the incident neutron energy in each experiment.

Level (keV)	Neutron Inelastic Scattering Cross Sections, in (mb), at 2.75 MeV	
	(n,n'γ) 3.20 MeV	(n,n') 2.75 MeV
934.1	633 ± 68	606 ± 64
1381.9	108 ± 12	109 ± 28
1494.8	183 ± 22	254 ± 46
1846.4	240 ± 26	340 ± 72
2066.1	240 ± 25	160 ± 57

B. DETECTION METHODS

1. A Secondary Standard Neutron Detector for Measuring Total Reaction Cross Sections (Sekharan, Laumer, and Gabbard)

A neutron detector has been constructed and calibrated for the accurate measurement of total neutron-production cross sections. The detector consists of a polyethylene sphere of 24" diameter in which 8-$^{10}BF_3$ counters have been installed radially. The relative efficiency of this detector has been determined for average neutron energies from 30 keV to 1.5 MeV by counting neutrons from $^7Li(p,n)^7Be$. By adjusting the radial positions of the BF_3 counters in the polyethylene sphere the efficiency for neutron detection was made nearly constant for this energy range. Measurement of absolute efficiency for the same neutron energy range has

been done by counting the neutrons from $^{51}V(p,n)\ ^{51}Cr$ and $^{57}Fe(p,n)^{57}Co$ reactions and determining the absolute number of residual nuclei produced during the measurement of neutron yield. Details of absolute efficiency measurements and the use of the detector for measurement of total neutron yields from neutron producing reactions such as $^{23}Na(p,n)^{23}Mg$ are available.

The detector efficiency is flat to within 2% for neutrons with energies between 30 keV and 1.56 MeV. Tests of detector response at higher energies are encouraging, but presently incomplete.

2. Finite Sample Corrections for (n,n'γ) Reactions
(F.D. McDaniel, G. P. Glasgow, and M. T. McEllistrem)

The accurate determinaton of (n,n') and (n,n'γ) cross sections from measurements with thick samples requires reliable methods of calculating finite sample effects such as flux attenuation (FA) and multiple scattering (MS). The amount of double scattering is proportional to the radius of the sample, while the desired yields are roughly proportional to sample volume. Hence a reduction of sample size has a much bigger effect on detected yield than on sample size. It is generally more efficient to use fairly large scattering volumes and correct the results for plural scattering. The samples generally used in inelastic scattering experiments include between 0.2 and 2 moles of material.

In the past Day[1] and Nishimura, et al[2] have assumed that for samples of ∿1 mole the effective increase of incident flux caused by MS was approximately equal to the loss of flux caused by FA. The inadequacy of the above assumption has been noted by other groups[3] as well as our own, although it has been frequently employed in experiments studying (n,n'γ) reactions. We have studied the importance of several finite-sample corrections on (n,n'γ) cross section measurements with the following results:

1. Uncorrected γ-ray angular distributions are asymmetric with respect to 90°, but correcting for γ-ray self absorption restores symmetry to within a few percent.

2. Tests of the FA and MS corrections are made to test the early assumption of Day that they almost cancel.

With this assumption, and using Pb and Fe scattering samples, at 3 MeV incident neutron energy, one finds values ∿10% too low for 2 cm diameter samples. If one includes only the MS correction and ignores FA, the results are ∿10% too high. Including both FA and MS corrections leads to sample size independent results. Those tests also included corrections for γ-ray selfabsorption in the sample.

C. COMPILATION AND EVALUATION

1. Nuclear Level Schemes for A = 145, 146, and 156 (T. W. Burrows*)

The revisions of compilations and evaluations of the level and decay schemes for A = 145 and A = 146 have been completed and recently published. The review for A = 156 has also been completed, and a manuscript submitted to the Nuclear Data Center at ORNL.

D. MEDICAL USES OF RADIOISOTOPES

1. ^{18}F and ^{13}N Production (M. F. Reed*, M. T. McEllistrem, and others)

The production of ^{18}F as an isotope for bone scans has been in routine use since 1972. More recently the production of ^{18}F labled 5-FU has been developed to study the tumor localizing properties of 5-FU. In an independent project, ^{13}N-labeled Nitrosoureas have been developed to study these as potential brain tumor localizing agents. Both of these labeling studies have been collaborations between M. F. Reed and members of the University of Kentucky Medical Center.

---

* Department of Nuclear Medicine, University of Kentucky

A. STANDARDS

1. ^{235}U Fission Cross Section Relative to n-p Scattering. (J. B. Czirr and G. S. Sidhu)

A paper (UCRL-76508) on this experiment was presented at the Conference on Nuclear Cross Sections and Technology in Washington, D.C., March 3-7, 1975. The abstract for this paper is quoted below.

> "Energy dependence of the fission cross section of ^{235}U with respect to the n-p scattering reaction was measured for neutron energies from 0.8 to 20 MeV. The LLL linac target was used as the pulsed neutron source; neutron energies were measured by time-of-flight techniques. A ^{235}U ion chamber was designed and operated to make the fission detection efficiency independent of the angular distribution of fission fragments. The neutron flux monitor consisted of an annular polyethylene radiator with a shielded proton recoil detector. Data in the energy range from 3 to 20 MeV were obtained with a 3.3 mg/cm^2 radiator; a 0.31 mg/cm^2 radiator was used for the range from 0.8 to 4 MeV. Both sets of data were normalized to yield the average fission cross section value of 1.98 b in the overlapping region from 3 to 4 MeV. Total error in the relative $^{235}U(n,f)$ cross section is ±2% at 14 MeV, and ±6% at 20 MeV."

2. A Measurement of the ^{235}U Fission Cross Section from Thermal to 1 MeV. (J. B. Czirr and G. S. Sidhu)

The ratio of the ^{235}U fission cross section to the $^{6}Li(n,\alpha)$ reaction has been measured for neutron energies from thermal to 1 MeV. Results of this measurement were presented at the Nuclear Cross Sections and Technology Conference mentioned above. (UCRL-76572).

B. NEUTRON DATA APPLICATIONS

1. High Energy Fission Cross Section Ratios Measurements. (G. W. Carlson and J. W. Behrens)

We have submitted results (UCRL-76219) to the Conference on Nuclear Cross Sections and Technology, March 3-7, 1975 for the fission cross section ratios: ^{233}U:^{235}U, ^{234}U:^{235}U, ^{236}U:^{235}U, ^{238}U:^{235}U and ^{238}U:^{233}U.[1] The measurements made at the LLL 100 MeV LINAC cover the energy

range from 1 keV to 30 MeV, except where limited by low cross sections on the threshold isotopes. We normalized the results independent of other measurements by using the threshold cross section method.[1,2]

We are presently repeating our measurements of ^{239}Pu:^{235}U and ^{238}U:^{239}Pu with new fission chambers designed to reduce the alpha pileup experienced with our preliminary measurements.[2]

During the year 1975, we also plan to measure the fission cross sections of ^{240}Pu, ^{241}Pu, ^{242}Pu and ^{244}Pu relative to ^{235}U in the energy range from about 100 keV to 20 MeV.

2. Fission $\bar{\nu}$ Measurements. (R. E. Howe and T. W. Phillips)

We have begun measurements of $\bar{\nu}$ for ^{235}U in the MeV region ($E_n \leq 20$ MeV) using the LLL linac with the same detector system used for precision $\bar{\nu}$ measurements in the ^{235}U resonance energy region.[3] Preliminary results are shown in Figure B-1.

3. Recent Measurements of the $^{93}Nb(n,2n)^{92m}Nb$ (10.16d) Cross Section. (D. R. Nethaway)

Table B-1 lists preliminary results for the $^{93}Nb(n,2n)^{92m}Nb$ (10.16d) cross section based on recent irradiations at the Livermore ICT facility, together with some revised results of work previously published.[4] The revisions were made because of a change in the ^{92m}Nb counting efficiency. The results listed in Table B-1 are accurate to ±5%.

Table B-1. $^{93}Nb(n,2n)^{92m}Nb$ (10.16d) Cross Section

Neutron Energy (MeV)	Cross Section (mb)
13.9	462
14.1	465
14.5	467
14.8	458

[1] J. W. Behrens, G. W. Carlson, and R. W. Bauer, Neutron-Induced Fission Cross Sections of ^{233}U, ^{234}U, ^{236}U, and ^{238}U with Respect to ^{235}U, UCRL-76219 submitted to Proceedings of the Conference on Nuclear Cross Sections and Technology, Washington, D.C., March 3-7, 1975.

[2] J. W. Behrens and G. W. Carlson, High Energy Measurements of Neutron-Induced Fission Cross Section Ratios Involving ^{233}U, ^{235}U, ^{238}U, and ^{239}Pu Using the Method of Threshold Cross Sections, UCID-16548 (1974).

[3] NCSAC Report, dated 10 November 1971, UCID-15937.

[4] D. R. Nethaway, Nucl. Phys. A190, 635 (1972).

4. Neutron Reactions on ^{239}U. (D. G. Gardner)

A paper (UCID-16679) on this topic has recently been written on this subject. A summary from this paper is quoted below.

> "Calculations were made of the major reactions induced by neutrons in the energy range of 10 eV to 2.5 MeV incident on ^{239}U. Both the 23.5 m $5/2^+$ ground state and the 0.78 μs $1/2^+$ isomeric state of ^{239}U were considered as targets. The bulk of the calculations were performed with the COMNUC and UHL statistical model codes using Moldauer's optical model parameters, although a rough correction for direct reactions was also made. Specifically, the total, shape elastic, compound elastic, inelastic, capture and fission cross sections are presented in tabular and graphic form over the specified neutron energy range. In addition, the fission cross sections were tentatively extrapolated down to thermal energy where they are compared with an unpublished measurement. For neutron energies above 500 keV the fission calculations are compared with predictions derived from published experimental measurements of the (t,pf) reaction on ^{238}U."

5. Model Calculations of Gamma-Ray Strength Functions. (D. G. Gardner)

A paper on this subject was presented at the Pittsburgh meeting of the APS, Oct. 31-Nov. 2, 1974. Results of these calculations for ^{182}Ta and ^{198}Au are contained in LLL Chemistry Dept. Technical Note No. 74-32. A comparison of the experimental and calculated γ-ray spectra for $^{197}Au(n,\gamma)$ are shown in Fig. B-2.

6. Tritium Depth Profiling by Neutron Time-of-Flight. (J. C. Davis and J. D. Anderson)

A paper (UCRL-75757, Rev. 1) on this topic was presented at the 21st National Symposium of the American Vacuum Society in Anaheim, California, Oct. 7-11, 1974. The abstract of this paper is quoted below.

> "A method has been developed to measure the depth profile of tritium implanted or absorbed in materials. The sample is bombarded with a pulsed proton beam. Neutron energies from T(p,n) reactions occurring in the target are measured by time-of-flight over a 10.8 m flight path. From the neutron energy the proton energy and thus the tritium depth in the target may be inferred. The measurements were initiated to determine the depletion of tritium absorbed in titanium layers. These layers had served as targets on a 400 keV T(d,n) neutron generator. A depth resolution of 0.4 mg/cm^2 of titanium (0.9 μm) was obtained. Unlike proton

backscattering methods, the technique can be used with thick samples. We estimate that a sensitivity of 0.1 at. % tritium in host materials can be obtained. Extension of the method to deuterium depth profiling is possible with the use of the D(d,n) reactions."

7. Comparison Between the Integral Gamma-Ray Measurements on Nitrogen and the Calculations using the ENDF/B-IV Library. (L. F. Hansen, T. T. Komoto, B. A. Pohl, C. Wong and J. D. Anderson)

The gamma-ray spectra from 0.5, 1.1 and 3.1 mean free paths (mfp) of nitrogen bombarded with 14-MeV neutrons, were reported in USNDC-11 (June 1974). These measurements, using the sphere transmission and time-of-flight techniques, were repeated with somewhat improved experimental conditions. NE 213 scintillators were used at angles of 26 and 120° and the flight paths were 769.62 and 912.42 cm, respectively. No major discrepancies were found with the earlier results.

Calculations have been carried out with the TARTNP Code using the ENDF/B-IV library. TARTNP is a coupled neutron-photon Monte Carlo Transport Code, which calculates the number of gammas/MeV/source neutron as function of gamma-ray energy. To this calculation is folded the recoil electron response of the detector calculated with the Monte Carlo Photon Transport Code TORTE.

Table B-2 gives the integral values of the measured and calculated spectra at 26° and 120° as function of mfp and the comparison for the 3 mfp is shown in Fig. B-3. The results show that the calculations are lower than the measurements with the discrepancy increasing as function of mfp.

Table B-2

Comparison between the measured integrals between 320 keV to 10 MeV gamma-ray energies and the calculations with the ENDF/B-IV library for nitrogen bombarded with 14-MeV neutrons.

mfp	θ	Experiment	ENDF/B-IV	Discrepancy (%)
0.5	26°	7.040	7.343	+4.3
	120°	4.68	4.48	-4.3
1.1	26°	10.02	9.87	-1.5
	120°	6.76	6.14	-9.1
3.1	30°*	15.87	12.41	-22.0
	120°	10.38	8.30	-20.0

C. NUCLEAR DATA FOR SAFEGUARDS

1. Photofission and Photoneutron Cross Sections for Actinide Nuclei. (R. A. Alvarez, B. L. Berman, and P. Meyer, LLL; J. T. Caldwell and E. J. Dowdy, LASL; T. F. Godlove, NRL)

Analysis of the data discussed in USNDC-11, p. 136, is proceeding. Results for ^{232}Th and ^{235,236,238}U will be presented at the Washington APS meeting in April. Further measurements are planned as well.

D. BASIC PHYSICS

1. Neutron Total Cross Section for Tritium. (T. W. Phillips, W. A. Barletta and B. L. Berman, LLL; J. D. Seagrave, LASL)

Measurements were completed in December, 1974; the data are being analyzed. The data analysis is expected to yield results in the neutron energy range from several tens of keV to several tens of MeV. The expected accuracy of the results is a few percent.

2. Neutron Capture Cross Sections for the Osmium Isotopes. (J. C. Browne and B. L. Berman).

The neutron capture cross sections for 186, 187, 188, 189, 190 and 192-Os have been measured from 2 eV to 300 keV. Data analysis is in progress. A paper on this experiment will be presented at the Washington APS meeting in late April.

3. High Resolution Neutron Resonance Measurements. (H. S. Camarda)

Using the LLL 100-MeV linac, high resolution transmission measurements on monoisotopic ^{89}Y are being performed over the energy range 20 keV to 250 keV for a range of sample thicknesses (1/n = 6, 12, 24, 50 barns/atom). The experiment employs Li glass detectors with $\sim$ 4 nsec timing jitter, a 250-meter flight path, 5 nsec beam burst and 36,000 timing channels (2 nsec width above 53 keV and 4 nsec below).

The large range of sample thicknesses and the excellent resolution coupled with shape and area analysis should enable a clean determination of the neutron width, spin and parity of most levels. With this information, various theoretical predictions will be examined.

4. Atlas of Photoneutron Cross Sections Obtained with Monoenergetic Photons. (B. L. Berman)

A second edition has been issued (UCRL-75694). A slightly revised version has been submitted for publication in Atomic Data and Nuclear Data Tables.

5. Photodisintegration of ^{18}O. (B. L. Berman, R. A. Alvarez, P. Meyer, and D. D. Faul)

Measurements have been taken in November, 1974 and February/March, 1975. Structure has been observed in all reaction channels [(γ,n), $(\gamma,2n)$, and (γ,p), the last obtained from observation of the delayed neutrons following the decay of ^{17}N] throughout the energy range measured [from the (γ,n) threshold at 8 MeV through the giant-resonance region].

6. Recent Developments in the Description of Odd-Mass Nuclei. (R. A. Meyer)

A paper (UCRL-76207) on this subject was submitted to the International Conference on Gamma-Ray Transition Probabilities in Delhi, India, November 11-15, 1974. The abstract for this paper is listed below.

> "A detailed survey of the medium-mass region ($60 < A < 140$) of the nuclear chart has been made to compare a number of recent theoretical calculations with the significant body of experimental information coming into the published literature. A comparison of the level properties of the Z = 51 antimony nuclei shows very good agreement with the recent calculations of Vanden Berghe, who includes two-particle one-hole configurations. The level structure and electromagnetic properties of the Z or N = 53 nuclei are not predicted so well as the antimony nuclei. Inclusion of three-particle clustering has improved the agreement between calculated and experimental electromagnetic transition rates for the low-lying levels in odd-mass nuclei. More recent calculations using a dressed quasi-particle formalism are shown to have some success. The detailed experimental study of odd-mass iodine near the neutron shell closure at N = 82 suggests that the particle-core interaction can account for a majority of the levels observed, if one uses an even-even core that includes known low-lying two-proton states. The nonnormal parity states in a given shell have higher J values than the normal parity states (e.g., $h_{11/2}$ in the g-d-s shell). This can cause significant deviations from the expected vibrational character. Studies of the odd-mass Z = 57 lanthanum nuclei suggest that the Coriolis force and its effect on high-J state coupling to the core can be used to account for the excess negative-parity states observed in the lathanum nuclei and

their electromagnetic decay properties. The deformability of the cadmium (Z = 48) core and the Coriolis force may be the causes of apparent rotationlike level structure observed in the experimental studies of the odd-mass indium nuclei. These results suggest that more attention should be paid to the inclusion of a dynamic rather than static core and that the Coriolis force should be included as part of any complete, effective interaction."

E. CONTROLLED THERMONUCLEAR RESEARCH APPLICATIONS

1. Use of Nuclear Reaction Models in Cross Section Calculations. (S. M. Grimes)

The following abstract is of an invited paper (Bull. Am. Phys. Soc. 19, 988 (1974)) presented at the Pittsburgh meeting of the Nuclear Physics Section of the American Physical Society:

> "The design of fusion reactors will require information about a large number of neutron cross sections in the MeV region. Because of the obvious experimental difficulties it is probable that all of the cross sections of interest will not be measured. Current direct and pre-equilibrium models will be used to calculate non-statistical contributions to neutron cross sections from information available from charged particle reaction studies; these will be added to the calculated statistical contribution. Estimates of the reliability of such calculations will be derived from comparisons with the available data."

In the talk comparisons between calculations and data were presented for Fe and Ni; similar calculations are now underway for Al and Nb. The text of the talk is available as UCRL-75991 and a more extensive report of the calculations will be available shortly.

2. ^{238}U Pulsed Sphere Measurements and CTR Fusion-Fission Blanket Calculations. (C. Wong, J. D. Anderson, R. C. Haight, L. F. Hansen and T. Komoto)

The neutron emission spectra from ^{238}U spheres pulsed with 14-MeV neutrons have been measured from the source energy down to 10 keV and have been compared with calculations employing ENDF/B-IV and (LLL) ENDL cross sections. The low energy spectra (10 keV to 1 MeV), (fig. E-1) are better described using ENDF/B-IV cross sections while the high energy spectra (2 MeV to 15 MeV), (fig. E-2) are better described using

ENDL cross sections. Discrepancies between calculation and experiment are apparent in all the figures, however. These experiments have particular relevance to fast fission blankets of hybrid fusion-fission reactors. For one conceptual design, significant differences exist in calculations done with previous versions of ENDF/B and ENDL data sets.[5] The present versions of these data sets continue to give large differences for three crucial reactor parameters (Table E-1).

Table E-1

Summary of Hybrid Reactor Calculations

	ENDF/B-IV	ENDL
Fissions		
^{235}U	.119	.127
^{238}U	.673	.737
Total	.792	.864
Tritium Breeding		
$^{6}Li(n,\alpha)T$	.900	1.040
$^{7}Li(n,n'\alpha)T$	.066	.067
Total	.966	1.107
Pu-Breeding		
$^{238}U(n,\gamma)$	2.225	2.143

All results are reactions per 14-MeV source neutron.

3. Cross Section for the $^{9}Be(n,t_1)\ ^{7}Li$ Reaction for E_n(lab) Between 13.3 and 15 MeV. (F. S. Dietrich, L. F. Hansen, and R. P. Koopman)

We have measured the magnitude and energy dependence of the $^{9}Be(n,t_1)\ ^{7}Li^*$ cross section in the 13.3 to 15 MeV energy range by observing the isotropic 481 keV decay gammas from the first-excited state of ^{7}Li. The experiment was performed in a ring-and-shadow-cone geometry, and the gammas were detected with a Ge(Li) spectrometer. The

[5] R. C. Haight and J. D. Lee, "Calculations of a Fast Fission Blanket for DT Fusion Reactors with Two Evaluated Data Libraries," Proc. of the First Topical Meeting of the Technology of Controlled Nuclear Fusion (CONF-740402-P1) p. 271.

neutrons were supplied by the Livermore ICT D-T neutron generator, and their energy was varied by changing the angle subtended by the Be ring. Neutron-induced backgrounds were reduced by time-of-flight discrimination. The results are shown in Fig. E-3, together with a recent estimate[6] of the cross-section at 14.0 MeV. These results are in disagreement with a previous measurement[7] using a NaI detector which yielded cross-sections in the range 10-30 mb, with a sharp dip near 14 MeV.

---

[6] J. P. Perroud and Ch. Sellem, Nucl. Phys. A227, 330 (1974).
[7] J. Benveniste et al. Nucl. Phys. 19, 52 (1960).

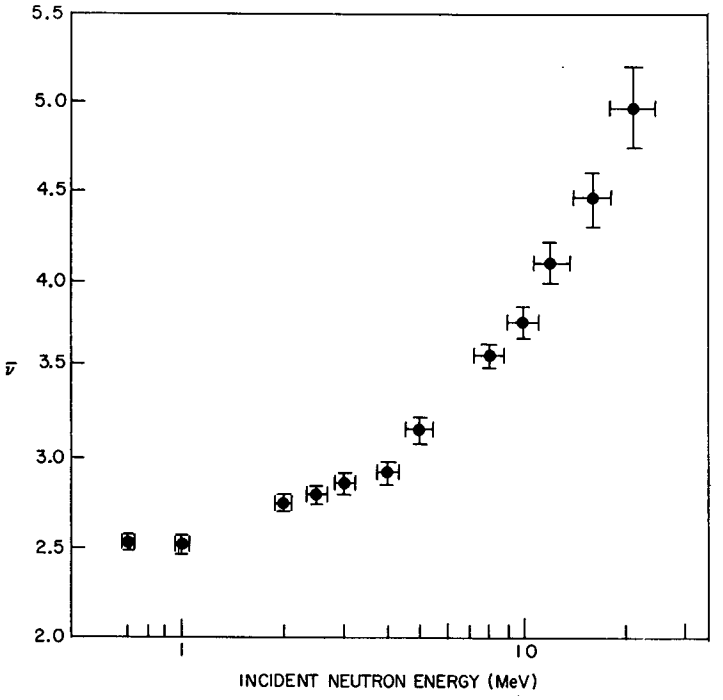

Fig. B-1. Prompt Fission Neutrons $\bar{\nu}$ as a function of incident neutron energy for $^{235}U(n,f)$. The data were normalized to $\bar{\nu}$ (1.0 MeV) = 2.51.

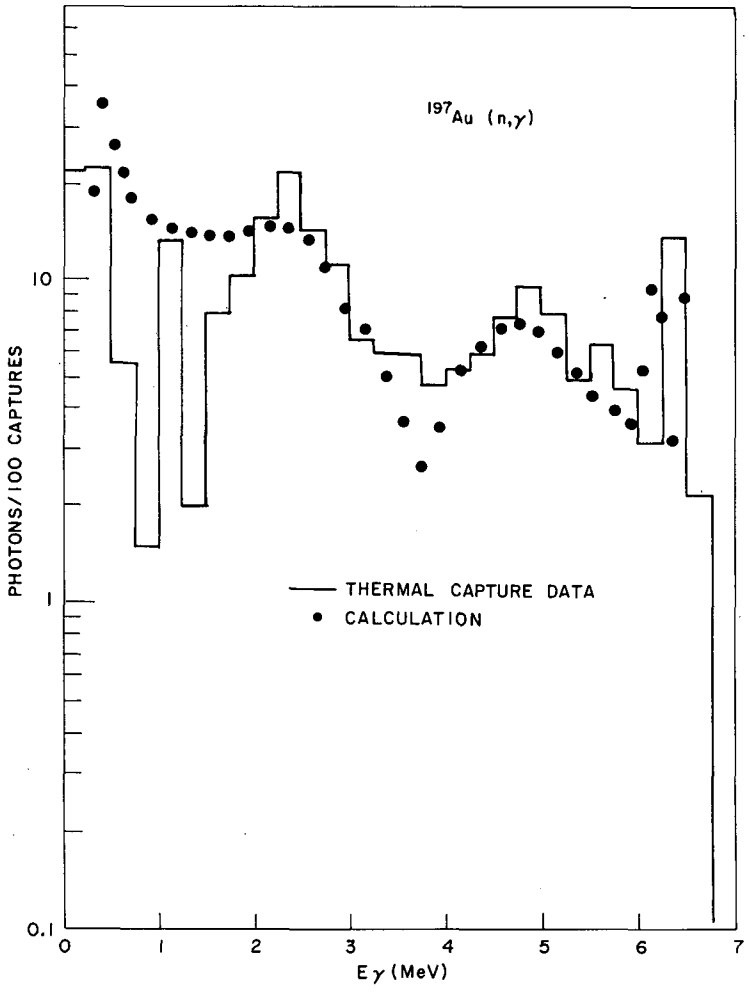

Fig. B-2. Calculation of the ^{197}Au(n,γ) capture spectrum compared with the thermal capture data of V. Orphan et al., Gulf General Atomic Report No. GA-10248 (1970).

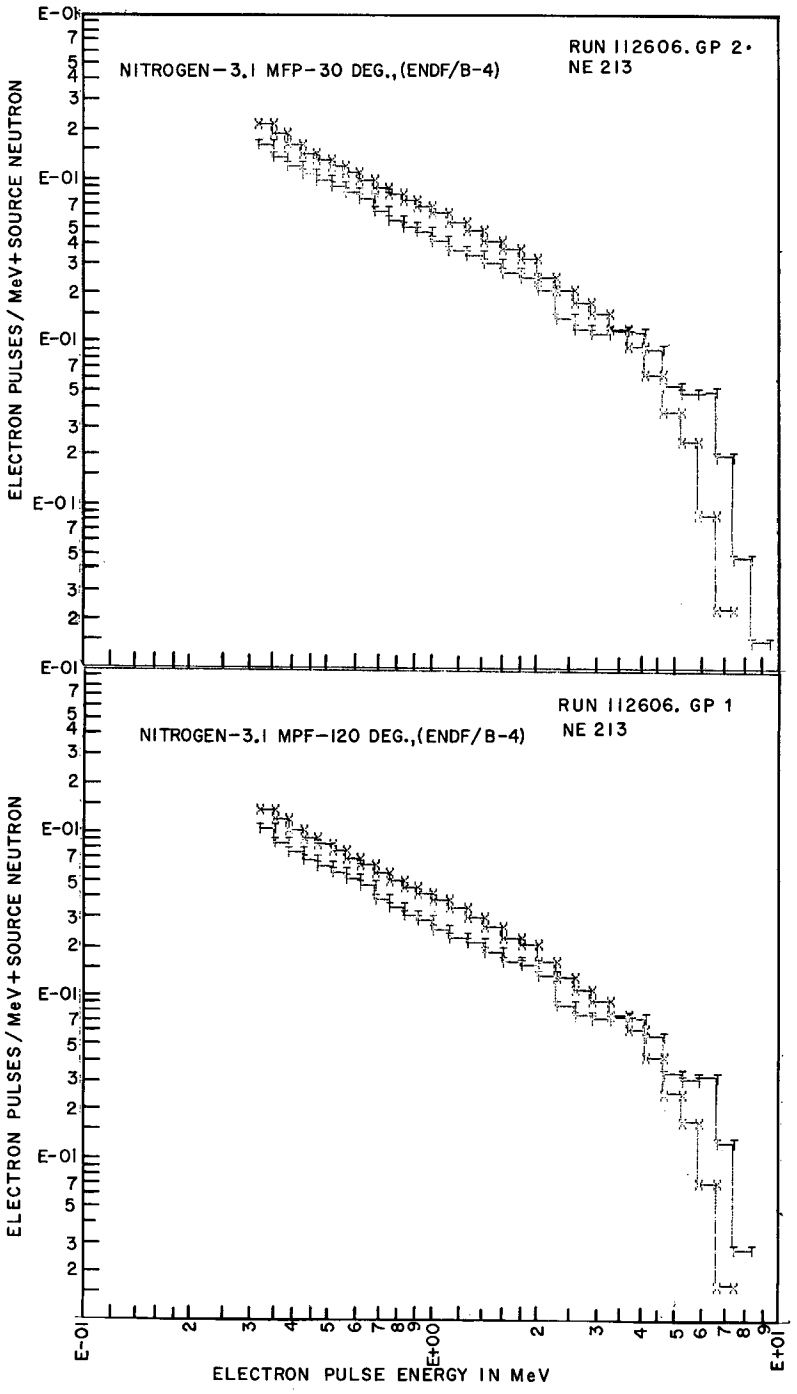

Fig. B-3. Comparison between the measured γ-ray spectra (X) and the calculation (T) using TARTNP with the ENDF/B-IV library for 3.1 m.f.p. of nitrogen at angles of 30° and 120°.

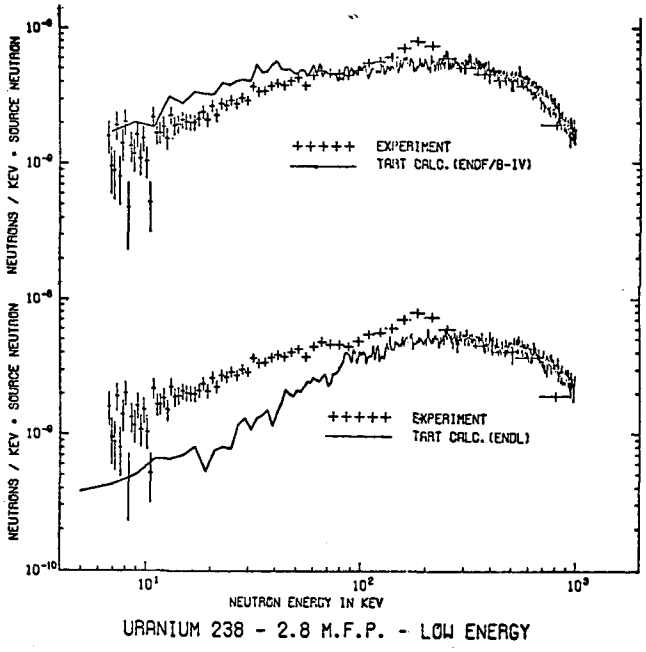

Fig. E-1. Comparison between the low energy measurements and calculations for the 2.8 m.f.p. ^{238}U sphere at 30°.

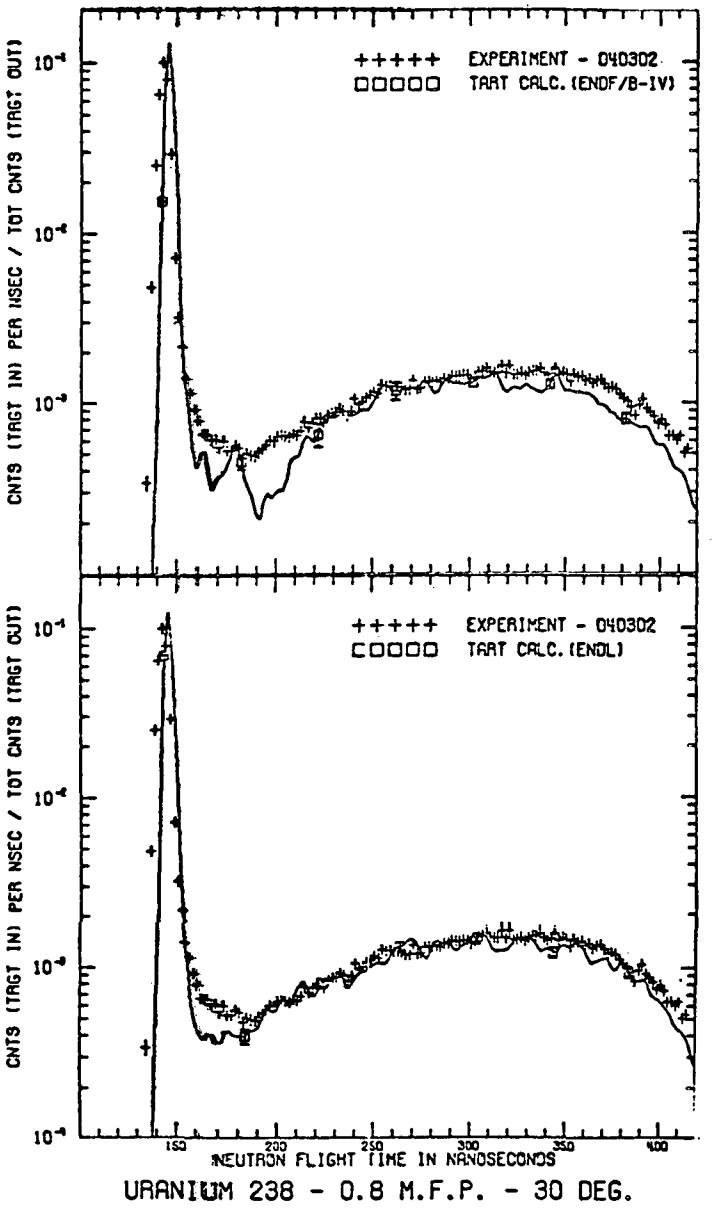

Fig. E-2. Comparison between the high energy measurements and calculations for the 0.8 m.f.p. sphere.

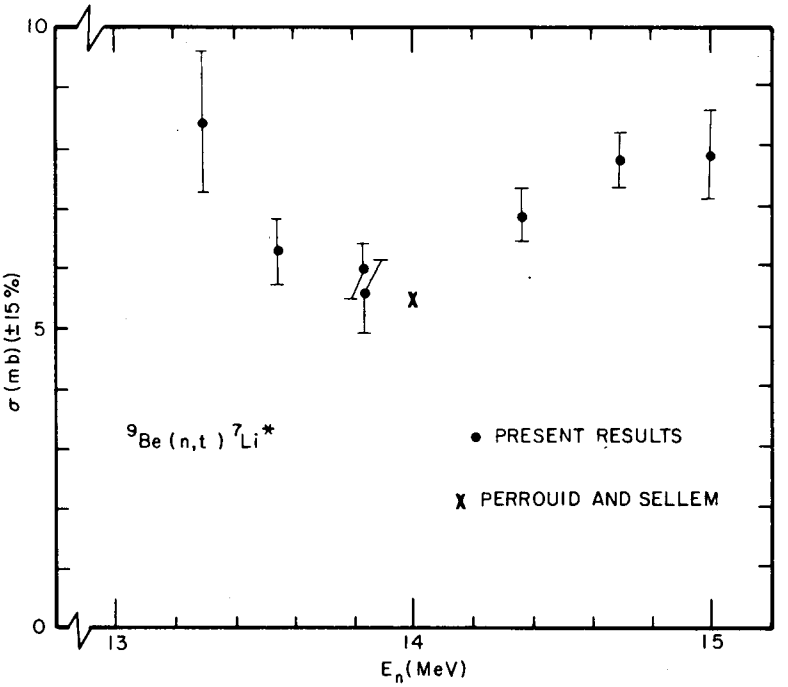

Fig. E-3. The $^{9}Be(n,t_1)\ ^{7}Li^{*}$ Cross Section.

LOS ALAMOS SCIENTIFIC LABORATORY, UNIVERSITY OF CALIFORNIA

A. STANDARDS

1. Elastic Scattering of 7-12 MeV Tritons by Alpha Particles (Jarmie, Ohlsen, Lovoi, Stupin, Hardekopf, Anderson, Sunier, Poore, Barrett, Hale, Dodder)

An abstract with the above title and with the following abstract was submitted for presentation at the Washington meeting of the American Physical Society, April 28 - May 1, 1975:

> The $^{6}Li(n,\alpha)T$ cross section at low energies is of importance in the design of fusion reactors and as a neutron flux standard. Ten to twenty percent discrepancies exist between various direct measurements of the cross section in the region of primary interest, i.e., near a narrow 5/2- resonance at a neutron energy of ~240 keV.[1] A multichannel R-matrix analysis code has been used to show that, near this essentially isolated resonance, accurate values of t-α elastic scattering cross sections can be used to determine the $^{6}Li(n,\alpha)T$ cross section. We have measured six t-α angular distributions at energies between 8.2 and 12.0 MeV, and excitation functions at six angles in the energy range 7.6 to 10 MeV. Over 700 data were obtained with absolute errors on the order of 1% or better. The data will be compared with the results of an earlier experiment.[2] R-matrix analysis of the data will be discussed.

2. $^{6}Li(n,\alpha)T$ Reaction (Hale)

New data have been included in the multichannel, multilevel R-matrix analysis of the ^{7}Li system which was used to provide neutron cross sections at low energies for the ENDF/B-IV evaluation of ^{6}Li. These include precision measurements just completed at LASL of t+α elastic scattering excitation functions and angular distributions for triton energies between 7.6 and 12 MeV. In addition, we replaced preliminary $^{6}Li(n,t)$ angular distribution measurements of Overley et al with their final values.[3] The present analysis also takes into account the pronounced forward peaking observed by Schröder et al[4] in the $^{6}Li(n,t)$ angular distribution of 25 keV.

---

[1] D. C. Dodder, G. M. Hale, R. A. Nisley, K. Witte, P. G. Young, Los Alamos Scientific Laboratory Report LA-UR-74-738.

[2] R. J. Spiger and T. A. Tombrello, Phys. Rev. 163, 964 (1967).

[3] J. C. Overley, R. M. Sealock, and D. H. Ehlers, Nucl. Phys. A221, 573 (1974).

[4] I. G. Schroder et al "Angular Anisotropy in the $^{6}Li(n,\alpha)^{3}H$ Reaction at 25 keV," Bull. Am. Phys. Soc. 20, 145 (1975).

The precise t+α measurements appear to determine values of the neutron total cross section and of the (n,α) cross section which peak at 11.1 and 3.4 barns, respectively. These values are .2 barns higher for the total cross section and .1 barn lower for the (n,α) cross section than had been obtained in the previous analysis. The asymmetry in the ^{6}Li(n,t) angular distribution is well reproduced at 25 keV, and satisfactory fits to the Overley data are obtained at higher energies, except for normalization differences near the resonance at 240 keV.

3. Total Cross Section of Tritium (Seagrave, with Berman and Phillips, LLL)

A three-week run in December for simultaneous measurement with a continuum neutron source of the total cross sections of hydrogen and tritium was completed without incident except for a false-alarm exercise caused by failure of one of the two sample-area tritium monitors. The 2520-psia tritium sample cell contained 19.1 grams of tritium. The three sample cells (tritium, hydrogen, and evacuated dummy) were mounted in a cylindrical total-containment vessel capable of confining the entire gas content at less than one atmosphere pressure. The samples were successively positioned in the collimated neutron beam by computer-controlled rotation of the vessel. Backgrounds measured with a meter-long copper "shadow bar" and with blocks of aluminum and graphite (which were "black" at the sharp resonances) were close to the machine-off time-dependent background in the detectors located at the end of the evacuated 250 m flight path. Neutron beam monitoring was accomplished by 90° scattering from a thin graphite sheet placed in the beam between the source collimator and the sample. In addition, high- and low-biased time-of-flight spectrum monitoring was recorded from a detector at 59 meters on a separate beam tube. To achieve a dynamic range from 50 keV to 50 MeV, signals from the matched-gain photomultiplier dynodes 9 and 14 were handled separately and recorded as two simultaneous data fields 64 pulse height channels by 4096 time channels, with an overlap in the most intense spectrum range between 2 and 3 MeV.

4. Spline-Fitting of Continuum Cross Section Data (Seagrave)

Tabular data was given in the May 1974 report for the RPI ^{3}He total cross section data.[5] Graphs and tables for ^{4}He have been deferred pending analysis of the new tritium data.

[5] C. A. Goulding, P. Stoler, and J. D. Seagrave, Nucl. Phys. A215, 253-259 (1973).

B. NEUTRON DATA APPLICATIONS

1. Radiative Thermal Neutron Capture by ^{59}Ni (Jurney)

The energy distribution of the gamma rays from $^{59}Ni(n,\gamma)^{60}Ni$ has been measured at the Los Alamos Omega West Reactor thermal neutron capture gamma ray facility. This facility makes use of an internal target configuration, in which the target under study is placed in the reactor thermal column at a position where the Cd ratio is ~1000; gamma rays from the capture process are extracted through collimators to a detector position external to the reactor structure. For the experiment described here, the target consisted of 9.8 mg of ^{59}Ni metal contained in a 1 cm diameter cavity in the center of a 2.5 cm diameter disk-shaped graphite holder. The detector was a 6.3 cm-dia by 15 cm-long NaI crystal surrounded by a 20 cm-dia by 25 cm-long NaI Compton suppression annulus. The combination of Compton suppression and collimation of the gamma-ray beam to an approximately 1 cm diameter spot at the center of the analyzing crystal results in an exceptionally clean, localized response function over a wide gamma ray energy range and reduces the burden on the process of unfolding the pulse-height spectrum into a spectrum composed of superimposed, full energy photopeaks. Calibration of the system in terms of capture cross section was made by substituting a 97 mg target of CH_2 for the ^{59}Ni target.

Summing the counts in the full energy peak from the single 2223 keV gamma ray from hydrogen capture permitted, through the use of a measured relative efficiency vs energy curve, a determination of the number of barns per count in the full-energy photopeaks in any part of the unfolded spectrum from ^{59}Ni.

Figure B-1 shows the photon spectrum from $^{59}Ni(n,\gamma)^{60}Ni$. Because the first few excited states in ^{60}Ni are widely spaced, the gamma ray spectrum above ~8.3 MeV contains only a very few isolated, intense transitions and, for this reason, provides an exceptionally good test of the system response matrix in the 8-12 MeV energy range.

The ^{59}Ni thermal (n,γ) cross section was computed by taking an energy-weighted sum of the individual bin yields. The value of the cross section thus determined is 53 ± 4 barns.

In a separate experiment, the gamma ray spectrum was measured with a 26 cm^3 Ge(Li) detector. Here the cross section was determined from an energy-weighted sum of the partial capture cross sections of the resolved gamma rays (235 in number). This measurement yielded a value of 51 ± 8 barns. The 846.75 keV transition representing the (n,α) branch to the 2^+ first excited state in ^{56}Fe was observed with an intensity corresponding to a partial cross section of 0.12 ± 0.03 barns.

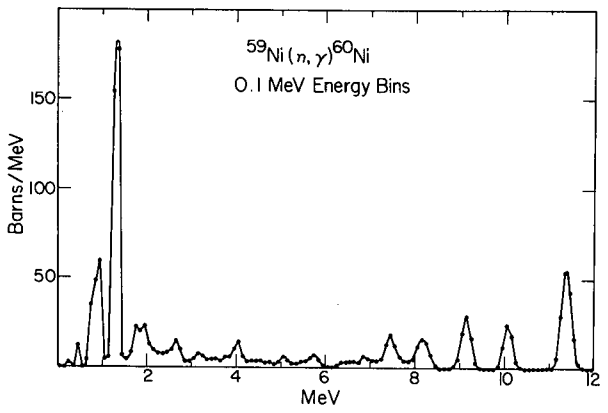

Fig. B-1. Photon spectrum from ^{59}Ni(n,γ)^{60}Ni.

2. Reactions of Polarized Neutrons on Polarized ^{235}U (Keyworth, Moses, Olsen, LASL; Dabbs, Hill, Oak Ridge National Laboratory)

A preliminary experiment[6] on reactions of polarized neutrons with a polarized ^{235}U target resulted in spin assignments for many resonances in ^{236}U below 60 eV. The experiment has been repeated with better counting statistics, and higher neutron polarization, and the results of the preliminary experiment have been confirmed and extended. The analysis of these data is not complete, but some results are available. We are able to make spin assignments up to at least 150 eV. At higher energies we are unable to identify individual resonances because of the limited energy resolution, but will probably be able to extract useful information from a statistical analysis of the data. Some results of this experiment have been presented in a paper contributed to the Conference on Nuclear Cross Sections and Technology. A copy of the abstract of that paper is included below:

> A polarized beam of neutrons and a polarized ^{235}U target have been used to determine the spins of resonances below 150 eV. Most spins are assigned by inspection of the data; others by comparison with multilevel or single-level fits. Previously published data on fission fragment angular distributions, in conjunction with our spin assignments, indicate that two or more fission channels are available to each spin state. The ratio of symmetric to asymmetric fission appears to be uncorrelated with the resonance spin.

3. Measurement of the Differential Elastic and Nonelastic Neutron Cross Sections and Emission Spectra from Beryllium for 6-, 10-, and 14-MeV Incident Neutrons (Auchampaugh, Drake)

Calculations of breeding ratios in proposed fusion blankets require a detailed knowledge of the neutron spectra from beryllium under bombardment by energetic neutrons. Little such information is available for beryllium, especially regarding the angular distribution of inelastic neutrons and those resulting from the (n,2n) reaction.

We have set up a neutron time-of-flight system at the Los Alamos Van de Graaff facility for measuring the angular distributions and spectra of neutrons emitted by targets bombarded by monoenergetic neutrons. The emitted neutrons are detected by a 10 cm-dia by 7.6 cm-thick

[6] G. A. Keyworth, C. E. Olsen, F. T. Seibel, J. W. T. Dabbs, and N. W. Hill, Phys. Rev. Lett., 31, 1077 (1973).

liquid scintillator located 2.7 meters from the sample. The detector was located inside a massive shield on a goniometer arm which could be remotely rotated about the sample axis. The gamma ray background was suppressed by operating the detector in the pulse shape discrimination mode.

The efficiency of the detector was measured relative to the H(n,n) elastic scattering cross section up to 7 MeV, and for higher energies the $T(d,n)^4He$ and $D(d,n)^3He$ cross sections were used as standards. A relative accuracy of ± 3% was achieved for $E_n > 1.5$ MeV, increasing to ± 30% near the detector bias threshold of 0.35 MeV.

Since the $T(p,n)^3He$ reactions, which is generally used as a monoenergetic neutron source in the 6-14 MeV energy region, produces a severe background from breakup of the tritons, the inverse reaction, $H(t,n)^3He$, was used. An additional advantage of the $H(t,n)^3He$ reaction over the inverse is an increase in neutron yield at 0° of an order of magnitude.

A summary of the data taken to date is given in Table B-1. The $H(t,n)^3He$ data at 10 MeV will be weighted more heavily than will the $T(p,n)^3He$ data because of the abovementioned background problem.

The secondary neutron emission spectra show strong variations, both as a function of angle and as a function of outgoing neutron energy. A preliminary analysis of the 6- and 10-MeV data using the $H(t,n)^3He$ reaction has been completed. A correction due to multiple scattering in the sample has been generated by a Monte Carlo code designed to mock up the experimental conditions. Our preliminary values for the differential elastic scattering cross section at 6 MeV agree well with previously published values. Little information regarding the neutron emission spectra was previously available. The measurements resulting from this work will make a substantial contribution.

4. Fourteen MeV, Neutron-Induced Gamma-Ray Production Cross Sections (Drake, Arthur, Silbert)

Gamma-ray production cross sections have been measured for samples of Mg, Al, Cr, Fe, Ni, Cu, Mo, Nb, Ta, Pt, ^{235}U, and ^{239}Pu. These samples were bombarded with a pulsed 14.2 MeV neutron beam obtained from the $^2H(t,n)^4He$ reaction. The samples located about 100 mm from the neutron source and the gamma rays produced by neutrons striking the samples were detected by a heavily shielded, NaI crystal, gamma-ray spectrometer system. An anti-Compton NaI scintillator surrounding the center crystal was used to suppress further the background events and improve the response functions.

TABLE B-I

Neutron Energy (MeV)	Source Reaction	Lab Angle	Number of Samples
5.87	H(t,n)	25, 35, 45, 60, 80, 100, 110, 125	2
5.87	T(p,n)	25, 35, 45, 60, 80, 100, 125	2
10.08	H(t,n)	25, 35, 45, 60, 80, 100, 110, 125	2
10.08	T(p,n)	35, 60, 125	2
14.2	D(t,n)	30, 45, 60, 80, 100, 125, 145	2

The pulsed neutron beam allowed time-of-flight discrimination, sorting out the desired gamma rays from extraneous neutron-related and other background events.

Net pulse height spectra (appropriate backgrounds subtracted) were converted to gamma-ray spectra by a stripping program NIBL.

Cross sections for gamma-ray production for the above samples are listed in Table B-2 as millibarns per steradian in 100 keV intervals from 300 to 4000 keV and in 500 keV intervals above 4000 keV.

5. (n,2n) and (n,3n) Measurements Using A Liquid Scintillator Tank (Veeser)

We have begun to measure (n,2n) and (n,3n) cross sections using a 75 cm-dia spherical liquid scintillator tank as a highly efficient neutron detector. Samples are placed at the center of the tank where they are struck by bursts of monoenergetic neutrons. When a neutron-emitting reaction takes place, the tank counts the number of neutrons released, and the (n,2n) and (n,3n) cross sections are determined from the probabilities of detecting two and three neutrons and from the detector efficiency, the target thickness, and the number of incident neutrons.

We have measured the cross sections of several nuclides which have radiochemically measurable residual nuclei because these can be used as neutron dosimeters. Measurements extend from 14.7 to 24 MeV for ^{45}Sc, ^{59}Co, ^{89}Y, ^{93}Nb, ^{103}Rh, ^{169}Tm, ^{175}Lu, ^{181}Ta, ^{197}Au, and ^{209}Bi. We have also begun to measure the (n,2n) cross section for beryllium which is of interest to the fusion reactor program. Where previous radiochemical measurements have been made, our cross sections are in general agreement except for lutetium for which our (n,2n) results are about 15% higher and our (n,3n) results are about 15% lower.

6. Cross Sections for (n,xn) Reactions Between 7.5 and 28 MeV (Bayhurst, Gilmore, Prestwood, Wilhelmy, Jarmie, Erkkila, Hardekopf)

An article with the above title and with the following abstract has been submitted to Physical Review C:

A total of 236 cross sections for (n,xn) reactions have been measured at neutron energies between 7.5 and 28 MeV, using radiochemical techniques. Cross sections for (n,n′) and (n,2n) reactions are reported on ^{193}Ir; (n,2n) cross sections on ^{45}Sc and ^{58}Ni; (n,2n), and (n,3n) cross sections on ^{89}Y, ^{90}Zr, and ^{107}Ag; (n,2n) (n,3n), and (n,4n) cross sections on ^{169}Tm, ^{175}Lu, ^{191}Ir, ^{197}Au, and ^{203}Tl; (n,3n) and (n,4n) cross sections on ^{151}Eu, and (n,4n)

TABLE B-2

DIFFERENTIAL GAMMA-RAY PRODUCTION CROSS SECTIONS AS A FUNCTION OF GAMMA-RAY ENERGY

Element →	MAGNESIUM				ALUMINUM		CHROMIUM		IRON			
Angle →	90°		128°		128°		120°		90°		120°	
Energy Interval (MeV)	Cross Section (mb/sr)	Est Uncertainty (mb/sr)	Cross Section (mb/sr)	Est Uncertainty (mb/sr)	Cross Section (mb/sr)	Est Uncertainty (mb/sr)	Cross Section (mb/sr)	Est Uncertainty (mb/sr)	Cross Section (mb/sr)	Est Uncertainty (mb/sr)	Cross Section (mb/sr)	Est Uncertainty (mb/sr)
0.3 - 0.4	5.1	0.6	7.2	1.0	2.3	0.6	6.5	0.9	6.2	0.6	8.1	1.3
0.4 - 0.5	2.8	0.4	3.7	0.8	3.2	0.6	9.8	1.1	12.1	1.3	10.2	1.2
0.5 - 0.6	1.7	0.3	1.8	0.5	0.61	0.36	9.1	1.0	8.3	0.9	4.2	0.3
0.6 - 0.7	0.56	0.21	0.36	0.46	0.0	0.35	9.8	1.1	5.0	0.5	1.8	0.7
0.7 - 0.8	1.5	0.2	2.0	0.5	3.2	0.5	10.4	1.1	15.0	1.5	15.7	2.0
0.8 - 0.9	2.7	0.3	2.3	0.5	3.4	0.5	10.5	1.1	34.5	3.5	43.4	4.6
0.9 - 1.0	2.0	0.3	2.0	0.5	6.0	0.7	12.2	1.3	11.8	1.2	12.8	1.5
1.0 - 1.1	1.9	0.3	1.5	0.5	4.1	0.5	5.0	0.6	6.5	0.7	6.9	0.8
1.1 - 1.2	2.8	0.3	2.3	0.5	1.2	0.3	6.1	0.6	9.7	1.1	11.0	1.4
1.2 - 1.3	5.5	0.6	6.2	0.8	1.5	0.3	11.6	1.2	18.6	1.8	23.3	2.4
1.3 - 1.4	16.5	1.7	17.9	1.9	1.3	0.3	29.5	3.0	10.0	1.0	13.3	1.4
1.4 - 1.5	8.3	0.9	8.5	1.0	1.2	0.3	33.7	3.4	4.1	0.4	4.9	0.6
1.5 - 1.6	2.2	0.3	1.3	0.4	1.4	0.3	12.4	1.3	2.7	0.3	3.0	0.5
1.6 - 1.7	2.3	0.3	1.8	0.4	3.1	0.4	2.8	0.4	3.6	0.4	4.0	0.5
1.7 - 1.8	3.6	0.4	3.1	0.5	7.1	0.8	3.4	0.4	4.5	0.5	5.4	0.6
1.8 - 1.9	3.6	0.4	3.4	0.5	6.5	0.7	2.2	0.3	4.3	0.5	4.7	0.6
1.9 - 2.0	2.0	0.2	2.5	0.4	2.9	0.4	2.3	0.3	3.1	0.3	3.5	0.4
2.0 - 2.1	1.1	0.2	1.1	0.3	2.4	0.3	2.6	0.4	2.9	0.3	3.2	0.4
2.1 - 2.2	1.0	0.2	0.75	0.27	4.7	0.5	2.2	0.3	3.0	0.3	3.2	0.4
2.2 - 2.3	0.97	0.15	0.49	0.25	6.0	0.7	2.3	0.3	2.3	0.3	2.4	0.3
2.3 - 2.4	0.98	0.14	1.1	0.3	3.6	0.4	2.3	0.3	2.2	0.3	2.5	0.4
2.4 - 2.5	1.3	0.2	0.93	0.24	2.3	0.3	1.7	0.3	2.7	0.3	2.7	0.4
2.5 - 2.6	1.4	0.2	1.4	0.3	1.7	0.3	1.8	0.2	3.2	0.4	3.6	0.5
2.6 - 2.7	1.7	0.2	1.8	0.3	1.3	0.2	1.6	0.2	2.7	0.3	3.2	0.4
2.7 - 2.8	1.9	0.2	2.3	0.3	1.4	0.2	1.7	0.2	2.1	0.2	2.4	0.3
2.8 - 2.9	1.7	0.2	2.0	0.3	1.9	0.3	1.6	0.2	1.9	0.2	2.0	0.3
2.9 - 3.0	1.1	0.1	1.2	0.3	3.7	0.4	1.7	0.2	1.9	0.2	2.1	0.3
3.0 - 3.1	0.97	0.14	1.0	0.2	3.9	0.5	2.3	0.3	1.8	0.2	2.0	0.3
3.1 - 3.2	0.79	0.12	1.1	0.2	2.4	0.3	2.3	0.3	2.0	0.2	2.2	0.3
3.2 - 3.3	0.67	0.11	0.67	0.21	1.4	0.2	2.3	0.3	2.0	0.2	2.5	0.3
3.3 - 3.4	0.54	0.10	0.84	0.20	0.96	0.18	1.8	0.3	1.9	0.2	2.3	0.3
3.4 - 3.5	0.75	0.12	1.1	0.2	0.62	0.16	1.3	0.2	1.9	0.2	2.2	0.3
3.5 - 3.6	0.69	0.11	0.5	0.21	0.53	0.16	1.6	0.2	1.9	0.2	2.3	0.3
3.6 - 3.7	0.92	0.13	0.95	0.22	0.78	0.17	1.8	0.2	1.8	0.2	2.2	0.3
3.7 - 3.8	1.34	0.2	1.0	0.2	0.90	0.18	1.5	0.2	1.7	0.2	2.0	0.3
3.8 - 3.9	1.5	0.2	1.5	0.3	0.88	0.18	1.7	0.2	1.4	0.2	1.7	0.3
3.9 - 4.0	1.4	0.2	1.4	0.3	1.2	0.2	1.4	0.2	1.4	0.2	1.7	0.3
4.0 - 4.5	1.3	0.27	1.3	0.27	0.84	0.20	1.4	0.2	1.2	0.2	1.4	0.2
4.5 - 5.0	0.71	0.23	0.71	0.23	0.90	0.20	1.4	0.2	1.0	0.2	1.2	0.2
5.0 - 5.5	0.51	0.21	0.51	0.21	0.75	0.19	1.2	0.2	0.99	0.14	1.2	0.2
5.5 - 6.0	0.56	0.21	0.56	0.21	0.73	0.19	1.3	0.2	0.99	0.15	1.1	0.2
6.0 - 6.5	0.56	0.24	0.56	0.24	0.56	0.21	1.0	0.2	0.98	0.17	1.2	0.2
6.5 - 7.0	0.50	0.25	0.50	0.25	0.49	0.24	0.87	0.24	0.98	0.18	1.1	0.2
7.0 - 7.5	0.59	0.24	0.59	0.24	0.56	0.23	0.84	0.25	0.88	0.16	1.0	0.2
7.5 - 8.0	0.64	0.22	0.64	0.27	0.53	0.16	0.91	0.18	0.79	0.15	0.90	0.17
8.0 - 8.5	0.41	0.13	0.41	0.13	0.32	0.11	0.91	0.18	0.69	0.13	0.79	0.18
8.5 - 9.0	0.61	0.14	0.61	0.14	0.45	0.13	0.71	0.16	0.60	0.12	0.84	0.14

TABLE B-2 (cont)

Element →	NICKEL		COPPER		MOLYBDENUM				NIOBIUM	
Angle →	120°		120°		90°		120°		120°	
Energy Interval (MeV)	Cross Section (mb/sr)	Est Uncertainty (mb/sr)	Cross Section (mb/sr)	Est Uncertainty (mb/sr)	Cross Section (mb/sr)	Est Uncertainty (mb/sr)	Cross Section (mb/sr)	Est Uncertainty (mb/sr)	Cross Section (mb/sr)	Est Uncertainty (mb/sr)
0.3 - 0.4	12.1	1.3	22.0	2.4	---	---	22.1	2.5	29.4	3.2
0.4 - 0.5	13.2	1.4	15.8	1.7	---	---	27.6	3.6	30.5	3.3
0.5 - 0.6	3.7	0.5	10.1	1.1	20.3	2.1	24.5	2.9	17.6	1.9
0.6 - 0.7	2.5	0.4	10.1	1.1	29.4	3.0	40.6	4.5	12.2	1.5
0.7 - 0.8	5.0	0.5	6.7	0.7	52.5	5.3	63.4	6.7	16.7	1.8
0.8 - 0.9	4.6	0.5	10.6	1.0	42.9	4.3	46.3	4.8	14.9	1.7
0.9 - 1.0	8.2	0.8	21.0	2.1	22.6	2.3	25.5	2.7	25.2	2.6
1.0 - 1.1	9.1	0.9	16.8	1.7	20.7	2.1	23.8	2.6	14.4	1.6
1.1 - 1.2	12.5	1.2	23.9	2.4	16.6	1.7	18.6	2.0	11.6	1.3
1.2 - 1.3	15.4	1.5	15.8	1.6	11.3	1.2	12.2	1.3	7.9	1.0
1.3 - 1.4	18.8	1.9	13.3	1.4	10.5	1.1	11.6	1.3	9.7	1.2
1.4 - 1.5	16.1	1.6	9.9	1.0	13.3	1.3	15.4	1.7	9.4	1.1
1.5 - 1.6	7.5	0.8	7.3	0.8	14.1	1.4	14.7	1.6	8.1	1.0
1.6 - 1.7	4.5	0.4	5.9	0.7	9.8	1.0	9.7	1.1	7.2	0.9
1.7 - 1.8	4.6	0.5	5.0	0.5	7.7	0.8	7.4	0.8	4.4	0.7
1.8 - 1.9	4.2	0.5	5.6	0.6	6.3	0.7	6.4	0.7	6.0	0.8
1.9 - 2.0	2.9	0.3	4.5	0.5	5.9	0.6	6.1	0.7	6.2	0.8
2.0 - 2.1	2.4	0.3	3.4	0.4	5.5	0.6	5.5	0.7	7.3	0.9
2.1 - 2.2	2.4	0.3	3.1	0.4	4.8	0.5	4.9	0.6	7.3	0.9
2.2 - 2.3	2.1	0.2	2.5	0.3	4.3	0.5	4.4	0.6	6.2	0.8
2.3 - 2.4	2.2	0.2	2.5	0.3	3.9	0.4	4.2	0.5	5.0	0.6
2.4 - 2.5	2.2	0.3	2.2	0.3	3.8	0.4	3.7	0.5	3.5	0.5
2.5 - 2.6	2.1	0.2	2.1	0.3	3.2	0.3	3.3	0.4	3.2	0.5
2.6 - 2.7	2.3	0.3	1.9	0.2	3.0	0.3	3.0	0.4	2.2	0.4
2.7 - 2.8	2.2	0.3	1.8	0.2	2.8	0.3	3.0	0.4	3.0	0.5
2.8 - 2.9	2.3	0.3	1.9	0.2	2.7	0.3	2.6	0.4	2.2	0.4
2.9 - 3.0	2.4	0.3	1.7	0.2	2.2	0.2	2.3	0.3	2.4	0.4
3.0 - 3.1	2.5	0.3	1.7	0.2	2.0	0.2	2.3	0.3	1.6	0.4
3.1 - 3.2	2.3	0.3	1.6	0.2	2.0	0.2	1.9	0.3	1.3	0.4
3.2 - 3.3	2.1	0.2	1.6	0.2	1.8	0.2	2.0	0.3	1.7	0.4
3.3 - 3.4	1.9	0.2	1.6	0.2	1.7	0.2	1.7	0.3	1.5	0.4
3.4 - 3.5	1.5	0.2	1.5	0.2	1.6	0.2	1.4	0.3	0.45	0.31
3.5 - 3.6	1.4	0.2	1.3	0.2	1.4	0.2	1.4	0.3	1.1	0.3
3.6 - 3.7	1.4	0.2	1.4	0.2	1.3	0.2	1.3	0.3	1.2	0.3
3.7 - 3.8	1.3	0.2	1.3	0.2	1.3	0.2	1.0	0.2	0.68	0.33
3.8 - 3.9	1.3	0.2	1.3	0.2	1.2	0.2	1.2	0.2	1.3	0.3
3.9 - 4.0	1.1	0.2	1.1	0.2	1.1	0.1	1.0	0.2	0.86	0.32
4.0 - 4.5	1.2	0.2	1.2	0.2	0.95	0.14	0.83	0.24	0.56	0.33
4.5 - 5.0	1.1	0.2	0.95	0.17	0.69	0.11	0.66	0.23	0.65	0.28
5.0 - 5.5	1.1	0.2	0.81	0.15	0.51	0.10	0.52	0.24	0.29	0.30
5.5 - 6.0	0.96	0.17	0.78	0.15	0.45	0.09	0.46	0.29	0.35	0.30
6.0 - 6.5	0.92	0.18	0.64	0.15	0.39	0.09	0.38	0.28	0.33	0.32
6.5 - 7.0	0.81	0.18	0.59	0.15	0.26	0.09	0.33	0.25	0.30	0.38
7.0 - 7.5	0.77	0.16	0.40	0.11	0.23	0.07	0.26	0.14	0.30	0.31
7.5 - 8.0	0.67	0.13	0.29	0.07	0.15	0.05	0.17	0.11	0.12	0.14
8.0 - 8.5	0.54	0.13	0.15	0.05	0.09	0.03	0.14	0.08	0.14	0.14
8.5 - 9.0	0.36	0.08	0.13	0.05	0.08	0.03	0.13	0.08	0.13	0.12

TABLE B-2 (cont)

Element →	TANTALUM		PLATINUM		URANIUM		PLUTONIUM	
Angle →	120°		122°		120°		120°	
Energy Interval (MeV)	Cross Section (mb/sr)	Est Uncer-tainty (mb/sr)	Cross Section (mb/sr)	Est Uncer-tainty (mb/sr)	Cross Section (mb/sr)	Est Uncer-tainty (mb/sr)	Cross Section (mb/sr)	Est Uncer-tainty (mb/sr)
0.3 - 0.4	63.4	7.4	128	13	201	20	281	29
0.4 - 0.5	71.4	7.7	152	15	217	22	262	27
0.5 - 0.6	31.0	3.7	88.5	8.9	161	17	202	21
0.6 - 0.7	16.6	2.4	35.6	3.7	130	13	154	15
0.7 - 0.8	15.9	2.3	22.4	2.4	111	11	126	13
0.8 - 0.9	17.3	2.4	20.0	2.1	93	10	102	11
0.9 - 1.0	19.4	2.5	17.6	1.9	78	7.8	81	9.6
1.0 - 1.1	23.3	2.8	20.3	2.2	63	6.4	70	8.3
1.1 - 1.2	23.1	2.8	19.8	2.1	60	6.0	65	8.1
1.2 - 1.3	16.6	2.2	16.7	1.8	55	5.5	58	7.3
1.3 - 1.4	19.0	2.4	16.8	1.8	48	4.8	48	6.1
1.4 - 1.5	16.9	2.2	16.9	1.8	40	4.1	40	4.9
1.5 - 1.6	13.9	1.9	16.9	1.8	37	3.7	36	4.5
1.6 - 1.7	13.4	1.8	16.2	1.7	34	3.3	31	4.2
1.7 - 1.8	12.0	1.7	16.2	1.7	32	3.4	29	3.8
1.8 - 1.9	12.4	1.7	13.8	1.5	28	2.8	24	3.1
1.9 - 2.0	11.5	1.5	11.3	1.2	25	2.6	21	2.7
2.0 - 2.1	10.6	1.4	10.7	1.2	21	2.2	20	2.8
2.1 - 2.2	11.2	1.5	8.8	1.0	19	2.1	19	2.6
2.2 - 2.3	9.6	1.3	8.3	0.9	18	2.0	15	2.2
2.3 - 2.4	8.9	1.2	7.9	0.9	15	1.7	14	2.1
2.4 - 2.5	7.8	1.1	7.4	0.8	14	1.5	12	2.0
2.5 - 2.6	6.7	1.0	6.5	0.7	13	1.3	12	2.0
2.6 - 2.7	6.4	1.0	6.4	0.7	12	1.3	10	1.8
2.7 - 2.8	6.8	1.0	5.4	0.6	9.9	1.1	9.5	1.7
2.8 - 2.9	5.8	0.9	5.3	0.6	9.2	1.1	9.7	1.8
2.9 - 3.0	5.2	0.9	3.7	0.5	8.6	1.0	8.0	1.6
3.0 - 3.1	4.7	0.9	3.1	0.5	6.2	0.9	5.7	1.4
3.1 - 3.2	3.4	0.8	2.6	0.4	5.8	0.8	4.7	1.4
3.2 - 3.3	4.6	0.9	3.1	0.4	5.7	0.8	8.2	1.6
3.3 - 3.4	4.1	0.8	2.3	0.4	5.3	0.8	4.5	1.3
3.4 - 3.5	2.2	0.7	1.8	0.3	4.7	0.7	4.5	1.4
3.5 - 3.6	2.6	0.8	1.9	0.3	3.7	0.7	2.3	1.3
3.6 - 3.7	2.3	0.7	1.4	0.3	3.6	0.6	4.3	1.3
3.7 - 3.8	1.2	0.7	1.9	0.4	4.0	0.7	2.3	1.3
3.8 - 3.9	3.0	0.7	1.3	0.3	4.0	0.7	3.4	1.3
3.9 - 4.0	1.8	0.7	1.5	0.3	2.9	0.7	3.6	1.3
4.0 - 4.5	1.2	0.7	0.66	0.29	2.6	0.6	1.7	1.2
4.5 - 5.0	0.77	0.61	0.71	0.25	1.8	0.6	1.4	1.0
5.0 - 5.5	0.40	0.63	0.56	0.27	1.2	0.6	1.4	1.0
5.5 - 6.0	0.60	0.64	0.14	0.27	0.7	0.6	0.6	0.6
6.0 - 6.5	0.59	0.77	0.30	0.30	0.9	0.6	0.8	0.7
6.5 - 7.0	0.84	0.93	0.35	0.37	0.7	0.7	0.9	0.8
7.0 - 7.5	0.37	0.60	0.17	0.19	0.6	0.4	0.8	0.4
7.5 - 8.0	0.19	0.35	0.19	0.15	0.3	0.2	0.5	0.3
8.0 - 8.5	0.27	0.22	0.09	0.08				
8.5 - 9.0	0.30	0.24	0.03	0.07				

cross sections on ^{205}Tl. Neutron fluences were determined by either the $^{27}Al(n,\alpha)^{24}Na$ or the $^{90}Zr(n,2n)^{89}Zr$ reactions appropriately combined with proton-recoil telescope measurements. The excitation functions are compared with calculations based on a model incorporating both compound-nucleus and pre-equilibrium decay modes. Cross sections for the $^{27}Al(n,$ $^{27}Al(n,\alpha)^{24}Na$ reaction between 21 and 26 MeV are also reported.

7. Prompt and Delayed Gamma Rays from Fission of ^{235}U and ^{239}Pu (Foster)

A preliminary evaluation has been completed of the yield and spectrum of gamma rays from the neutron-induced fission of ^{235}U and ^{239}Pu. The evaluation covers the range from prompt (<1 nsec) to 60 sec and is in ENDF/B format. The data up to 1 msec are taken from various publications of Sund, Walton, et al[7]; and later data are from Fisher and Engle.[8] The uncertainties are estimated to be less than 20% except at the highest photon energies.

8. Calculated Medium-Energy Cross Sections and Secondary Spectra of Light Nuclei (Foster)

Two-million-word histories (30,000-100,000 events) have been generated for ^{12}C and ^{16}O bombarded by protons at each of 15 selected energies from 20 MeV to 3.5 GeV, using the ORNL intranuclear-cascade code with a rewritten evaporation module. The light nuclei present special problems because the cascade module frequently emits more particles, charge, or energy than is available in the nucleus. These problems have been addressed by renormalizing the spectra for minor energy overshoots and by discarding events which produce pathological nuclei or large energy overshoots. The evaporation module treats the kinematics exactly in the nonrelativistic approximation, and is fully protected against various contingencies which arise when the target nucleus is completely disintegrated. Energies and directions of all secondary products up to alpha particles are preserved, since they are markedly anisotropic in the laboratory system. The data are stored as individual histories to permit various analyses of them to be performed without having to repeat the Monte Carlo calculations.

---

[7] For example, R. B. Walton and R. E. Sund, Phys. Rev. 178, 1894 (1969); V. V. Verbinski and R. E. Sund, "Measurement of Prompt Gamma-Rays from Thermal-Neutron Fission of ^{235}U and ^{239}Pu, and from Spontaneous Fission of ^{252}Cf," Gulf General Atomic report GA-9148, (1969).

[8] P. C. Fisher and L. B. Engle, Phys. Rev. 134, B796 (1964).

9. Model Code Development (Young and Arthur)

We have developed a model code based on statistical theory and incorporating a gamma-ray cascade routine that permits calculation of level activation cross sections, discrete gamma-ray cross sections, isomer ratios, and particle and gamma-ray spectra from arbitrary reactions. The code follows closely the theory described by Uhl[9] and permits calculation for six decay channels each for up to ten decaying nuclei. Externally calculated optical model transmission coefficients are used to compute particle-decay widths, and either the Weisskopf[10] single particle estimate or the Brink-Axel[11] giant dipole resonance model is used to estimate gamma-ray widths. Gamma-ray emission by electric and magnetic dipole or quadrupole transitions are allowed. The Gilbert and Cameron[12] form of level density function is used and is matched with inputted discrete level data for up to 50 low-lying states per residual nucleus. A simple preequilibrium model is used to correct the particle spectra for semi-direct processes.

10. Fission-Product Data Base (England and Stamatelatos)

We have participated in a national task force to include fission yield, cross sections and decay data in Version IV of ENDF/B.[13] Our major responsibility is in the area of direct fission yields, and to date 10 sets of direct yields each covering > 1100 nuclides are available in the data file.

The fission yield and decay data file have been used to calculate time-dependent photon spectra and photoneutron spectra at various times between 1 and 1000 hours after thermal and fast fission of ^{233}U, ^{235}U, ^{238}U, and ^{239}Pu.[14] Yield and decay data for all fission products with half-lives $\geq$ 15 minutes and gamma energies above the $^{9}Be(\gamma,n)^{8}Be$ threshold were used in the calculations.

---

[9] M. Uhl, Acta Physica Aust. 31, 245 (1970).

[10] J. M. Blatt and V. F. Weisskopf, Theoretical Nuclear Physics, Wiley, New York, (1952).

[11] D. M. Brink, Thesis, Oxford University, 1955; P. Axel, Phys. Rev. 126, 671 (1962).

[12] A. Gilbert and A. G. W. Cameron, Can. J. Phys. 43, 1446 (1965).

[13] R. E. Schenter and T. R. England, "Nuclear Data for Calculation of Radioactivity Effects," Trans. Am. Nucl. Soc., to be published, (June, 1975).

[14] M. G. Stamatelatos and T. R. England, "Fission-Product Gamma-Ray and Photoneutron Spectra," Conference on Nuclear Cross Sections and Technology, Washington, D. C. (March, 1975).

C. NON-NEUTRON NUCLEAR DATA

1. Half-Lives of ^{129m}Xe, ^{131m}Xe, ^{133m}Xe, and ^{135g}Xe (Hoffman, Barnes, Dropesky, Lawrence, Kelley, Ott)

The half-lives of several Xe isotopes were remeasured because accurate values were needed in our determinations of the isomer ratios and yields of the Xe isotopes from various types of fission. The values reported in the literature at the time the study was begun were rather old and did not appear to be of sufficient accuracy. Since then a number of very accurate values have been reported.

Approximately 3 mg samples of Xe gas in quartz capsules were irradiated in the Los Alamos Omega West Reactor for about 30 minutes at a flux of 5-7 x 10^{13} n-cm^{-2} -sec^{-1}. The samples were then processed in an electromagnetic isotope separator[15] using the conventional oscillating electron ion source. Separation times were typically 2 to 3 hours, and the yields as estimated from integration of ^{134}Xe ion current approached 20%. Following separation, the aluminum collection foil was cut into strips representing the 129, 131, 133, and 135 mass fractions. The strips were mounted on standard counting plates and covered with transparent tape. (Previous studies showed that no Xe activity was lost even from uncovered sample foils.) The decay of each sample was followed for eight half-lives or more with standard end-window, β-proportional counters. No contamination with other activities was detected except in the case of the ^{135g}Xe samples in which (3-8) x 10^{-5} of the total activity was ^{133g}Xe. Computer least-squares analyses of the β-decay data by the "Skitzo" program gave the half-lives and standard deviations shown in Table C-1. The final quoted errors are estimated "overall" errors.

Our values for ^{133m}Xe, ^{133g}Xe, and ^{135g}Xe of 2.19 ± 0.05 days, 5.25 ± 0.02 days, and 9.104 ± 0.020 hr are in good agreement with those of 2.188 ± 0.008 days, 5.240 ± 0.006 days, and 9.083 ± 0.013 hr recently reported by Fontanilla et al,[16] and of 5.245 ± 0.006 days for ^{133g}Xe reported by Cavallo et al.[17] Our value of 8.87 ± 0.03 days for ^{129m}Xe agrees within the estimated error with that of 8.89 ± 0.02 days given by Miller et al.[18] Our value of 11.92 ± 0.03 days for ^{131m}Xe is in agreement with that of 11.9 ± 0.1 days reported by Martin and Blichert-Toft.[19] A value of 12.00 ± 0.02 days has also been reported by Emery et al.[20]

---

[15] The Los Alamos Isotope Separator was built by K/CM Mileikowsky and Co., Stockholm, Sweden.

[16] J. Fontanilla, A. L. Prindle, J. H. Landrum, and R. A. Meyer, BAPS 19, 501 (1974).

[17] L. M. Cavallo, F. J. Schima, and M. P. Unterweger, Phys. Rev. C10, 2631 (1974).

[18] L. D. Miller and F. J. Schima, Int. J. appl. Rad. Isotop. 24, 353 (1973).

[19] M. J. Martin and P. H. Blichert-Toft, Nucl. Data Tables A8, 1 (1970).

[20] J. F. Emery, S. A. Reynolds, E. I. Wyatt, and G. I. Gleason, Nucl. Sci. Eng. 48, 319 (1972).

Table C-1. Half-Lives of Xe Isotopes

Nuclide	Individual determinations[a]	Time followed	Weighted average[b]
^{129m}Xe	8.844 ± 0.003 days	3-120 days	8.87 ± 0.03 days
	8.872 ± 0.001 days	4-189 days	
^{131m}Xe	11.930 ± 0.004 days	3-98 days	11.92 ± 0.03 days
	11.921 ± 0.001 days	4-189 days	
^{133m}Xe	2.19 ± 0.03 days	2-85 days	2.19 ± 0.05 days
^{133g}Xe	5.247 ± 0.003 days	2-85 days	5.25 ± 0.02 days
	5.251 ± 0.002 days	4-98 days	
^{135g}Xe	9.095 ± 0.002 hr	0.5-27 days	
	9.107 ± 0.002 hr	0.5-27 days	9.104 ± 0.020 hr
	9.110 ± 0.002 hr	0.5-27 days	

[a]The error quoted on the individual determinations is the standard deviation from least-squares analysis of the data.

[b]The error quoted on the average is an estimated "overall" error.

2. Studies of (^{3}He,df) and ^{3}He,tf) Reactions (Britt, Gavron, Weber, and Wilhelmy)

The (^{3}He,df) and (^{3}He,tf) reactions have been used to measure fission probability distributions ($P_f = \Gamma_f/(\Gamma_f+\Gamma_n)$) for 26 actinide nuclei including $^{230-233}$Pa, $^{231-232}$U, $^{233-239}$Np, $^{239-243}$Am, $^{241-244}$Cm, and $^{248-249}$Bk. Measurements include excitation energies from threshold up to ~ 12 MeV. This technique for measuring Γ_f/Γ_n up to high excitation energies has been tested by comparing several cases where (^{3}He,df) and (^{3}He,tf) reactions can be used to excite the same residual nucleus, and by comparing (^{3}He,df) and (n,f) results. Results indicate that these reactions can be used to measure absolute fission probabilities to an accuracy of ~ ± 10% up to an excitation energy of ~ 12 MeV.

In order to try to understand these data in a more fundamental way we have improved our previous microscopic statistical model[21] by incorporating the enhancements to the nuclear level densities due to coupling to collective degrees of freedom as suggested by Bjørnholm, Bohr, and Mottelson.[22] With this improved statistical theory we found that we could reproduce the absolute values and energy variations of the fission probabilities for all nuclei from Pa through Bk without using any arbitrary adjustable parameters. The key to obtaining absolute calculations of fission probabilities was to assume that the nucleus passes over the first peak of the fission barrier with an axially asymmetric shape while its shape is axially symmetric at both the equilibrium deformation and the second peak of the fission barrier. Thus, these results give the first direct experimental confirmation of an axially asymmetric shape at the first barrier as has been predicted by several theoretical calculations.

In addition, equivalent neutron fission cross sections for these nuclei have been estimated using the relations: $\sigma_{n,F}(E_n) = P_f(E_n + B_n) \cdot \sigma_{cn}(E_n)$ where σ_{cn} is the total compound nucleus formation cross section for an incident neutron taken from optical model calculations. Preliminary results indicate that this technique can yield reasonable (n,f) cross sections for $E_n > 2$ MeV. For $E_n < 2$ MeV deviations of ~ 20-30% sometimes occur between measured (n,f) cross sections and values deduced from the direct reaction experiments. For the region $E_n < 2$ MeV we are currently investigating both possible improvements in the optical model calculations and corrections for the different angular momentun distribution excited in two types of reactions.

[21] B. B. Back, H. C. Britt, Ole Hansen, B. Leroux, and J. D. Garrett Phys. Rev. C10, 1948 (1974).

[22] S. Bjørnholm, A. Bohr, and B. R. Mottelson, in Proceedings of the Third International Atomic Energy Symposium on the Physics and Chemistry of Fission, Rochester, 1973.

D. NUCLEAR DATA FOR CTR

1. $T(d,n)^4He$ Reaction (Hale and Stewart)

Most measurements of the $T(d,n)^4He$ cross section at low deuteron energies are nearly 20 years old, and considerable uncertainty occurs in extrapolating the measurements to zero energy for fusion applications. Many of the measurements have been checked by including them in a preliminary, but comprehensive, R-matrix analysis of reactions in the five-nucleon system at low energies. The analysis includes data from the reactions $T(d,d)T$, $T(d,n)^4He$, and $^4He(n,n)^4He$ in the ^5He system, as well as data from the reactions $^3He(d,d)^3He$, $^3He(d,p)^4He$, and $^4He(p,p)^4He$ in the ^5Li system. In addition to the integrated reaction cross sections, these data include differential cross sections, polarizations, and analyzing tensors for the deuteron-induced reactions. Resonance parameters in the two systems (^5He and ^5Li) are related by charge symmetry, so that all the reactions are analyzed simultaneously.

A satisfactory fit to all data included in the analysis has been obtained. The calculated cross sections produce much better agreement with low energy measurements by Arnold et al[23] than was obtained with a Gamow extrapolation. This information has been included in a report[24] discussing the status of measurements and parameterizations for two of the important fusion reactions, $T(d,n)^4He$ and $T(t,2n)^4He$, at energies below 1 MeV.

2. (n,2n) Cross Sections for ^{93}Nb and ^{169}Tm (Young of LASL and Philis of Centre d'Etudes de Bruyères-le-Châtel, Montrouge, France)

Preliminary evaluations of the total (n,2n) cross sections of ^{93}Nb and ^{169}Tm and of the $^{93}Nb(n,2n)$ activation cross section leading to the first excited state of ^{92}Nb have been completed for neutron energies from threshold to 20 MeV. Where sufficient information was available, the measurements were renormalized to modern standards and a set of recommended values and errors was determined from the corrected measurements.

3. Laser Fusion Applications (Seagrave)

More discriminating methods than are presently in use are desirable for selection and inspection of the tiny glass microballoons used for D-T gas-containing laser targets. Present methods include liquid-floatation screening, high-pressure crushing and liquid pressure cycling to sink

---

[23] W. R. Arnold, J. A. Phillips, G. H. Sawyer, E. J. Stovall, and J. L. Tuck, "Cross Sections for the Reactions $D(d,p)T$, $D(d,n)^3He$, $T(d,n)^3He$, and $^3He(d,p)^4He$ Below 120 keV," Phys. Rev. 93, 483 (1954).

[24] Leona Stewart and Gerald M. Hale, "The $T(d,n)^4He$ and $T(t,2n)$ Cross Sections at Low Energies," Los Alamos Scientific Laboratory Report LA-5828-MS, (1975).

leaky balloons, and floatation in compressed SF_6. The yield from the bulk material is about 10^{-6}, and radiography is then used to assess wall uniformity. The existing methods are more effective in eliminating poor specimens than in assessing the quality for final selection. A typical size of interest might be 50 μm in diameter with 1-2 μm wall, the exact dimensions being less important than the uniformities: ± 0.5 μm on the diameter and ± 0.1 μm on the thickness being the sort of precision desired. Livermore uses an interference scheme[25] for this purpose, but a faster and selective system is desirable. Several other optical methods are being investigated at LASL.

a. Video Microscopy

The equipment available is comparable in scope with the video and densitometer systems used at Livermore,[26] but the real-time 3-D display and the color-band area measurement features offer variations which may be more satisfactory for screening purposes. Also, our flexibility of adaptation to different microscopes is a distinct advantage, as preliminary visual observation with dark-field and phase-contrast microscopes show much higher detail. The system in the densitometric mode can also be applied to the radiographs.

b. Mie Scattering

A code for calculating the light scattering from concentric spheres is being adapted to larger spheres, and will be run for some representative cases. It will also apply to a core of frozen D-T and to the changes associated with an immersion fluid. (Matching the glass index will permit observation of scattering from the inner surface alone.)

c. Ring/Wedge Detector Analysis

A Recognition System, Ins. (RSI) 32-ring/32-wedge photodetector for Fourier transform analysis and feature characterization has been set up with a 64-channel multiplex interface, which permits output of the detector data to an incremental plotter and a digital printer. The RSI detector is appropriate for direct scattering distribution characterization as well as Fourier transform dissection. The wedge distribution

[25] R. R. Stone and P. C. Souers, "Nondestructive Inspection of Transparent Microtargets for Laser Fusion" (Preprint and Private Communication).
[26] R. P. Reedy, "Nondestructive Testing of Laser Targets," UCRL-51630 (1974).

gives an immediate test of the uniformity of scattering independent of the complexity of the radial distribution. The advantage of the Fourier transform optical setup is that the pattern of the detector is insensitive to position of the sample, and a slide or pellicle supporting a balloon can be presented rapidly in several orientations to the laser beam and moreover masked for successive testing of balloons located in a rough array. Transform analysis can also be applied to the radiographs.

d. Glory Scattering

This special case of 180° scattering[27] seems most apposite to this problem, as the peaking in the backward direction involves a surface wave as well as a refractive trajectory (in raindrops). The latter may prove negligible in the thin-walled spheres, but is likely to be compensated by a wave-guide effect which may greatly enhance the coupling between surface waves at the two interfaces. The glory effect in raindrops is strongly resonant in wavelength, and if it proves to be so in balloons, one may envision a large field of them illuminated with parallel light from a monochromater, perhaps viewed by the video system. As the light is swept in wavelength, good spheres will "flash" at their resonant point, giving dimensional data, and the intensity of the flash will give a measure of the uniformity of the dimension.

E. MEDICAL APPLICATIONS

1. Excitation Functions for the $^{12}C(\pi^{\pm},\pi N)^{11}C$ Reactions over the Region of the (3,3) Resonance (Dropesky, Butler, Orth, Williams, LASL; Friedlander, BNL; Yates, CMU; Kaufman, ANL)

The need to establish the $^{12}C(\pi^{\pm},\pi N)^{11}C$ reaction as a foil activation flux monitor for pion beams, in analogy with the widely used $^{12}C(p,pn)^{11}C$ reaction for proton beams, called for a careful remeasurement of the excitation functions for the formation of ^{11}C by π^+ and π^- over the energy range available at the Clinton P. Anderson Meson Physics Facility (LAMPF). A paper with the above title and authors and with the following abstract has been submitted to Physical Review Letters:

> The excitation functions for the $^{12}C(\pi^{\pm},\pi N)^{11}C$ reactions have been measured over the energy ranges 50 to 470 MeV for π^+ and 40 to 550 MeV for π^-. These excitation functions, clearly reflecting the (3,3) pion-nucleon resonance, show an upward energy shift in the resonance peak for π^- and a downward shift for π^+. The $\sigma_{\pi^-}/\sigma_{\pi^+}$ ratio at 180 MeV is 1.55 ± -.10.

[27] H. C. Bryant and N. Jarmie, "The Glory," Scientific American 231.1 (July 1974) 60-71.

A. INTRODUCTION

We continue to place primary emphasis on the absolute measurement of cross sections in nearly-monoenergetic neutron fluxes produced by photoneutron sources. These measurements are intended to provide independent normalization points to cross section data produced at linacs and other TOF facilities. Our facilities for the irradiation, rapid transfer, and calibration of photoneutron sources are now well-developed, and work is continuing on additional sources to supplement those which were used in the measurements reported here.

B. ABSOLUTE FISSION CROSS SECTION OF ^{235}U. (J. C. Robertson, M. C. Davis, J. C. Engdahl, G. F. Knoll)

Work completed earlier using a Na-Be source was recently reported at the Conference on Nuclear Cross Sections and Technology.[1] Final value obtained is 1.21 ± .025 barns at 964 keV.

Primary measurements have been completed using a newly-fabricated Na-D source. A preliminary value of 1.32 barns has been obtained for the source median energy of 265 keV. Until secondary measurements relating to various correction factors are completed, an estimated uncertainty of about 3% should be associated with the present value. Final corrections and error checks are expected to reduce this uncertainty to approximately 2%. Measurements at the new source energy were carried out in a very similar manner to those reported earlier.[1] Dual target geometry, limited solid angle fission fragment recording, track-etch detectors with manual counting, and manganese bath calibration of the source were all features of the experimental method. A paper describing this measurement will be given at the June ANS meeting.

C. ABSOLUTE FISSION CROSS SECTION OF ^{239}Pu. (J. C. Robertson, M. C. Davis, J. C. Engdahl, G. F. Knoll)

Primary measurements are nearly completed using both the Na-Be and Na-D sources. The fission rate determinations are carried out in vacuum, rather than in a helium atmosphere as in the ^{235}U measurements, but otherwise the techniques are very similar to our earlier fission experiments. The added alpha flux causes a marked increase in background pitting of the polyester track recorders, but a simple size

[1] D. M. Gilliam, G. F. Knoll, Paper GB 25

discrimination appears adequate to unambiguously count the fission fragment tracks. We hope to report preliminary results at the November ANS meeting.

D. THE $^{6}Li(n,\alpha)$ CROSS SECTION AT 964 keV. (W. P. Stephany, G. F. Knoll)

This experiment has been described at the Conference on Nuclear Cross Sections and Technology.[2] Since the present result of 356 mb ± 12% is somewhat higher than prior measurements, efforts will continue to check various aspects of the measurement. We are also evaluating the possibility of remeasuring this cross section, replacing the surface barrier detector by alpha track-etch recorders and external ^{6}Li targets. Considerably better precision should be possible through this substitution.

E. FISSION MEASUREMENTS IN A ^{252}Cf FISSION NEUTRON SPECTRUM. (M. C. Davis, G. F. Knoll)

In order to achieve the desired precision in this measurement (~2%), a more intense ^{252}Cf source will be obtained to supplement the $\sim 10^{6}$/sec source now in use. Efforts are continuing in the study of problems associated with the measurement, including methods to eliminate the effects of possible source anisotropy and in the manganese bath calibration of the source.

F. Nu-Bar MEASUREMENT ON ^{252}Cf. (H. Bozorgmanesh)

A calibration of the absolute emission rate of Californium sources in our manganese bath is necessary for both the integral measurements described above and the Californium nu-bar determinations we are also undertaking. Because of the relatively high neutron energies involved in this spectrum compared with our more common photoneutron sources, we are investigating some additional effects in the bath which are important when calibrating high energy sources. These include the obvious increase in bulk leakage due to the greater penetrability of high energy neutrons as well as the parasitic capture of fast neutrons in sulphur and oxygen contained in the bath solution. Here we propose to use both analytical and experimental techniques. One-dimensional neutron transport codes such as ANISN have been sufficiently developed so that reasonably accurate predictions are possible of the neutron flux in the critical energy groups in which this absorption is important. We propose to couple the analytical description of the absorption with experiments designed to test the accuracy of the analytical models in order to assess the residual uncertainty of the method.

---

[2] W. P. Stephany, G. F. Knoll, Paper DB 2

A chamber for limited solid angle fission counting has been constructed with remotely adjustable apertures and counting geometry. Work is underway in its calibration and application to absolute fission counting.

G. CAPTURE CROSS SECTION AT ^{115}In. (J. C. Robertson)

In a recent paper,[3] the results of measurements of the ^{238}U and ^{115}In capture cross sections in the keV energy region and their ratios were presented by a group at NPL. The results given for the ^{238}U capture cross section were about 10% lower than the values predicted in recent evaluations based on the simultaneous evaluations of many interrelated cross sections. This difference could be attributed to either the assumed ^{235}U fission cross sections or their ratios to the ^{238}U capture cross sections used in the evaluations being in error. A direct measurement of the ^{238}U captive to ^{235}U fission cross section ratio would clarify the situation.

However, it is not possible to measure this ratio directly using photoneutron sources since the yield from the ^{238}U reaction is too low in an activation measurement. It is therefore proposed to use the ^{115}In cross section as an intermediary. Measurements of this cross section when combined with the prior ^{235}U fission cross section measurements made at Michigan and the ^{115}In/^{238}U capture cross section ratios measured in (3) will give ^{238}U fission to ^{238}U capture cross section ratios. This will check the consistency of the recent measurements in (3) and the data used in the evaluations.

There are two other reasons for measuring the ^{115}In cross section. Firstly, the use of indium as a secondary flux standard is much more convenient in activation cross sections than gold because of its 54 minute half life. Secondly, the use of indium will enable a more accurate determination of the room-return component, common to all measurements made using our facility, to be made. For these reasons we feel a measurement of the indium cross section is important and will contribute both to the nuclear data and neutron standards field. In order to carry out the indium measurements we have constructed a 4π continuous flow proportional counter for use in absolute beta counting.

We expect that the necessary neutron irradiations and absolute data counting can be carried out over the next year to yield cross section values for indium at both 964 and 265 keV. The measurements will be carried out in a manner similar to those of our fission determinations.

---

[3] J. Nucl. Energy 27, 519, 1973

A light weight structure will be used to support both a photoneutron source and a symmetric pair of indium foils on either side of the source. Procedures identical to those of the fission measurements will be used to carry out the foil irradiations and calibration of the source, but the ^{116}In activity induced in the indium will be determined using the 4π counter rather than the hand counting necessary for fission track registration.

NATIONAL BUREAU OF STANDARDS

A. NEUTRON PHYSICS

1. ^{235}U Neutron Fission Cross Section (A. Carlson)

Measurements have begun of the ^{235}U fission cross section in the MeV region. The first data have been obtained for neutron energies from about 0.8 MeV to 5 MeV. The neutron flux was measured with a proton "counter telescope" used in ring geometry with a lead bar shielding the Si (Li) proton detector from the direct beam. The radiation foil was a 0.8 mg/cm^2 polystyrene film. The ^{235}U fission reaction events were detected with a parallel plate ionization chamber. Both of these detectors are located at the 60m end station of the new Above-Ground Neutron Time-of-Flight Facility. The measurements are now being analyzed.

2. $^{10}B(n,\alpha,\gamma)^7$ Li Cross Section Measurement (R. A. Schrack, G. P. Lamaze, and O. A. Wasson)

Preliminary measurements of the ^{10}B cross section, from 300 keV to 1 MeV, have been started at the 68 meter station of the 200 meter flight path of the NBC Linac facility. Relative cross section measurements and background determinations have been made using the Nel10 black detector at 200 meters to monitor the neutron flux.

3. Calculation of Detector Responses in Fast Reactor Fluxes (C. Eisenhauer)

The DETAN 74 computer code has been used to calculate responses for $^{239}Pu(n,f)$, $^{237}Np(n,f)$, $^{115}In(n,n')$, $^{238}U(n,f)$, and $^{58}Ni(n,p)$ detectors in ^{252}Cf and ^{235}U fission neutron spectra and in a number of fast reactor spectra. Calculations indicate that the shape of the fission spectrum is preserved above about 1 MeV in these reactor spectra. Therefore fast fluxes in these reactors can be estimated with threshold detectors which have been calibrated in a known spectrum such as the ^{252}Cf fission neutron spectrum. Also, total fluxes can be estimated in neutron fields which do not have a significant low-energy component by using ^{239}Pu detectors which are energy-independent to within $\pm$6% between 10 keV and 5 MeV.

4. Measurement of Absolute Fission Rates (J. A. Grundl, D. M. Gilliam, N. Dudey,[1] and R. Popek[1])

---

[1] ANL

An article entitled "Measurement of Absolute Fission Rates" was published in Nuclear Technology, Vol. 25, p. 237-257 (Feb. 1975). The abstract and an excerpt from the conclusion of that paper follow:

> "The capability to measure absolute fission rates per nucleus at a remote laboratory site (the Coupled Fast Reactivity Measurement Facility (CFRMF) at Aerojet Nuclear Company) has been established to a precision level of better than $\pm 1\%$ and was sustained at that level for a period of two years. Double fission ionization chambers and solid-state track recorders were used in a series of irradiations designed to calibrate fission activation detectors used for reactor fuels and materials dosimetry. The array of reference and working fissionable deposits involved in the measurements included five isotopes: ^{239}Pu, ^{235}U, ^{238}U, ^{237}Np, and ^{234}U. Isotopic masses for the fissionable deposits were determined from interrelated components of mass assay: (a) relative and absolute alpha counting, (b) fission comparison counting in thermal-neutron beams, (c) mass spectrometry, and (d) quantitative deposition employing solutions of known fissionable element concentration. Absolute accuracies for the fission rates per nucleus measured in CFRMF are in the range of ± 1.5 to $\pm 2.5\%$ and are dominated by uncertainties in the fissionable deposit masses. Fission cross-section ratios for the CFRMF central spectrum are (1.000 : 1.145 $\pm$ 0.017 : 0.0485 $\pm$ 0.0007 : 0.354 $\pm$ 0.008) for (^{235}U: ^{239}Pu: ^{238}U: ^{237}Np), respectively."

Conclusions. The capability to measure absolute fission rates per nucleus on a sustained basis at a remote laboratory site has been established to a precision level of better than $\pm 1\%$. The techniques developed are convenient to apply and maintain, and they require a minimal investment of equipment and manpower. The dynamic range of measurement demanded by reactor fuels and materials dosimetry applications was met for the CFRMF measurements. With the reactor operating at its maximum power level of 10.4 kW, satisfactory fission chamber pulse rate data were taken up to 6000/sec. Certain compromises were required, however, to reach these high neutron fluxes. Not all fissionable isotopes could be run at the maximum power levels, and ^{235}U fissionable deposits with mass ratios of 1:40 relative to the NBS reference deposits had to be procured and calibrated. Because comparison with the ^{235}U reference deposit by means of alpha counting was not feasible, the mass calibration of these low-mass deposits ($\sim 4\ \mu g/cm^2$) was based on fission counting alone. The related problem of establishing a proper extrapolation-to-zero for various fissionable deposit thicknesses was

investigated--see Fig. 1. Accuracy levels attained in the course of the CFRMF measurements were in the range ±1.5% to ±2.5% and are dominated by uncertainties assigned to the isotopic masses of the NBS reference fissionable deposit (see Table I). These uncertainties were reduced by nearly a factor of two since the CFRMF measurements began, and efforts to improve the mass assignments to near ±1%, and to achieve added confidence by means of interlaboratory comparisons, is an ongoing project.

Fission cross-section ratios provide a useful characterization of the high-energy component of a neutron spectrum like that of CFRMF. The fission rate ratios obtained in CFRMF are listed in Table I and compared with predicted values based on neutron transport computations. A linear interpolation of 69-group CFRMF calculations was used to generate the predicted values, and except for ^{237}Np, the fission cross sections employed are ENDF/B-III. The observed spectral index, $\overline{\sigma}_f(^{238}U)/\overline{\sigma}_f(^{235}U)$, characterizes the spectrum as more energetic than computed. This is a commonly observed feature of fast-neutron spectra, although later versions of ENDF/B have tended to improve agreement for fast metal critical assemblies. Of equal interest is the rather good agreement between the observed and computed ^{239}Pu to ^{235}U fission cross-section ratios in Table I.

TABLE I

Average Fission Cross-Section Ratios for CFRMF

	Observed	$\frac{\text{Observed}}{\text{Computed}}$
$\overline{\sigma}_f(^{238}U)/\overline{\sigma}_f(^{235}U)$	0.0485 ± 1.4%	1.138
$\overline{\sigma}_f(^{237}Np)/\overline{\sigma}_f(^{238}U)$	7.34 ± 2.3%	0.975
$\overline{\sigma}_f(^{239}Pu)/\overline{\sigma}_f(^{235}U)$	1.145 ± 1.5%	1.034

5. Fission Rate Ratios in Big Ten (J. A. Grundl, D. M. Gilliam, G. E. Hansen[1], and H. H. Helmik[1])

Absolute fission rate ratio measurements were performed in the Big Ten Critical Assembly at the Los Alamos Scientific Laboratory. Two NBS double fission chambers and associated electronics were on-site for the measurements. Preliminary fission rate ratios, reported with a nominally large error of ±2.5% pending final analysis of all available fission rate data, are as follows: $\overline{\sigma}_f(^{239}Pu) = 1.19$; $\overline{\sigma}_f(^{238}U) = 0.0361$;

[1] LASL

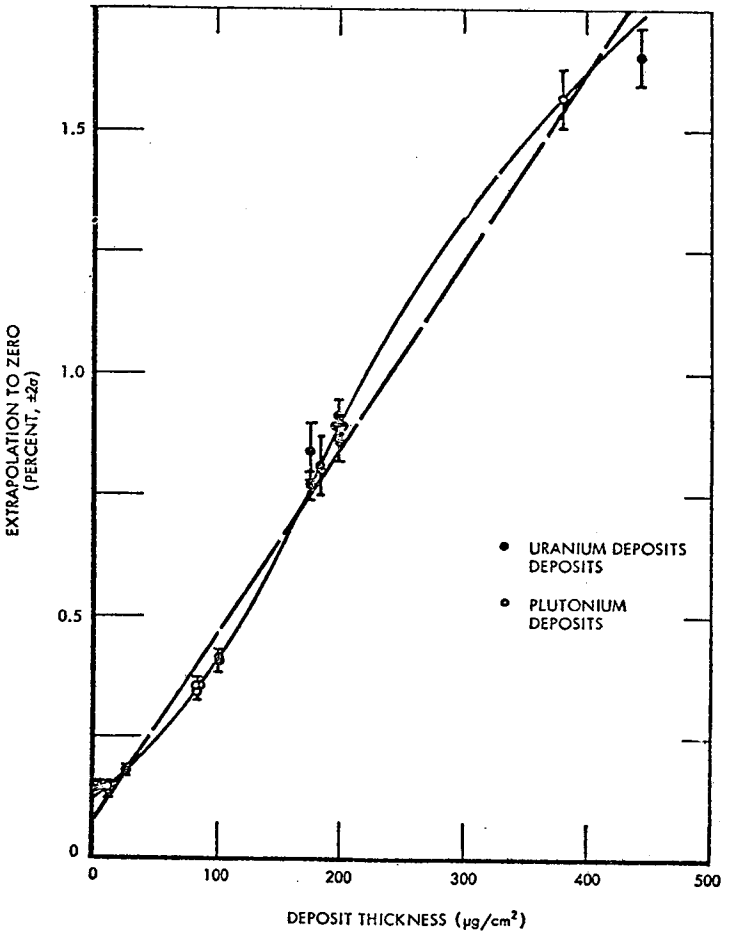

Fig. 1. The etz correction for extrapolation to zero pulse height is plotted in units of percent

TABLE II

YIELDS RELATIVE TO ^{140}Ba

(FOR THERMAL NEUTRON FISSION OF ^{235}U)

Fission Product Nuclide	Yield[a] Relative to ^{140}Ba (Average of Tests 74-1,2,3)
^{95}Zr	1.03 ± 3.3%
^{97}Zr	1.11 ± 2.9%[b,c]
^{99}Mo	1.00 ± 3.3%[b,c]
^{103}Ru	0.491 ± 4.2%
^{131}I	0.478 ± 2.8%[b,c]
^{132}Te	0.690 ± 7.4%
^{133}I	1.06 ± 2.8%[b,c]
^{137}Cs	1.00 ± 3.6%
^{141}Ce	1.12 ± 3.1%[b,c]
^{143}Cc	0.95 ± 2.8%[b,c]
^{144}Ce	0.96 ± 7.6%

[a] The error in the relative yields is taken as the root-sum-square combination of the gamma counting errors in the ^{140}Ba yield and the gamma counting errors in the yield of the nuclide of interest. (These relative yields are independent of errors in the fission counting or foil mass analysis.)

[b] No error was assigned to the branching ratio.

[c] Only one laboratory reported a result for this nuclide.

and $\bar{\sigma}_f(^{237}Np) = 0.317$ relative to $\bar{\sigma}_f(^{235}U) = 1.000$. Instrumentation and procedures for monitoring absolute fission rates in ^{235}U and ^{238}U during subsequent high-fluence dosimetry foil activation irradiation were established. The primary feature of the monitoring scheme is the placement of the fission chamber at the center of Big Ten along with the irradiation samples and operation of the chamber there throughout the course of nominal $10^{15}n/cm^2$ irradiations. A precision of $\pm 0.3\%$ for relative fluences are expected with fission chamber pulse rates of up to 2000/sec and a total exposed fluence of $10^{16}n/cm^2$.

6. Interlaboratory Comparison of Absolute Reaction Rate Measurement Scales (J. A. Grundl, D. Gilliam, and E. Eisenhauer; in cooperation with staff members of CEN-SCK, Mol, Belgium; Gfk, Karlshruhe, Germany; and RCN, Pettem, Netherlands)

A paper entitled "Interlaboratory Comparison of Absolute Fission Rate and Uranium-238 Capture Rate Measurements in the Mol-ΣΣ Secondary Intermediate-Energy Standard Neutron Field" was given at the Conference on Nuclear Cross Sections and Technology in March 1975. The abstract published in the program bulletin is as follows:

> "Interlaboratory comparisons have been made during the past two years, of techniques that are currently applied for the measurement of fission rates and uranium-238 capture rates in a number of German-Dutch, Belgian and American zero-power fast assemblies related to the LMFBR program. This sustained intercomparison effort has involved multiple exposure of absolute fission chambers and of activation foils, at the center of the MOL-ΣΣ Secondary Intermediate-Energy Standard Neutron field. Considerable care is required to achieve a long-term flux level monitoring accuracy of better than ±1% in MOL-ΣΣ. This has been accomplished by the redundant use of monitoring fission chambers and of up to four independent activation foils. The perturbation of the neutron field by the fission chambers and by the related access hole has been studied extensively by complementary computational and experimental methods. Corrections for neutron self-shielding and gamma-ray self absorption with the uranium-238 capture foils have been experimentally investigated. Estimated uncertainties in measured reaction rates relative to flux monitors are between ±2% and 2.5%. Excellent agreement is observed for fission rate ratios, but it is found that absolute fission rates may differ by up to 3.5%. A set of ΣΣ preferred values of central reaction rate ratios and their associated estimated uncertainties will be presented for nuclear data testing purposes."

7. The following papers were submitted for presentation at the Nuclear Cross Sections and Technology Conference held in Washington on March 3 - 7.

a. A Black Detector for 250 keV--1000 keV Neutrons (G. P. Lamaze, M. M. Meier, O. A. Wasson)

A detector has been designed to have a greater than 95% efficiency in the range of 250--1000 keV neutron energy. The detector is modeled from a similar but larger detector by Poenitz.[1] The efficiency calculations were made with a modified version of Carlo Black,[1] which is a Monte Carlo calculation of multiple neutron scattering in a scintillator. The detector is a 12.6cm x 17.78cm cylinder of NE110 with a 5.08cm x 2.54cm reentrant hole. The scintillator is mounted on an RCA8854 photomultiplier tube which has been selected for low noise. Calculated efficiencies will be presented as well as comparisons with experimental measurements.

b. Detector Calibration with an Associated Particle Apparatus (M. M. Meier, A. D. Carlson and G. P. Lamaze)

An associated particle apparatus employing the $T(p,n)^3He$ reaction is now in routine use at the NBS. The apparatus consists of two target chambers with ports at 10^o and 25^o which give a useful neutron energy range of 100 keV to 1 MeV for protons from the 3 MV Van de Graaff. Electrostatic deflection, fast energy discrimination and pulsed beam time of flight techniques are used to reduce background in the neutron-associated $^3He^{++}$ pulse height spectrum to less than 1%. Neutron fluxes in the associated cone range between 30 and 100 n/sec at the lowest and highest bombarding energies. The spatial profile of the neutron cone is broadened by coulomb scattering of the $^3He^{++}$ in the tritiated titanium target and has a width less than 12^o (full width at one-tenth maximum) for neutron energies above 300 keV. The apparatus has been used to calibrate a "black" detector described by Lamaze.[2] The results of this calibration will be compared to a Monte Carlo calculation of the efficiency.

c. Use of Gas Proportional Counters for Neutron Flux Monitors at the NBS Linac (O. A. Wasson)

The program at the NBS linac to measure neutron reaction cross sections in the energy range from 1 eV to 20 MeV requires various neutron flux monitors since no existing detector can cover this entire energy

[1] W. P. Poenitz. ANL-7915, Argonne National Laboratory (1972).

[2] G. P. Lamaze, M. M. Meier and A. O. Wasson, Conference on Nuclear Cross Sections and Technology, 1975.

range. We have selected hydrogen and methane filled gas proportional counters for use in the region from 10 keV to 1 MeV because hydrogen scattering is the best known cross section in this energy range. The accuracy of these counters is limited at low energies by the uncertainties in the relationship between recoil energy and ionization and on the high energy end by the range of the recoil proton. Because of the slow timing, both counters are located at the 200m flight path. The counters are 5cm diameter and 60cm length and placed in a 2.5cm diameter neutron beam. This beam collimation eliminates the wall effect correction for the incident beam while the long length reduces the error in the end effect corrections. A 1 atmosphere H_2 gas mixture is used from 10 keV to 100 keV while 2 atmospheres of pure methane is used from 50 keV to 1 MeV. Detailed measurements of counting rate, background, timing, spectral shapes, and efficiency uncertainties will be presented.

d. Angular Anisotropy in the $^6Li(n,\alpha)^3H$ Reaction at 25 keV
(I. G. Schroder, E. D. McGarry,[1] S. De Leeuw,[2] and G. De Leeuw-Gierts[2]

This anisotropy was measured in 2 sets of experiments performed at the NBS reactor iron filtered beam facility (99.1% at 25 keV). 1) A surface barrier detector coated with 80 $\mu gm/cm^2$ ^6LiF (front face) was used as a 2π detector. This detector was placed in four different angular positions with respect to the neutron beam; front face 90^o and 45^o to beam; back face 90^o and 45^o to beam. The pulse height distribution of both ^3H and ^4He were recorded for these four positions yielding a forward to backward asymmetry of 1.66 ± 0.11. 2) A second detector was placed coaxially with the first (at 90^o to the beam) and such as to subtend a 45^o cone. Coincidence measurements which recorded simultaneously the distributions in both detectors yielded an asymmetry in the forward to backward 45^o of 1.96 ± 0.06. The existence of such a large aniostropy at this low energy and the possibility of similar behavior at still lower energies (i.e. 1-2 keV) which could arise from s-p interference with the bound level (G. M. Hale) is under investigation. Implications to neutron spectroscopy and to the wide use of the ^6Li reaction in cross sections measurements will be discussed.

---

[1] HDL, USA

[2] CEN-SCK, Mol, Belgium

B. ELECTRONUCLEAR PHYSICS

1. Measurement of Nuclear Structure (S. Penner, J. W. Lightbody,Jr. and S. P. Fivozinsky)

The following papers were submitted for presentation at the Washington Meeting of the American Physical Society. The abstracts follow:

Electron Scattering Studies of $^{50,52,54}Cr$. (J. W. Lightbody,Jr. J. B. Bellicard,[1] P. de Witt-Hubert,[2] B. Frois,[1] Phan Xuan Ho,[1] P. Leconte,[1] A, Nakada,[3] S. Turck[1])-- Angular distributions for the states in $^{50,52,54}Cr$ below 4 MeV excitation have been measured at Saclay using a 400 MeV electron beam and covering a momentum transfer range from 1.0 to 2.5 fm^{-1}. The resolution of 4×10^{-4} $\Delta p/p$ permitted clean separation of most low lying levels. Form factors, extracted transition probabilities, and radial transition charge for the 2^+, 4^+, and 6^+ states will be presented and discussed.

Measurement of Charge Radii of ^{36}Ar and ^{40}Ar by Elastic Electron Scattering. (J. M. Finn,[4] Hall Crannell,[4] J. T. O'Brien,[5] S. P. Fivozinsky, and S. Penner)--The charge structures of ^{36}Ar and ^{40}Ar have been investigated using the electron scattering facilities at the National Bureau of Standards. A small volume, sealed gas-target cell was designed for this work and was used in transmission geometry. Substraction for scattering from the target windows was performed simultaneously by employing a multielement detector that takes advantage of the double focusing properties of the NBS momentum-analyzing spectrometer. Data were collected at values of q^2 between 0.29 fm^{-2} with an overall resolution of 0.1%. Phase shift fits to a 2-parameter Fermi distribution yield model dependent values for the rms radii of 3.3 ± 0.02 fm for ^{36}Ar and 3.39 ± 0.02 fm for ^{40}Ar.

Inelastic Electron Scattering from Low-Lying States in ^{36}Ar and ^{40}Ar. (Hall Crannell,[4] J. M. Finn,[4] J. T. O'Brien,[5] S. Fivozinsky and S. Penner)--The low-lying levels of ^{36}Ar and ^{40}Ar have been investigated at the NBS electron scattering facility. Data were collected at incident electron energies from 60 to 115 MeV for scattering angles of 92.5° and 110°. The first 2+ and 3- levels in both isotopes were observed, as were additional levels in ^{40}Ar at 2.52 MeV (2+) and at 3.12 MeV. The transition form factor to the 3.21 MeV level exhibits momentum dependence which is consitent with a 2+ spin-parity assignment for this state. The "two-phonon" triplet in the region of 4.4 MeV in ^{36}Ar was not seen. Transition radii and strengths for the observed levels will be presented.

[1] Saclay, France
[2] On leave from the Institut voor Kernphysisch Onderzoek, Amsterdam, Holland
[3] On leave from the Laboratory for Nuclear Science, Tokyo University, Sendai, Japan
[4] Catholic U.
[5] Catholic U./Montgomery College

Electroexcitation of Giant Resonances in ^{20}Ne. (Z. M. Szalata,[6] P. T. Kan,[6] F. J. Kline,[6] G. A. Peterson,[6] S. Penner, S. P. Fivozinsky, and J. W. Lightbody, Jr.)--At the NBS linear accelerator facility we have measured with high resolution the elastic and inelastic scattering of electrons from ^{20}Ne. Incident beams of 60, 90 and 120 MeV were used, and scattered electrons were observed at 75.4°. The gas was contained in a 350 cm^3 sealed rectangular gas cell pressurized to 10 atmospheres. Ten prominent peaks were observed between the 12.9 MeV proton emission threshold and 22 MeV. Variable width Lorentzian peaks and a phenomenological quasielastic continuum were fitted to the radiatively unfolded data. The 6 peaks below the neutron emission threshold at 16.8 MeV have form factors of an E2 or E0 character, whereas the peaks above that energy have form factors of an E1 character.

Giant M2 States in ^{58}Ni and ^{208}Pb. (R. A. Lindgren,[7] W. L. Bendel,[8] L. W. Fagg,[8] E. I. Jones, Jr.,[8] J. W. Lightbody, Jr. and S. P. Fivozinsky)--Inelastic electron scattering on targets of ^{58}Ni and ^{208}Pb[9] at incident electron energies between 37 MeV and 75 MeV at angles of 163° and 180° has revealed that the multipolarity of levels at 5.94, 6.41, 6.82, 7.15, 7.45, 8.24, 8.50, and 9.81 MeV in ^{58}Ni and 7.3 MeV in ^{208}Pb are probably magnetic quadrupole. In each case the q dependence of the cross section is different fromthat of identified magnetic dipole states and also is consistent with DWBA M2 predictions. Strong M2 transitions from the ground state to levels at 7.8 MeV in ^{58}Ni and 7.5 MeV in ^{208}Pb have been predicted by RPA particle-hole calculations.[10,11] Extracted strengths will be presented and compared with current model and sum rule predictions.

A paper entitled "Observation of Electric Monopole Strength in the Electrodisintegration of ^3He" (P. T. Kan,[6] G. A. Peterson,[6] D. V. Webb,[6] Z. M. Szalata,[1] S. P. Fivozinsky, J. W. Lightbody, Jr., and S. Penner) was submitted to Physical Review Letters. The abstract follows:

> A broad electric monopole excitation peaking at 6.4 MeV has been observed in the breakup of ^3He induced by inelastic electron scattering. The monopole cross section was obtained by subtracting from the observed cross section electric dipole contributions converted from photodisintegration cross sections by using the virtual photon theory, and magnetic multipole contributions obtained from a 180° electron scattering experiment. The extracted monopole matrix element is 2.4 ± 0.5 fm^2.

[6]Univ. of Massachusetts at Amherst
[7]On leave from the University of Rochester
[8]Naval Research Lab.
[9]L. W. Fagg et al., Proc. of the Int. Conf. on Nucle
[10]C. Ngo-Trong, Thesis 1975. U. of Toronto
[11]P. Ring and J. Speth, Phys, Lett. 44B, 477 (1973).

2. Proton and α Particle Yields from the Electrodisintegration of Be, Ag, and Au (W. R. Dodge)

We measured the (e,p) and (e,α) energy and angular distributions from Be, Ag, and Au at several electron bombarding energies between 50 and 115 MeV. Our Ag and Au proton angular distributions exhibit an asymmetric component which increases with proton energy from about 0 to 50% as the proton energy increases from the Coulomb barrier to 25 MeV. Our α-particle angular distributions exhibit an asymmetric component which increases from about 0 to 30% as the α-energy is increased from the Coulomb barrier to 25 MeV. Below the Coulomb barrier our α-particle angular distributions are backward peaked. Reactions which exhibit angular distributions with these asymmetries as a function of the particle kinetic energy are typical of fast or direct reactions. Therefore, we conclude that the asymmetric component of our yield must be attributed to a direct or secondary mechanism involving αs not formed by statistical processes during de-excitation of the nucleus.

C. DATA COMPILATION

1. X-Ray and Ionizing Radiation Data Center (J. H. Hubbell)

The name of this OSRD-sponsored literature-surveillance, data-evaluation, compilation, and information-service program was changed from "X-Ray Attenuation Coefficient Information Center" to "X-Ray and Ionizing Radiation Data Center" to reflect an intended broadened scope to include electron and other charged-particle microscopic cross sections, as well as buildup-factor and other radiation transport data.

The previous USNDC report from this center contained an abstract of a manuscript in progress for the Journal of Physical and Chemical Reference Data: "Calculated Tables of the Atomic Form Factor and Incoherent Scattering Function for $0.005\ \text{Å}^{-1} \leq \sin(\theta/2)/\lambda \leq 10^9\ \text{Å}^{-1}$, and Photon Coherent and Incoherent Scattering Cross Sections for $0.1\ \text{keV} \leq E\gamma \leq 100\ \text{MeV}$, for $1 \leq Z \leq 100$", a collaborative effort with Wm. J. Veigele and E. Briggs of Kaman Sciences Corp., Colorado Springs, and with R. T. Brown and D. T. Cromer of Los Alamos. This manuscript, now completed, is presently undergoing NBS editorial review, and the tables have been translated into ENDF format by J. B. Wright and R. W. Roussin (Radiation Shielding Information Center, Oak Ridge) and are available from RSIC as part of the new photon interaction ENDF data-tape DLC-7E.

An invited keynote address "Present Status of Photon Cross Section Data" was presented at the International Symposium on Radiation Physics (co-sponsored by the Dept. of Atomic Energy, Govt. of India, with assistance from the International Atomic Energy Agency and the National Bureau of Standards, USA) Bose Inst., Calcutta, India, Nov. 30-Dec. 4, 1975. The abstract follows:

"Recent developments in theoretical and experimental cross sections for the basic photon interactions with atoms (photoeffect, coherent and incoherent scattering, and electron-postron pair production) are reviewed. Emphasis is on the extensive total and subshell, photoeffect calculations by J. Scofield, and on the atomic form factor and incoherent scattering function data calculated by D. Cromer and by R. Brown. Some comparisons of these theoretical results with available explicit cross section and total attenuation coefficient measurements are presented."

2. Energy Spectra of Fission Neutrons (J. Grundl, C. Eisenhauer)

We have begun a compilation of measured energy spectra of neutrons from fission. Initially, the compilation has been restricted to induced fission in ^{235}U and spontaneous fission in ^{252}Cf. The purpose of this compilation is to recommend a simple analytical form which best fits the measured data, together with some statement on the probable departure of the spectrum from this form within several energy ranges.

Least squares fit have been made to each set of experimental data to determine an effective average energy, E_{AV} from the expression

$$N(E)dE = A \quad E\exp(-1.5\ E/E_{AV})dE$$

The parameters A and E_{AV} are used to normalize each set of data to unit integral.

A reference Maxwellian is then determined by estimating a reference energy E_{AV} from the average energies E_{AV} of all the sets of data. Finally, the departures of the experimental data from the reference Maxwellian are calculated.

The values deduced for ^{235}U and ^{252}Cf spectra are, respectively, $E_{AV} = 1.97 \pm .03$ MeV and $E_{AV} = 2.13 \pm .03$ MeV.

The following is an abstract of a paper submitted to the Nuclear Cross Sections and Technology, March 1975:

"Fission Spectrum Neutrons for Cross Section Validation and Neutron Flux Transfer. A variety of measurement methods over more than two decades provides a base for proper evaluation of the fission spectrum shape. Such an evaluation will be presented and will include a recommended fission neutron spectrum shape for ^{235}U (thermal-neutron-induced fission) and ^{252}Cf (spontaneous fission) and an estimate of maximum credible

departures from those shapes. Two features of fission neutrons make them a useful reference for certain measurement problems in nuclear technology. First, the fission spectrum shape is preserved above about 1 MeV in breeder, fuels test, and light water reactor cores, as well as in clean and prototype critical assemblies; second, small intense sources of pure ^{252}Cf fission neutrons (5×10^9 n/s source emission localized to $\pm$ 0.05 cm) are now available, and their absolute source strength can be determined to $\pm$ 1% or better. The application at NBS of such ^{252}Cf fifssion sources (and related ^{235}U and ^{239}Pu cavity fission sources) to neutron cross section normalizations and validation for reactor design and operation will be desribed. Also to be outlined are methods of absolute neutron flux transfer from isolated fission neutron fields of known intensity to reactor neutron fields important for technology."

3. Nuclear Data Applications (S. M. Seltzer, C. S. Dyer,[1] and J. I. Trombka[2]

A paper entitled "Nuclear Data for Assessment of Activation of Scintillator Materials During Spaceflight" was given at the Washington Meeting of The American Physical Society. The abstract follows:

"Activation of detector materials by cosmic rays and trapped protons is a major problem in gamma-ray spectrometry performed in a space environment. In lightweight spacecraft, direct spallation interactions of the primary particles provide most of the activation. A computation scheme for prediction of this background is under development. An electron-photon transport code used the latest available decay scheme data to compute energy-loss spectra for decaying nuclides inside detector materials. The computation of isotope production rates requires spallation cross-sections covering all possible particle energies, and these are drawn from both semi-empirical formulae and estimates based on Monte Carlo intranuclear cascade simulations. Interaction between this calculation

---

[1] NAS/NRC Resident Research Associate

[2] NASA-Goddard Space Flight Center

and monoenergetic beam irradiation results can be used to improve cross-section prediction for scintillator materials. In heavy spacecraft, secondary neutrons are an important source of activation and neutron cross sections are required as well as accurate codes for assessing neutron production and transport."

D. FACILITIES

1. Associated Particle Facility (M. M. Meier)

A description of the associated particle facility was presented to the Third Conference on Application of Small Accelerators. The abstract follows:

> "The neutron standards program at NBS is discussed with emphasis on Van de Graaff contributions to the overall program. In particular, the characteristics of an associated particle apparatus, which serves as a primary standard for flux normalization at the three percent accuracy level are presented. The "black" detector, a secondary standard, suitable as a flux monitor for linac applications and for dosimetry is characterized and its calibration with the associated particle technique is described. Future goals of the program are outlined and the Van de Graaff/associated particle system's future role in achieving them are discussed."

The associated particle facility is currently being used in the calibration of a NE110 "black" detector as described elsewhere in this report. Two chambers, with ports at 10^{o} and 25^{o}, for production of kinematically collimated neutron beams in the ranges 100 to 500 keV and 500 to 1000 keV have been constructed. The calibration has focussed on the lower energy range, but the second chamber will be put to use by early spring.

Since the last report, the background in the $^{3}He^{++}$ peak has been reduced from three percent to less than one percent. Also, a more accurate measurement of the neutron spatial profile has been made at 300 keV with a resulting cone width (full width at one-tenth maximum) of 11^{o}. An attempt to reduce the width by employing thinner TiT_2 targets was not successful due to increased backgrounds produced by enhanced proton scattering in the thicker Ni substrate. A 25 $\mu g/cm^2$ target deposited on a 100 $\mu g/cm^2$ Al substrate is currently on order and should considerably reduce the cone width.

Following the "black" detector calibration from 100 keV to 1 MeV, we plan a threefold increase in the neutron flux by improving the beam transport system and will then undertake measurement of the ^{6}Li(n,d) cross section with thin scintillators.

2. 3 MV Positive Ion Van de Graaff (M. M. Meier)

Van de Graaff operation has been satisfactory with most down time accounted for by routine source replacement. In-house source bottle refurbishing has improved in quality and efficiency and we have regularly been operating in pulsed mode for more than 250 hours between changes.

Planned improvements in the transport system include an electrostatic quadrupole and afterpulser, which should increase pulsed beam transmission through the analysing magnet by a factor of three with no increase in dark current. These will be implemented as need arises, probably with the measurement of the ^{6}Li(n,a) cross section using the associated particle technique and thin scintillators.

The Datacraft 6024/5 computer has been interfaced to a CAMAC system including 3 ADCs and 8 scalers. Debugging of the data acquisition software has begun. A second magnetic tape unit for the system is on order.

3. The following papers covering recent developments in NBS facilities were submitted for presentation at the Nuclear Cross Sections and Technology Conference held in Washington, March 3-7:

a. After-Pulse Suppression for 8850 and 8854 Photomultipliers (G. P. Lamaze, J. K. Whittaker, R. A. Schrack and O. A. Wasson)

Spurious pulses occurring after large light output events in a scintillator (after pulsing) have been observed in semi-conducting first dynode photomultipliers (RCA 8850 series). The after-pulsing apparently has two components, an isochronous component occurring at a fixed time interval after the initial light pulse and an asynchronous component with a long duration lasting at least 40 μsec. The time interval between the isochronous bursts is related to the types of residual gases in the photomultiplier. In the RCA 8850 series tubes, the asynchronous after-pulsing consists of very low amplitude pulses and appears to be primarily due to single electron events, the number of these events being related to the main pulse amplitude. To obtain after pulse suppression, a fine stainless steel mesh was stretched tightly over the glass window of the photocathode. The mesh was then pulsed (FWHM = 250 ns) during the light flash to +300 volts relative to the photocathode potential. The isochronous and asynchronous after-pulsing was completely suppressed. Further details will be presented.

b. A Modular Minicomputer Multiparameter Data Gathering and Virtual Memory Operating System for the NBS Neutron Standards Program (R. A. Schrack, H. T. Heaton II, D. Green)

A new aboveground neutron time-of-flight system has recently been completed at the National Bureau of Standards Linear Accelerator facility. A relatively inexpensive computer system has been developed that will permit the accumulation of multiparameter data simultaneously from several experiments using a minicomputer and a small moving head disc storage unit. The operating system is modular in form allowing different experimenters to rapidly construct a software system to their requirements. Data gathering and analysis programs are interchanged between core and disc as required. Interfacing hardware has been modularized using the CAMAC system. The central processing unit has 1 microsecond cycle time, 16 thousand word memory, and a 24 bit word length. The cartridge type moving head disc unit has a 1,800,000 word storage capacity. Data input rates of over 400 counts per second of a flat spectrum into a 1 million word data field are achieved by the system. Higher input rates are attainable with (a) more core storage, (b) smaller data fields, or (c) non-flat spectra.

c. The 2 keV Filtered Beam Facility at the NBS Reactor (I. G. Schroder, R. B. Schwartz, and E. D. McGarry[1])

A Sc filter which views a Mn scatterer has been installed in a through tube of the NBSR. The use of a resonant scatterer eliminates unwanted core neutrons and core gammas; this results in a pure 2 keV neutron beam with only 3% high energy contamination and a 1 mR/hr gamma background. This should be compared to previous reported results in which the high energy contaminant was greater than 50% thus severely limiting the utility of such a filter. Details of the filter construction, the use of Ti (1 cm) with the Sc to reduce background, optimization of the beam for different types of experiments and the application of the filter-resonant scatterer technique to Fe (25 keV) and Si (144 keV) will be discussed. Applications to neutron dosimetry, spectroscopy, cross section measurements and capture gamma rays will be presented.

d. A 25-keV Neutron Beam Facility at NBS (E. D. McGarry[1] and I. G. Schroder)

An iron-filtered, neutron-beam facility has been installed at the NBS reactor. This facility provides a well collimated beam of 99% 25 keV neutrons with a flux of 5×10^5 n/cm^2 sec. and a gamma

---

[1] HDL-USA

background less than 2 mR/hr. This beam is obtained by preferentially scattering 25-keV neutrons from titanium placed tangential to the reactor fuel and by optimizing a secondary aluminum filter to provide the desired purity. Applications of this beam to neutron dosimetry and cross section measurements will be discussed. For other experiments, such as intercalibration of fast-neutron spectrometers, fluxes of 10^6 n/cm^2 sec. are obtained by modification of the aluminum filter. This provides a beam with as many as 13 identifiable peaks in the energy range 25 keV to 1.5 MeV. Furthermore, the use of gamma sources of varying intensity together with the extremely low gamma background of the present beam permits controlled studies of gamma discrimination techniques in proportional counter measurements.

OAK RIDGE NATIONAL LABORATORY

A. NEUTRON DATA APPLICATIONS SUBCOMMITTEE

1. Neutron Measurements

a. Fluorine and Silicon Total Cross-Section Measurements (D. Larson, C. H. Johnson, J. A. Harvey and N. W. Hill)

In the process of performing evaluations of fluorine[1] and silicon[2] for ENDF/B-IV, it was noted that deficiencies existed in the total cross-section data of these materials. In order to provide high resolution data for ENDF/B-V, we have measured the transmission through samples of teflon $(CF_2)_n$ and transistor-grade natural silicon using the ORELA facility. Two samples of teflon (n = .1309, .0169) and two samples of silicon (n = .0746, .0376) were used. The fluorine measurements are from 5 eV to 20 MeV, while the silicon measurements were taken from 5 eV to 700 keV. The data have been reduced to cross sections and will be sent to the National Neutron Cross Section Center (NNCSC) at Brookhaven National Laboratory.

b. ORNL Neutron Scattering Cross Section Measurements from 4 to 8.5 MeV: A Summary*,** (W. E. Kinney and F. G. Perey)

The ORNL program to measure neutron elastic and inelastic scattering cross sections for 26 nuclides from C to ^{238}U in the 4-8.5 MeV incident neutron energy range is summarized. Data acquisition and reduction techniques are reviewed and typical results given. The nuclides investigated are tabulated.

c. Cross Sections for the Production of Low Energy Photons by Neutron Interactions with Fluorine and Tantalum† (J. K. Dickens, G. L. Morgan and F. G. Perey)

Differential cross sections for the production of low energy photons (< 240 keV) by neutron interactions in fluorine and tantalum have been measured for neutron energies between 0.1 and 20 MeV. Photons were detected at 92° using an intrinsic germanium detector. Incident neutron energies were determined by time-of-flight techniques for a white source spectrum.

---

* Conf. on Nuclear Cross Sections and Technology, Washington, March 1975.

** Relevant to request Nos. 56, 58, 61, 64-66, 69, 83, 84, 91, 116, 119, 120, 129-131, 147, 149, 150, 153, 154, 182-184, 201, 381, 396, 465-7.

† Relevant to request Nos. 76, 78, 379.

[1] C. Y. Fu and D. C. Larson, ENDF/B-IV, MAT 1277, available from NNCSC.

[2] D. C. Larson, ENDF/B-IV, MAT 1194, available from NNCSC, Brookhaven.

d. Gamma-Ray Production Measurements due to Interactions of Neutrons with Elements Required for Nuclear Power Applications and Design*,**(Chapman, Dickens, Love, Morgan and Newman)

For the past three years neutron-induced gamma-ray production cross sections have been made for a variety of elements at the Oak Ridge Electron Linear Accelerator (ORELA). A large, well shielded, NaI spectrometer was used as the gamma-ray detector and ORELA as the neutron source. The facility provides a consistent data set for neutron energies from 0.7 to 20 MeV and photon energies from 0.3 to 10.5 MeV. Typically the samples are flat plates of the element of $\tilde{\sim}$ 0.02 atoms/barn thickness, although several elements studied required samples in compound form. The data are accumulated in a two-parameter array, gamma-ray pulse height versus neutron time-of-flight. Data reduction was accomplished by binning in desired neutron-energy groups and in fixed photon-energy groups. For each neutron-energy group the data were unfolded using FERD unfolding routine, and the results are in the form of absolute differential cross sections, $d^2\sigma/d\omega dE$, for each photon-energy bin. So far data have been obtained for 20 elements (Li, C, N, O, F, Mg, Al, Si, Ca, Fe, Ni, Cu, Zn, Nb, Ag, Sn, Ta, W, Au, and Pb).

e. Gamma-Ray Production due to Neutron Interactions with ^{68}Zn and the Level Structure of ^{68}Zn†,‡ (J. K. Dickens)

Numerical values of differential cross sections for gamma rays produced by neutron interactions with ^{68}Zn have been measured for an incident energy of 5.4 MeV and gamma-ray scattering angle of 55 deg. The $d\sigma/d\omega$ data were obtained using a 60 cm^3 Ge(Li) detector. The data consist of cross section values for 164 gamma rays or gamma-ray groups having gamma-ray energies between 413 and 4998 keV. These data were analyzed to obtain information on the level structure of ^{68}Zn, and 131 transitions were assigned among 78 known or postulated new levels in ^{68}Zn.

f. Fission Product Capture Cross Section Data for ^{105}Pd (R. L. Macklin)

Fission product capture cross sections needs for fast reactor calculations have been listed. Palladium isotopes, particularly 105, ranked high. Last November that sample was run at ORELA, and the data were processed. There was a cluster of sharp peaks at a few keV with the effective capture cross section (for 0.0041 atom/barn sample thickness) reaching 12.9 barns at 2.665 keV. A valley at 2.618 keV shows only 0.094 barns for a ratio of 135.

* Conf. on Nuclear Cross Sections and Technology, Washington, March 1975.

** Relevant to request Nos. 11, 59, 68, 72, 96, 98, 107, 160, 163-5, 192, 195-6, 207, 209, 216, 281, 283-4, 380, 382-3, 397-8.

† Abstract of ORNL-4985.

‡ Relevant to request No. 216.

g. Neutron Capture and Absorption of ^{59}Ni for Thermal and Resonance Energy Neutrons* (Raman, Harvey, Jurney**and Hill)

A consideration of the rate of helium production in reactor structural materials arising from an anomalously high (n,α) cross section for slow neutrons in ^{59}Ni has prompted a re-examination of the (n,γ) cross section at thermal and absorption cross section at both thermal and resonance neutron energies.

The thermal (n,γ) part was done at Los Alamos Omega West Reactor Thermal Neutron Capture γ-Ray Facility. This facility makes use of an internal target which consisted of 9.8 mg of Ni metal enriched to 95% in ^{59}Ni. Using a 6.3 cm dia. x 15 cm long NaI crystal surrounded by a 20 cm dia. x 25 cm NaI annulus, a value of 53 ± 4 b was obtained for the thermal (n,γ) cross section. In a separate experiment, the ^{59}Ni(n,γ) γ-ray spectrum was measured with a 26 cm^3 Ge(Li) detector. This measurement yielded a value of $\sigma_{n,\gamma}$ = 51 ± 8 b.

The neutron transmission measurements were carried out at the Oak Ridge Electron Linear Accelerator with a 9.6 mg metallic powder sample (95% ^{59}Ni) placed in a small holder 3 mm dia. by P. R. Keuhn, Isotopes Division. Both the thermal and resonance energy measurements were made using a ^{6}Li glass scintillator at a 17.890 m flight path using 30 nsec bursts from the accelerator.

The total cross-section data from 0.02 eV to 3 eV have been fitted to a constant plus a $1/\sqrt{E}$ dependence. The $1/\sqrt{E}$ slope corresponds to an absorption cross section of 66 ± 5 b at 2200 m/sec. This value is considerably lower than the value of 92 ± 4 b obtained from pile oscillator measurements.[1] Our absorption cross section is, however, consistent with the capture cross section of 53 b and an (n,α) cross section[2] of ≈ 18 b. In addition to the known large resonance[1] at 204 eV, small resonances were observed at higher energies at 3.21, 4.22, 6.30 and 9.16 keV. The 204 eV resonance has been analyzed using a shape analysis program and the following parameters were obtained based on an inverse sample thickness of Ni of 846 atoms per barn: E_o = 203.9 ± 0.2 eV, Γ = 13.9 ± 0.2 eV and Γ_n = 5.2 ± 0.1 eV assuming g = 3/8. Earlier measurements by Kirouac and Eiland[1] gave E_o = 204 eV, Γ = 13.9 ± 1.0 eV, g = 3/8 and Γ_n = 10.5 ± 0.3 eV. The disagreement for Γ_n cannot be explained. We plan to make additional measurements with a larger ^{59}Ni sample (enriched to ∿4%) in order to eliminate the possibility that the thickness of the sample is in error.

---

* Physics Div. Ann. Prog. Rept., Period Ending Dec. 1974, ORNL-5025 (1975).

** Los Alamos Scientific Laboratory.

[1] G. J. Kirouac and H. M. Eiland, Bull. Am. Phys. Soc. 20, 149 (1975).

[2] R. D. Werner and D. C. Santry, to be published.

h. Neutron Total Cross Section of ^{6}Li (J. A. Harvey and N. W. Hill)

Transmission measurements have been made upon two metal samples of ^{6}Li (98.72%) with inverse thicknesses of ^{6}Li of 11.994 and 2.987 barns/atom. Data for many discrete energies have been taken with an iron-filtered beam where signal/background ratios of >1000 to 1 were obtained. Total cross section values (accurate to 1%) are given in the following table:

E(keV)	(barns)
24.58	1.79 ± 0.02
81.64	1.45 ± 0.02
128.60	1.74 ± 0.02
137.16	1.90 ± 0.02
167.71	2.86 ± 0.03
183.74	3.91 ± 0.04
219.06	8.44 ± 0.08
244.05	10.8 ± 0.1
273.57	8.70 ± 0.08
312.48	5.28 ± 0.05
352.02	3.63 ± 0.03
375.70	3.09 ± 0.03
404.10	2.66 ± 0.05
436.87	2.34 ± 0.03
468.09	2.11 ± 0.02
497.76	1.94 ± 0.03

i. Level Spacing and S-Wave Neutron Strength Function of $^{180}Ta+n$* (J. A. Harvey, N. W. Hill and E. R. Mapoles)

We have measured the transmission of a 155 mgm sample of Ta enriched to 5.47% in ^{180}Ta (valued at $1175 per mgm of sample) and a matching sample of natural tantalum (which contains only 0.01% ^{180}Ta) in order to correct for the ^{181}Ta resonances. A small sample holder ($\sim$3 mm dia.) and the filling and emptying equipment to minimize the loss of sample were designed by R. H. Ward. The holder was filled by P. R. Kuehn of the Isotopes Division with essentially no loss of material. The measurements were made using a ^{6}Li glass scintillator at an 18-meter flight path at ORELA. Data were obtained from 0.3 to 200 eV with an energy resolution of 0.3%.

The resonances in ^{180}Ta up to 20 eV have been analyzed by a shape analysis program and final results are available. The radiation widths (Γ_γ) are consistent with a constant average radiation width of (51±1) x 10^{-3} eV. From 20 to 102 eV the ^{180}Ta data have been analyzed using an area analysis program to determine the resonance energies and the neutron widths of the resonances. The average level spacing for

* Physics Div. Ann. Prog. Rept., Period Ending Dec. 1974, ORNL-5025 (1975).

both spin states after correcting for "missed" small resonances assuming a Porter-Thomas neutron width distribution was 1.1 ± 0.1 eV. This experimental value although a little larger than the predicted values including rotational motion certainly confirms the claim that rotational effects are important for deformed nuclei at high excitation but indicates that the moment of inertia at high excitation is less than the rigid moment of inertia. The s-wave neutron strength function was determined from the data up to 100 eV and a value of $(2.4 \pm 0.4) \times 10^{-4}$ was obtained. This value is in agreement with those of other nuclides in this mass region.

j. Dependence of Level Spacing of the Isotopes of Fe upon Parity*,** (Pandey,† Garg,† Harvey and Good)

Measurements have been made upon the isotopes ^{54}Fe and ^{57}Fe up to ∿600 keV using an 80-meter flight path resulting in an energy resolution ∿0.1%. Measurements were made with a ^{6}Li glass scintillation detector using 30 nsec pulses below 50 keV and using an NE-110 scintillation detector and 8 nsec pulses above 20 keV. The measurements upon ^{58}Fe and ^{56}Fe were made with the NE-110 detector at a 200-meter flight path. For the ^{56}Fe measurements 5 nsec bursts were used resulting in an energy resolution of 0.05 to 0.1% from 20 to 1000 keV. For the ^{58}Fe measurements 16 nsec bursts were used giving a resolution of 0.05 to 0.2% from 20 to 600 keV. The cross sections for ^{54}Fe and ^{56}Fe have been analyzed using the R-matrix formalism for broad resonances and an area analysis program for the narrow resonances. The ^{57}Fe data have been analyzed with a single level R-matrix program up to ∿50 keV, but a detailed analysis of the ^{58}Fe data has yet to be made.

For ^{54}Fe+n the level spacing of $1/2^+$ states is 25 keV obtained from the s-wave resonances from the data up to ∿600 keV. This is in reasonable agreement with a value of 20 keV from earlier data and is somewhat smaller than the value of 31 keV predicted by Soloviev. For ^{56}Fe+n the level spacing of $1/2^+$ states is 27 keV from the data up to 500 keV. This is in agreement with the predicted value of 25 keV. The predicted level spacing for 0^- and 1^- states for ^{57}Fe+n was 5 keV, which is slightly smaller than the experimental value of 8 keV determined from the six s-wave resonances up to 50 keV.

For all the isotopes many more p-wave than s-wave resonances were observed. For example, for ^{54}Fe+n the average level spacing for both the $1/2^-$ and $3/2^-$ states is 5 keV. This is significantly smaller (by a factor of ∿2) than would have been observed if the level spacing were independent of parity. However, it is not as small as the predicted value of ∿2 keV. The analysis of the ^{57}Fe and ^{58}Fe data is incomplete but it also indicates several times more p-wave resonances than s-wave resonances but not as large a factor as predicted.

* Physics Div. Ann. Prog. Rept., Per. End. Dec. 1974, ORNL-5025 (1975).
** Relevant to request No. 146.
† State University of New York at Albany.

k. The Neutron Capture Cross Section of ^{33}S to 850 keV*
(J. Halperin and R. L. Macklin)

A measurement of the conversion rate of ^{32}S to ^{36}S relative to other nuclides produced during nucleosynthesis provides a test of the adequacy of explosive carbon burning to explain the abundance of the rare and neutron rich nuclide ^{36}S(140 ppm in natural sulfur). A critical uncertainty in this conversion rate concerns the branching ratio in the decay of ^{34}S ($\sim$11.5 MeV above ground) by charged particle emission compared to gamma-ray de-excitation. This problem is being investigated in a collaborative effort[1] and we report here only on the production path leading to ^{36}S.

In view of the essential non-existence of $^{33}S(n,\gamma)^{34}S$ data in the literature, measurements were carried out on the radiative capture neutron cross section of ^{33}S (0.76% in nature) at the ORELA time-of-flight facility. The energy region spanned ranged from 2.5-850 keV, at which point the onset of gamma rays from inelastic neutron scattering would be expected. The measurement was carried out at 40 meters with 5 ns pulses at a repetition rate of 1000 pps. A 1.1 gm sample of ^{33}S (88.21% abundance) with an areal density of 0.0132 atoms/barn was viewed by two total energy detectors utilizing on-line pulse-height weighting. This resulted in an average detector response essentially independent of the gamma cascade from the compound nucleus,[2,3] and proportional to the total energy (i.e., binding energy plus center-of-mass neutron energy). The neutron flux was measured with 0.5 mm thick ^{6}Li glass in transmission.

Following the usual corrections for deadtime, time independent background, time and sample dependent backgrounds, the effective capture cross section of ^{33}S versus energy has been evaluated. Resonance parameters were extracted from an area analysis of observed resonances using first, an automatic Gaussian fitting computer code, followed by an analysis folding in Doppler broadening, instrumental resolution, self-shielding and multiple scattering. Some 39 resonances are listed up to 549 keV more than doubling the number of resonances previously recognized based upon a transmission measurement.[4] A cumulative distribution plot of the number of resonances observed in the interval from 13 to 240 keV suggests that to that energy very few resonances are missed, and yields an average level spacing, D, of 9.1 ± 0.9 keV. The resonances integral ($\int_{0.5} \sigma_\gamma dE/E$) is calculated to be 33.4 ± 5.0 mb.

---

* Physics Div. Ann. Prog. Rept., Per. End. Dec. 1974, ORNL-5025 (1975).

[1] G. F. Auchampaugh, J. Halperin, R. L. Macklin, and W. M. Howard, "Kilovolt $^{33}S(n,\alpha_0)$ and $^{33}S(n,\gamma)$ Cross Sections: Importance in the Nucleosynthesis of the Rare Nucleus ^{36}S," to be submitted to Phys. Rev.

[2] R. L. Macklin and J. H. Gibbons, Phys. Rev. 159, 1007 (1967).

[3] R. L. Macklin and B. J. Allen, NIM 91, 565 (1971).

[4] "Neutron Cross Sections," compiled by S. F. Mughabghab and D. I. Garber, Brookhaven National Laboratory Report BNL-325, 3rd Edition, Vol. 1 (1973).

l. Gold Neutron Capture Cross Section from 3 to 550 keV*,**

(R. L. Macklin, J. Halperin and R. R. Winters†)

One of the principal standards used in quantitative neutron cross section and flux measurement work has been gold. Its advantages include high chemical and isotopic purity, large thermal neutron capture and resonance integral, leading to a convenient radioactivity for post-exposure laboratory detection. It has also been used extensively as a neutron capture standard in the fast fission reactor energy range. For that purpose, the highest possible accuracy in cross section is desired. As this can only be achieved through evaluation and consensus of independent studies at many laboratories, we have undertaken a careful measurement of the capture cross section at the Oak Ridge Electron Linear Accelerator.

At neutron energies of a few keV, many sharp "compound" nuclear resonances are seen. The average behavior of the cross section up to 150 keV is well described by standard nuclear reaction statistics and four strength function parameters. Our fitted average is also in excellent agreement with an evaluation of the earlier work[1] and above 70 keV, with recent French results.[2]

It is clear that the underlying resonance structure produces significant departures from the average at the few percent level. Only for very broad energy spread can one assume the average cross section to 1%. For higher resolution work the details of the local fluctuations must be taken into account. Thus while we have achieved respectable precision and unprecedented resolution in remeasuring the standard gold capture cross section, the result is to point up its unappreciated weaknesses as a standard.

m. Neutron Capture Cross Section of Niobium from 2.6 to 700 keV

(R. L. Macklin)

The neutron capture cross section of stable ^{93}Nb was measured by time of flight at the Oak Ridge Electron Linear Accelerator. Individual resonances were parameterized to 7.4 keV with energy resolution $\leq$ 0.14% FWHM. The average cross section was deduced from 3 to 700 keV with accuracy estimated at 3-5% S.D. The average data to 100 keV are well fitted by strength functions, but the fluctuations about the fit are not consistent with an energy independent level density proportional to 2J+1 beyond 20 keV.

---

* Phys. Div. Ann. Prog. Rept., Per. End. Dec. 1974, ORNL-5025 (1975).

** Relevant to request No. 394.

† Denison University, Granville, Ohio.

[1] W. P. Poenitz, in Neutron Standards and Flux Normalization, A.B. Smith, Coordinator, AEC Symposium Series Report 23 (August 1971).

[2] C. le Rigoleur, et al., Mesure de la Section Efficace de Capture Radiative des Neutrons per l'Or Entre 75 keV et 550 keV, report CEA-N-1662 (Aout 1973).

n. keV Neutron Resonance Capture in ^{138}Ba (Musgrove,* Allen,* Boldeman* and Macklin)

The neutron capture cross section of ^{138}Ba has been measured with high resolution to 100 keV and resonance parameters have been extracted for a number of new levels. The s-wave radiative width is found to be a factor of six greater than the p-wave radiative width and it is also considerably larger than for other nuclei in this mass region. Valence capture and enhanced decay to single particle final states could account for the large s-wave radiative strength. A large positive correlation between Γ_n^0 and Γ_γ for ten s-wave levels is found ($\rho = 0.67$).

The following average resonance parameters are deduced: $\langle D \rangle = 7.5 \pm 1.5$ keV, $10^4 S_0 = 0.9 \pm 0.4$, $10^4 S_1 = 0.5$; $\langle \Gamma_\gamma \rangle_s = 310 \pm 25$ meV and $\langle \Gamma_\gamma \rangle_p = 47 \pm 5$ meV.

Evidence for a predominant direct capture mechanism for thermal capture is presented.

o. keV Neutron Resonance Capture in ^{40}Ca (Musgrove,* Allen,* Boldeman,* Chan** and Macklin)

The neutron capture cross section of ^{40}Ca was measured at high resolution and resonance parameters have been extracted for levels below 360 keV. Many new p- and d-wave resonances are reported.

The average resonance parameters obtained from our data are as follows: $\langle D \rangle = 37 \pm 3$ keV, $10^4 S_0 = 2.9 \pm 1.9$, $10^4 S_1 \simeq 0.1$, $10^4 S_2 = 2.3 \pm 0.5$. The average radiative widths were found to be dependent on ℓ as follows: $\langle \Gamma_\gamma \rangle_s = 2.5 \pm 1.7$ eV, $\langle \Gamma_\gamma \rangle_p = 0.32 \pm 0.09$ eV and $\langle \Gamma_\gamma \rangle_d = 0.60 \pm 0.1$ eV, where the quoted errors are standard deviations. A strong positive correlation between Γ_n^0 and Γ_γ of 0.76 was found for the nine s-wave levels observed in the range.

Optical model calculations show that valence transitions to low lying shell model P orbitals account for 0.86 eV of the s-wave radiative strength on average. A further important contribution of the same order of magnitude results from enhanced transitions to the same p-wave final states, and which arise in the presence of two particle-two hole excitations of the core. These enhanced transitions are seen to be present in s- and p-wave neutron capture and the great difference between the respective radiative widths can be in part attributed to the difference in strengths between E1 and M1 transitions to the same final states of ^{41}Ca.

---

* Australian Atomic Energy Commission, Lucas Heights, NSW, Australia.

** University of Melbourne, Parkville, Vic., Australia.

p. Valence Component in the Neutron Capture Cross Section of ^{90}Zr* (Boldeman,** Allen,** Musgrove** and Macklin)

The neutron capture cross section of ^{90}Zr has been measured with high energy resolution between 3 and 200 keV using the capture cross section facility at the 40 meter station on the Oak Ridge Electron Linear Accelerator. Through the comparison of the present data with the total cross section and inverse ^{91}Zr(γ,n) data from Toohey and Jackson, complete resonance parameters have been extracted for 37 $p_{3/2}$, 12 $p_{1/2}$ and 11 s-wave resonances out of a total of 101 observed resonances. The neutron strength functions extracted from the resonance parameters are $S_0 = 0.56 \times 10^{-4}$, $S_1 = 3.8 \times 10^{-4}$, $S_1(p_{3/2}) = 4.7 \times 10^{-4}$ and $S_1(p_{1/2}) = 1.9 \times 10^{-4}$. It is noteworthy that the $S_1(p_{3/2})$ strength function is significantly larger than the $S(p_{1/2})$ strength function in agreement with theoretical expectation.

A significant correlation ($\rho = 0.58$) exists between the reduced neutron widths and the radiative widths for the 37 $p_{3/2}$ resonances. The data give strong confirmation of the Valence Neutron Model. With standard valence calculations all radiative widths can be calculated reasonably from the associated reduced neutron width. However, to explain the measured correlation coefficient, it has been necessary to include with the valence component, single particle transitions to the ground and low excited states of ^{91}Zr, which are uncorrelated with the resonance reduced neutron width.

The average capture gamma spectrum for neutron capture in ^{90}Zr between 2 and 80 keV has been calculated from the valence model and the present data and is found to be in very close agreement with published experimental data.

q. The Pb(n,xγ) Reaction for Incident Neutron Energies Between 0.6 and 20.0 MeV†,‡ (G. T. Chapman and G. L. Morgan)

Numerical values of the differential cross sections for gamma rays produced by neutron reactions with natural lead have been measured for neutron energies between 0.6 and 20 MeV. The data were obtained using an electron linac as a neutron source in conjunction with a NaI spectrometer located at an angle of 125°. The data consist of the doubly differential cross section, $d^2\sigma/d\Omega dE$, for gamma rays between 0.3 and 10.5 MeV for coarse intervals in incident neutron energy and the integrated yield of gamma rays of energy greater than 0.3 MeV with high resolution in the incident neutron energy. The measured results are compared with the current ENDF/B data.

---

* Relevant to request No. 234.

** AAECRE, Lucas Heights, NSW, Australia.

† Abstract of ORNL-TM-4822.

‡ Relevant to request Nos. 397 and 398.

r. Gamma-Ray Transitions in ^{181}Ta Observed in ^{181}Ta(n,n'γ) Reactions* (J. K. Dickens and G. G. Slaughter)

The level structure of ^{181}Ta has been studied by observing gamma radiation due to inelastic neutron scattering by Ta. Of the 131 gamma rays (or groups of unresolved gamma rays) observed, 60 could be placed as transitions among 42 levels in ^{181}Ta. These include 24 new levels having $E_x > 990$ keV, and verification of previously reported results. Possible quantum assignments based upon the Nilsson single-particle rotational bands are suggested for 4 of the new levels.

s. Gamma-Ray Production due to Neutron Interactions with ^{208}Pb for E_γ Between 5 and 8 MeV** (J. K. Dickens)

Reduction of ^{208}Pb(n,n'γ) spectra obtained using a Ge(Li) detection system and monoenergetic neutrons (produced by pulsed deuterons impinging on a deuterium-filled gas cell)[1] has been completed, and an analysis of the resulting cross-section data is in progress. For two important transitions, E_γ = 0.583 and 2.614 MeV, the present data have been compared with recent work of Nellis, et al.[2] and with the current evaluation.[3] This comparison is shown in Fig. A-1.

t. The ^{120}Sn(n,γ)^{121}Sn Reaction (R. F. Carlton†, G. G. Slaughter and S. Raman)

Resonance (n,γ) measurements from sixteen neutron resonances have been carried out for an enriched sample of ^{120}Sn with neutrons from the Oak Ridge Electron Linear Accelerator. Eighteen gamma rays were assigned as primary γ-rays. The resulting level scheme with $\approx$ 20 states is in good agreement with that obtained from (t,d) and (t,p) studies[4] and from recent (d,p) studies.[5] Gamma-ray branching ratios have been determined for various levels in ^{121}Sn. Available data on the odd tin isotopes have been used to investigate the systematic behavior of levels as the filling of neutron shells occurs. These are discussed within the framework of the quasiparticle description of single closed shell nuclei.

---

* Abstract of ORNL-TM Report (to be published).

** Relevant to request No. 398.

† Middle Tennessee State University.

[1] See J. K. Dickens and F. G. Perey, Nucl. Inst. Meth. 82, 301 (1970) for a description of the experimental system.

[2] D. O. Nellis, I. L. Morgan and E. L. Hudspeth, Phys. Rev. C9, 1972 (1974).

[3] C. Y. Fu and F. G. Perey, ORNL-4765 (March, 1972).

[4] R. F. Casten, et al., Nucl. Phys. A180, 49 (1972).

[5] M. J. Bechara, O. Dietzsch, and E. W. Hamburger, Private Communication.

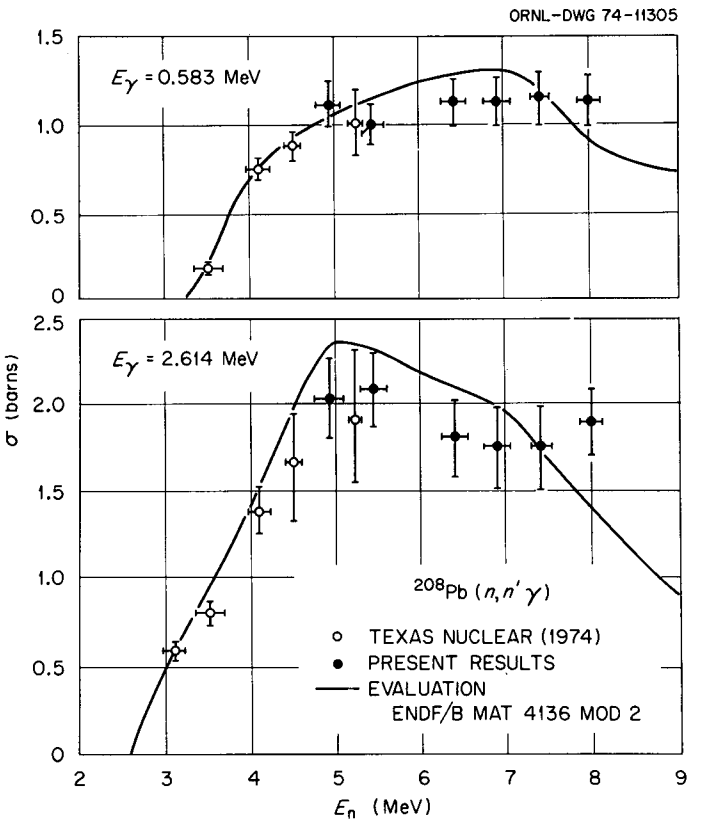

Fig. A-1. Comparison of present cross sections for production of gamma rays in ^{208}Pb with prior results and evaluation. The present σ are $4\pi\ d\sigma/d\omega$ for θ_γ = 55 or 125 deg, and the error bars are absolute.

u. Neutron Separation Energies of Tin Isotopes (G. G. Slaughter and S. Raman)

We have carried out resonance (n,γ) measurements at ORELA on a natural tin target in order to obtain the neutron separation energies, S_n, of several tin isotopes. The results are summarized below:

Final Nucleus	E_n (eV)	E_γ(keV) ±2	E(level) keV	S_n (keV)
^{113}Sn	99	7245.2	496.5	7741.9 ± 2.3
^{117}Sn	148	6942.4	g.s.	6942.5 ± 2.0
^{118}Sn	39	8094.8	1229.6	9324.8 ± 2.1
^{119}Sn	46	6482.8	g.s.	6483.0 ± 2.0
^{121}Sn	427	6170.7	g.s.	6170.5 ± 2.0
^{123}Sn	107	5921.1	24 ± 2	5945.2 ± 2.9
^{125}Sn	62	5706.0	26 ± 2	5732.1 ± 2.9

The present S_n value for ^{121}Sn is in good agreement with S_n = 6173 ± 4 keV obtained earlier in (n,γ) measurements but not with S_n = 6191 ± 6 keV deduced from $Q_\beta(^{121}Sn \rightarrow ^{121}Sb)$ and the known masses for ^{120}Sn and ^{121}Sb from mass doublets.

v. Precise Measurements and Calculations of ^{238}U Neutron Transmissions*,**(Olsen, de Saussure, Silver and Perez)

We have measured the total neutron cross section of ^{238}U below 1 keV in precise transmission experiments and have compared the results with ENDF/B-IV. Special emphasis was placed on measuring transmissions through thick samples to obtain accurate total cross sections in the potential-resonance interference regions between resonances. These total cross sections are important in computing shielded capture integrals, and it has been observed that such shielded integrals are overestimated by ENDF/B-IV.

The neutron energies were determined by time of flight along a 40 m flight path at ORELA. The detector was a 7.62-cm diameter, 1.0-mm thick Li-glass disk viewed edge-on by two RCA-7585 phototubes. At 20 m from the neutron source isotopically enriched ^{238}U disks with inverse thicknesses of 1/n = 5405, 1603, 807, 266, 80.7, 19.2, and 5.7 barns/atom were alternated in and out of the beam with 10 minute cycles. At least four different transmission measurements with various combinations of Cd, In, Co, Al, Mn, and Au beam filters were made for each sample thickness. Blackened resonances from these filters aided in estimating the background levels.

After subtracting the background and deadtime-correcting the sample-in and sample-out time-of-flight spectra, the resulting transmissions for

* Relevant to request Nos. 475 and 476.

** To be presented at ANS Meeting, New Orleans, La., June 1975.

each sample thickness were combined and compared with a Doppler and resolution broadened transmission calculated from ENDF/B-IV total cross sections. In particular Fig. A-2 shows the experimental transmission of 50- to 300-eV neutrons through 3.62 cm (1/n = 5.7 barns/atom) of ^{238}U. The upper curve is the corresponding transmission calculated using the ENDF/B-IV procedure. For energies larger than 40 eV, the calculated transmission between resonances is greater than the measured transmission and, in fact, calculates to be greater than unity (negative cross section) at some interference minima in the cross section. The lower curve shows the transmission as obtained from an exact R-matrix calculation of the total cross section using: (1) the random phase approximation for the radiative channels; (2) the resonance parameters and scattering radius from ENDF/B-IV; and (3) the "picket fence" approach (uniform spacings and widths) for levels outside the resolved resonance region. This more exact calculation of the total cross section reproduces the measured transmission much better and does not yield negative cross sections. It is very likely that the failure of ENDF/B-IV to reproduce measured thick sample transmission as shown above is the cause of the overestimation of the strongly self-shielded capture resonance integrals. In particular, the capture integral from 100 to 680 eV shielded down to 10.0 barns decreases by 4.6% when the multilevel formalism is used in place of ENDF/B-IV procedures.

w. Measurements on the 22 eV Doublet in $^{232}Th(n,\gamma)$*,** (Halperin, de Saussure, Perez and Macklin)

The 22 eV doublet in the $^{232}Th(n,\gamma)$ reaction contributes about half the thin-sample resonance capture integral for ^{232}Th. A discrepancy of some 15% in the measured neutron width for the 23.439 eV resonance is apparent among several recent measurements. In view of the special interest in ^{232}Th as the fertile nuclide in the ^{233}U breeder, we have remeasured the capture cross section with a relatively thin (0.0002375 a/b) metal sample. The measurement was carried out at the 40-meter flight path of the ORELA time-of-flight facility. The capture gamma cascade was measured with nonhydrogenous total gamma energy detectors. The incident neutron spectrum was measured with a thin ^{6}Li glass in transmission displaced 0.4 meter forward in the beam. Since the gamma width dominates in these two resonances, the capture area predominantly provides a measurement of the neutron width. Monte Carlo calculations evaluating the capture area of the resonance at 23.439 eV (provisionally normalized to the better known 21.783 eV resonance) yield a measure of $g\Gamma_n = 3.72 \pm 0.11$ meV. This value is consistent with an unpublished ORNL value of J. A. Harvey of $g\Gamma_n = 3.74 \pm 0.15$ meV.

---

* Relevant to request No. 404.

** Conf. on Nuclear Cross Sections and Technology, Washington, March 1975.

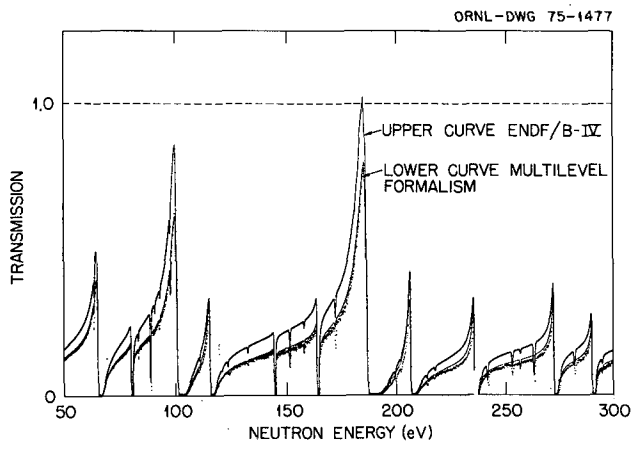

Fig. A-2. Measured Transmission of 50- to 300-eV Neutrons Through 3.62 cm of ^{238}U. The upper curve is the transmission calculated from a Doppler broadened ENDF/B-IV cross section, whereas the lower curve was obtained from a multilevel formalism.

x. A Direct Comparison of Different Experimental Techniques for Measuring Neutron Capture and Fission Cross Sections*,** (Gwin, Weston, Todd, Ingle and Weaver)

Measurements of the neutron capture, σ_c, and fission cross sections, σ_f, of ^{239}Pu have been obtained at ORNL using different detectors for both fission and capture. These experiments were normalized to the same 2200 m/sec cross sections and extended into the keV region. In one experiment fission was detected by means of the prompt neutrons and absorption. The other technique detected fission fragments to measure fission and a large liquid scintillator detected the prompt gamma rays from absorption. Auxiliary experiments were used to investigate the neutron flux measurements, and to test the fast neutron detected with the pulse shape discrimination method for measuring fission events in ^{239}Pu. For the 28 decade energy intervals between 0.1 to 200 keV, the ratio $\langle\sigma_c\rangle/\langle\sigma_f\rangle$ obtained in the two experiments differ on the average by 6%. The cross sections are in good agreement ($\sim$ 2%) up to 8 keV.

y. Measurement of the Neutron Capture Cross Sections of the Actinides*,† (L. W. Weston and J. H. Todd)

The capture cross sections of the isotopes heavier than ^{239}Pu are of great importance for the core physics, fuel management, and waste management of power reactors. Since integral measurements and total cross sections are not sufficient, a program for the measurement of these needed capture cross sections is being carried out at ORNL. Measurements have been completed on ^{240}Pu, ^{241}Pu, ^{241}Am and have been planned for ^{242}Pu and ^{237}Np. The capture gamma-ray detector used is the "total energy detector" which is a modification of the Moxon-Rae detector. Fission, when present, is detected with fast neutron counters. Results obtained on ^{240}Pu, ^{241}Pu, and ^{241}Am extend continuously from thermal neutron energies to 300 keV. The cross sections are normalized at thermal neutron energies and the neutron flux is measured relative to the ^{10}B(n,α) cross section up to 20 keV and ^{6}Li(n,α) at higher neutron energies. The accuracy of the techniques used varies with the sample but is about 8%. With such cross sections the long-range management of the actinides produced in power reactors can be planned on a more systematic basis. The basic neutron energy resolution of the system is about 0.4 nsec/m.

---

* Conf. on Nuclear Cross Sections and Technology, Washington, March 1975.

** Relevant to request Nos. 501 and 507.

† Relevant to request Nos. 521, 522, 530, 543, and 544.

z. Measurement of $\bar{\nu}_p$ for ^{252}Cf* (Spencer, Gwin, Ingle and Weaver)

Preliminary studies of the efficiency calibration of the 1.1 meter diameter, Gd poisoned, liquid scintillator tank have been initiated using a neutron beam from ORELA and a proton recoil detector. These measurements will be used in conjunction with two-dimensional DOT code computations, which are being carried out by Joe Pace of the Computer Sciences Division, to give the absolute efficiency of the tank for ^{252}Cf spontaneous fission neutrons. Ths efficiency will be used in an absolute determination of $\bar{\nu}_p$ for a high-purity ^{252}Cf source.

2. Charged Particle Experiments

a. ^{131}Ba Levels by the $^{122}Sn(^{12}C,3n\gamma)$ Reaction (J. Gizon,** A. Gizon** and D. J. Horen†)

Recently the structure of some odd neutron-deficient nuclei has been studied by heavy-ion reactions.[1] From the "band structure" based upon the $9/2^-$ ground state which was observed in ^{133}Ce and ^{135}Nd with N = 75, it was concluded that these nuclei have a prolate deformation. From previous work,[2] it is known that in the ^{131}Ba isotone a $9/2^-$ level occurs as an isomeric state. The present study was undertaken in an attempt to determine whether or not this latter level is analogous to the $9/2^-$ "band" head observed in the Ce and Nd isotones, as well as to extend the systematics of this "band."

The variable energy cyclotron at Grenoble was used to accelerate ^{12}C ions to energies between 46-57 MeV to irradiate a target of ^{122}Sn. Excitation functions, prompt and delayed γ-ray spectra, angular distributions, and γ-γ coincidence measurements have been made. Based upon preliminary analysis, we obtain a level scheme which contains the major portion of the observed intensity.

The "band structure" based upon the $9/2^-$ level is almost identical to that observed previously in the Ce and Nd isotones, thereby indicating that this "band" is essentially due to the neutron configuration and is little influenced by changing the number of protons from 56 to 60. Indeed, the energies and relative intensities of the transitions are very similar for these three isotopes. The main difference seems to be the relative spacing between the $11/2^-$ and $9/2^-$ levels which decreases monotonically with Z.

---

* Relevant to request Nos. 579 and 580.

** Institut des Sciences Nucléaires, Grenoble, France.

† Work performed while on assignment at Institut des Sciences Nucléaires.

[1] J. Gizon et al., Nucl. Phys. (to be published).

[2] D. J. Horen et al., Phys. Rev. 129, 1712 (1963).

From the angular distributions, it appears that the sign of A_2 for the M1 + E2 transitions is negative. Using the arguments previously given,[1] one can conclude that ^{131}Ba has a prolate deformation for this odd-parity band.

Data pertaining to the positive-parity states in these nuclei are not yet very extensive. The ground-state "band" proposed here is consistent with the results of Spalek et al.[2] As in ^{135}Ce and ^{137}Nd, the main feeding of this "band" is via the high-spin negative-parity isomeric state. A tentative level scheme was attained.

b. Study of Giant Resonances with ^{3}He Ions* (Horen,** Arvieux,† Buenerd,† Cole,† Saintignon† and Perrin†)

The excitation of the giant resonance regions in ^{48}Ti, ^{56}Fe, ^{59}Co, ^{60}Ni, ^{144,154}Sm, ^{159}Tb, ^{165}Ho, ^{169}Tm, and ^{208}Pb was studied by use of inelastic scattering of 80-MeV ^{3}He ions using the Grenoble isochronous cyclotron. The impetus for this work was basically threefold:

1. To attempt to obtain angular distribution data that would clearly demonstrate the multipole character of the giant resonance(s).
2. To attempt to determine whether or not excitation of the GDR is observable in ^{3}He scattering.
3. To investigate the relative shape of the GR region for spherical and deformed nuclei and to make comparisons with the results obtained in proton scattering.[3]

The scattered particles were detected with silicon detector telescopes and analyzed with an electronic particle-identification system. Measurements were made between 8° and 40° in the laboratory system. Extensive care was taken to ensure that the incident beam on target was clean. In addition, the effect of reactions induced in the E detector by elastically scattered ^{3}He ions was thoroughly investigated. After

---

* Condensation of two papers accepted for publication in Nuclear Physics and The Physical Review.

** Work performed while on assignment at Institut des Sciences Nucléaires, Grenoble, France.

† Institut des Sciences Nucléaires, Grenoble, France.

[1] J. Gizon et al., Nucl. Phys. (to be published).

[2] A. Spalek et al., Nucl. Phys. A118, 161 (1968).

[3] D. J. Horen, F. E. Bertrand, and M. B. Lewis, Phys. Rev. C 9, 1607 (1974).

reduction, the data were compared with theoretical calculations based upon the works of Satchler.[1] In general, the present work is in excellent agreement with the earlier results and conclusions based upon proton scattering at ORNL.[2]

Angular distributions were obtained for the first-excited state (2^+) in ^{56}Fe and the 16.6-MeV giant resonance which represent the first data obtained in ^{3}He scattering which unambiguously demonstrate the L = 2 character of this resonance. Each of the targets in the light-mass region (i.e., A = 48-60) exhibited similar characteristics. These consisted of a broad peak (FWHM $\approx$ 6 MeV) located at an energy of about 63 $A^{-1/3}$ MeV and a much narrower satellite peak at about 51 $A^{-1/3}$ MeV. The broad peaks all had angular distributions which could best be reproduced with L = 2. A search was made for evidence of excitation of the GDR by comparing spectra obtained at the laboratory angle where an L = 2 angular distribution has a minimum to those at other angles. No significant differences in the shape of the GR region were found. These results tend to confirm the theoretical prediction that the excitation of a G.T. GDR is small compared to excitation of an E2 GR. The strength of the giant resonance for the light elements was found to exhaust $\approx$ 50-60% of the isoscalar E2 EWSR.

The spectra obtained for the Sm-Pb group of targets were very similar to each other. In particular, there was little difference observed between the ^{144}Sm and ^{154}Sm spectra in the GR region, as was also the case for proton scattering.[3] Assumption that the integrated cross section for the resonance region is solely due to an isoscalar E2 excitation implies exhaustion of the E2 EWSR of $\gtrsim$ 100%.

c. Inelastic Scattering of Polarized Protons by ^{12}C (G. Perrin,* Arvieux,* Buenerd,* Cole,* Durand,* Horen,** Martin,* C. Perrin* and P. de Saintignon*)

The cross sections and analyzing powers of polarized protons scattered by ^{12}C have been measured at 22.3, 26.7 and 30.5 MeV for all states up to the 14.1 MeV. A coupled-channel analysis of the 0^+, 2^+ and 3^- states has been done with the code ECIS 72 and the following combinations:

---

* Institut des Sciences Nucléaires, Grenoble, France.

** Work performed while on assignment at Institut des Sciences Nucléaires.

[1] G. R. Satchler, Nucl. Phys. A195, 1 (1972); erratum, Nucl. Phys. A224, 546 (1974); and Part. Nucl. 5, 105 (1973).

[2] The reader is referred to the summary contained in Physics Division Annual Progress Report, ORNL-4937, p. 2 (May 1974) or the open literature, references for which are given in G. R. Satchler, Physics Reports 14C, No. 3 (1974).

[3] D. J. Horen, F. E. Bertrand and M. B. Lewis, Phys. Rev. C 9, 1607 (1974).

0^+-2^+ (rotation $\beta_2 = -0.6$), 0^+-3^- (vibration $\beta_3 = 0.4$), and 0^+-2^+-3^- (vibrations $\beta_2 = 0.4$, $\beta_3 = 0.6$). These deformations are average values extracted from different experiments. Different sets of optical parameters have been tried, but no one is able to reproduce the elastic data in this energy range. The data cannot be fitted with a single set of parameters. This may indicate that resonance effects, and particularly core-polarization, are quite strong in all channels and must be included in a meaningful analysis.

3. Theoretical Analysis, Compilation, and Evaluations

a. Intermediate Structure in the ^{238}U Neutron Capture Cross Section (R. B. Perez and G. de Saussure)

Recent measurements of the ^{238}U neutron capture cross section show large fluctuations in the unresolved resonance region. To test whether the observed local enhancements of the neutron capture are randomly distributed or, on the contrary, represent departures from the statistical nuclear model, the Wald-Wolfowitz runs and correlation tests were applied to the ^{238}U neutron capture data obtained at ORELA. The Wald-Wolfowitz runs test deals with the statistic, R, which is the number of unbroken sequences of data points above or below a given reference line. This statistic is to be compared with the expected value of runs $E(R)\pm\sigma(R)$ arising from randomly distributed data. In the correlation test we have computed the first serial correlation coefficient of the data as well as its expected value and variance for a set of random data. In both tests one computes the probability, P, for the given statistic entity to depart from its expected value by more than F standard deviations. Both tests yield $P<10^{-4}$ between 10 and 100 keV confirming the presence of intermediate structure. The range of the structure far exceeds the width of the experimental resolution.

b. Representation of Neutron Cross Sections in the Unresolved Resonance Region (G. de Saussure and R. B. Perez)

In the unresolved resonance region, the statistical properties of neutron cross sections are usually specified by the average values and distribution functions of the resonance parameters. We discuss deficiencies of this treatment: In particular, it is based on the statistical model of nuclear reactions, a model which is inconsistent with the intermediate structure observed in many heavy nuclei. Present technology allows the measurement of cross sections with an instrumental resolution broadening which is small compared to the Doppler broadening. From the results of such measurements, the Doppler broadened cross sections may be obtained directly by kernel broadening. We propose to replace the statistical treatment of the unresolved region by a parametric description of the actual cross sections. The use of this cross section, rather than a representation of their statistical properties, is expected to yield more accurate estimates of resonance absorption and self-shielding factors.

c. Intermediate Structure in the Neutron Induced ^{235}U Cross Sections (G. D. James, G. de Saussure and R. B. Perez)

The ^{235}U fission cross section exhibits large fluctuations in the unresolved resonance region. One asks whether this phenomenon can be explained in terms of the statistical nuclear model, or whether, on the contrary, these fluctuations represent departures from it, in localized energy regions, where enhancements of the reaction widths occur.

Two statistical tests have been proposed to determine whether these fluctuations are of a random nature: the Wald-Wolfowitz[1] and the Levene-Wolfowitz[1] tests. In the former one counts the number of runs, R, of consecutive observed values which lie above or below a reference value (ideally the median). In the latter one counts the number of consecutive observed pairs of values of increasing or decreasing magnitude (runs up or down), thus creating a set of runs, $R(\ell)$, of length, ℓ. Both statistics provide the number of runs, E(R), expected from random statistical data, as well as the standard deviation, $\sigma(R)$, and the probability, P(R), for R to depart from its expected value by more than F standard deviations.

To utilize these tests with confidence, one has to prove that cross sections obtained from the statistical nuclear model do indeed satisfy both statistics. The ^{235}U fission cross section was simulated by Monte Carlo techniques for neutron energies between 10 and 40 keV, and averaged over 100-eV energy intervals. The result of the statistical tests shows the adequacy of both statistics.

The capability of detecting the presence of intermediate structure was tested by mocking-up fission width enhancement on the basis of the double-humped fission barrier model. In this case the fission widths, $\Gamma'_{\lambda f}$, of fine structure resonances (Class I levels) are modulated by the presence of levels in the second fission potential barrier minimum (Class II levels) according to the equation:[2]

$$\Gamma'_{\lambda f} = \Gamma_{\lambda f} + \sum_{\mu} \frac{A^2_{\lambda\mu}\Gamma_{\mu}}{(E - E_{\mu})^2 = (1/4)\Gamma^2_{\mu}} \qquad (1)$$

where $\Gamma_{\lambda f}$ belongs to the Class I levels, Γ_{μ} and E are the fission widths and level energies for the Class II levels and $A_{\lambda\mu}$ is the coupling between the two potential wells. Data generated according to Eq. (1) show large departures from random statistical behavior in both statistical tests.

Next the ^{235}U fission and capture cross sections measured at ORELA were averaged over 100 eV intervals between 10 and 40 keV and tested. The significant deviations from random statistical behavior which are observed confirm the presence of an intermediate structure in both the ^{235}U fission and capture cross sections. This finding has implications in regard to our understanding of the unresolved resonance region and treatment of cross sections in this region for reactor design.

---

[1] A. Wald and J. Wolfowitz, Annals Math. Stat. XI, No. 2 (1940).

[2] R. B. Perez et al., ORNL-TM-3696 (1972).

d. Estimated Data Covariance Files of Evaluated Cross Sections -- Examples for ^{235}U and ^{238}U (F. G. Perey, G. de Saussure and R. B. Perez)

We review the status of development of formats and methods to represent uncertainty information of evaluated microscopic data in the ENDF/B system. Some examples of methods to obtain the data covariances of important cross sections for fertile and fissile nuclides are given. We give some examples of typical group cross sections covariance matrices obtained by processing the ENDF/B estimated data covariance files.

e. Use of Nuclear Reaction Models in Evaluating Gamma-Ray Production Data (F. G. Perey)

An extensive body of neutron-induced gamma production cross sections has been collected recently as a result of major advances in experimental technique.[1] The use of nuclear-reaction theories in evaluating these results has proved surprisingly successful[2] and the excellent agreement suggests that these reaction models can be used to generate cross sections for materials and targets for which data are not feasible or not yet available.

f. Estimated Uncertainties in Nuclear Data -- an Approach (F. G. Perey)

The need to communicate estimated uncertainties in evaluated nuclear data to be used in the assessment of their adequacy in applications has been recognized in the ENDF/B system. Starting with ENDF/B-IV, the data files contain formatted data describing the estimated covariances of some of the microscopic cross sections in such a form that they can be processed by computer codes to generate covariance matrices of quantities used in solving neutron transport problems such as group cross sections. The basic concepts behind the representation of such quantities will be described and the work done so far in the representation and manipulation of such quantities will be discussed. Problem areas not yet addressed in ENDF/B-IV but under study will be discussed.

g. Description of the ENDF/B-IV Silicon Evaluation (D. Larson)

The ENDF/B-IV version of the silicon evaluation is considered as an example of an evaluation which includes angle and energy distributions of outgoing charged particles. Relevant optical model parameters were determined by careful fitting to available elastic scattering data. Competition among open channels was calculated using the Hauser-Feshbach

---

[1] J. K. Dickens, G. L. Morgan and F. G. Perey, Nucl. Sci. Eng. 50, 311-336 (1973).

[2] C. Y. Fu and D. C. Larson, ORNL, to be published.

formalism, including direct reaction components where appropriate. Gilbert-Cameron level density parameters were modified to reproduce available data and also checked against predictions from shell model calculations. Gamma-ray production for binary channels was calculated from the Hauser-Feshbach results, with the branching ratios taken from the literature and shell model calculations. The tertiary reaction cross sections and associated gamma-ray productions were calculated using a statistical model with empirical angular momentum corrections. Energy distributions of both neutrons and charged particles are given as probability distributions and are obtained from the Hauser-Feshbach and tertiary calculations. Comparisons of the evaluation to available data will be shown.

h. Reaction List for Charged-Particle-Induced Nuclear Reactions Z = 1 to 98 (H to Cf), July 1973 - September 1974*
(F. K. McGowan and W. T. Milner)

This reaction list for charged-particle-induced nuclear reactions has been prepared from the journal literature for the period from July 1973 through September 1974. Each published experimental paper is listed under the target nucleus in the nuclear reaction with a brief statement of the type of data in the paper. The nuclear reaction is denoted by A(a,b)B, where $M_a \geq$ (one nucleon mass). There is no restriction on energy. Nuclear reactions involving mesons in the outgoing channel are not included. Theoretical papers which treat directly with the analysis of nuclear reaction data and results are included in the reaction list.

i. "Anomalous" Ground States in the Neutron-Deficient $171 \leq A \leq 185$ Region (B. Harmatz, D. J. Horen and Y. A. Ellis)

Recently revised nuclear data compilations[1-5] for odd-mass ($171 \leq A \leq 185$) nuclei far from the β-stability line have indicated possible variations from the regional systematics of Nilsson ground-state assignments for ^{177}W, ^{181}Os, and ^{171,173}Ta. Other shifts from ground-state systematics have been recently proposed by experimenters for ^{165}Lu, ^{177}Re, and ^{185}Ir. This behavior has been ascribed to changes in quadrupole and/or hexadecapole deformation. The cases cited above occur in nuclei 9±1 neutrons removed from the β-stability line. To determine the relevance of various factors such as deformation parameter, a horizontal study is in process.

Although $5/2^-[512]$ has been regularly ascribed to 103-neutron ground states (e.g., ^{175}Hf, ^{173}Yb, ^{171}Er), a shift to $1/2^-[521]$ probably occurs for the more neutron-deficient ^{177}W isotone based on our experimental conversion-electron study. A first level scheme for ^{177}Re (14 m) decay to ^{177}W is proposed in which most of the transition intensity is accounted for in the rotational $1/2^-[521]$ configuration up to spin 9/2. Intraband

* To be published in Atomic Data and Nuclear Data Tables.

Placements are consistent with multipolarity information, E2 branching ratios, band parameters, and empirical systematics. Furthermore, a large fraction of ^{177}W β-decay strength is to low-spin ($\lesssim$3/2) members of K = 1/2 bands in ^{177}Ta. The 1/2$^-$[521] orbital appears at ground also in isotone ^{183}Hg, based on measured J and μ values.[6]

Compilers have noted that β-branchings from ^{171,173}Ta differ from heavier off-A tantalums. Branchings from both ^{175,177}Ta(7/2$^+$[404]) are mainly to various K = 7/2 excitations in hafnium. In contrast, strong β-transitions (60%) from ^{173}Ta proceed to the 3/2, 5/2, 7/2 sequence of 1/2$^-$[521] states in ^{173}Hf. Similar decays to K = 1/2, 3/2 bands were observed for ^{171}Ta.[1] The nature of β-feeding precludes 7/2$^+$[404] as the ground state of lighter tantalums, but is compatible with J = 5/2, 1/2$^-$[541]. The state J = 5/2, 1/2$^-$[541] is populated in ^{175,177}Ta at 51 and 186 keV, respectively.

The sharply different character of isomeric decays of isotones ^{179}W and ^{181}Os can be explained by an inversion of 7/2$^-$[512] and 1/2$^-$[521], the lowest-lying neutron orbitals. A fast β-transition (log ft $\approx$ 4.5) connects $7/2^-[512]_n \leftrightarrow 9/2^-[514]_p$ states in decays of ^{179}W and ^{181}Os. In contrast with ^{181}Os, 99% of ^{179}W (1/2$^-$[521]) decay strength is isomeric, via a 222-keV M3 γ-ray. There is no evidence of M3 isomerism or a genetic relationship between 2.7-m and 105-m ^{181}Os decay spectra. From consideration of limits of detection, calculated M3 branching intensity, and decay properties of the ^{179}W analog, the 1/2$^-$[521] orbital probably lies at ground in ^{181}Os. As for ^{181}Os, the ground state of isotone ^{185}Hg has been assigned as 1/2$^-$[521] from measured spin and magnetic moment.[6]

A 5/2, 1/2$^-$[541] assignment for ^{185}Ir at ground is consistent with strong β-transitions from ^{185}Ir to J = 5/2, 7/2 members of 1/2$^-$[510] and 3/2$^-$[512] bands in ^{185}Os. The shift from 3/2$^+$[402], which is regularly ascribed to odd-A Ir ($\geq$187) ground states, is confirmed by a recent revision of ^{185}Ir ground-state spin to 5/2 (atomic beam.)[7]

Odd-mass Re isotopes ($181 \leq A \leq 187$) are regularly classified as 5/2$^+$[402] at ground. In-beam heavy-ion reactions populate 1/2$^-$[541] and 5/2$^+$[402] bands in ^{179}Re and ^{177}Re, up to high spins, with an inversion of the Nilsson states. A K = 1/2 ground state for ^{177}Re is consistent with strong β-transitions to a 1/2$^-$[521] configuration in ^{177}W.

Our phenomenological survey of deviations from the regional trend of Nilsson ground-state assignments extends from $71 \leq Z \leq 77$, where the neutron deficiency is 8 to 10 units. An interesting aspect of this behavior is the movement of low-lying $K^\pi = 1/2^\pm$ orbitals to ground for the seven cases noted to date.

---

[1] D. J. Horen and B. Harmatz, Nucl. Data Sheets 11, 549 (1974).

[2] B. Harmatz and D. J. Horen, Nucl. Data Sheets 14, 297 (1975).

[3] Y. A. Ellis and B. Harmatz, Nucl. Data Sheets for A = 177, to be published.

[4] Y. A. Ellis, Nucl. Data Sheets 9, 319 (1973).

[5] Y. A. Ellis, Nucl. Data Sheets for A = 185, to be published.

[6] J. Bonn, G. Huber, H. Kluge, and E.W. Otten, Phys. Lett. 38B, 308 (1972).

[7] C. Ekström, private communication (December 1974).

4. Status Report of the Nuclear Data Project (R. L. Auble, J. B. Ball,[1] F. E. Bertrand, Y. A. Ellis, W. B. Ewbank, B. Harmatz, D. J. Horen,[2] H. J. Kim,[3] D. C. Kocher,[4] M. B. Lewis,[5] M. J. Martin, F. K. McGowan,[6] S. Raman,[7] and M. R. Schmorak)

During the calendar year 1974, the Nuclear Data Project (NDP) published 31 mass-chain compilations and three issues of Recent References. In addition, the Project provided information in the form of selected reference lists and nuclear data to a variety of persons and groups. From the 14 persons listed above, only *10 man-years* were devoted to the NDP. These resulted in the publication of 14 mass-chain compilations, 14 research papers, deliverance of 23 talks (4 invited), review of about 30 NIRA compilations, and review of about 15 papers for physics journals. Work in progress includes the preparation of 20 mass-chain compilations by *Project staff*, production of 11 NIRA compilations, and near completion of preparation of radioactive decay data on about 190 radionuclides for inclusion in a forthcoming handbook of the National Bureau of Standards. Not included in this report are the contributions of the NDP to the atomic mass compilation of A. H. Wapstra *et al.* In the process of preparing a mass-chain compilation the compilers usually detect on the average of about four errors or corrections to the input values. Most of these only surface when the compiler has considered all the available structure data, *i.e.*, the correlations between reaction results, level schemes, etc.

Utilization of NDP products in the form of references and evaluated data compilations by applied workers and basic researchers continues to grow.

A horizontal type compilation in the deformed region has exhibited an interesting trend in the ground-state spins of nuclei with $171 \leq A \leq 185$.

The computer-based Evaluated Nuclear Structure Data File (ENSDF) is in regular use. Data from 30 mass chains have been placed on permanent disk storage; 30 mass chains are in a working area of the data cell. Data cards for 30-40 additional mass chains are being upgraded to current data bank standards and will be added to the permanent files. A special computer program has been developed (with the aid of Marian Kowalski) to prepare directly from ENSDF standard data sets tabulations of pertinent radiative data required for biomedical dose calculations.

Status of Data File

The card-image format for the computerized data file has been finalized, and the system is routinely being utilized by NDP compilers.

---

[1]Heavy-Ion Facility. Acting Director NDP till July 1974.
[2]On foreign assignment till August 1974.
[3]Half-time Project member, on foreign assignment till September 1974.
[4]Commenced May 1974.
[5]Full-time Project member till September 1974.
[6]Half-time Project member.
[7]ORELA. Half-time Project member till July 1974.

Basically, the procedures are as follows:

a) The compiler examines the literature for each type experiment and makes a decision as to which data he wishes to adopt. This is then entered in the standard data format.

b) Programs have been developed which utilize these standard data sets as input and which can perform a number of functions such as data checking, data analysis, plotting of level schemes, printing, *etc.* All drawings for the *Nuclear Data Sheets* are produced by the computer.

Present efforts are well underway to *redefine* the content of *Nuclear Data Sheets* so that the *Sheets* will include only such information as is contained in the Data File. The text pages of *Nuclear Data Sheets* will then be prepared directly from the computer file (ENSDF) just as is the case now with drawings.

Selective retrieval from the Data File can be used to prepare special lists or tape copies of special classes of data, *e.g.*, absolute photon intensity from radioactive decay (where normalization factors are known), energy and relative intensity of photons from neutron capture. It will also be possible to prepare directly from the ENSDF various types of tabulations, *e.g.*, listings of gamma rays by energy, intensity, half-life, isotope, *etc.* In addition, searches can be made to examine trends in selective nuclear properties.

Decay Data for Biomedical and Environmental Usage

As indicated above, with the assistance of Marian Kowalski, who was working under the Great Lakes College Association Program, a computer program has been developed which uses the information contained in standard ENSDF data sets as input, and in conjunction with existing programs for calculating fluorescence yields, conversion coefficients, average beta energies, *etc.*, generates tabulations of radiative particles, *i.e.*, energies and absolute intensities. The latter then serve as the input to existing programs used to calculate biological dose (*e.g.*, at the Information Center for Internal Exposure at ORNL). The NDP programs are written so as to propagate the uncertainties involved. Sample data sets for radioactive decays are shown in Fig. 1. An intensity cutoff limit is built into the program and can be chosen to suit the needs of the user.

Revised Mass-Chain Compilations

Mass chains revised during calendar year 1974 are as follows:

A = 62, H. Verheul[8]
A = 63, R.L. Auble
A = 64, R.L. Auble
A = 68, M.B. Lewis
A = 73, K.R. Alvar[9]
A = 99, L.R. Medsker[9]
A = 103, D.C. Kocher
A = 105, F.E. Bertrand

[8]Consultant.
[9]Nuclear Information Research Associate (NIRA).

199AU B- DECAY			$T_{1/2}$ = 3.139 D 7
Type		Radiations Energy (keV)	Intensity (%)
Auger-L		7.6	23.4 18
ce-L- 1		34.989 5	2.8 3
ce-MNO- 1		46.266 5	0.87 9
Auger-K		53.8	0.6 4
ce-K- 2		75.268 10	11.8 6
ce-K- 3		125.0977 8	6.9 8
ce-L- 2		143.531 10	18.4 10
ce-MNO- 2		154.808 10	6.4 4
ce-L- 3		193.3607 10	1.29 15
ce-MNO- 3		204.6384 11	0.41 5
β- 1	max	250.0 10	
	avg	67.40 20	23.0 20
β- 2	max	292.0 10	
	avg	82.50 20	70 4
β- 3	max	453.0 10	
	avg	133.0 10	7.0 10
total β-			
	avg	82.6 7	100 5
X-ray L		10	14.3 14
γ 1		49.828 4	0.32 3
X-ray $K\alpha_2$		68.8950 20	5.2 4
X-ray $K\alpha_1$		70.8190 20	8.9 5
X-ray Kβ		80.3	3.92 24
γ 2		158.370 10	40.0 20
γ 3		208.2	9.1 10

58CO EC-DECAY			$T_{1/2}$ = 70.8 D 1
Type		Radiations Energy (keV)	Intensity (%)
Auger-L		0.67	116.3 13
Auger-K		5.62	49.3 7
ce-K- 1		803.638 20	0.0298 10
β+ 1	max	475 3	
	avg	201.0 20	15.00 5
X-ray L		0.7	0.36 12
X-ray $K\alpha_2$		6.39084 3	7.77 25
X-ray $K\alpha_1$		6.40384 3	15.3 4
X-ray Kβ		7	3.10 10
γ 1		810.750 20	99.450 10
γ 2		863.940 20	0.680 10
γ 3		1674.73 4	0.520 10

Fig. 1. Decay data sets from the Nuclear Data Project's Evaluated Nuclear Structure Data File (ENSDF).

A = 106, F.E. Bertrand
A = 116, G.H. Carlson,[9] W.L. Talbert, Jr.,[10] and S. Raman
A = 130, H.R. Hiddleston[9]
A = 133, E.A. Henry[9]
A = 135, E.A. Henry[9]
A = 136, R.L. Bunting[9]
A = 139, L.R. Greenwood[9]
A = 140, L.K. Peker,[11] V.M. Sigalov,[11] and Yu.I. Kharitonov[11]
A = 143, J.F. Lemming[9]
A = 145, T.W. Burrows[9]
A = 146, T.W. Burrows[9]
A = 158, J.K. Tuli[9]
A = 160, J.K. Tuli[9]
A = 161, J.K. Tuli[9]
A = 166, A. Buyrn[9]
A = 171, D.J. Horen and B. Harmatz
A = 173, B. Harmatz and D.J. Horen
A = 178, L.R. Greenwood[9]
A = 182, M.R. Schmorak
A = 185, Y.A. Ellis
A = 186, M.R. Schmorak
A = 187, Y.A. Ellis
A = 189, M.B. Lewis

Recent References

Recent References is published three times a year as part of *Nuclear Data Sheets*. These contain an index to nuclear structure data listed first by mass number, followed by a section which tabulates references according to specific nuclear reactions studied. Issues published during calendar year 1974 are as follows:

Recent References (September 1973-December 1973), R.N. Dietrich, W.B. Ewbank, F.W. Hurley, and M.R. McGinnis

Recent References (January 1974-April 1974), R.L. Auble, W.B. Ewbank, F.W. Hurley, M.J. Martin, and M.R. McGinnis

Recent References (May 1974-August 1974), W.B. Ewbank, R.L. Haese, F.W. Hurley, and M.R. McGinnis

Reaction List for Charged-Particle-Induced Nuclear Reactions, Cross-Section Data File

A *Reaction List* for charged-particle-induced nuclear reactions has been prepared from the journal literature for the period from July 1973 through September 1974, and has been submitted for publication. Each published experimental paper is listed under the target nucleus in the nuclear reaction with a brief statement of the type of data in the paper. The nuclear reaction is denoted by A(a,b)B, where $M_a \geq$ (one nucleon mass). There is no restriction on energy. Nuclear reactions involving mesons in the outgoing channel are not included. Theoretical papers which treat directly with the analysis of nuclear reaction data and results are included in the *Reaction List*. These reaction lists, which were originally published in *Nuclear Data Tables A*, appear in *Atomic Data and Nuclear Data Tables*, a journal published by Academic Press. The cross-section data file has been maintained.

---

[10]Ames Laboratory, Ames, Iowa.
[11]Leningrad Institute of Nuclear Physics, Gatchina, USSR.

Supportive Activities to the NIRA Program

The NIRA Program has not yet been completed officially. At the conclusion of calendar year 1974, the Project was still processing (or expecting to receive) work from 15 of the original 21 NIRA's assigned to prepare mass-chain compilations. The number of such compilations still outstanding amounts to about 35, of which 11 are well into the production process. In addition to providing reference lists, Project staff have participated by performing reviews and in a number of cases by acting as coauthors.

Indexes to Nuclear Structure Literature

Complete, cumulated files of nuclear structure references are maintained at the NDP so the Project can answer inquiries about the current status of an experiment. The files are arranged according to nucleus, reaction, and type of measurement for fast and efficient response.

A portion of the reference file has been prepared for testing through the RECON network. When the complete file is placed on RECON in February 1975, it will be possible for any user at one of the 27 RECON sites (within the USA) to search the cumulated indexed reference files of the Nuclear Data Project.

Additional Services to the Nuclear Physics and Applied Communities

A. A Few Examples of Applied Uses of Large Quantities of NDP Products

Photon dosimetry calculations for accelerator, CTR, and fast breeder applications - Neutron Physics Division, ORNL

Data for internal dose calculation - Information Center for Internal Exposure, ORNL

Decay data for reactor heating calculations - Chemical Technology Division, ORNL

E_γ, I_γ for radioactive decay - W. Bowman and K. MacMurdo, Savannah River; published in *Atomic Data and Nuclear Data Tables* 13, 89 (1974)

National Bureau of Standards - M.J. Berger for dose calculations published in the *Journal of Nuclear Medicine*

Mossbauer Effect Data Index - J.G. Stevens and V.E. Stevens, references and evaluated data

Charged-Particle Nuclear Data Group (Karlsruhe) - H. Munzel *et al.*

French Table of Evaluated Radionuclide Decay Scheme Parameters - J. Blachot *et al.*

ENDF Fission Product Decay File - BNL

Table of Isotopes - LBL

Nuclear Data and Measurements Series - ANL

B. Current Awareness Services (one-month intervals)

1. Approximately 300 lists of newly identified references were sent to the 23 Nuclear Information Research Associates (NIRA's) still active during 1974.

2. New references for A < 20 - F. Ajzenberg-Selove (University of Pennsylvania)

C. Regular Reference Services (four-month intervals)

1. A magnetic-tape copy of *Recent References* was sent to the Table of Isotopes Project.

2. Preprint copies of *Recent References* were sent to:

a) B.S. Dzhelepov (Leningrad)
b) L.K. Peker (Leningrad)
c) C. van der Leun (Utrecht)
d) A.H. Wapstra (Amsterdam)
e) H. Ikegami (Tokyo)
f) E.G. Fuller (NBS, Washington)
g) F. Ajzenberg-Selove (Univ.Pa.)
h) C.M. Lederer (Berkeley)
i) S. Pearlstein (BNL)
j) J.A. Harvey (ORNL)
k) P.H. Stelson (ORNL)
l) C.D. Moak (ORNL)
m) E.E. Gross (ORNL)
n) E. Eichler (ORNL)

3. New references for special topics (from inverted index) were sent to:

a) Nuclear Reaction Q-Values - A.H. Wapstra (Amsterdam)
b) μ, Q - G.H. Fuller (NBS, Washington)
c) μ, Q - V. Shirley (Berkeley)

D. Special Reference Requests during 1974

Three-body problems - Y.E. Kim (Los Alamos), F. Roig (Manchester), Shin Nan Yang (Brookhaven), B. Sundqvist (Uppsala)

Th, Pa, U - L.J. Nugent (Berkeley)

B(E2) for even nuclei - S. Raman and P.H. Stelson (ORNL)

Gamma-ray transition probability - G.S. Goldhaber (Brookhaven)

^{12}C, ^{16}O (p,p′), (α,α′) - F. Wong (Oak Ridge)

$^{117\text{-}125}Sb$, $^{117\text{-}124}Sn$ - C.H. Johnson (Oak Ridge)

Level $T_{1/2}$ in Ni, Cu, Zn, Ga - S. Roodbergen (Amsterdam)

Several rare-earth isotopes - F.C. Von der Lage (Oak Ridge)

All measured $T_{1/2}$ - G.N. Rao (Kanpur, India and Berkeley)

Gamma-ray mixing ratios - K.S. Krane (Berkeley)

$^{112\text{-}115}Sb$, Te - M.E.J. Wigmanns (Amsterdam)

$T_{1/2}$ for fission fragments - L. Hjärne (Malmö, Sweden)

Proton-induced reactions - J. Rapaport (Ohio)

Nuclear fp-shell studies - K. Bhatt (Ahmedabad, India)

^{111}Ag, Cd - S. Sharma (Udaipur, India)

Superallowed β-decay - S. Raman (Oak Ridge)

(p,n) reactions - K. Heinbach (Chicago)

Inter-nuclear fields in Se - W.C. Koehler (Oak Ridge)

E. Adjusted Nuclear Masses

1. Magnetic tape copies - E. Sutter (Argonne), D. Hendrie (Berkeley), G.T. Emery (Indiana), L. Friesen (Aerospace Corp.)
2. Computer listings - J.L. Weil (Kentucky), G. Blum (Bettis Atomic Power Lab)

F. Special Data Requests during 1974

1. Reaction data - Cross-section data were supplied on request to the following institutions: Lawrence Livermore Laboratory, Battelle Pacific Northwest Laboratories, DCTR of AEC, NASA, Air Force Weapons Laboratory at Albuquerque, New England Nuclear, Naval Research Laboratory, Fusion Energy Institute, Sandia Laboratories, and California Institute of Technology.

   The complete *Reaction List* and cross-section data files were provided on magnetic tape to Livermore Laboratory. The *Reaction List* file has received wide use at Livermore where several groups are routinely preparing specialized reaction lists based on the indexing available in the *Reaction List* file. Because of the enthusiastic response to this file, Livermore has requested a copy on magnetic tape of the annual update to the *Reaction List* file.

2. Structure information

   $T_{1/2}$ (^{10}Be) - W.S. Lyon (Oak Ridge)

   n-p mass difference - R.L. Cohen (Rockwell International)

   ^{4}He mass - S. Austin (Michigan State)

   γ/α in ^{210}Po decay - J. Ramberg (3M Company)

   Absolute I_γ in ^{212}Pb decay - D. Olsen (Idaho Falls)

   Levels with $T_{1/2}$ < 10 ps, E_γ < 200 keV - M.L. Weiss (Livermore)

   Level $T_{1/2}$ in ^{75}As - G.H. Fuller (National Bureau of Standards)

   Levels in ^{139}Ba - A.R. Musgrove (Australian AEC)

   ^{181}Hf, ^{181}Ta decay and others - P. Schmidt (Bell Laboratories)

   A = 186 - A.B. Smith (Argonne)

   $^{131-136}$I decay data - F. Patti (Burns & Rowe, Inc.)

   Decay data for monitoring systems for nuclear power reactors - R.E. Sinclair (Nuclear Data, Inc.)

G. Special Computer Program Services during 1974

Conversion coefficients for Mossbauer transitions - J. Stevens (North Carolina)

E_γ to level energy by least-squares - R.G. Helmer (Idaho Falls)

H. Data Bank Services

Standard data sets for several β^+-decay isotopes $100 < A < 130$ - F.F. Dyer (Goddard Space Flight Center)

I. Miscellaneous Services

An average of 1-2 persons per week (ORNL staff or visitors) visit the Nuclear Data Project Library either to find a reference or data value or to read a report or an article that is not available elsewhere.

Research Reports

Most members of the NDP participate to a small degree ($\lesssim$20%) in experimental research, mainly at accelerator facilities at ORNL. The titles of work resulting therefrom are given below.

Studies of the Giant Resonance Region of the Nuclear Continuum via Inelastic Proton Scattering - F.E. Bertrand, E.E. Gross, D.C. Kocher, and E. Newman

Study of the Giant Resonance Region and Bound States in ^{58}Ni Using Inelastic Scattering of Polarized Protons - D.C. Kocher, F.E. Bertrand, E.E. Gross, and E. Newman

Isolation of the Giant Quadrupole Resonance in ^{58}Ni via Deuteron Inelastic Scattering - F.E. Bertrand, E.E. Gross, D.C. Kocher, E. Newman, and C.C. Chang

Qxygen Diffusion in β-Zircaloy - R. Perkins, F.E. Bertrand, and M.J. Saltmarsh

Isospin Makeup of Giant Resonances - C.D. Goodman, F.E. Bertrand, D.C. Kocher, and R.L. Auble

"Anomalous" Ground States in the Neutron-Deficient $171 \leq A \leq 181$ Region - B. Harmatz, D.J. Horen, and Y.A. Ellis

^{131}Ba Levels by the ^{122}Sn(^{12}C,3nγ) Reaction - J. Gizon, A. Gizon, and D.J. Horen

Study of Giant Resonances with ^{3}He Ions - D.J. Horen, J. Arvieux, M. Buenerd, A.J. Cole, P. de Saintignon, and G. Perrin

Inelastic Scattering of Polarized Protons by ^{12}C - G. Perrin, J. Arvieux, M. Buenerd, J. Cole, J.L. Durand, D.J. Horen, P. Martin, C. Perrin, and P. de Saintignon

OHIO UNIVERSITY

A. TANDEM ACCELERATOR PROGRAM.

1. High Energy Neutron Scattering

a. Neutron Elastic Scattering at 11 MeV.* (J.C. Ferrer, J.D. Carlson and J. Rapaport)

Elastic scattering of 11 MeV neutrons has been obtained for the following natural samples: Mg, Al, S, Ca, V, Mn, Fe, Co, Ni, Nb, In, Ho, Ta, Pb, Bi as well as the following enriched isotopes ^{92,96,98,100}Mo, ^{120}Sn and ^{206}Pb. The D(d,n)^{3}He reaction provided the required neutrons. Data between θ_{lab}=15° and 155° in steps of $\Delta\theta$=5° has been obtained. A pulsed beam time of flight technique using five large area liquid scintillators simultaneously and a monitor was employed. The energy resolution was 200-300 keV. Absolute normalization was obtained both by measurement of the 0° flux and by the observation of scattered neutrons from a CH_2 sample, at several angles. Extracted yields are in the process of being corrected for dead time, attenuation, detector efficiency, multiple scattering and fine geometry.

---

* Work supported in part by the National Science Foundation.

b. 26 MeV Neutron Elastic Scattering.* (J.D. Carlson, J. Rapaport)

Neutron angular distributions have been obtained at 26 MeV using the T(d,n) reaction as a neutron source. Data over the same angular range as in a) has been obtained for the following natural samples: Al, Fe, Nb, Pb as well as for the following enriched samples: ^{92,96,98}, ^{100}Mo and ^{120}Sn. The extracted yields are in the process of being corrected by attenuation, multiple scattering and finite geometry.

---

* Work supported in part by the National Science Foundation.

c. Neutron Inelastic Scattering on Sulphur.* (Bainum, Carlson, Ferrer, Finlay, and Rapaport)

Inelastic Scattering of 11 and 26 MeV neutrons on natural sulphur has been measured between the angle of 15° and 145°; the data were taken using a time of flight spectrometer with resolution less than

700 keV, with a 6.61 m flight path and using the D(d,n) and T(d,n) neutron source reactions. The data for the 2^+ state at 2.24 MeV and for the 3^- state at 5.01 MeV in ^{32}S, once analyzed, will be compared to DWBA calculations.

---

* Work supported in part by the National Science Foundation.

d. Lane Model analysis of Nucleon Elastic and Quasielastic Scattering from ^{96}Mo.* (J.D. Carlson, J. Ferrer and J. Rapaport)

Neutron elastic scattering cross sections have been measured for ^{96}Mo at 11 MeV. The results have been analyzed in terms of the generalized nucleon optical model due to Lane along with previously measured proton elastic[1] and (p,n) quasielastic[2] scattering cross sections on the same nuclide at 23 MeV. The neutron energy in the (n,n) work was chosen to equal the energy of the outgoing neutron in the (p,n)-IAS reaction.

---

* Supported in part by the National Science Foundation.

1 R.I. Bentley, J.D. Carlson, H.W. Fielding, D.A. Lind and C.D. Zafiratos, unpublished.

2 R.I. Bentley, et al., Phys. Rev. Lett. 27 (1971) 1081.

e. 11 MeV Neutron Elastic Scattering on T=0 Nuclei: ^{32}S and ^{40}Ca. J.C. Ferrer, J.D. Carlson and J. Rapaport.

The Ohio University 11 MeV Tandem was used to produce 11 MeV neutrons by means of the $D(d,n)^3He$ reaction. Elastic scattering on ^{32}S and ^{40}Ca was measured between 15° and 155° with and energy resolution less than 300 keV. The analysis of the data within the frame of an optical model DWBA will be presented. The neutron parameters compared with those obtained in proton elastic scattering at the same energy should provide an experimental determination of the Coulomb correction term, usuall quoted as $0.4ZA^{-1/3}$. (To be presented at the APS Washington meeting, April '75)

---

2. Unbound States of ^{27}Al from the Reactions: $^{26}Mg(p,n)^{26}Al$ and

^{23}Na(α,n)^{26}Al.* (G. Doukellis and J. Rapaport)

Unbound states in ^{27}Al between 13.0 and 15.0 MeV excitation energy were studied by means of the ^{26}Mg(p,n)^{26}Al and ^{23}Na(α,n)^{26}Al reactions. The Ohio University 11 MeV Tandem Van de Graaff was used to provide protons between 5.2 and 7.0 MeV, in 30 keV steps. The outgoing neutrons populating the first three states of ^{26}Al were measured at six angles by means of a pulsed-beam-time-of-flight spectrometer. The excitation functions and angular distributions, thus measured were fitted to a multilevel multichannel R-matrix code, MULTI.[1] Preliminary spin-parity assignments and partial widths, based upon those fits will be presented for the observed resonances. (To be presented at the APS Washington Meeting April '75)

---

* Supported in part by the National Science Foundation

1 D.L. Lellin, H. Weller, private communication.

3. Level Structure of ^{76}As.* (J.F. Lemming,** J. Rapaport, A.J. Elwyn.†)

The energy-level structure of ^{76}As has been studied by the ^{75}As(d,p) reaction with 12.0 MeV incident deuterons. Eighty-seven energy levels up to 2.5 MeV have been identified. The angular distributions for thirty-nine of the observed transitions are compared with distorted-wave Born approximation calculations. Angular momentum transfers are determined and spectroscopic strengths are deduced from the data. The results are compared with shell-model sum rules and with (d,p) results on N=42 isotones. Possible spin values are assigned for some of the levels based on the present results, (n,γ), (p,n) and (p,nγ) studies. (Abstract of a paper to appear in Nucl. Phys.)

---

* Work performed under the auspices of U.S. Atomic Energy Commission.

** Nuclear Information Research Associate. Work supported by NSF through the NAS-NRC Committee on Nuclear Science.

† Argonne National Lab.

4. Anomalies in the ^{72}Ge(α,n)^{75}Se Reaction Near Isobaric Analog Resonances in ^{76}Se.* (Elwyn,** Monahan,** Lemming, Rapaport, and Sample)

Anomalies in the excitation function of the reaction $^{72}Ge(\alpha,n)^{75}Se$ are compared with isobaric analog resonances observed in the $^{75}As(p,n)^{75}Se$ reaction. The results are consistent with the interpretation that the same analog resonance is populated in both reactions. Since the (α,n) reaction through isobaric analog states is isospin forbidden in both entrance and exit channels, these results imply some isospin-breaking mechanism for the excitation of analog resonances via alpha and/or neutron channels. (Published in Phys. Rev. C10 (1974) 1939.)

---

* Work performed under the auspices of the U.S. Atomic Energy Commission.

** Argonne National Laboratory.

5. Low Lying States of ^{96}Tc.* (Doukellis, McKenna, Finlay, Rapaport, and Kim.**)

The $^{96}Mo(p,n)$ and $^{96}Mo(p,n\gamma)$ reactions have been studied for proton energies between 3.8 and 5.5 MeV. Energy levels in ^{96}Tc up to 632 keV excitation energy have been determined. Possible spin and parity assignments are given for several levels based on the neutron enhancement and angular distributions observed on and off resonance of the $5/2^+$ isobaric analog state in ^{96}Tc, as well as the observed γ-yields. The first excited state reported at 34 keV was found to be a close doublet only 0.8 keV apart. The observation of this doublet in the (p,n) reaction was used to determine the ground state Q-value Q= -3.760±0.010 MeV. (Published in Nucl. Phys. A229 (1974) 47.

---

* Work supported in part by the U.S. Atomic Energy Commission.

** Oak Ridge National Lab.

6. Masses of Technetium Isotopes.* (J.R. Comfort, R.W. Finlay and P.T. Debevec**)

The masses of $^{96,97,98}Tc$ have been determined by studying the (p,n) reaction on $^{96,97,98}Mo$ at E_p = 4.0-5.0 MeV and the (^{3}He,d) reaction on $^{96,97}Mo$ at $E_{^3He}$ = 19.0 and 23.0 MeV. Time-of-flight techniques were used for the (p,n) measurements at the Ohio University Tandem Van de Graaf laboratory. The (^{3}He,d) reactions were studied at Argonne National Laboratory and the University of Pittsburgh. Reaction Q-values and the implied mass excesses are given in Table A-6.

TABLE A-6. The Q values for (p,n) and (^{3}He,d) reactions leading to technetium isotopes, and the mass excesses for the residual nuclei. The mass excesses are revised from the 1971 atomic mass compilation (Ref. 1).

Reaction	Q value (MeV)	Mass Excess (MeV)
^{96}Mo(p,n)^{96}Tc	-3.760(10)[a]	-85.820(10)
^{96}Mo(p,n)^{96}Tc	-3.755(6)[b]	-85.825(6)
^{97}Mo(p,n)^{97}Tc	-1.102(6)	-87.221(6)
^{96}Mo(^{3}He,d)^{97}Tc	0.229(8)[c]	-87.230(8)
	0.220(8)[d]	-87.221(8)
^{98}Mo(p,n)^{98}Tc	-2.458(10)	-86.432(10)
^{97}Mo(^{3}He,d)^{98}Tc	0.680(8)	-86.420(8)

[a] Reference 2.
[b] Reference 3.
[c] Argonne data.
[d] Pittsburgh data.

---

* Phys. Rev. C10 (1974) 1236.

** Physics Division, Argonne National Laboratory.

1 A.H. Wapstra and N.B. Gove, Nucl Data A9 (1971) 265.

2 G. Doukellis et al., Nucl. Phys. A229 (1974) 47.

3 R.G. Kruzek et al., Bull. Am. Phys. Soc. 17 (1972) 514; but see also Nucl. Data B8 (1972) 615.

7. Neutron Radiative Capture Pb(n,γ). (C.E. Brient and K.R.S. Devan)

Neutron capture gamma rays have been measured using a D(d,n) neutron source at E_n = 5.7 MeV. Spectra were obtained with pulsed neutron beams and with direct unpulsed beams to determine the response of 9 inch by 9 inch annular triple crystal NaI spectrometer to the direct neutrons. A 4 inch plastic scintillator was used for both neutron shielding and an anti-coincidence shield for escaping radiation from the central NaI crystal. The gamma rays from Pb^{206,207} and ^{208} were observed with a total

crystal ratio of 2 X 10^{-3} at a total count rate of 5 X 10^{4} per second. The time response from the time to amplitude converter was flat with a gamma peak only, indicating no direct neutron contributions. These measurements indicate that the detector is quite suitable for these measurements and shielding and anti-coincidence modifications are now in progress.

B. A-CHAIN COMPILATIONS

1. Nuclear Data Sheets for A=81 and A=82 (J. Lemming* and J. Rapaport)

Level schemes and decay characteristics have been compiled for all nuclei with mass number 81 and 82. Experimental data, adopted values, comparisons with theory and arguments for spin and parity assignments are indicated.

The adopted level schemes and decay properties are based on data received before August 1974. (To be published)

---

* Nuclear Information Research Associate. Work supported by the National Science Foundation through the National Academy of Sciences-National Research Council, Committee on Nuclear Science.

RENSSELAER POLYTECHNIC INSTITUTE

A. NEUTRON DATA APPLICATIONS - EXPERIMENTAL

1. KeV Capture Cross Section of ^{242}Pu. (R. W. Hockenbury, A. J. Sanislo and N. N. Kaushal)

The neutron capture cross section of ^{242}Pu has been measured from 5 to 70 keV. The high-low bias method was used to distinguish between capture and fission events. Transmission experiments were also made in the resonance region. The high spontaneous fission activity of the ^{242}Pu sample presented difficulties in the normalization of the capture cross section data. A normalization method was developed using the absorption and transmission data from six resonances. This normalization is consistent with that obtained by using published results of ^{242}Pu transmission measurements. The theory of Lane and Lynn was used to calculate the keV capture cross section for comparison to our experimental results. Using an average s-wave radiation width of 22 meV, an s-wave strength function of 1.16×10^{-4} and our measured capture cross section, we have determined the s-wave and p-wave contributions to the ^{242}Pu capture cross section below 70 keV.

2. Resonance and KeV Neutron Cross Sections of ^{145}Nd, ^{149}Sm, and $^{101, 102, 104}$Ru. (R. W. Hockenbury, W. R. Koste, and R. A. Shaw)

Neutron capture and transmission measurements have been made on separated isotopes of ^{145}Nd, ^{149}Sm, and ^{101,102,104}Ru from 20 eV to 150 keV using the RPI Linac. The observed level spacings are 17.9 ± 1.9, 109.8 ± 15.7, and 125.1 ± 19.1 eV for ^{101,102,104}Ru. For ^{145}Nd and ^{149}Sm, the level spacings are 14.4 ± 2.0, and 2.7 ± 0.3 eV, respectively. The ratio of capture cross sections of the Ru isotopes between 20 and 60 keV is approximately 11:2.5:1 for masses 101, 102 and 104, respectively. Resonance parameters and keV capture cross sections will be presented for these five isotopes.

3. Capture Cross Sections of ^{103}Rh, ^{105}Pd, ^{151}Eu and ^{153}Eu in the keV Region (R. W. Hockenbury, H. Knox and N. N. Kaushal)

The first and fifth most important fission products in the LMFBR are ^{105}Pd and ^{103}Rh. The isotopes ^{151}Eu and ^{153}Eu are of interest in reactor control applications as well. Capture cross section measurements have been made on four nuclei from 20 eV to 90 eV. Capture data in the resolved resonance region are combined with our own transmission data to obtain a consistent capture normalization which

can be more precise than that of conventional methods. For these experiments, the statistical uncertainty of the normalization is ± 4% for ^{151}Eu, ^{153}Eu and ^{105}Pd, and ± 8% for ^{103}Rh. The statistical uncertainty of the keV capture cross section point data is about ± 4%. The s and p wave capture components in the keV region have been determined from our experimental results. The information derived from these measurements then is the measured keV capture cross section and the average s and p wave parameters $\bar{\Gamma}_\gamma$, S^o and S^1.

4. The Rensselaer Intense Neutron Spectrometer
(R. C. Block, R. W. Hockenbury, J. R. Valentine, R. E. Slovacek, E. B. Bean, and D. S. Cramer)

The Rensselaer Intense Neutron Spectrometer (RINS) is obtained by driving a 75-ton lead slowing down spectrometer with the intense pulsed neutron source from the RPI 100-MeV electron Linac. For the same Linac beam power, the RINS system produces a usable neutron flux which is $10^3 \sim 10^4$ times greater than that obtained with a conventional time-of-flight spectrometer. RINS is being used to measure extremely small neutron cross sections, such as (n, α) and subthreshold fission. Figure A-1 illustrates the counting rate vs. slowing-down time for alpha particles detected from the ^{145}Nd (n,α) reaction. A 7.2 mgm sample of $^{145}Nd_2O_3$ and a 2 cm^2 diffused-junction silicon detector were used for this measurement. The data were obtained in 2-1/2 hours with 330 watts of electron beam power on the neutron target. The two lowest energy resonances are clearly resolved with the intrinsic spectrometer resolution of $dE/E \approx .33$.

The ^{238}U (n,f) cross section has been measured from ≈ 1 eV to 35 keV with RINS. Ionization chambers containing ≈ 0.8g of ^{238}U (4ppm ^{235}U) were used in the measurement. The fission widths of the 6.7, 21 and 37 eV resonances were measured as (10 ± 5),(70 ± 30) and (8 ± 6) neV respectively. The cross section integrated over the two subthreshold groups at 720 and 1200 eV and the average cross section from 10 to 30 keV are in agreement with our previous measurement[1]. The fission width at 6.7 eV is 20 times smaller than the earlier reported upper limit[2], and these fission widths are consistent with the (30 ± 50) neV average width for the resonances between 37 and 327 eV[3]. The net ^{238}U fission counts per μsec channel width are plotted from 1.5 eV to 35 keV in figure A-2.

---

[1]Phys. Rev. Lett. 31, 247 (1973).

[2]Leonard & Odegaarden, Bull. Am. Phys. Soc. 6, 8 (1961).

[3]Silbert & Bergen, Phys. Rev. C4, 220 (1971).

5. Measurement of Neutron Total Cross Sections of Sodium Near Minima* (P. H. Brown, B. L. Quan, J. J. Weiss, R. C. Block and R. W. Hockenbury)

Because of the large quantities of sodium in an LMFBR it is important that the neutron total cross section (σ_t) of Na is known to a high degree of precision. The deep minima in σ_t are especially important since it is these minima which determine the characteristics of a deeply penetrating flux.

We have performed thick-sample Na neutron transmission measurements using the filtered-beam technique[1,2] to determine these minima with high precision. A Na filter 62.2 or 93.3 cm thick is placed in a collimated neutron beam and a 31.1 cm Na sample is cycled in and out of the beam. The transmitted beam is detected by a neutron detector located at the RPI Linac 100 m flight path. The thick filter results in a filtered beam containing mainly neutrons with energies near the deep minima.

Table 1 shows a comparison between ENDF/B IV[3] and our data for the minima at 0.297, 0.521, 1.680, 1.885 and 3.075 MeV. No resolution corrections have been applied to the data, although the resolution of 0.15 nsec/m and the identical results for two different filter thicknesses indicates that the minima are fully resolved.

The results shown in Table 1 agree with ENDF/B IV to within experimental errors. Figure A-3 shows our data along with ENDF/B IV near the minimum at 297 keV. This figure shows that our data covers a much finer mesh of neutron energies than does ENDF/B IV. Thus, while ENDF/B IV may be considered accurate at an actual minimum value, it is not as useful as our data for determining the detailed shape of a minimum which is, perhaps, as important as the actual minimum for determining the characteristics of the flux emerging from a thick Na blanket. Figure A-4 shows the transmission through 1 m of Na as determined here and by ENDF/B IV. A preliminary analysis shows the area under our transmission data to be 46% greater than the area under the ENDF/B transmission data..

The analysis of data for the other minima and final area and shape analysis of all minima is proceeding.

*Sponsored by US AEC Contract AT(11-1)-2479

1. R. C. Block, N. N. Kaushal, R. W. Hockenbury, Proc. ANS Topical Meetings on New Developments in Reactor Physics and Shielding, Kiamesha Lake, New York, CONF-72091, 1107 (1972).
2. K. A. Alfieri, R. C. Block, P. J. Turinsky, Nucl.Sci. Eng. 51,25 (1973).
3. ENDF/B Version IV, MAT1156, National Neutron Cross Section Center, Brookhaven National Laboratory, Upton, New York, (1974).

TABLE 1

Minima E_n (MeV)	RPI* (b)	ENDF/B IV (b)
0.297	1.25 ± 0.05	1.20
0.521	1.97 ± 0.05	1.96
1.680	1.88 ± 0.05	1.86
1.885	1.74 ± 0.04	1.72
3.075	1.57 ± 0.04	1.58

*Combined results for 62.2 cm and 93.3 cm thick sodium filter measurements, except 3.075 MeV which is for 93.3 cm filter only.

B. NEUTRON DATA APPLICATIONS - THEORETICAL

1. Processing Nuclear Data with Deep Minima (M. Becker)

It has been determined that standard data processing code procedures, which utilize inverse cross-section weighting, can lead to serious excessive influence of minima on group constants for single materials. Serious errors in the prediction of spectra measured in iron at RPI have been attributed to this phenomenon. In the B_N approximation to the transport equation, it can be shown that the flux approaches a finite limit even when the cross-section tends to vanish. Weighting spectra can be formulated accounting for this observation. This topic is discussed more fully in a forthcoming issue of Nuclear Science and Engineering.[1]

2. Interactive Graphics and Data Adjustment (A. Parvez, M. Becker)

Interactive graphics is being utilized to help identify cross-section uncertainties from discrepancies between calculation and measurement for integral experiments. The combination of an interactive analysis system developed at RPI to incorporate a large number of options and adjustments[2] and of a generalized continuous slowing down theory which permits rapid and reasonably accurate predictions[3] has made for a flexible and useful system. Recent modifications have been in the direction of permitting direct data adjustment rather than

1. M. Becker, "Influence of Deep Minima on Multigroup Cross-Section Generation," Nucl. Sci. Eng. (in press).

adjusting continuous slowing down theory parameters and then inferring data uncertainties. The current system leads to more specific evaluations.

2. M. Danchak, W. R. Moyer, M. Becker, "The Rensselaer Interactive Graphics Analysis System," Trans. Am. Nucl. Soc. 18, 159 (1974).

3. M. Danchak, M. Becker, W. R. Moyer, "Utilization of Interactive Graphics and Continuous Slowing Down Theory," Trans. Am. Nucl. Soc. 19, 175 (1974).

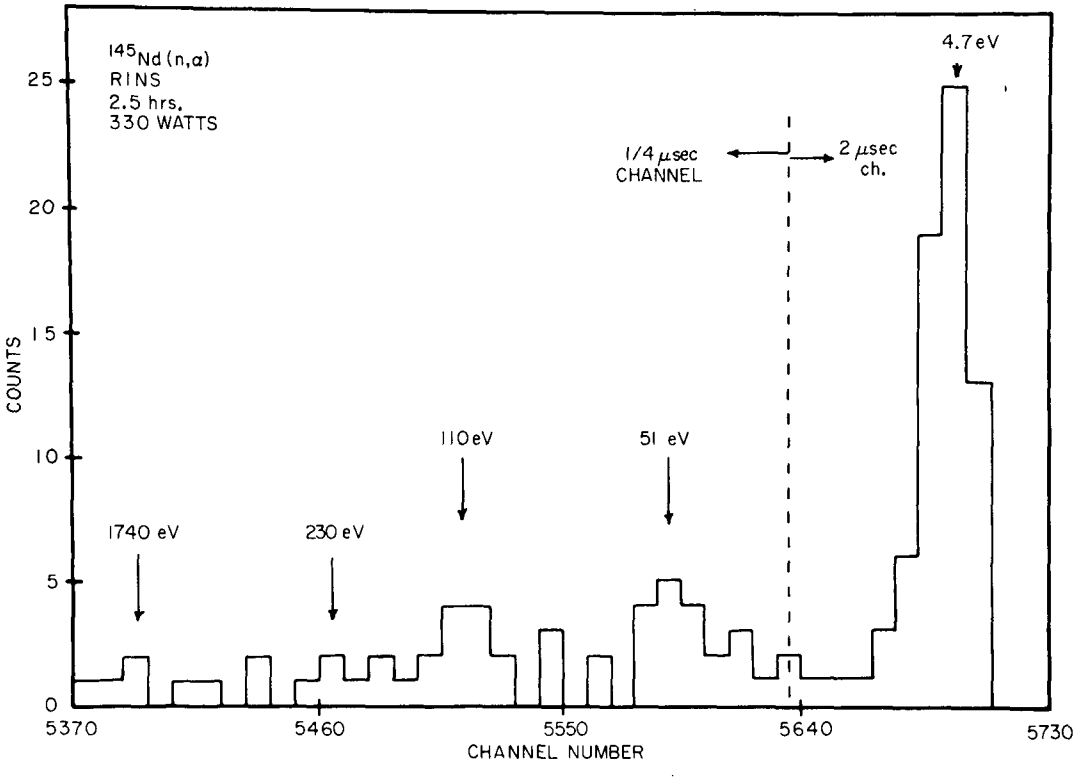

Fig. A-1 The $^{145}Nd(n, \alpha)$ counts vs slowing down time.

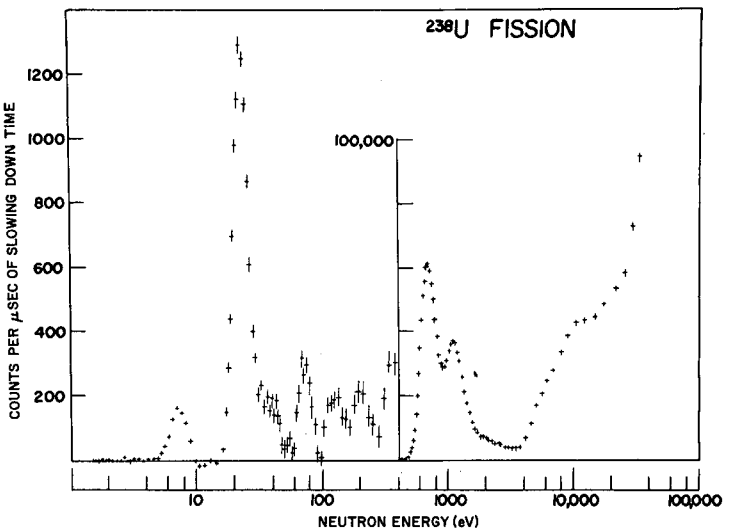

Fig. A-2 The $^{238}U(n,f)$ counts per μsec slowing down time vs neutron energy.

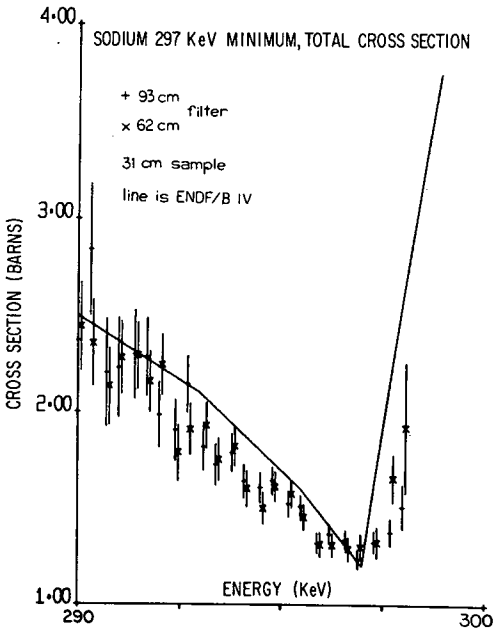

Fig. A-3 The Na neutron total cross section near the 297 keV minimum.

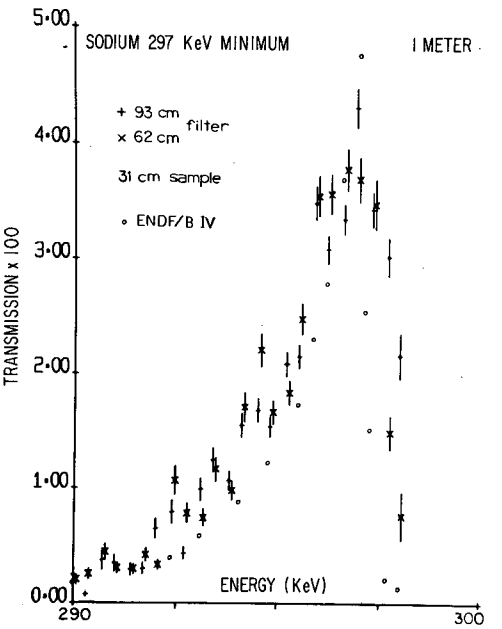

Fig. A-4 Neutron transmission through 1 m of Na near the 297 keV minimum.

TRIANGLE UNIVERSITIES NUCLEAR LABORATORY

A. NEUTRON AND FISSION PHYSICS

1. Fast Neutron Differential Cross Sections, 9-15 MeV (D. W. Glasgow, F. O. Purser, C. R. Gould, D. E. Epperson, H. H. Hogue, G. Glendenning, E. G. Bilpuch, H. W. Newson, S. G. Buccino, P. W. Lisowski)

In support of the CTR program the Cyclo-Graaff neutron time-of-flight facility has been utilized to measure the differential elastic and inelastic cross sections for the scattering of 9-15 MeV neutrons from natural carbon (USNDC-6, Request No. 56). The measurements were performed with a high precision goniometer time-of-flight spectrometer which utilizes a heavily shielded (6000 lb. Cu and 1000 lb. $(CH_2)_x$-Li_2CO_3), precision machined, double truncated conical collimator, NE-218 liquid scintillator detectors coupled to bi-alkali photomultiplier tubes, wide dynamic range pulse shape discrimination; excellent beam optics; and an all metal, ultra clean beam transport system to obtain unusual freedom from extraneous neutron and gamma ray background.

The cross sections were measured (by using a cylindrical scatterer) at 28 angles each in 5° increments (2.5° increments at cross section minima) spanning the angular range 25-160° for E_n = 9.0, 9.2, 9.6, 10.0, 10.25, 10.74, 11.0, 11.2, 11.79, 12.0, 13.0, 14.0, 14.5 and 15.0 MeV. The data were converted to absolute cross sections by normalizing to the existing high accuracy n-p scattering cross sections. The energy dependence of the neutron detection efficiency was measured relative to the known $D(d,n)^3He$ source reaction cross sections and the n,p scattering cross sections. The experimental cross sections were corrected for the finite size and anisotropy of the primary $D(d,n)^3He$ neutron source, differences in neutron fluence for the carbon scattering sample and the polyethylene normalization sample, attenuation of the incident and scattered neutron flux density, angular resolution, and multiple scattering by Monte Carlo simulation. Relative uncertainties in the measured elastic scattering cross sections are typically 2-3% and the normalization uncertainties are 3-4%. The cross section measurements at 14 MeV were performed with 3/8" dia. x 1" long and 3/4" dia. x 1" long carbon scatterers in order to check the multiple-scattering corrections. The corrected angular distributions easily agree within statistics. The above set of measurements partially fill the 9-15 MeV carbon data set required for the proper design of prototype fusion power reactors. Since carbon is also one of the major constituents of human tissue, these cross sections are of value in transport calculations for predicting the neutron dose as a function of depth in fast neutron therapy of deep-

seated, anoxic tumors. This program will continue with measurements of the differential elastic and inelastic scattering cross sections for the scattering of 9-15 MeV neutrons from ^{9}Be and ^{6}Li both of which are required for the CTR program.

2. Resolved Neutron Total Cross Sections and Intermediate Structure (J. Clement,* B.-H. Choi,** W. F. E. Pineo, M. Divadeenam,*** H. W. Newson)

A paper entitled "Intermediate Structure: ^{28}Si" is ready for submission to Annals of Physics as Part Xd of our series "s- and p-Wave Neutron Spectroscopy." The abstract was included in our last report, TUNL-XII.

A paper on intermediate structure (Part Xc) of neutron scattering on Sr will appear in Annals of Physics 89, 555 (1975). No additional measurements and few additional R-Matrix analyses are planned. However much unpublished information is still of interest. The following additional papers are now in various stages of preparation: $^{32}S(n,n)$, $Pb(n,n)$, $^{33}S(n,n)$, $^{60}Ni(n,n)$, $^{34}S(n,n)$, $^{40}A(n,n)$, etc.

3. Averaged Cross Sections, Strength Functions, and Intermediate Structure (W. F. E. Pineo, M. Divadeenam, E. G. Bilpuch, H. W. Newson)

Part III of the series on Strength Functions and Average Cross Sections is still to appear in Annals of Physics. The abstract was in our last report.

4. Charged Particle Fission (F. O. Purser, D. E. Epperson, H. W. Newson, E. G. Bilpuch, H. W. Schmitt+)

a. Analysis of Fission Cross Section Measurements

This program has been inactive for this report period.

b. Fragment Mass and Kinetic Energy Measurements

A total of 35 fission fragment mass and kinetic energy distributions have been measured for proton induced fission of ^{235}U and ^{236}U. The measurements are concentrated in the first and second chance fission region

---

* Now at T. W. Bonner Laboratory, Rice University, Houston, Texas
** Now at Pacific Lutheran University, Tacoma, Washington
*** Now at Brookhaven National Laboratory, Upton, New York
\+ Oak Ridge National Laboratory, Oak Ridge, Tennessee

($5.0 \leq E_p \leq 13$ MeV) to allow a definitive study of the effect on measured mass and energy distributions of multi-chance fission processes. Analysis techniques developed in this energy region will be extended to mugh higher energy measurements to allow unambiguous fragment mass and kinetic energy studies as a function of the excitation energy of the fissioning nucleus.

For charged particle induced fission, the resolution obtainable from fission-fragment correlation measurements can be adversely affected by pulse-height dispersion introduced by charging of the input capacitances of the detector systems. The degree of the dispersion is beam current and geometry dependent and appears to be due to elastic and Rutherford scattered particles, other than fission fragments, intercepted by the detectors. This problem has been studied and computer analysis techniques developed to minimize its effect upon the measured masses kinetic energies.

c. Cross Section Measurements

This program has been inactive for this report period.

5. A Selectively Excited And Distorted (SEXD) Liquid Drop Model
(H. W. Newson)

It is hoped that a preprint will be available for circulation before the next meeting of the USNDC.

6. Cross-Section Measurements for $^4He(n,n)^4He$ from 8 to 16 MeV
(G. Mack,* R. C. Byrd, S. Skubic, P. W. Lisowski, R. L. Walter)

Recoil angular distribution data for ^4He contained in a high pressure gas scintillator have been measured for neutron bombarding energies from 8 to 16 MeV to provide accurate cross-section information in this energy range. From the R-Matrix analyses, on the mass-5 systems, it was evident that new information was required here. Pulsed neutron beams produced in the D(d,n) reaction provided a clean flux of neutrons for these data. Numerous tests were made to avoid problems that might exist in previously reported data.

---

* University of Tuebingen, Tuebingen, West Germany

7. Cross-Section and Polarization in (^{3}He,n) Reactions from ^{12}C and ^{13}C from 8 to 22 MeV (T. C. Rhea, R. A. Hardekopf,* P. W. Lisowski, J. M. Joyce,** R. Bass,+ R. L. Walter)

This work has been inactive but a publication on the results shall be prepared in the near future.

8. Neutron Polarizations Produced by the Breakup of Polarized Deuterons on D and ^{4}He (P. W. Lisowski, R. C. Byrd, T. B. Clegg, R. L. Walter)

The previously obtained polarization transfer coefficients $K_y^{y'}$ have been put in final form and were reported at the International Conference on Few Body Problems in Nuclear and Particle Physics at Laval University, Quebec, Canada. The data will be submitted for formal publication.

9. Transfer Polarizations Studies of $^{12}C(\vec{d},\vec{n})$ $^{28}Si(\vec{d},\vec{n})$ and $^{16}O(\vec{d},\vec{n})$ at A Reaction Angle of 0° (P. W. Lisowski, R. C. Byrd, G. Mack, T. B. Clegg, R. L. Walter)

Previously reported polarizations produced at a reaction angle of 0° were used to deduce final values of polarization transfer coefficients for $^{12}C(\vec{d},\vec{n})$ and $^{28}Si(\vec{d},\vec{n})$. Measurements for $^{16}O(\vec{d},\vec{n}_0)$ and $^{16}O(\vec{d},\vec{n}_1)$ have been made from 5 to 15 MeV and show large $K_y^{y'}$ values for the (d,n_1) group. The large $K_y^{y'}$ values for the $^{12}C(\vec{d},\vec{n})$ and $^{28}Si(\vec{d},\vec{n})$ were reported at the Atlanta meeting of the American Physical Society.

10. Neutron Scattering Studies Using Polarized Neutrons Produced by Polarized Deuteron Beams (P. W. Lisowski, T. C. Rhea, C. E. Busch, T. B. Clegg, R. L. Walter)

a. $^3He(\vec{n},\vec{n})^3He$

The results for these previously obtained data are complete and were reported at the International Conference on Few Body Problems in Nuclear and Particle Physics at Laval University, Quebec, Canada. Work on preparing a report for formal publication is in the final stages.

---

* Now at Los Alamos Scientific Laboratory, Los Alamos, New Mexico
** Now at East Carolina University, Greenville, North Carolina
\+ Now at Frankfurt University, Frankfurt, Germany

b. $^4He(\vec{n},\vec{n})^4He$

The results of earlier $^4He(\vec{p},p)^4He$ asymmetry measurements from an investigation of the quench ratio method for determining beam polarizations have been incorporated in an R-matrix analysis of the n-^{4}He and p-^{4}He systems. The data were reported at the Atlanta meeting of the American Physical Society. Revisions to the R-matrix computer calculation have been made to permit a reduction in computation time by about 80%. Final searching of the data for the R-matrix parameterization of these mass-5 systems will be made prior to publication.

11. Transfer Polarization Studies in $(\vec{p},\vec{n})$ Reactions (P. W. Lisowski, G. Mack, R. C. Byrd, T. B. Clegg, R. L. Walter)

Polarization transfer coefficients have been deduced from measurements of the outgoing 0° neutron polarizations for the following reactions:

a. $D(\vec{p},\vec{n})pp$
b. $^{11}B(\vec{p},\vec{n})$
c. $^{13}C(\vec{p},\vec{n})$
d. $^{9}Be(\vec{p},\vec{n})$
e. $Cu(\vec{p},\vec{n})$

The results for the $D(\vec{p},\vec{n})2p$ reaction were reported at the International Conference on Few Body Problems in Nuclear and Particle Physics at Laval University, Quebec, Canada.

Additional data have been taken for $^9Be(p,n)$. From 10 to 15 MeV cross-section angular distributions and 0° yield data were recorded using the new pulser and buncher apparatus. It is believed that these data will be useful in interpreting the $^9Be(\vec{p},\vec{n})$ polarization transfer data.

12. Polarization Transfer at 0° in the D(d,n) Reaction (P. W. Lisowski, C. E. Busch, T. B. Clegg, R. L. Walter)

These data have been submitted for final publication in Nuclear Physics.

13. Analyzing Power Angular Distribution Measurements for $^{9}Be(\vec{p},\vec{n})$
(G. Mack, P. W. Lisowski, T. B. Clegg, R. L. Walter)

Seven angular distributions of the asymmetry produced in the $^{9}Be(\vec{p},n)$ reaction have been obtained with proton energies from 8 to 15 MeV. It is expected that the cross-section measurements of Section 11 will aid in estimation of the uncertainties due to background and breakup effects. The preliminary analyzing power angular distributions are similar to polarization angular distributions for $^{9}Be(p,\vec{n})$ but are of smaller magnitude.

14. Theoretical Investigation of Neutron Cross Section Measurements
(M. Divadeenam, B.-H. Choi, W. P. Beres,* S. and K. Ramavataram,** A. Lev,* R. Y. Cusson, H. W. Newson)

$^{28}Si+n$: A paper (by Divadeenam and Cusson) incorporating the 2p-1h doorway calculations has been accepted by Physical Review Letters. The abstract follows:

> "A suitable treatment of the neutron single-particle continuum is given. The $1f_{5/2}$ single-particle strength distribution is predicted to be among doorway states below 4 MeV neutron bombarding energy, as a result of choosing a restricted shell model for the calculation. Combining the predicted continuum single particle and 2p-1h contributions accounts well for the observed strong $5/2^{-}$ resonance structure in ^{28}Si neutron scattering below 4 MeV."

Papers on the following are in various stages of preparation by M. Divadeenam, a former member of the TUNL staff:

$^{89}Y(n,n)$ a preliminary report appeared in the Amsterdam Conference, Sept. 9-13, 1974.

Ca and Pb isotope shell model and particle-vibration doorway calculations.

---

* Wayne State University, Detroit, Michigan

** Universite Laval, Quebec, Canada

15. Investigation of Nuclear Widths Using The Doorway Concept And The Shell Model (S. Maripuu, M. Divadeenam)

The study of neutron resonance widths in the ^{28}Si+n and ^{32}S+n compound systems is in progress.

The proton and gamma-ray partial widths are being calculated for the A = 15 and A = 55 giant dipole resonances using similar techniques. Furthermore the effect of 3p-2h excitations is being included in the configurations of the giant dipole resonance.

B. CHARGED PARTICLE REACTIONS

1. Fine Structure of Isobaric Analogue States--Elastic Scattering (E. G. Bilpuch, G. E. Mitchell, H. W. Newson, D. Flynn, D. A. Outlaw, W. M. Wilson,* J. D. Moses**)

a. Iron and Nickel Isotopes

Work has continued on the development of a high resolution system for the 4 MeV accelerator. A number of experimental improvements were achieved. The beam was completely realigned through the analyzing magnet, with a resulting decrease in dome ripple from ~ 4 keV to ~ 2 keV. The water-vapor stripper was moved back 2 feet and a magnetic-slit system installed. The purpose was to keep unwanted components of the beam off the analyzer plates and thus reduce the drift in energy calibration. Both resolution and reproducibility have improved after these changes.

The following data have now been measured (at four angles for elastic scattering and three for inelastic scattering): ^{54}Fe (to 4.5 MeV), ^{58} Ni (to 4.1 MeV), ^{60}Ni (to 3.2 MeV). We are now extending the ^{58}Ni measurements to higher energies. Preliminary results indicate that these higher energy data may be satisfactorily analyzed with the present analysis codes.

---

* Now at Argonne National Laboratory

** Now at Los Alamos National Laboratory

b. Calcium Isotopes

A paper has been published on the results from $^{40}Ca(p,p)$: "Thomas-Ehrman Shifts in ^{41}Ca-^{41}Sc", by W. M. Wilson, J. D. Moses, E. G. Bilpuch and G. E. Mitchell, Nuclear Physics A227 (1974) 277.

A paper entitled "Fine Structure of Analogue States in ^{45}Sc" has been submitted for publication. The abstract follows:

> "Differential cross sections were measured for $^{44}Ca(p,p)$ and $^{44}Ca(p,p')$ at four angles between E_p = 1.5 and 3.0 MeV, with an overall energy resolution of about 325 eV. Spins, parities, total and partial widths were extracted for 429 resonances. Five analogue states were identified and fits to the fine structure were obtained for four of these analogues."

c. ^{30}Si, ^{34}S and ^{92}Mo

A dissertation entitled "A High-Resolution Study of Proton Resonances in ^{31}P, ^{35}Cl and ^{93}Tc" by D. A. Outlaw has been completed. The following is the abstract of that dissertation.

> "Differential cross sections were measured for $^{30}Si(p,p)$ from 1.08 to 3.00 MeV and $^{34}S(p,p)$ from 1.46 to 2.82 MeV at laboratory angles of 160°, 135°, 105°, and 90° using the TUNL 3 MV Van de Graaff accelerator and associated electrostatic analyzer-homogenizer system. The differential cross section for $^{92}Mo(p,p)$ was measured from 5.13 to 5.43 MeV at 160°, 125°, and 90° using the TUNL tandem Van de Graaff accelerator and magnetic analyzer-homogenizer system. All targets were 1-2 $\mu g/cm^2$ of enriched (95.5% $^{30}SiO_2$, 90.0% $Cd^{34}S$, and 98.3% $^{92}MoO_3$) isotope deposited on thin carbon backings. A total energy resolution of 350-450 eV was maintained for the ^{30}Si and ^{34}S excitation functions: the resolution was about 500 eV for the ^{92}Mo excitation function.

"The resonances observed in the excitation functions were analyzed in terms of the parameters of the R-matrix theory of nuclear reactions. Resonance energies, spins, parities, and proton widths were extracted for 62 resonances in ^{31}P, 59 resonances in ^{35}Cl, and 125 resonances in ^{93}Tc.

"The analogues of the 2.317 and 3.133 MeV states in ^{31}Si were positively identified and the analogue of the 2.790 MeV state was tentatively identified. The analogue of the 2.348 MeV state in ^{35}S was positively identified and the analogues of the 2.718, 2.939, and 3.421 states were tentatively identified. The highly fragmented analogue of the first excited state in ^{93}Mo was studied. Coulomb energies for each of the analogue states were determined and found to be internally consistent and in agreement with other experiments. Spectroscopic factors were determined for each of the observed analogue states and compared with (d,p) spectroscopic factors. A fit to the theoretical fine-structure distribution was obtained for the highly fragmented s-wave analogue state in ^{93}Tc and the fine-structure parameters were extracted.

Seven very large $3/2^-$ states were observed in ^{31}P. These resonances contain a large fraction of the $3/2^-$ single-particle strength. The proton widths obtained in these experiments were combined with capture data in order to extract gamma-ray widths for resonances in ^{31}P and ^{35}Cl. The proton strength functions for each spin and parity observed were determined for each isotope studied. These strength-function data were combined with the previous data taken at this laboratory. The qualitative features of the proton strength functions from A = 30 to A = 64 were discussed. These proton strength functions were compared with general optical-model predictions and to the limited results of the proton strength function measurements obtained from (p,n) reaction data."

A paper has been published on the results for ^{92}Mo: "High-Resolution Study of the $1/2^+$ Analog State in ^{93}Tc", by E. G. Bilpuch, J. D. Moses, F. O. Purser, H. W. Newson, G. E. Mitchell, R. O. Nelson and D. A. Outlaw, Physical Review C, 9 (1974) 1589.

Papers for results on ^{30}Si and ^{34}S are in preparation.

2. Fine Structure of Analogue States--The Capture Reaction (G. E. Mitchell, E. G. Bilpuch, K. Wells, J. F. Wimpey*)

a. ^{62}Ni

A paper has been published on these results: "Electromagnetic Decay of a Fragmented Analogue State in ^{63}Cu", by J. F. Wimpey, G. E. Mitchell and E. G. Bilpuch, Nuclear Physics A233 (1974) 9. The following is the abstract of this paper:

> "The ^{62}Ni (p,p), (p,p'γ) and (p,γ) reactions were studied in the vicinity of the $3/2^-$ fragmented analogue of the first excited state of ^{63}Ni. The overall proton energy resolution was about 300 eV. The γ-rays were detected with both NaI(Tl) and Ge(Li) detectors. Elastic and inelastic proton widths and partial and total γ-ray widths were measured for each of the fourteen fine structure states of the analogue. Statistically significant correlations were observed between the elastic proton widths, the inelastic proton widths and the total γ-ray widths."

b. ^{44}Ca

Further analysis of the large body of data on ^{44}Ca (p,γ) is in progress.

3. High Resolution Inelastic Scattering (G. E. Mitchell, E. G. Bilpuch, T. Dittrich, K. Stelzer,**C. R. Gould)

A program of measurements of the (p,p') and the (p,p'γ) reactions is currently in progress to extend and check the results of earlier high resolution

---

* Now at Gulf Atomic

** Now at Frankfurt University, Frankfurt, Germany

elastic scattering and capture studies. Elastic scattering measurements determine the ℓ-value of a resonance very well, but often leave the j-value in doubt. Our primary concern is the assignment of p-wave resonances. The combined measurement of p' and γ angular distributions in singles ($1/2^-$, $3/2^- \rightarrow 2^+ \rightarrow 0$) provide a unique spin assignment.

For $3/2^-$ resonances, the measurement of the two angular distributions provides (in almost all cases) a unique value of the magnitude and sign of the channel spin mixing ratio.

Both particle and γ-ray angular distributions were measured for all p-wave resonances previously observed in $^{50}Cr(p,p)$ from 2 to 3 MeV. Preliminary analysis indicates excellent internal agreement between the results of the two sets of measurements. Detailed analysis is in progress. The γ-ray angular distributions for $^{44}Ca(p,p'\gamma)$ were also studied for all p-wave resonances from 2 to 3 MeV. This reaction has a much higher density of resonances than for ^{50}Cr. Particle angular distributions are necessary to aid in interpreting the ^{44}Ca results.

4. Statistical Properties of Nuclei from Proton Resonance Reactions
(E. G. Bilpuch, G. E. Mitchell, H. W. Newson, W. M. Wilson*)

A paper entitled "Applications of Statistical Tests to Proton Resonances in ^{45}Sc and ^{49}V" has been submitted for publication. The abstract appears below:

> "Several statistical tests have been applied to $1/2^-$ and $1/2^+$ proton resonances observed in $^{44}Ca(p,p)$ and to $1/2^+$ resonances observed in $^{48}Ti(p,p)$. The energy dependence of the density was unfolded (to a constant density) in order to make comparison with theoretical spacing predictions for single level populations. The functional form for the density does not appear to significantly affect the results: a constant temperature density function was adopted for simplicity. The ^{44}Ca data overall indicate missing and spurious levels. However for a subsection of these data, where the observed total number of resonances of all spins and parities is relatively lower, and where the effects of $1/2^+$ and $1/2^-$ analogue states enhance the widths, the data appear nearly complete. For 52 $1/2^-$ levels in ^{45}Sc, $\Delta_3^{exp} = 0.39$ ($\langle\Delta_3\rangle$ correlated $= 0.35$) and $\rho^{exp}(S_i, S_{i+1}) = -.32$ ($\langle\rho\rangle_{correlated} = -0.27$). For 39 $1/2^+$ levels in ^{45}Sc, $\Delta_3^{exp} = 0.34$ ($\langle\Delta_3\rangle_{correlated} = 0.35$) and $\rho^{exp} = -0.35$ ($\langle\rho\rangle_{correlated} = -0.28$). For ^{48}Ti all of the

$1/2^+$ levels were included. For 66 $1/2^+$ levels in ^{49}V, $\Delta_3^{exp} = 0.51$ ($\langle\Delta_3\rangle^{correlated} = 0.38$) and $\rho^{exp} = -0.21$ ($\langle\rho\rangle^{correlated} = -0.27$). Dyson's F-statistic test was applied to all of these data, and the kth nearest spacing distributions were calculated for k = 0 through 10. All of these results appear internally consistent. There is thus strong evidence for both short and long range correlations in the spacings of single level populations observed by proton resonance reactions. These results are consistent with the first experimental demonstration of such correlations by the Columbia group in total neutron cross section measurements."

5. Studies of The Gamma Decay of Excited Levels of ^{51}Ti (G. P. Lamaze,* C. R. Gould, N. R. Roberson, D. R. Tilley)

This work is inactive.

6. Mean Lifetimes of Excited States in ^{38}Ca (E. C. Hagen,** S. Maripuu, N. R. Roberson, D. R. Tilley)

This work comprises the Ph.D. dissertation of E. C. Hagen. The abstract follows:

"The Doppler shift attenuation method (DSAM) has been used to measure the mean lifetimes of low-lying excited states of ^{38}Ca. The levels were populated by the $^{36}Ar(^3He,n\gamma)^{38}Ca$ reaction at ^3He bombarding energies of 9.0, 10.0 and 10.5 MeV. Both enriched (99.6%) ^{36}Ar gas and solid targets were used. The solid target was a tantalum foil with ^{36}Ar embedded in it. Precise energies for the first six levels have been determined. A doublet at 3.7 MeV was resolved as a $J^\pi = 3^-$ state at 3.703 MeV and a $J^\pi = 2^+$ state at 3.684 MeV. The lifetimes determined in this study are $98 \pm {}^{44}_{40}$ fs, $27 \pm {}^{17}_{11}$ ps, < 8 fs, $225 \pm {}^{100}_{85}$ fs and 35 ± 17 fs for the levels at 2.213, 3.084, 3.684, 3.703 and 4.384 MeV. The lifetime of the level at 4.193 MeV was not determined.

---

* Now at National Bureau of Standards, Gaithersburg, Maryland

** Now at the University of Kentucky, Lexington, Kentucky

"The experimental level scheme is compared with other A = 38 nuclei and with a calculation performed with the Oak Ridge-Rochester shell model code. The model used $(s_{1/2})^j(d_{3/2})^k(f_{7/2})^l(p_{3/2})^m$ configurations with $1 + m \leq 2$, $j \geq 2$ and $k \geq 4$."

7. Study of Excited States of ^{39}Ca and ^{39}K (W. Kessel, R. Bass, E. C. Hagen, N. R. Roberson, C. R. Gould, D. R. Tilley)

A paper has been published in Nuclear Physics A223 (1974) 253. The abstract is given below.

"States in ^{39}Ca up to 4 MeV excitation energy have been studied with the ^{36}Ar(x,nγ)^{39}Ca reaction. Outgoing γ-rays were measured in coincidence with either neutrons or γ-rays detected at 0° with respect to the beam axis. Excitation energies for levels in ^{39}Ca have been measured; doublets have been found near 3.88 and 3.95 MeV. Mean lifetimes of excited states have been determined by the Doppler-shift attenuation method. The results are 90 ± 24 ps, 24 ± 15 ps and 30 ± 25 ps for the levels at 2.80 MeV, 3.64 MeV and 3.95 MeV in ^{39}Ca, respectively. Upper limits on the mean lifetimes of several other states were determined. From the γ-γ coincidence data, a mean lifetime of 18 ± 10 ps was deduced for the state at 5.16 MeV in ^{39}K. The results are compared with existing data and theoretical calculations."

8. Measurement of (d,pγ) Angular Correlations in ^{33,35}S with Polarized Deuterons (J. D. Hutton, R. D. Ledford, D. G. Rickel, N. R. Roberson, C. R. Gould, R. O. Nelson, D. R. Tilley, S. Maripuu, T. B. Clegg)

This work is complete and a paper has been submitted for publication. The abstract is given below.

"Electromagnetic mixing ratios for the decay of a number of the low-lying levels of ^{33}S and ^{35}S have been determined via the (d,pγ) reaction. The experiment utilized a tensor-polarized deuteron beam and a collinear geometry for measuring particle-gamma angular correlations. The polarized deuteron beam was accelerated to 4.72 MeV and used to bombard 80 $\mu g/cm^2$ sulfur targets. An array of NaI scintillators detected gamma-rays in

coincidence with protons observed at 180°. A detailed shell-model calculation for ^{35}S has been made with a model space that provides states of positive and negative parities. Comparisons are made with available experimental results."

9. Linear Polarization Measurements in ^{29}Al (J. R. Williams,* C. R. Gould, R. O. Nelson, D. R. Tilley)

Linear polarization measurements for the γ-rays from the low lying levels of ^{29}Al have been made with a 5-crystal NaI polarimeter (see Sec. C-8, TUNL XI). A paper describing the results of this work has been submitted to the Physical Review. The abstract follows:

"Levels of ^{29}Al were populated with the $^{26}Mg(\alpha,p)^{29}Al$ reaction at E_α = 11.26 MeV. The linear polarizations of gamma rays emitted in the decays of the 1.40-, 1.75-, 2.22-, and 2.87-MeV levels were measured. The polarization measurements are consistent with known spin-parity assignments for the 1.40- and 2.87-MeV levels respectively. When combined with previously available information they indicate an assignment of $3/2^+$ for the 2.22-MeV level and $7/2^+$ $(3/2^+)$ for the 1.75-MeV level."

10. Angular Correlation, Linear Polarization, and Lifetime Studies in ^{61}Ni (J. R. Williams, R. O. Nelson, C. R. Gould, D. R. Tilley, D. G. Rickel, N. R. Roberson)

This work is being prepared for publication. In addition, it has been the subject of a Ph.D. dissertation by J. R. Williams. The relevant portion of the dissertation abstract follows:

"A Compton polarimeter, purchased commercially and consisting of two 30 cc., germanium (GeLi) crystals, has been employed in a comprehensive study of the seventeen levels in ^{61}Ni below 2200 keV. This study has also included lifetime measurements using the Doppler shift attenuation method and gamma ray angular correlation measurements based on Method II of Litherland and Ferguson. The excited states in ^{61}Ni were populated using the $^{58}Fe(\alpha,n\gamma)^{61}Ni$ reaction with E_α = 8.0 MeV.

* Now at Auburn University, Auburn, Alabama

The results of these measurements confirm most of the spin-parity assignments made previously from stripping and pick-up reaction studies and studies of the β^+-decay of the ground state of ^{61}Cu. Additional J^π assignments of $7/2^-$, $5/2^-$, $3/2^-$, and $7/2^-$ have been made for the levels at 1016, 1611, 1730, and 2020 keV, respectively. The experimental results are compared to recent theoretical calculations made using the shell model and the core coupling model. The experimental M1E2 transition strengths have been found to be in agreement with those measured for other 1f 7/2 shell nuclei."

11. The Decay Properties of Low Lying Levels of ^{53}Fe (R. O. Nelson, N.R. Roberson, C. R. Gould, D. R. Tilley)

This work has been published in Nuclear Physics A215 (1973) 541.

12. The Decay Properties of Low Lying Levels in ^{55}Co (R. O. Nelson, J.R. Williams, D. R. Tilley, D. G. Rickel, N. R. Roberson)

The work described on ^{55}Co in the previous report (TUNL XII) has continued and is now being prepared for publication. In the past year we have acquired additional data by the (^{3}He,d) reaction with a specially designed particle telescope placed at 0° and with the Ge(Li) detector at the zero of $P_2(\cos\theta)$. This procedure allowed us to determine branching ratios without the necessity of taking angular distributions.

13. The $(\vec{d},t)$ and $(\vec{d},{}^3He)$ Reactions with 15 MeV Polarized Deuterons (S. Datta, M. Kaitchuck, E. J. Ludwig, W. Jacobs, T. B. Clegg)

a. Targets of ^{10}B, ^{13}C, ^{14}N, ^{16}O

A paper discussing (d,t) and (d,^{3}He) cross sections and vector analyzing powers from deuteron bombardment of the targets above has been published in Nuclear Physics A230 (1974) 271. This work constituted part of the Ph.D. thesis of S. Datta.

b. Ca Target

The ^{40}Ca(d,^{3}He)^{39}K reaction has been studied using 15 MeV vector polarized deuterons. Cross sections and vactor analyzing powers have been obtained over the angular range 20° -90° which will provide information about spins,

parities and spectroscopic factors for the lowest several states in ^{39}K. This work will form part of the Master's degree thesis of M. Kaitchuck.

14. $(\vec{d},\alpha)$ Reactions with Polarized Deuterons (M. Jones, M. Kaitchuck, E. J. Ludwig, W. Jacobs, T. B. Clegg)

a. ^{14}N and ^{40}Ca Targets

The $^{14}N(\vec{d},\alpha)^{12}C$ and $^{40}Ca(\vec{d},\alpha)^{38}K$ reactions are being studied using vector polarized deuterons at 15 MeV. The cross section and vector analyzing power data (for 25° -115°) for the lowest three states of ^{12}C and lowest 5 states of ^{38}K are being used to evaluate the angular momentum values (J, L and S) transferred by the particles picked up from the target nucleus. Especially interesting for the case of the ^{14}N target is the question of whether the two pick-up particles are transferred as a deuteron cluster. The vector analyzing powers for these reactions are generally quite oscillatory and the measured values as large as 0.6. A preliminary analysis of the $^{14}N(\vec{d},\alpha)\ ^{12}C_{GS}$ reaction shows great sensitivity to the α-particle optical model parameters. The analysis indicates that the orbital angular momentum transfer is zero.

b. ^{16}O Target

Vactor and tensor polarized deuteron beams have been used to study the $^{16}O(\vec{d},\alpha)^{14}N_{2.31\ MeV}$ reaction at 7.8 MeV and 10.0 MeV. This reaction has been used to calibrate the tensor polarization of the deuteron beam in states 1 and 2 since the tensor analyzing powers calculated when this state is populated are independent of beam energy, scattering angle and reaction mechanism. The reaction also has no vector analyzing power which makes it useful for determining scattering asymmetries due to unwanted causes. A report on this work has been presented at the Southeastern Section meeting of the American Physical Society. It constitutes the Master's degree thesis of Michael Jones.

15. Lifetimes of Levels in ^{59}Cu (R. O. Nelson, C. R. Gould, D. R. Tilley, N. R. Roberson)

This work has been published in Phys. Rev. C9, 2193 (1974).

16. Multistep Processes in The (d,t) And (d,^{3}He) Reactions on ^{30}Si And The Structure of Mass 29 Nuclei (R. A. Hilko, R. O. Nelson, N. R. Roberson)

The dissertation of R. A. Hilko has been completed. The following is

the abstract of that dissertation:

> "Sixteen states with excitation energies < 6.2 MeV and the 8.34 MeV $5/2^+$ t = 3/2 state were studied in ^{29}Si. The first eight levels in ^{29}Al with excitation energies < 3.5 MeV were studied. The coupled-channel Born approximation (CCBA) was used to test two nuclear models, the rotational model with bandmixing and the shell model. The study of the inelastic effects in the scattering from the target nucleus was done for each level, but due to current limitations the study of the inelastic effects in the residual nucleus could only be done properly for the ground state rotational band of ^{29}Si. The need for multistep processes was found in the majority of levels.
>
> With the use of the rotational model with bandmixing electromagnetic transition rates, lifetimes and branching ratios were determined. This calculation supported the CCBA results in favoring this model over the shell model. A complete calculation in a deformed Woods-Saxon potential was performed to determine energy levels and wave functions for various orbits. The results are very similar to the work of Nilsson who used a harmonic oscillator basis."

17. A Study of The Proton Widths for The Lower T = 3/2 States in 4N+1 Nuclei Utilizing Polarized Protons (P. G. Ikossi, W. W. Jacobs, T. B. Clegg, E. J. Ludwig, W. J. Thompson)

a. ^{25}Al via ^{24}Mg+$\vec{p}$

The study with the polarized beam of the two lower T = 3/2 resonances in ^{25}Al discussed in the previous report was continued. Complementary data over the two T = 3/2 resonances have been taken in steps of 150 eV with a 120 eV thick target using the TUNL high resolution system. The beam resolution was measured by repeating previous measurements over the lower T = 3/2 resonance in ^{41}Sc. Difficulties encountered in the description of the background in the neighborhood of the T = 3/2 resonances hopefully will be resolved by fitting the cross section and analyzing power data over the T = 1/2 resonances in the energy region where the T = 3/2 states occur.

b. ^{28}P via $^{28}Si + \vec{p}$

Cross section and analyzing power data have been taken in the region 5.6 - 5.9 MeV in 10 keV steps with an 8 keV thick SiO target. Data over the lowest T = 3/2 resonance have been taken in 2 keV steps with a polarized beam. In addition high resolution data were taken in steps of 150 eV. The target thickness for these data was 200 eV and the beam resolution 800 eV. This resonance is very well pronounced both in the elastic and first inelastic channel. A rough estimate of the proton partial width for the elastic channel is 300 ± 50 eV in contradiction with previous measurements (140 ± 40).[1]

c. ^{33}Cl via $^{32}S + p$

Cross section and analyzing power angular distributions have been taken using a H_2S gas target at proton energies 3.0, 3.4 and 3.9 MeV. The 3.9 MeV off-resonance angular distribution was fitted with an optical model to obtain background phase shifts, which in turn were used to fit cross section and analyzing power excitation function data taken in the energy region 3.0-3.9 MeV. The resonance parameters for the broad T = 1/2 resonances obtained from these fits are in very good agreement with results of previous works.[2]

High resolution data for the lowest T = 3/2 resonance in ^{33}Cl at 3.371 MeV proton Laboratory energy, taken in 180 keV steps with an Sb_2S_3 300 eV thick target, were fitted using the phase shifts and resonance parameters of the T = 1/2 states to describe the background. The beam resolution for these data was deduced from data taken over the 325 eV wide ^{55}Co resonance at 3.229 MeV proton energy. In a different approach phase shifts obtained by fitting an angular distribution at 3.355 MeV were used to describe the background. The resonance parameters obtained for the T = 3/2 resonance with the two methods are in very good agreement and suggest a width of 92 ± 7 eV $J^\pi = 1/2^+$ in agreement with previous results.

A report on the progress of this work was given in the meeting of the American Physical Society in Pittsburgh.

A paper describing our earlier work with $p + ^{40}Ca$ scattering has appeared since the last report in Phys. Rev. Lett. 33 (1974) 229.

---

[1] B. Teitelmann and G. H. Temmer, Phys. Rev. 177 (1969) 1656.

[2] J. W. Olness, W. Haeberli and H. W. Lewis, Phys. Rev. 112 (1958) 1702.

[3] U. Abbondanno et al., Nuovo Cimento 70A (1970) 391.

18. $^{208}Pb(p,p')$, $^{208}Pb(p,d)$ and $^{208}Pb(p,t)$ Reactions from 16.7 to 27.3 MeV (E. J. Ludwig, P. Nettles, C. Busch, M. Divadeenam)

This work is inactive at present.

19. Isobaric Analog Resonances in ^{71}Ge (P. G. Ikossi, C. E. Busch, T. B. E. J. Ludwig, W. J. Thompson)

This work has been published in Nuclear Physics

20. Study of Isobaric Analog Resonances in ^{209}Bi via $^{207}Pb(\vec{d},p)$ and $^{207}Pb(\vec{d},d)$ Reactions (S. Tonsfeldt, T. B. Clegg, W. W. Jacobs, E. J. Ludwig, W. J. Thompson)

Interest in these reactions exists because we wish to determine to what extent these reactions occur via isospin mixing in the compound nucleus. Excitation functions were taken at lab angles 90° , 110° , 130° and 150° at bombarding energies varied between 9.0 and 13.0 MeV in steps of 50 keV or 100 keV. Strong structure was observed in the present $(\vec{d},p)$ studies in both cross section and vector analyzing power in the vicinity of the single particle resonances. Angular distributions for the $^{207}Pb(\vec{d},d)$ were taken at 10.2 and 13.2 MeV to obtain optical model parameters. Also $^{207}Pb(\vec{d},d)$ excitation functions for σ and Ay were taken with good statistics to obtain an upper limit on the resonance widths in the deuteron channel. A paper on the present state of this work was given at the Pittsburgh Meeting of the American Physical Society.

21. Depolarization Measurements in $^{14}N + p$ Elastic Scattering (T. B. Clegg R. A. Hardekopf, G. G. Ohlsen ((Los Alamos)))

The Wofenstein depolarization parameter $D(\theta)$ was measured for $^{14}N + p$ elastic scattering for an incident proton energy of 16.15 MeV. A report of this work was made at the Pittsburgh meeting of the American Physical Society in November 1974, and a paper is being prepared for publication.

22. Measurement of Mean Lifetimes, γ-Ray Angular Distributions And Linear Polarizations for Low-Lying Levels of ^{50}V (D. G. Rickel, N. R. Roberson, R. O. Nelson, J. R. Williams, D. R. Tilley)

A paper has been published in Nuclear Physics A232 (1974) 200. The abstract is given below.

"Levels of ^{50}V were populated with the $^{50}Ti(p,n)^{50}V$ reaction at E_p = 4.50, 4.62 and 4.80 MeV. Gamma rays were measured in singles. From Doppler shift attenuation measurements mean lifetimes have been deduced for 9 levels below E_x = 2 MeV. The J^π assignments for 8 of these levels follows from γ-ray angular distribution and linear polarization measurements. The transition strengths have been compared with calculations based on the wave functions of McCullen, Bayman and Zamick."

23. Studies of The Gamma-Decay of Excited Levels in ^{117}Sb (C. Schiffel, C. Cameron, R. D. Ledford, D. G. Rickel, N. R. Roberson, K. Stelzer, D. R. Tilley)

To obtain unique spin-assignments for levels in ^{117}Sb above 1.3 MeV excitation energy and mixing ratios for the γ-radiation from the decay of the states, angular distribution and γ-ray polarization measurements have been made. The reaction $^{117}Sn(p,n\gamma)^{117}Sb$ at a proton-energy of E_p = 4.15 MeV was used to populate the levels. The polarization was determined by a Ge(Li)-Polarimeter.

In order to obtain a complete set of information on the nuclear structure of the states it is planned to take also n- γ-correlations and make Doppler-shift lifetime measurements using the reaction $^{116}Sn(He^3,d)^{117}Sb$.

24. The GDR of ^{15}N from $^{14}C(\vec{p},\vec{p})$ Measurements (H. R. Weller, D. G. Rickel, N. R. Roberson, D. R. Tilley) Phys. Rev. Lett., 33, 657 (1974).

25. Study of The Giant Dipole Resonances in The Co Isotopes Using Proton Capture and Polarized Proton Capture Measurements (H. R. Weller, R. A. Blue, D. Griggs ((Univ. of Florida)), N. R. Roberson, D. Rickel, C. Cameron, R. D. Ledford, D. R. Tilley)

Previous workers[1] have measured $^{54,56}Fe(p,\gamma)$ cross sections in the giant dipole resonance (GDR) region of $^{55,57}Co$. We have initiated a program to measure the analyzing powers for these reactions utilizing our recently installed 10"x10" NaI spectrometer. In addition, both the cross sections and analyzing powers are being measured for ^{58}Fe. These ^{58}Fe data should be especially significant with regard to the understanding of the possible presence of isospin splitting of the GDR since a systematic behavior of the relative strengths and positions of the T< and T> components is predicted as one goes from a T= 1 to a T= 2 to a T= 3 target.

[1] J. V. Maher et al., Phys. Rev. C9, 1440 (1974)

A preliminary analysis of the ^{54}Fe and ^{56}Fe analyzing power and cross section data indicate that the giant resonance in ^{55}Co and ^{57}Co can be accounted for with the g7/2 configuration (the spin flip transition) set equal to zero. When this is done, two solutions are obtained which correspond to a mixture of g9/2 and d5/2 strengths. It is observed that the normalized strengths of these configurations is remarkably constant over the GDR region, whereas the relative phase angle between the g and d transition matrix elements changes dramatically. This result resembles the $^{15}N(p,\gamma)$ result obtained by Hanna.[2] Furthermore, our solutions indicate that the configuration of the GDR changes smoothly through that energy region which was suggested in Ref. 1 to be the energy of transition from T < to T >. The authors of Ref. 1 noted that the sign of a_2 changes at this energy and suggested that this could be correlated with the isospin. The fact that the configurations which are necessary to account for this sign change do not show any distinct change casts serious doubt on this suggestion's validity.

26. Further Development of The PIXEA System (R. D. Willis, W. Gutknecht, R. L. Walter)

Utilizing 3-MeV proton beams, a Proton-Induced X-ray Emission Analysis system has been developed in the 4-MeV Van de Graaff laboratory. Partial support for studying the applicability of the method was received from EPA and the National Institute for Environmental Health Sciences. A major report on the technique is being written presently and will include an overview of about 4000 runs. Main concentration has been placed upon calibration, sensitivity and analysis of samples from the following categories: environmental, medical, biological, geochemical, marine life, and biochemical. Numerous useful applications appear worthwhile to pursue. Reports on our work in 1974 appeared in Anal. Chem. 46, 440 (1974), Anal. Chem. 46, 843 (1974), Anal. Biochem. 57, 618 (1974), and Proc. of Applications of Small Accelerators (1974 Conference). Papers have been submitted to Geochimica et Cosmochemica Acta, Nature, and another to Anal. Chem. A continuing cooperation in energy-related studies with NIEHS will be arranged in the near future.

27. $^{6}Li(p,^{3}He)^{4}He$ Reaction from 3 to 12 MeV (C. R. Gould, J. R. Boyce, J. R. Williams)

The experimental phase of this work has been completed and the results are being prepared for publication. Our data for this reaction indicate the total cross section to be monoatomically decreasing from ~ 150 mb at 3 MeV down to

[2] S. S. Hanna et al., Physics Letters 40B, 631 (1972).

~ 40 mb at 12 MeV with little indication of resonance structure. These results agree well with those of Hooton and Ivanovich[1] at 3 MeV and support their contention that the cross section in this region is much higher than had previously been supposed. Additional measurements of proton elastic and inelastic scattering from ^{6}Li made in the region 4 to 8 MeV imply cross sections for these reactions are also higher than earlier results.[2] This work was reported at the Chicago meeting of the American Physical Society. Investigations are planned for other absolute cross section measurements of interest to thermonuclear reactor studies, in particular those involving light mass nuclei.

This work has been published in Nucl. Sci. and Eng. 55, 267 (1974). The abstract is given below.

> "Absolute cross section measurements for reactions among light mass nuclei ($A < 10$) are important in feasibility studies of controlled thermonuclear reactor systems. For a ^{6}Li-d fueled fusion reactor, the ^{6}Li(p,^{3}He)α reaction is of particular interest. The absolute cross sections for this reaction are incomplete and poorly known, and have accordingly been remeasured in the range E_p = 3 - 12 MeV. The results support recent measurements below 3 MeV in finding the cross section to be higher in this region than previously supposed. Additional results for the ^{6}Li(p,p)^{6}Li and ^{6}Li(p,p')^{6}Li* reactions imply the cross sections for these reactions are ~40% higher than earlier measurements. A plot of the Maxwell averaged reaction rage parameter $\bar{\sigma}_v$ for the ^{6}Li(p,^{3}He)α reaction is presented as a function of kT, the temperature of a p - ^{6}Li plasma."

28. ^{6}Li(^{3}He,p)^{8}Be Reaction from 3 to 6 MeV (C. R. Gould, J. R. Boyce)

This reaction has a large positive Q value and is of interest to thermonuclear reactor studies including only charged particles. We have measured the cross sections for excitation of ^{8}Be in its ground and first excited states and have also parameterized the three body break up continuum from $^8\text{Be} \rightarrow \alpha + \alpha$ using the statistical density of states factor. Our cross sections are a factor of three lower than the only other known absolute values,[1] being of the order of ~ 25 mb for the 2.9 MeV state of ^{8}Be and ~ 6 mb for the ground state. This work was performed in response to cross section request No. 32 of Report LA-5253-M5 and is currently being prepared for publication in Nucl. Sci. and Eng.

---

[1] J. P. Schiffer et al., Phys. Rev. 104, 1064 (1956)

C. DEVELOPMENT

1. Accelerator Improvements (F. O. Purser, H. W. Newson, E. G. Bilpuch, R. L. Rummel, D. E. Epperson)

a. Tandem Accelerator

Only routine maintenance has been performed during this report period.

b. Injector Cyclotron

No development work was undertaken during this period.

2. Pulsed Beams (F. O. Purser, H. W. Newson, N. R. Roberson, T. B. Clegg, D. W. Glasgow, D. E. Epperson)

a. Neutron Time-of-Flight System

Construction of the outer shield and radial carriage of the massive γ-ray detection system has been completed. Design work for the baffle and collimator system is in progress. Pending completion of this unit, the outer shield, consisting of approximately 6000 lbs. of copper, is being used as a pre-shield for the main neutron collimator to reduce background levels for high energy cross section measurements.

A neutron collimator designed to permit neutron cross section measurements over the angular range $1\text{-}1/2° \leq \theta \leq 15°$ has been obtained on loan from the Ballistic Research Laboratory, Edgewood Arsenal. With its associated detectors and electronics, this system will make a significant addition to our ability to measure accurate high energy angular distributions. Modification of the equipment to fit it into our experimental area is underway and it is anticipated that it will be in use by mid-1975.

3. Polarized Ion Source Operation (T. B. Clegg, P. W. Lisowski, R. Henneck, W. W. Jacobs)

The polarized-ion source has continued to be used extensively for experiments since the last report--usually for an average of 10 - 15 days/month. Accelerated beams are down somewhat from those last reported and are typically 80-120 μA for both protons and deuterons. The operation of the source has been accomplished with a minimum of maintenance--usually several hours work before

each accelerator run of 4 - 8 days. A new polarized-ion source Faraday cup has been constructed and will be installed as soon as there is a period when the ion source and low energy vacuum systems can be bented without interfering with experiments.

Two papers describing the polarized-ion source hardware have appeared since the last report: 1) Nucl. Inst. Meth. 120 (1974) 445 and 2) Proceedings of The Second Symposium on Ion Sources and The Formation of Ion Beams, Berkeley, Calif., Oct. 22-25, 1974, Lawrence Berkeley Laboratory Report LBL-3399, pg. IV-5-1.

4. Hardware and Software for Tensor Polarization Experiments (R. F. Haglund, Jr., R. J. Eastgate, T. B. Clegg)

The circuitry for remote-controlled rotation of the 60 cm. diam. scattering chamber was installed in September and has been used in several experiments. At present, only manual controls are available. However, most of the interface circuit for the DDP-224 computer has been built, and its completion and installation are expected in a few weeks. This will permit complete computer control of the chamber rotation, including remote sensing of chamber position.

The data acquisition program DMASS is still being used for tensor polarization measurements. Current programming efforts center around standardizing and optimizing the various vector and tensor polarization data acquisition programs used in the laboratory.

5. Beam Optics Calculations (T. B. Clegg, D. Stevenson)

The interactive matrix optics computer program, which was reported previously and which allows the operator to simulate focal conditions in the low-energy region of the accelerator and in target area beam lines, has been improved. A version has been written for the IBM-360 system at the Triangle Universities Computation Center which allows the calculated beam envelope to be displayed on a storage oscilloscope or to be output on a CALCOMP plotter. Major improvements have been made in the organization of the program making it much more easily understood by new users and much easier to modify for new problems. At present checks must be made to establish the accuracy of the program before we can actually use it to try to improve the beam optics systems currently used in the laboratory.

6. Polarized Triton Source (T. B. Clegg, with J. L. McKibben and R. A. Hardekopf ((Los Alamos)))

The Lamb-shift polarized source for triton beams which was designed during the summer of 1972 has been constructed over the past two years. During the six-week visit of one of the above participants (TBC) to the Los Alamos laboratory this past summer, final construction was completed and beams of polarized protons of up to ~ 320 nA of ~ 85% beam polarization were obtained. The ion source is now being installed on the tandem accelerator at Los Alamos. The first polarized triton beams should be available for experiment in ~ April 1975.

7. Scattering Chamber for (p,n) Cross-Section Measurements (M. Kaitchuck, E. J. Ludwig, R. L. Walter)

A scattering chamber has been designed and built to allow (p,n) measurements to be made with the neutron spectrometer system. The chamber has been designed to be of a minimum mass and to have no outgassing from vacuum seals. The chamber also incorporates particle detectors for beam monitoring purposes.

8. Split Faraday Cup for Beam Centering (M. Jones, E. J. Ludwig)

A Faraday cup has been built which consiste of four isolated segments which can be used to separately measure and compare beam currents. This will allow a correction signal to be sent to a beam steerer for centering of the accelerator beam. The control electronics is now being assembled.

9. Pulsed Polarized Beam Studies (P. W. Lisowski, F. O. Purser, R. C. Byrd, S. Skubic, T. B. Clegg, R. L. Walter)

The use of the chopper-buncher system for the production of pulsed polarized beams has been investigated by observing gamma ray and neutron peak widths produced in the $D(d,n)^3He$ reaction. Pulsing and bunching the polarized beam decreases the average current on target by about a factor of 10. The principal difficulty was one of obtaining a satisfactory beam pick-off timing signal when working with nanoampere pulsed beams. The results obtained in our preliminary investigation show that polarized beams yielding an average target current as low as 6 nA may be successfully pulsed and bunched and that neutron time-of-flight peaks of less than 4 ns full width at half maximum are currently obtainable. Further development is planned.

10. Computer Improvements (C. R. Gould, D. Lupo, N. R. Roberson, D. G. Rickel, P. W. Lisowski)

The on-line DDP-224 computer has been in operation since January 1966; the off-line DDP-224 since 1970. During this time, the system has been steadily improved, primarily through software development but with some small additions of hardware. Recent acquisitions of both new and surplus equipment will permit significant expansion. These improvements or planned improvements are listed below.

1. A 200K fast drum has been installed on the off-line computer. All support software has been completed. A second 100K drum will be added during the year.

2. A surplus DDP-224 with over 120K of fast memory has been obtained. The CPU will be used as a supply for parts which are no longer commercially available. The memory will be used to expand each of our two systems to 64K. This will enlarge the off-line computer from 12K and the on-line computer from 24K. The expansions will be made in 32K steps.

3. A CAMAC interface is on order and will be delivered in March 1975. This interfact will bring our PRIME-300 computer on-line for use with the high-resolution work being carried out at the 3 MeV accelerator.

4. An "almost new" off-line 30 inch CALCOMP plotter with magnetic tape input has been obtained from surplus. The software is now complete and high quality inked drawings are being routinely produced.

D. THEORY

1. Compound Elastic Scattering and Tensor Analyzing Powers (R. J. Eastgate, W. J. Thompson)

Final analysis of thick-target cross sections and vector and tensor analyzing powers for $^{28}Si(d,d)^{28}Si$ at mean energy 6.75 MeV is underway. This will be described in the Ph.D. thesis of R. J. Eastgate. Compound-elastic scattering probably has important effects in backward-angle tensor analyzing powers for (d,d) as well as for (d,p).

2. Studies of Deuteron Scattering Potentials (J. A. Ramirez, W. J. Thompson)

Analysis of many of the d-induced reactions studied at TUNL requires reliable d-scattering potentials. We are calculating d potentials from n and p potentials which describe scattering from the same target as for the d scattering. The nucleon potentials are averaged over the d internal motion. Numerical tabulations of the potentials and analytic approximations to these are being studied.

A modified and improved version of a computer code from the Univ. of Wisconsin, Madison, calculates elastic scattering including the full tensor potential for (d,d). Effects of terms which couple different partial waves to the same total angular momentum are large; this suggests that some previous analyses of d tensor polarizations are incorrect.

3. Total Wave Functions and Fluxes in Elastic Scattering (E. A. Olszewski, W. J. Thompson)

Calculation and computer display of total scattering wave functions in three-dimensional views is nearing completion. Insight into several phenomena in elastic scattering by optical-model potentials, both for nucleons and for heavy ions, will be obtained thereby.

4. Isospin-Consistent DWBA Analyses of Cross Section and Vector Analyzing Powers for (d,t) and (d,^{3}He) Reactions in Light Nuclei (S. K. Datta, W. J. Thompson)

Analyses have been made for self-conjugate target nuclei ^{10}B, ^{14}N, ^{16}O and ^{32}S leading to mirror states for d lab energy 15 MeV. A modified DWBA formalism[1] which includes isospin conservation throughout has been used. Isospin-coupling effects are similar to those produced by non-locality and finite-range corrections. This work is described in the Ph.D. thesis of S. K. Datta. The abstract of this thesis is given below:

> "The isospin-coupled Distorted-Waves-Born-Approximation (DWBA) theory for single nucleon transfer reactions is used to fit cross-section and vector-analyzing-power data obtained with 15-MeV vector-polarized deuteron beams. The reactions measured and analyzed are (d,t) and (d,^{3}He) on ^{10}B, ^{14}N and ^{32}S. For $l = 0$ transfers the weakly-bound-projectile-model (WBP) is discussed as an alternative to the DWBA approach and the evidence of the vector-analyzing-power data in its favor is presented.

The differences between isospin-coupled DWBA and uncoupled DWBA are investigated by varying the isospin parameters and studying the sensitivity of the isospin-coupled calculations to such variations. A comparison is made between the isospin-coupled and the uncoupled theory on the basis of their agreement with experimental data. The need of making non-locality and finite-range corrections to isospin-coupled DWBA calculations is discussed."

5. Nuclear DWBA Transfer-Reaction Code for Small Computers (S. K. Datta, W. J. Thompson)

The DWBA has been coded in FORTRAN for computers with about 10K words of core storage, rather than the customary 25K words usually required. The program, which we wrote and debugged on a PDP-15 computer at Kansas State University, will be adapted to the TUNL DDP-224 as soon as the drum storage feature is fully operative.

6. Version of a Nuclear Optical Model Code for Small Computers Designed to Run on a PDP-15 (S. K. Datta, W. J. Thompson, D. O. Elliott ((Kan-State U.)))

This is a version of OPTICS[1] which has been modified to run on a PDP-15 computer with DECtape input and storage-oscilliscope display. Heavy-ion elastic scattering in an optical-model potential can be readily calculated for up to 80 partial waves. This work is published in Computer Physics Communications 7, 343 (1974).

7. Projectile Size Effects in Quadrupole Deformation Measurements (J. S. Eck, D. O. Elliott ((Kansas State U.)), W. J. Thompson)

The effects of projectile size in determining potential shape quadrupole deformations have been shown to be such as to keep the deformation length, rather than the deformation parameter, independent of projectile size. These results have been obtained for targets of ^{24}Mg and ^{28}Si for projectiles of e, n, p, ^{3}He, ^{4}He, d, ^{12}C, ^{16}O and ^{18}O, and are reported at the Anaheim meeting of the American Physical Society. These analyses are being extended to include the target nuclei ^{12}C and ^{20}Ne.

---

[1] R. J. Eastgate, W. J. Thompson and R. A. Hardekopf, Comp. Phys. Comm. 5, 69 (1973).

8. Optical-Model and Coupled-Channels Calculations in Quantum Mechanics (S. D. Doyle, J. S. Eck, O. L. Weaver ((Kansas State U.,)) W. J. Thompson)

Potentials such as the optical-model potential are widely used in research but are seldom considered in introductory quantum mechanics. Similarly, the coupled-channels technique is usually encountered only in complicated research-level problems. We have studied the two-state scattering system of two one-dimensional square wells solved by the coupled-channels method. An approximate solution for one state is obtained by introducing a suitable optical-model potential. Comparisons of exact and approximation solutions are illustrated by the example of the n strength-function maximum near A = 55. This pedagogical research has been submitted for publication in the American Journal of Physics.

9. Depolarization Mechanisms and the Nucleon Elastic-Scattering Interaction (W. J. Thompson, T. B. Clegg with J. S. Blair ((Univ. Washington)) and H. Sherif ((Univ. of Alberta)))

Interpretation of the depolarization parameter D (occurring in the double scattering of polarized nucleons) as differing from unity only because of a spin-spin term in the nucleon-nucleus optical potential has recently been questioned by Blair and Sherif. They showed that a major contribution for target nuclei with ground-state spin I greater than 1/2 can be a combined effect of spin-orbit and quadrupole-moment coupling (LSQ). This is particularly important for highly-collective target nuclei. Our calculations for $^{9}Be(p,p)^{9}Be$ (I = 3/2) with only LSQ substantially explain the available D data without any spin-spin terms. Currently, analysis of D for $^{14}N(p,p)$ (I = 1) is underway and the feasibility of $^{13}C(p,p)$ (I = 1/2) measurements to unambiguously extract the spin-spin term from D data is being studied.

10. Spin-Orbit Coupling in Heavy-Ion Scattering (W. J. Thompson)

Heavy-ion, spin-orbit coupling has previously been ignored because simple kinematic arguments suggest that the strength of the spin-orbit coupling would decrease inversely with the projectile mass A. A model of the heavy-ion spin-orbit interaction has been derived and the resulting elastic-scattering polarization shown to be probably large (greater than 50%) at energies above the Coulomb barrier. Reports of this work were prepared for the Nashville International Conference on Reactions Between Complex Nuclei, presented at the Pittsburgh American Physical Society Nuclear Division meeting, and submitted to Physical Review Letters. The Calculation of ^{6}Li spin-orbit potentials is in progress.

11. Systematics of Backward-Angle Alpha Elastic Scattering (J. S. Eck ((Kansas State U.)), K. A. Eberhard, J. Schiele and W. Trombik ((Univ. of Munich)), W. J. Thompson)

Backward-angle (beyond 90°) cross sections for elastic alpha scattering from target nuclei with $32 \lesssim A \lesssim 100$, for bombarding energies $15 \lesssim E \lesssim 40$ MeV have been systematically investigated using all available data. A simple quantitative prescription for estimating the degree of backward enhancement is given. The enhancement is shown to be strongly correlated with (α,n) and (α,α') Q values. This correlation is discussed in terms of the ℓ-dependent absorption model, and (in work reported at the Washington American Physical Society meeting by W. J. Thompson) in terms of compound-elastic scattering. An experimental determination of the compound-elastic contribution by analysis of the excitation-function fluctuations is in progress at Argonne National Laboratory (K. A. Eberhard and J. P. Schiffer, private communication).

12. Proton Optical-Model Potential Near the Coulomb Barrier (J. S. Eck ((Kansas State U.)), W. J. Thompson)

An anomalously rapid energy dependence of local optical-model potentials which describe p elastic scattering near the Coulomb barrier in heavy nuclei has been determined from the analysis of elastic-scattering cross section and polarization data. The anomalies are related to the replacement of non-local potentials by equivalent local potentials. A report on this work is to be published in Nuclear Physics.

13. Ericson Fluctuation Theory for Polarized Beams (R. F. Haglund, R. Henneck, W. J. Thompson, T. B. Clegg)

Measurements of fluctuations in cross-section and analyzing power for the reactions ^{28}Si(d,d) and ^{28}Si(d,p) over the energy range 6.5-11.5 MeV were completed in March. Since that time, considerable effort has been devoted to theoretical problems of fluctuation analysis. Several areas of investigation have developed:

a. The theory of compound-nucleus cross section fluctuations and their analysis by statistical methods (Ericson theory) has not been investigated in sufficient detail for our analyses of TUNL vector-polarization analyzing power excitation function data for deuteron bombardment. Important questions, from the viewpoint of tractable statistical analyses, are whether the total-angular momentum compound-nucleus amplitudes are the random variables considered, or whether the helicity amplitudes are random, or whether the former implies the latter. To resolve

these questions we are calculating realistic synthetic excitation functions with known statistical properties for the amplitudes, then making statistical tests for randomness and independence of the resulting observables.

b. The functional form of the probability distribution of the vector analyzing power fluctuations has been investigated. We are trying to find out how best to extract information from this distribution function about the relative amounts of compound and direct contributions in the analyzing power excitation functions.

c. A number of recent articles in the field of statistics suggest that the ordinary congruential pseudo-random number generator is inadequate for multi-dimensional simulations, such as fluctuation analyses. A shift-register sequence generator available at the Triangle Universities Computing Center is being adapted for the TUNL DDP-224 computer to permit more reliable calculations of random numbers on this smaller machine.

14. Shell-Model Calculations (R. D. Ledford, S. Maripuu)

A large version of the Oak Ridge-Rochester shell-model code, MULTI, (requiring 450K of core memory) is in operation at the TUCC, IBM 360/165 computer. The code TRANS for calculation of electromagnetic multipole transition strengths, log ft values for Gamow-Teller and Fermi β-decay and static multipole moments as well as the code SFACTOR for calculation of spectroscopic factors for one-nucleon transfer reactions are also in operation and require the same core space as the code MULTI. The mixing of shell model operators and vectors is achieved by a special code REDMES (version requiring 200K is in operation). All the above mentioned codes are stored permanently. A write-up for users is in preparation.

a. Shell-Model Calculations of ^{35}S Structure

Excitation energies, dipole and quadrupole transition strengths, ground state magnetic dipole and electric quadrupole moments and spectroscopic factors for the ^{34}S(d,p)^{35}S reaction have been calculated for the low-lying spectrum of ^{35}S. The model space includes $2s_{1/2}$ and $1d_{3/2}$ orbits for $\pi = +$ states and excitation of one particle into $1f_{7/2}$ or $2p_{3/2}$ orbits for $\pi = -$ states. The modified surface delta interaction (MSDI) has been used as two-body interaction. Most observables are in good agreement with the predictions. The extremely weak $1/2^+$ (1:st. exc.)$\rightarrow$ $3/2^+$ (g.s.) E1 transition is explained in terms of a cancellation between two fairly large contributions. It appears possible that the lowest $J^\pi = 5/2^+$ state predicted at $E_x = 1.96$ MeV is still experimentally unobserved. The calculations strongly favor a positive ground state magnetic dipole moment. These calculations are in-

cluded in a paper "Measurement of (d,pγ) Angular Correlations in $^{33,35}S$ with Polarized Deuterons" recently submitted to the Physical Review.

b. Bound State Structure Calculations for ^{55}Co

The shell model calculations of negative parity states of ^{55}Co have been nearly completed. Predictions have been made for excitation energies, M1 and E2 transition strengths and spectroscopic factors for the $^{54}Fe(^3He,d)^{55}Co$ reaction. The model space includes up to two holes in the $1f_{7/2}$ shell and all possible combinations of particles in the $2p_{3/2}$, $1f_{5/2}$ and $2p_{1/2}$ shells. The model interaction used is the Kuo-Brown realistic interaction with ^{40}Ca core. The single particle energies are taken from a simultaneous best fit to ^{55}Co and ^{56}Co experimental spectra. Also in this calculation the agreement between experiment and theory is very good. The complicated distribution of single particle strengths is correctly predicted. The E_x = 2.66 MeV level is predicted to be a $J^\pi = 5/2^-$ state with negligible single particle strength.

15. Shell Model Study of ^{38}Ca and Argon Isotopes (S. Maripuu)

Two- and four-hole configurations in the (sd)-shell and particle excitations into $1f_{7/2}$ and $2p_{3/2}$ shells have been included to study energy levels of ^{38}Ca and Argon isotopes with A = 38 - 46. Some of the results for more "exotic" Argon isotopes are shown in Fig. 1. The experimentally observed level at E_x = 0.75 MeV in ^{44}Ar[1] is predicted to be a $J^\pi = 2^+$ level and not $J^\pi = 0^+$ as suggested in an unmixed configuration calculation.[2] The shell-model calculations of $^{43,44,45}Ar$ suggest that the $(\alpha,^9Be)$, $(^3He,^7Be)$ and $(\alpha,^7Be)$ reactions[1,3] populate levels quite selectively.

16. Self-Consistent K-Matrix Model Calculation for Finite And Super Heavy Nuclei (R. Y. Cusson, H. W. Meldner ((U.C.S.D.)), M. S. Weiss ((Livermore)), H. P. Trivedi)

No further progress has been made since the last report.

---

[1] W. F. Steele, G. M. Crawley and S. Maripuu, MSU Cyclotron Report 98 (1973)
[2] D. H. Gloecker, R. D. Lawson and F. J. D. Serduke, Phys. Rev. C9 (1974) 2071
[3] N. A. Jelley et al., Phys. Rev. C9 (1974) 2067

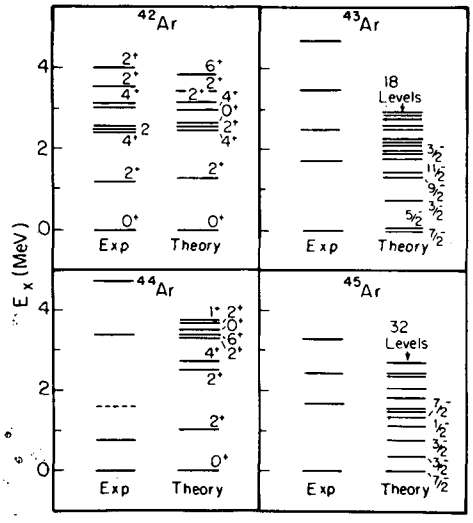

Fig. 1. Comparisons of shell model predictions with experimentally observed levels in Ar isotopes.

17. Computer Codes for High Accuracy Single Particle States (R. Y. Cusson, E. G. Bilpuch, R. A. Hilko)

A computer program to compute single-particle states of finite nuclei in the spherical shell model, starting from the self-consistent K-Matrix model mentioned in the previous entry has been stored on disk and is available for general service usage. The code is useful to give very good first approximations to many single-particle properties of finite nuclei such as radii, density distributions, total and single-particle energies.

18. Single-Particle Wavefunctions and Energies for Stripping and Pickup Reactions (R. Y. Cusson, G. R. Satchler ((ORNL)))

Inactive during this progress report period.

19. Realistic Single Particle Hamiltonian for Fission and Heavy Ion Calculations (R. Y. Cusson, R. A. Hilko, D. Kolb ((G.S.I., Darmstadt)))

The K-matrix model mentioned in Item D-16, TUNL XII, has been used to construct a new fission code to succeed the one used in the paper of the next entry. The new fission and heavy ion code has realistic nuclear matter, symmetry energy, surface energy, and shell correction energies. Thus it should do all that used to require the Nilsson-Strutinsky renormalization. The code accepts up to 200 x 200 matrices for K = 1/2 and is only limited by the available CPU time on the computer. Tests made on lighter nuclei such as the fission of ^{12}C into 3 α particles show a promise of great realism in mapping out the total energy versus the nuclear shape parameters.

Several points on the heavy ion reaction $^{16}O + ^{208}Pb$, of the cluster potential vs. separation distance have been obtained and confirm earlier beliefs concerning the properties of this potential. Further calculations are planned before the work is written up for publication. A paper to the Anaheim meeting of the American Physical Society will be presented.

20. Realistic α-particle Potentials (R. Y. Cusson, R. A. Hilko, K. Sage)

The heavy ion code discussed above has been used to calculate the (real part of the) optical potential for the α-α, α-^{12}C, α-^{16}O reactions. These idealistic potentials are being used to extract the amount of polarization induced in the target by the neighborhood of the α particle. A paper discussing the results is in preparation.

21. Asymmetric Fission of ^{236}U in A Realistic K-Matrix Model (R. Y. Cusson, D. Kolb, H. W. Schmitt ((ORNL)))
A paper has appeared in Phys. Rev. C10 (1974) 1529.

22. Coriolis Anti-Stretching in ^{20}Ne and α Widths (H. C. Lee and R. Y. Cusson)

Inactive.

23. Applications of Group Theory to Rotational Vibrational Bands on Nuclei (R. Y. Cusson, L. C. Biedenharn, O. L. Weaver ((Kansas State University)))

In a recent study we used the group $T_5 \circledcirc SU(2)$ to describe rotational bands in nuclei (Annals of Physics 77 (1973) 250) and we suggested to use the group $CM(3) = T_6 \circledcirc SL(3,R)$ to include vibrational excitations. This work has been carried out and a class of rotational-vibrational bands has been discovered. Each rotational-vibrational band is characterized by a fixed quantized vorticity, v. The $v = 0$ bands are the well-known SO(5) Bohr-Hottelsen bands. The new $v \neq 0$ bands play the role of particle-rotational couplings, without the need to introduce explicitly the degrees of freedom of the decoupled particles. Applications to back bending rotational bands are envisaged. A paper on those results is being written.

24. Exotic Configurations of Superheavy Nuclei, Bubbles, Torus, etc. (R. Y. Cusson, C. Y. Wang ((ORNL)))

Starting from classical liquid drop properties of finite nuclei, C. Y. Wang recently predicted the existence of bubble nuclei, having both an inner and an outer surface, in the mass region $A \sim 800$. The existence of these exotics has been confirmed using the K-matrix code mentioned in entry number 14. Although these species are too heavy to be made by present heavy-ion techniques, so that their existence is largely of academic interest (they have very short positron decay half-life anyway), the present result is most important in that it strengthens our belief in both the liquid drop theory, which predicts doughnut-like exotics near $A = 400$ and is manufacturable in the laboratory, and in the K-Matrix model's ability to correct by predicting liquid drop properties. Whenever computing time is available we hope to use the new deformed code to study the torus exotics near $A = 400$.

A paper on the spherical bubble nuclei is being written.

25. Do Protons and Neutrons Have Internal Rotational Vibrational Excitations? (S. Brown, R. Y. Cusson)

Inactive.

E. ATOMIC PHYSICS

1. Ion Induced X-Ray Studies (B. L. Doyle, W. W. Jacobs, S. M. Shafroth, A. W. Waltner)

a. Ag K and L and Au L X-rays Produced by 12-50 MeV ^{16}O Bombardment

A paper entitled "X-ray Production Cross Sections, Intensity Ratios, And Centroid Energy Shifts of Ag K and L and Au L X-Rays Produced by ^{16}O Beams of 12-50 MeV" by G. A. Bissinger,* P. H. Nettles,** S. M. Shafroth and A. W. Waltner has been published--Phys. Rev. A10, 1932 (1974).

b. High Resolution Study of Ag L X-rays

A paper covering some of this work, entitled "Silver L X-Ray Satellites Arising from Heavy Ion Bombardment of Silver" by B. L. Doyle, K. W. Hill,+ W. W. Jacobs, S. M. Shafroth, J. Wu and R. D. Deslattes,++ was given at the Fourth International Conference on Atomic Physics at Heidelberg, Germany, July 22-26, 1974 and was published in the conference proceedings, pages 647-650. A draft of a full length paper on this work is being prepared by Mr. B. L. Doyle. It is entitled "Rearrangement Calculations for The Production of Ag L_α Satellites by Heavy Charged Particles". The abstract follows:

> "Ag L_α x rays and satellites (L_3M^n, n = 0-10) have been produced by bombarding thick Ag targets with beams of H^+, He^{++}, Li^{+++}, C^{++}, and O^{+5} having velocities ranging from one to five MeV/amu. A Bragg spectrometer was used to detect the radiation. Intensity ratios were obtained from the spectra and fit with a modified binomial distribution incorporating a fitting parameter p_m, the probability of M-shell exci-

---

* Present address: East Carolina University, Greenville, N. C.
** Present address: Scientific Atlanta +Naval Research Lab., Wash., D.C.
++ National Bureau of Standards, Washington, D. C.

tation. This distribution was formulated by assuming that the initial number of M holes was described by a simple binomial distribution. The resulting combinations of L and M vacancies were then allowed to redistribute themselves, with the probability of each rearrangement being determined by theoretical branching ratios. The inclusion of these redistribution effects is important since transitions like the L_1-$L_3M_{4,5}$ Coster-Kronig and L_3M - L_3 XY Auger will respectively increase and decrease the number of M holes present at the time of L_α x ray emission. The extracted fitting parameters, p_m, were plotted in the form p_m/Z projectile vs. $V_{projectile}$, and, as the Binary Encounter Approximation (BEA) predicts, most of the points fall on a common curve. Theoretical values of p_m were obtained by extending published work to include M shell excitation, and the results, although predicting the correct trends, lie about a factor of 2 above our data."

c. Bi and Po K X-rays Arising from Proton Bombardment of Bi, E_p = 3 - 13 MeV

A paper including this subject as well as others has been published in the Journal of The Franklin Institute on the occasion of the fiftieth anniversary of the Bartol Research Foundation. It is entitled "Coulomb Excitation of Atomic Electrons in Heavy Ion-Atom Collisions" by S. M. Shafroth, Jour. Franklin Inst. 298, 333 (1974). The abstract follows:

"The relationship between Coulomb excitation of collective nuclear levels and Coulomb ionization of atomic electrons is discussed. Particular emphasis is placed on K shell ionization in this paper. Results of initial experiments with the Triangle Universities Laboratory Cyclo-Graaff where K x-ray production cross-sections were measured for Ca, Ti and Ni are given. The energies at which these cross-sections reach a maximum value were found and agreed well with theory. The experimental cross-sections had the same trend with energy as the theory but were too high by typically 25 percent. Reasons for this disagreement are discussed. A similar experiment is described where Ag was the target. In this case theory and experiment agreed quite well. An experiment is

described where Bi is bombarded with protons from 2-15 MeV and the K x-ray production cross-sections are measured. Also Po K x-rays are detected at the higher bombarding energies and it is shown that Coulomb ionization cannot be responsible. The most likely process for production of these x-rays is internal conversion of excited reaction products following (p,n) and (p,2n) reactions."

Further work with the object of understanding the origin of the Po K x-rays has been undertaken. Gamma ray production cross sections for the $^{209}Bi(p,n\gamma)$ and $(p,2n\gamma)$ reactions have been measured. Using available information on internal conversion coefficients for the major γ transitions in ^{208}Po and ^{209}Po, Po x ray production cross sections have been estimated. The trend with proton energy is in agreement with experiment but the x-ray yield so calculated is roughly a factor of 2 lower than experiment.

d. U and Np K x ray Production Arising from 2-15 MeV Proton Bombardment of U

Professor Waltner is preparing this work for publication.

e. Au K x rays Excited by Protons (2 - 14 MeV) And ^{16}O Ions (18 - 42 MeV)

No progress has been made since the last report.

f. L and M x rays of Bi and U Arising from 0.5 - 15 MeV and 2 - 15 MeV Proton Bombardment of Bi and U

An oral presentation of some of this work was given at the International Conference on X Ray Processes in Matter, Helsinki University of Technology, Otaniemi, Finland, July 28-August 1, 1974 entitled "L Subshell Ionization Probability in U due to 3 - 14 MeV Protons, Internal Conversion, and Photoexcitation". It appears in Physica Fennica 9, Supplement S1, 267 (1974). The authors are A. W. Waltner, J. T. May, K. V. Mani and S. M. Shafroth.

The main point of this work was to show how different excitation mechanisms give rise to quite different L subshell vacancy distributions which in turn cause the L x-ray spectra to differ markedly.

g. High Resolution Study of Ti K x rays Excited by Photons, P, He^{++}, Li^{+++}, O^{n+} Ion Beams

A paper entitled "Energy Shift, vs. Projectile Z for Ti K_α X-rays and Satellites" by D. H. Madison, K. W. Hill, B. L. Doyle, S. M. Shafroth and R. L. Deslattes has been published, Phys. Letters 48A, 249 (1974). A paper entitled "Shifts, Widths, and Intensities of Ti K_α Satellites vs. Projectile Z and Energy" by K. W. Hill, B. L. Doyle, D. H. Madison, S. M. Shafroth and R. L. Deslattes was published in Physica Fennica 9, Supplement S1, 28 (1974). It was also given orally by one of us (SMS) at the Helsinki Conference. A full length paper concerning part of the Ph.D. thesis work of Dr. K. W. Hill entitled "Ti K X Rays and Satellites Following Excitation by Fast Heavy Ions" by K. W. Hill, B. L. Doyle, D. H. Madison, S. M. Shafroth and R. D. Deslattes is in the final stages of preparation. The abstract follows:

> "High resolution measurements have been made of Ti K_α x rays and satellites (KL^n, n = 0-4) following bombardment of thick Ti targets by H, He, Li, C, and O ions at energies of 1-5 MeV/amu. A systematic study was made of the effect of projectile atomic number Z_1 and energy E_1 upon the relative intensities, centroid energies, and widths of the various x-ray peaks. Also studied was the dependence of peak widths upon n, the number of L-shell vacancies at the time of x-ray emission. Relative satellite intensities increase sharply with increasing Z_1. Both the Z_1 and E_1 dependence of these intensities agree reasonably well with a preliminary theoretical model and described elsewhere. Deviations of peak intensities from theory are discussed in terms of deficiencies in the theory, including the use of approximate wavefunctions and perturbation theory, statistical correlations between ejected electrons, and rearrangement of vacancies before x-ray emission. Energy positions of the peaks increase approximately linearly with Z_1 at a rate of $\sim$ 1 eV/Z. These energy shifts are compared with Hartree-Fock calculations of the x-ray energies for various numbers of M-shell (3s and 3p) electronic vacancies. Peak widths range from 10 to 37 eV, increasing monotonically with Z_1 for most peaks and increasing monotonically with n for all projectiles. No variation of peak positions or widths was ob-

served for different values of E_1 and fixed Z_1. The observed energy shifts and peak width variations are discussed in terms of ionization of the M shell, varying distributions of L-shell vacancies among the 2s and 2p subshells, and possible multiplet splittings."

h. High Resolution Study of Zr L X-rays excited by Heavy Ion Bombardment

This paper is being prepared by J. W. Cooper of NBS. It will include rearrangement calculations.

i. Development Progress

Having returned the NBS flat crystal x ray spectrometer in May 1974, we proceeded to replace it with an ARL 4^{11} curved crystal spectrometer which is being placed on line at TUNL. Also a GE spectrogoniometer with various flat crystals is on line at TUNL. A stepping motor has been added and the system is now computer controlled. A few preliminary x-ray spectra have been obtained. Finally a surplus G.E. spectrogoniometer has been converted into a double crystal instrument. Rocking curves of the crystals used can be obtained with this device. It is planned to take it to TUNL if higher resolution is required.

U.S. ARMY BALLISTIC RESEARCH LABORATORIES

A. NEUTRON PHYSICS

1. Small-Angle Elastic Scattering of Fast Neutrons by Nuclei (W. Bucher, C.E. Hollandsworth and J.E. Youngblood)

The elastic scattering of 7.55, 11.0, and 14.0 MeV neutrons through small angles by Be, C, Al, Fe, Cu, Ni, Sn, W and Bi has been measured. Part of these data are plotted in Figs. A1 to A3. The solid curves are predictions calculated from the optical-model parameters of Wilmore and Hodgson, which basically are local equivalents to the energy-independent, non-local potential of Perey and Buck. It is important to note that no normalization factors have been applied to either the data or calculated curves. The data have been corrected for finite geometry, multiple scattering, and other effects. Schwinger scattering has been subtracted. The error flag assigned to each data point includes contributions due to counting statistics (0.5 to 2.5%), uncertainties in each of the corrections, and other experimental uncertainties such as in the detector efficiency and in the transmission of the sample.

2. Do Anomalies Exist in the Small-Angle Scattering of Neutrons by Heavy Nuclei? (W. Bucher, C.E. Hollandsworth and J.E. Youngblood)

Previous experimental studies of the forward elastic scattering of fast neutrons from heavy nuclei are conflicting and have not clearly resolved the question of possible anomalies in the scattering cross sections at small angles. In order to contribute to the resolution of this problem, absolute measurements of the elastic scattering of neutrons by Pb and U were carried out to high accuracy for angles in the interval 3 to 15 degrees and over the range of energies from 7 to 14 MeV. This energy range spans a large body of existing data and, in addition, is sufficiently wide to provide a good test for optical model predictions of differential scattering cross sections at small angles. The present data for either element are well represented by a functional relationship of the form

$$\ln \sigma\ (\theta,E) = A(E) + B(E)\mu + C(E)\mu^2, \qquad (1)$$

where $\mu = 1-\cos\theta$. The curves shown in Fig. A4 are the result of a least-squares fit of Eq. (1) to the present data; data of other workers are also included for comparison. (Note displacement of vertical scales in Fig. A4; U scale displaced as indicated; and Pb scale displaced by amount E(MeV) in b/sr.). Figure A5 in a plot of the percent deviation of optical model predictions (calculated from Wilmore-Hodgson parameters) from the present data for Pb. The theoretical curve of Palla which

takes into account the effects of the nuclear deformation on the scattering of 14.7 MeV neutrons agrees well with the present U data at this energy. It is concluded that: (1) Optical model potentials based on the energy-independent non-local potential of Perey and Buck describe reasonably well the shape but not the magnitude of the small-angle scattering from Pb. (2) Spherical potentials fail to describe the scattering from U over the 7 to 14 MeV energy range; the nuclear deformation must be taken into account. (3) To within approximately ±2% there are no anomalous effects in small-angle neutrons scattering from either Pb or U in this energy range; previous reports of anomalies were due primarily to insufficient accuracy in the measurements and, in some cases, to specialized nuclear models which were used to interpret the data.

3. Small-Angle Elastic Scattering of Fast Neutrons from Nitrogen and Oxygen (C.E. Hollandsworth, W.P. Bucher, and J.E. Youngblood)

Absolute cross sections for the small-angle elastic scattering of 7.65, 7.88, 8.11, 10.95, and 14.00 MeV neutrons from nitrogen and 10.25, 10.75, 10.95, 11.25, and 14.10 MeV neutrons from oxygen have been obtained from previously measured data. Some of the nitrogen results are shown in Fig. A6. The neutron energy spread for these measurements was 75 keV.

All of the measurements are in good agreement with the most recent evaluations except for oxygen near 11 MeV where a minimum occurs in the total cross section. The measured differential cross sections for oxygen at 10.75 and 10.95 MeV are significantly lower than the evaluated ones.

4. Small-Angle Scattering of 14 MeV Neutrons from Niobium (C.E. Hollandsworth, W.P. Bucher, and J.E. Youngblood)

It is planned to measure the small-angle scattering cross sections of Nb at 14.0 MeV and several neighboring energies. This task is on a list of neutron cross section discrepancies which was compiled by H. Goldstein. A descrepancy of about 15% exists between the measured nonelastic cross section and that determined by subtraction of the total elastic from total cross section. Measurements are needed over the angular range 0-25° in order to determine more accurately the total elastic cross section. These data are of particular interest in CTR design studies.

B. A STUDY OF STATES POPULATED WITH THE (d,n) REACTION (J. Horton and C.E. Hollandsworth)

A series of (d,n) experiments were performed on targets of ^{13}C, ^{25}Mg, ^{86}Sr, ^{87}Sr, and ^{88}Sr. Preliminary data reduction of ^{86}Sr and ^{87}Sr is

underway. The distorted wave Born approximation analysis of ^{13}C, ^{25}Mg and ^{88}Sr is nearing completion. These results indicate a ^{88}Sr ground state with a predominant $(p_{1/2})^{-2}$ component but with significant components of $(p_{1/2})^2$ $(p_{3/2})^{-2}$ and $(p_{1/2})^2$ $(f_{5/2})^{-2}$. The ^{13}C experiments were performed at 10, 12, and 15 MeV incident energy. Although no energy dependence was observed, the previously reported discrepancy between spectroscopic factors of the 2.311 MeV T=1 state extracted from the (d,n) reaction and the (^{3}He,d) reaction still exists.

C. ERODED GUN BORE SURFACE DIAGNOSTICS (A. Niiler, and S. Caldwell)

It has been shown that the (d,α) and (d,p) reactions can be used to measure the depth concentration profiles of oxygen and nitrogen in thick steel surfaces. Depth resolutions of 0.2μm and concentration detectability limits of 10 $^{16}at/cm^2$ have been achieved at 3 MeV. The $^{16}O(d,\alpha_0)$, $^{16}O(d,p_0)$, and $^{16}O(d,p1)$ cross sections have been measured in the 0.50 to 1.00 MeV energy range, the results being in good agreement with earlier. published data. Oxygen depth profiling has been done at 650 keV with better detectability but somewhat poorer depth resolution than was achieved at 3 MeV.

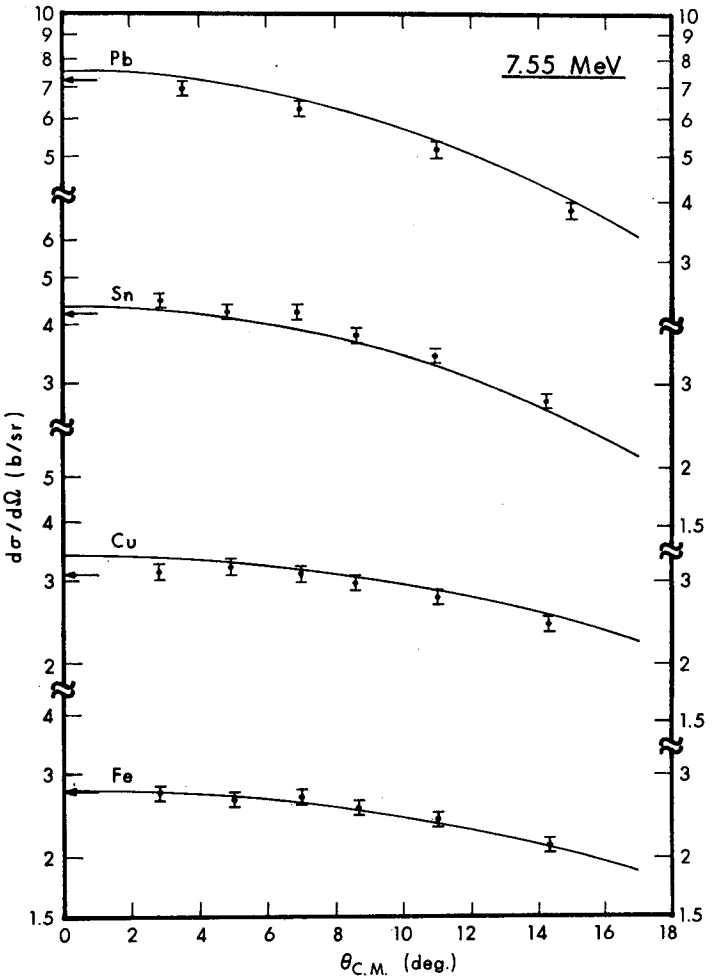

Figure A.1

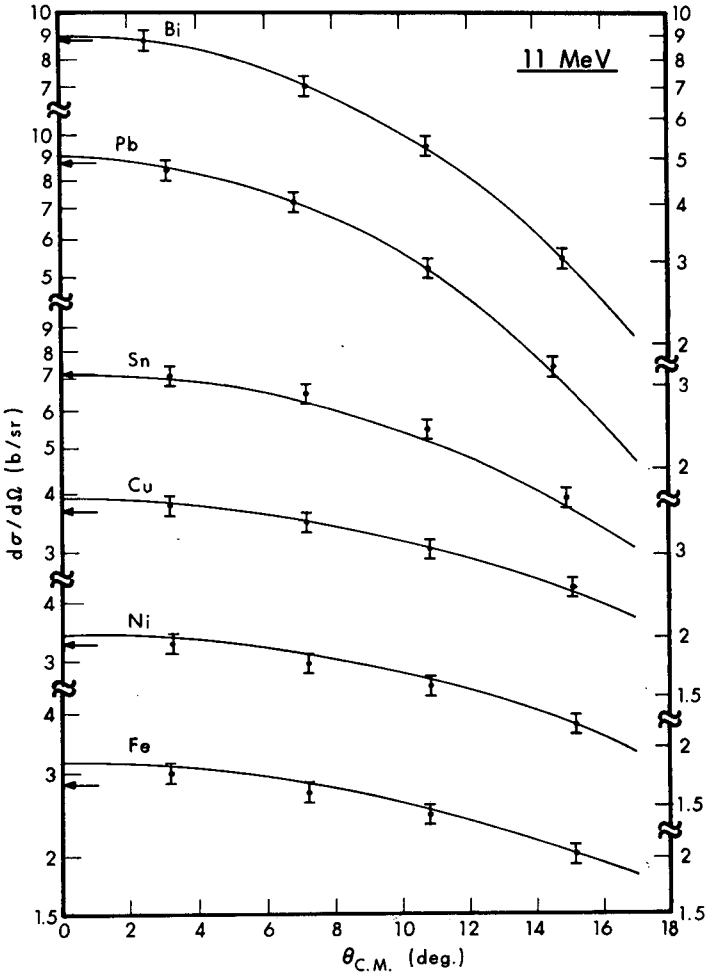

Figure A.2

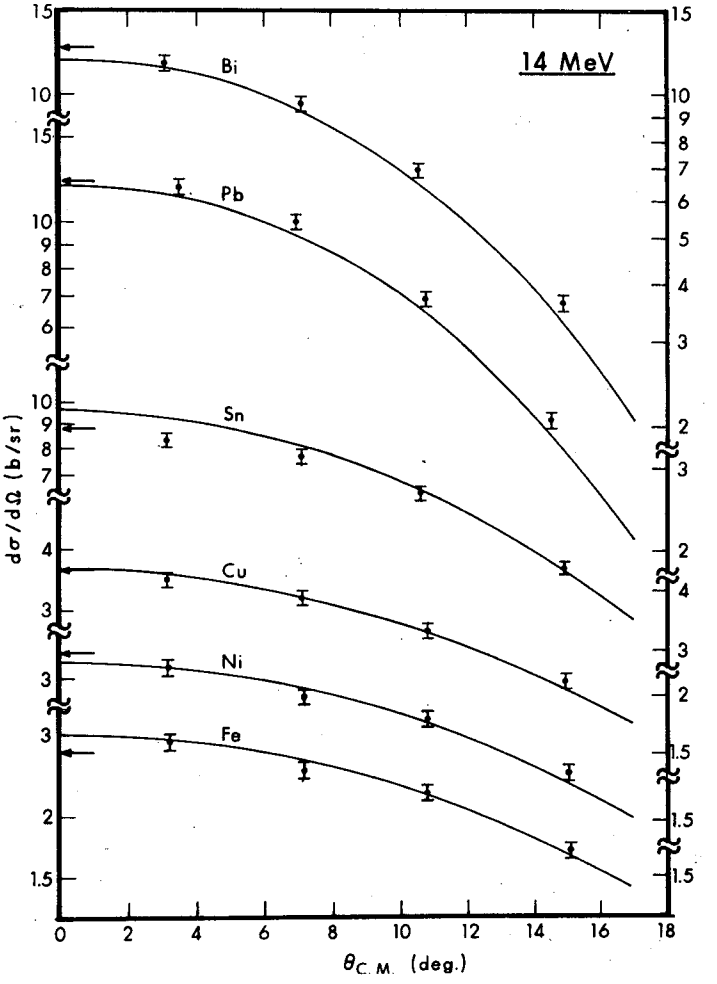

Figure A.3

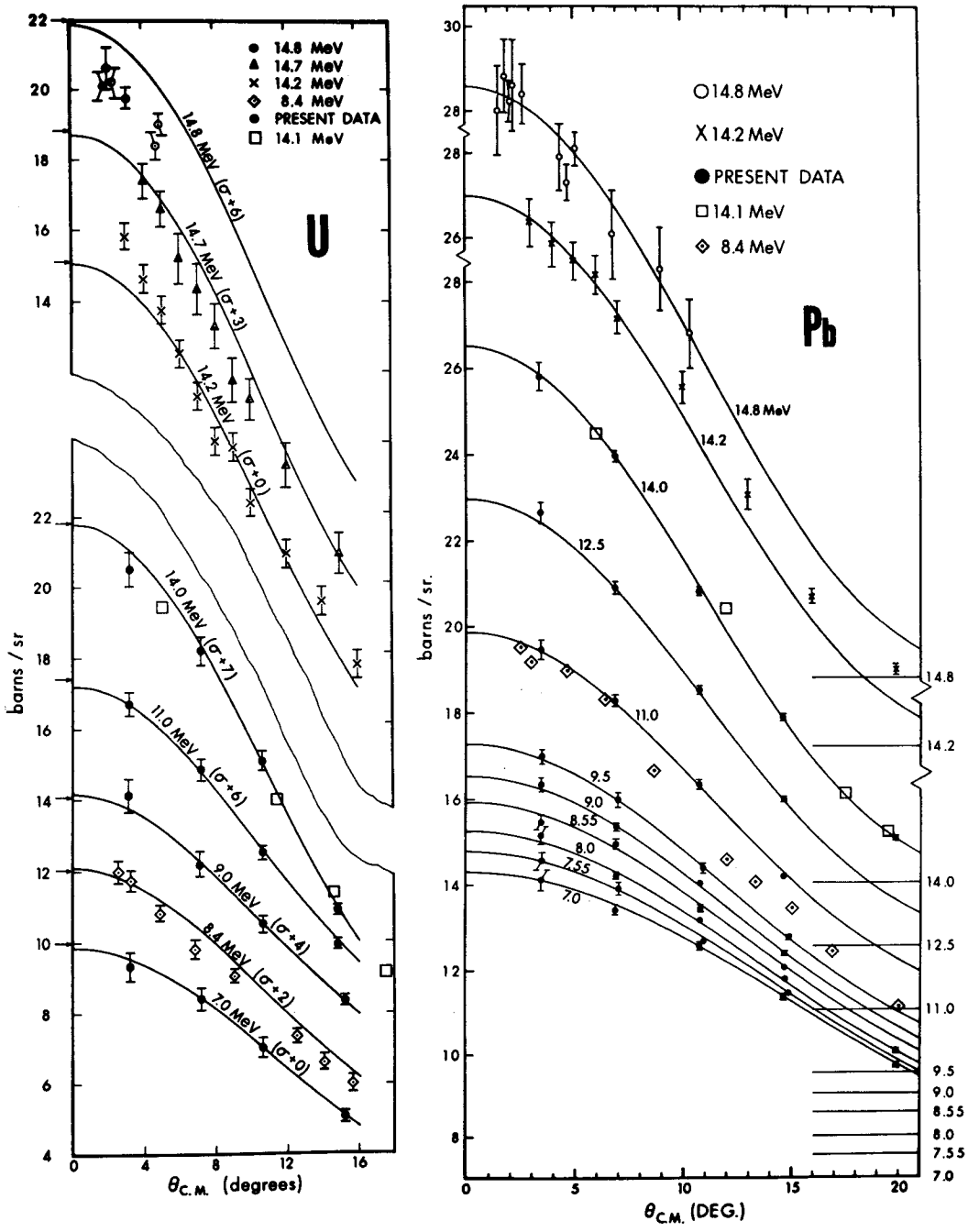
14.8 MeV
14.7 MeV
14.2 MeV
8.4 MeV
PRESENT DATA
14.1 MeV
U
14.8 MeV (σ+6)
14.7 MeV (σ+3)
14.2 MeV (σ+0)
14.0 MeV (σ+7)
11.0 MeV (σ+6)
9.0 MeV (σ+4)
8.4 MeV (σ+2)
7.0 MeV (σ+0)
barns / sr
θC.M. (degrees)
14.8 MeV
14.2 MeV
PRESENT DATA
14.1 MeV
8.4 MeV
Pb
14.8 MeV
14.2
14.0
12.5
11.0
9.5
9.0
8.55
8.0
7.55
7.0
barns / sr.
θC.M. (DEG.)

Figure A.4

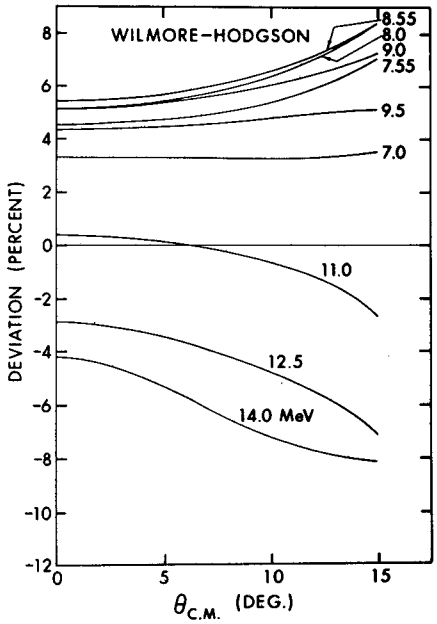
WILMORE-HODGSON
8.55
8.0
9.0
7.55
9.5
7.0
11.0
12.5
14.0 MeV
DEVIATION (PERCENT)
8
6
4
2
0
-2
-4
-6
-8
-10
-12
0
5
10
15
$\theta_{C.M.}$ (DEG.)

Figure A.5

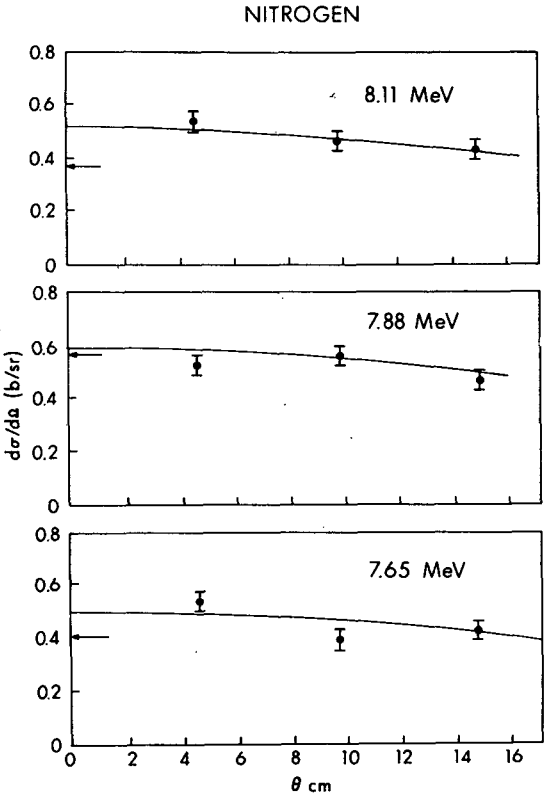
NITROGEN
8.11 MeV
7.88 MeV
7.65 MeV
dσ/dΩ (b/sr)
θ cm
0.8
0.6
0.4
0.2
0
0
2
4
6
8
10
12
14
16

Figure A.6

YALE UNIVERSITY

A. FAST NEUTRON POLARIZATION STUDIES (F.W.K. Firk, J.E. Bond, R. Nath and H.L. Schultz.)

1. Polarization of Neutrons in n-^{4}He Scattering

Our previously measured asymmetries of polarized neutrons elastically scattered from a target of liquid He have been analyzed to give R-matrix parameters and phase-shifts in the neutron energy range from 2 to 6 MeV. As a result of these analyses, it has become clear that additional measurements are necessary at angles less than 40° in order to determine the parameters with confidence. Such measurements are currently being made.

2. Polarization of Neutrons in n-^{9}Be Scattering (with R.J. Holt*)

The general analysis of neutron polarization developed for target nuclei with non-zero spins has been used to analyze our measurements of the $\vec{n}$-^{9}Be reaction in the MeV-region. Preliminary results are listed in TABLE I.

B. POLARIZATION OF PHOTONEUTRONS

1. Differential Polarization of Photoneutrons from Liquid Deuterium (F.W.K. Firk, L. Drooks and H.L. Schultz)

Measurements of the polarization of photoneutrons emerging from a liquid deuterium target are now well-advanced. Results have been obtained at angles of 90° and 120° using an absolutely calibrated analyzer of ^{12}C. The photon energy range covered extends from 6 to 15 MeV. A

* Now at ANL, Argonne, Ill.

TABLE I

ℓ J S	$E_{\lambda\ell JS}$ (MeV)	$\gamma^2_{\lambda\ell JS}$ (MeV)	$R^{\infty}_{\ell JS}$	$B_{\ell JS}$
0 1 1	-0.885	0.4	0	0
0 2 2	-0.555	0.4	0	0
1 0 2	0.7	2.4	0.4	-0.7
1 1 1	-	-	0.4	0
1 2 1	2.75	0.2	0	-0.4
1 1 2	-	-	0.2	0
1 2 2	2.75	1.0	0	-0.4
1 3 2	-	-	0.2	0
2 1 1	-	-	-	0
2 2 1	-	-	-	0
2 3 1	0.63	0.6	0	-1.9
2 0 2	-	-	-	0
2 1 2	-	-	-	0
2 2 2	-	-	-	0
2 3 2	-	-	-	0
2 4 2	2.71	0.8	0	-1.4

Interaction radius = 4.3 fm
The symbols have their usual significance.

detailed Monte Carlo calculation of the effects of multiple scattering in the target has been completed. Measurements are continuing at other reaction angles. The objectives of these measurements are to obtain results that will hopefully shed light on the question of meson effects at these low energies.